Environment Canada Environnement Canada

Assessment of Water Quality Simulation Capability for Lake Ontario

SCIENTIFIC SERIES NO. 111
(Résumé en français)

INLAND WATERS DIRECTORATE,
NATIONAL WATER RESEARCH INSTITUTE,
CANADA CENTRE FOR INLAND WATERS,
BURLINGTON, ONTARIO, 1979.

Environment Canada Environnement Canada

Assessment of Water Quality Simulation Capability for Lake Ontario*

*Contributions from F.M. Boyce, A.S. Fraser, E. Halfon, D. Hyde, D.C.L. Lam, W.M. Schertzer, A.H. El-Shaarawi, T.J. Simons and K. Willson of the Applied Research Division and D. Warry of the Water Quality Branch. Project Leader—T.J. Simons.

SCIENTIFIC SERIES NO. 111
(Résumé en français)

INLAND WATERS DIRECTORATE,
NATIONAL WATER RESEARCH INSTITUTE,
CANADA CENTRE FOR INLAND WATERS,
BURLINGTON, ONTARIO, 1979.

Cat. No. En 36-502/111
ISBN 0-662-10652-0

TABLE OF CONTENTS

ABSTRACT

This report evaluates the ability of current water quality models to simulate seasonal variations, long-term trends, and spatial variations in Lake Ontario. The analysis relies on routine surveillance data collected during the last decade and especially on observations taken during the International Field Year on the Great Lakes (IFYGL). The model evaluations concentrate on conceptual frameworks rather than mathematical formulations.

By fitting dynamic models to a seasonal data base, it is shown that equally satisfactory simulations can be obtained by a variety of parameterizations and regardless of conditions of annual periodicity. By comparison of model output with long-term observations, it is demonstrated that such seasonal verification studies are of little use in diagnosing the utility of these models for predicting long-term trends. It is concluded that the uncertainty surrounding the formulation of sedimentation and nutrient regeneration, as well as the sensitivity of models to assumptions regarding dynamic balance between lake concentrations and nutrient loadings, undermine the predictive capability of dynamic water quality models.

With regard to spatial variations, it is concluded that the lakewide response can be simulated reasonably well by simplified horizontally mixed models but that three-dimensional models are necessary to simulate the very important differences in biochemical properties between nearshore and offshore zones.

RÉSUMÉ

Le rapport évalue la capacité des modèles actuels de la qualité des eaux à en simuler les variations saisonnières, les tendances à long terme et les variations spatiales dans le lac Ontario. Cette analyse s'appuie sur des données de contrôles réguliers de la dernière décennie, et tout particulièrement sur les résultats d'observations effectuées pendant l'Année internationale d'étude des Grands lacs (IFYGL). L'évaluation traite davantage des cadres conceptuels de travail que des formules mathématiques utilisées par les modèles.

L'adaptation des modèles dynamiques à des données saisonnières montre qu'il est possible de bien simuler des phénomènes à partir d'un éventail de paramètres et sans égard aux conditions de périodicité annuelle. La comparaison des résultats des modèles et de ceux des observations à long terme montre le peu d'utilité des études de vérification des conditions saisonnières dans l'évaluation de l'utilité des modèles de prévision des tendances à long terme. On peut donc conclure que l'incertitude qui entoure l'établissement de formules qui décrivent la sédimentation et le recyclage des substances nutritives ainsi que la dépendance des modèles face aux suppositions qui touchent à l'équilibre dynamique entre les teneurs dans le lac et l'apport de substances nutritives réduisent la capacité de prévision des modèles dynamiques de la qualité des eaux.

En ce qui concerne les variations spatiales, il est possible de simuler de façon assez juste la réaction du lac pris dans son ensemble à l'aide de modèles bidimensionnels simplifiés qui supposent l'homogénéité de chaque paramètre sur le plan horizontal. Toutefois, les modèles tridimensionnels s'avèrent nécessaires pour la simulation des différences extrêmement importantes qui existent entre les propriétés biochimiques des zones près des rives et du centre.

ASSESSMENT OF WATER QUALITY SIMULATION CAPABILITY FOR LAKE ONTARIO

SUMMARY AND CRITIQUE

The report evaluates the ability of current water quality models to simulate seasonal variations, long-term trends, and spatial variations in Lake Ontario. The analysis relies on routine surveillance data collected during the last decade, and especially on observations taken during the International Field Year on the Great Lakes (IFYGL). In addition to a brief introduction, the report consists of three main chapters, addressing each of the above areas of simulation in turn. A considerable proportion of the discussion is devoted to the available data base, and the model evaluations tend to be more diagnostic than prognostic in nature, concentrating on the conceptual framework rather than mathematical formulations.

Seasonal Analysis and Simulation

The data used in this chapter were collected during the IFYGL program, April 1972 to March 1973. In particular, the biochemical data were obtained during the "Ontario Organic Particle Study" (OOPS) program, a series of nine ship surveys at approximately six-week intervals. Primary production measurements are available only for two stations, one inshore and one offshore, again at the same intervals. In order to extrapolate these observations to different times and other stations, an empirical regression model is constructed for observed algal growth as a function of light, temperature, and nutrients. It shows that almost all the observed variation can be explained in terms of light and temperature. A rigorous statistical analysis points to an inverse relationship between photosynthesis and concurrent phosphate concentrations, thus showing that this particular data set cannot be used to validate a primary production model incorporating an instantaneous nutrient limitation effect. By introducing a priori a conventional formulation of the nutrient effect, however, a quite acceptable fit to the data is obtained if the temperature effect is adjusted to reflect the inverse correlation between temperature and nutrients.

A two-layer, two-component dynamic phosphorus model, the variables being orthophosphate and total phosphorus, is then fitted to the IFYGL data base by application of mass balance principles as well as optimization techniques. Diffusive fluxes across the thermocline are computed by recourse to exchange coefficients derived fron concurrent temperature observations. Seasonal variations of net sedimentation of particulate phosphorus and net biological conversion from organic to inorganic phosphorus are obtained from mass balance equations for each of these components, including observed net loading. It is shown that the net biological conversion can be equally well reproduced by a range of primary production and respiration concepts, among them a model postulating that low nutrient concentrations do not inhibit primary production but rather require a faster regeneration of nutrients. It is also shown that the highly variable sedimentation cannot properly be simulated by invoking a constant settling velocity for the whole year.

The discussion of seasonal simulations is concluded with a review of dynamic plankton models including interactions of various nutrients, phytoplankton, and zooplankton species. By analyzing typical model experiments, attention is drawn to the fact that seemingly acceptable simulations of seasonal variations can be achieved without meeting reasonable mass balance conditions. In particular, the experiments with the dynamic models in this chapter show that equally satisfactory seasonal simulations are obtained with and without imposing conditions of annual periodicity, and hence they do not answer the question whether the lake is in equilibrium with the loading. It is then argued that seasonal verification studies of dynamic models by themselves are not sufficient to diagnose the utility of such models for predicting long-term trends.

Long-term Variations

This chapter starts with a compilation of nutrient loading data and a summary of physical and biochemical observations on Lake Ontario taken in the course of routine surveillance as well as special research programs during the twelve-year period 1966-1977. This period is roughly equivalent to the hydraulic retention time of Lake Ontario. Statistical analyses are carried out to estimate trends of nutrient concentrations and

chlorophyll in the lake for this period. Both the phosphorus and the phytoplankton levels appear to have peaked around 1970 to 1971 and display statistically significant decreasing trends since that time. According to the analyses, the extreme east end of the lake and the areas along the north shore are showing most improvement. In the area near Toronto, for example, the decrease in phosphorus concentrations between 1971 and 1977 is found to be one-third of the maximum level of 28 mg/l observed in 1971. It appears, therefore, that the combination of improved sewage treatment and the ban on phosphorus in detergents has resulted in a significant decrease of concentrations in the lake.

Experiments are then carried out with dynamic models to simulate the response of Lake Ontario to observed changes of light, temperature, and especially nutrient loading during the past 12 years. Particular attention is paid to the question of whether dynamic plankton models, including a variety of kinetic interactions and, as seen above, producing acceptable seasonal simulations, are better suited to predict the response of a lake to changing loads than relatively simple empirical relationships. It is found that the uncertainty surrounding the formulation of sedimentation and nutrient regeneration, in conjunction with the sensitivity of the models to assumptions regarding dynamic balance between lake concentrations and nutrient loadings, undermine the long-term predictive capability of such models. In essence, it is concluded that any presently available model, be it empirical or dynamic, can give at most a qualitative indication of the response of the lake to anticipated or postulated changes in loading conditions.

Spatial Variations

This chapter again utilizes the observational data gathered during the 1972 IFYGL program. The modeling experiments emphasize three-dimensional hydrodynamic simulations and the horizontal and vertical transports of materials in large lakes. It is concluded that hydrodynamic models are reasonably successful in simulating the immediate response of a lake to forcing by wind but much less capable of dealing with situations where cause-effect relationships are less well understood. Calculations are made of the vertical exchange of nutrients across the thermocline

during the stratified season, using exchange coefficients obtained from heat budgets. They indicate that vertical mixing has significant effects on the total rate of change of epilimnion concentrations especially during the spring bloom. Calculations of horizontal transports are made by combining observed nutrient concentrations with currents computed by a hydrodynamic model. The results show that the nearshore and offshore zones are intimately linked by horizontal transports and that their biochemical properties cannot be considered in isolation.

Experiments with a three-dimensional water quality model, combining a hydrodynamic model with a plankton model, are described and the results are compared with those obtained from horizontally mixed lake models. It is concluded that lake-wide averages of solutions for the segmented model correspond closely to results from the simple model, implying that the lake-wide response can be simulated reasonably well by the latter type of model. It is also shown that three-dimensional models appear capable of simulating the very important differences in biochemical properties between different lake areas, in particular, between nearshore and offshore zones.

It is concluded that major gaps remain in our knowledge of the system which can only be addressed by highly specialized disciplinary research.

Critique

The present report addresses only one particular aspect of ecological modeling, namely, the practical utility of first-generation dynamic water quality models. It reaches the conclusion that we still have some way to go before such models can, with confidence, be used as a management tool. There is, however, considerable danger involved in making the results of such a critical analysis available to a wide audience, including individuals with little background in this field of science. Thus, the somewhat negative tone of this study might be interpreted to mean that the authors do not believe in the use of mathematical modeling techniques in environmental science and management. Nothing could be farther from the truth. Throughout this report it is shown that such techniques provide a powerful diagnostic tool in trying to understand what goes on in the

highly complicated lake environment. Furthermore, while it is concluded that long-term quantitative predictions of the response of a lake to loading, based on dynamic plankton models, should be approached with much caution, the same is true for empirical methods. Perhaps the problem is best illustrated by quoting from a critique written by Dr. R.V. Thomann, Manhattan College, in response to an earlier draft of this report. He writes: *There are no doubt many unresolved questions,... areas of uncertain understanding, and discrepancies between models and data. But, the report seems to betray a certain negative bias that is probably at the opposite end of the enthusiastic bias that I have exhibited at various times. In my opinion, the water quality models do reproduce a number of the basic dynamic features of the Lake Ontario system and at the same time, have revealed any number of areas which require further investigation and field and laboratory work. ....The authors seem to maintain that an almost complete level of certainty of model ability is required before any predictive statements can be made. As a consequence, the report fails to reach any firm conclusions on some of the more basic questions of eutrophication in Lake Ontario. For example, on the basis of the assessment, do the authors believe that the models will provide at least a partial answer to whether reduction of phosphorus discharge will reduce phytoplankton biomass? The report is quite ambivalent on this question."*

Dr. Thomann is right in pointing out that this report tends to be more negative than the usual publications in the field of environmental modeling, not only his but ours as well. The reason is, of course, that unlike the observationally oriented scientist, who can publish any result, the modeler can only present a model that works. But here we are facing the question whether a model that works for us in helping us understand some of the workings of the system, also works for the decision maker. This report obviously arrives at the uncomfortable conclusion that in the latter case a much more complete level of certainty is required. Thus the authors do believe that the models provide some answer, but the whole purpose of the exercise is to show that the answer is indeed partial. That then leads to the crucial question of what to do while we are waiting

for the ultimate answer. Again, we like to quote from Dr. Thomann's review:

"Can the authors offer no other avenue for assisting decision making in environmental management than the approach of more "highly specialized disciplinary research?" Are the authors suggesting, as a result of their rather negative findings, that present models offer no simulation or prediction capability for water quality and that resources presently devoted to predictive modelling be diverted to more specialized process or mechanism-oriented research? These questions lead me to conclude that the authors have ducked the issues that occur in the real world and have opted for the illusionary comfort of wanting to know system behavior perfectly before venturing into the problem solving arena. It makes me wonder what the authors would have said ten years ago in response to Vollenweider's offering of the delineation between "dangerous" and "admissable" phosphorus loading as a basis for making decisions on eutrophication control."

And that, of course, is the heart of the matter: science on the one side, the real world on the other, and the modeler in the middle.

Chapter 1

INTRODUCTION

1.1 Outline of Study

Long-term records of physical, chemical, and biological variables in a lake often resemble typical climatological records of atmospheric temperature and radiation. Thus, large seasonal fluctuations are superposed on smaller but still appreciable, year-to-year variations. Formally, any record of observations can be decomposed into a series of sinusoidal functions of time with periods ranging from the fastest to the slowest variations present in the record. If this were done for typical biochemical variables such as nutrients or plankton biomass, one would expect to find two major periodicities in the series, the first one representing the seasonal cycle, the second one associated with the hydraulic retention time of the lake under consideration. Any modeling effort, therefore, must start by investigating which processes and parameters affect these periodicities individually, and to what extent, if any, the short-term and long-term variations can interact.

The seasonal variations of limnological variables, biological as well as physical, are directly related to corresponding changes in surface radiation. The associated heat fluxes across the air-water interface result in seasonal variations of temperature accompanied by the formation of thermoclines which inhibit mixing between warm surface water and cold bottom water. The latter process, and to a lesser extent also the direct effect of radiation, determines the month-to-month changes of nutrients and plankton in a deep lake such as Lake Ontario. For a large lake or sea, the immediate effects of nutrient loading are negligible in the sense that biological production in the stratified season is mostly controlled by nutrient concentrations at the end of spring overturn. Other processes, such as sedimentation, play an important role, but not to such an extent that changes of sedimentation parameters within reasonable limits would lead to essential modifications of typical seasonal cycles.

By contrast, limnological variations with time scales corresponding to the retention time of a given lake, are naturally governed by

net loading and net sedimentation. The retention time enters into the problem because a lake does not respond to changing loadings instantaneously, but rather gradually tries to reach a new state of equilibrium. This balance between lake concentrations and loadings will be achieved when the gains from external inputs are exactly compensated by losses due to river outflow and exchanges at the sediment-water interface. Since these losses are proportional, or at least related, to the concentrations in the lake itself, the whole mass of water contained in the lake has to adjust itself to any new loading conditions. Essentially, all the old water must be replaced, which requires a time span comparable to the flushing time, i.e., a decade or so for Lake Ontario.

At first glance, the foregoing would indicate that the primary periodicities in the response of the Lake Ontario system can be modeled independently from each other. It is indeed true that seasonal variations can be simulated quite accurately without regard to the long-term behaviour of the Lake, but the reverse does not necessarily hold true. This will be clear if one considers the relationship between chemical concentrations in a lake and exchanges at the sediment interface. For example, it is reasonable to postulate that the loss of phosphorus due to sedimentation is in some way proportional to the particulate fraction. Since sedimentation constitutes the primary factor in the long-term response of the lake to loading, the seasonal variation of particulate matter could be an important area of interaction between the two basic periodicities. Consequently, it may be necessary to develop fairly detailed "process" models instead of simple "input-output" models even if the sole purpose of the exercise is to predict some future trophic state of a lake.

This leads to a basic difficulty in constructing a long-term predictive model of a large lake. If one adopts the viewpoint that such a model should incorporate a reasonable description of the primary kinetics, then one would naturally first try to verify the postulated set of model parameters by comparison with observed seasonal variations. The amplitudes of the seasonal periodicities, however, are usually an order of magnitude larger than the year-to-year changes which may be expected to result from feasible changes in loading conditions for Lake Ontario.

Furthermore, the rate coefficients estimated from a seasonal verification study are far from unique and one can accommodate a substantial range of sedimentation rates by adopting different kinetics. The problem is compounded by the inherent uncertainty in the data base. Consequently, this procedure by itself can never be a sufficient test for a predictive model. At the same time, it is obviously tempting to ascribe such long-term predictive powers to a model which appears capable of simulating seasonal features, in particular if the model is so complex as to obscure the basic cause-effect relationships. In that sense, then, it may be more dangerous to have a sophisticated model than to have no model at all.

A similar difficulty relates to the above-mentioned time lag between external loading and equilibrium concentration. Clearly, if a lake at any given time is not in balance with the nutrient inputs, the future conditions will change even if the loading is held constant. Again, a seasonal model validation would not answer the question whether or not Lake Ontario is in equilibrium with the loading. Compared to the seasonal variations and in view of the error margin in the data base, the values of the variables after one year are in either case so close to the initial values that satisfactory simulations can be obtained without ever considering this problem. Naturally, it is extremely unlikely for all variables to be exactly periodic unless this condition is specifically imposed on the model. Since this is usually not done, a typical seasonal model will produce different results for consecutive years of simulation, regardless of actual equilibrium conditions in the real lake.

In addition to the above considerations of temporal characteristics of limnological variables, there is the problem of spatial variations in a large lake. It is generally recognized that vertical variations of biochemical processes must be included in an ecological model because of the large gradients of dissolved and suspended matter in stratified water bodies. Also, in a lake of the size of Lake Ontario, considerable horizontal gradients of nutrients and plankton populations may develop as a result of local environmental conditions such as temperature and nutrient loading. Even though different layers and zones of a lake may display quite specific properties, they are effectively coupled together by horizontal and vertical transport and dispersion

mechanisms. The question is then to what extent the local response is affected by the interactions between different volume elements; and specifically, what level of sophistication is required to simulate such physical processes. An equally relevant question is whether such three-dimensional simulations, when suitably averaged in space and time, show a significantly different "whole-lake" response as compared to much simpler models.

It follows from the foregoing discussion that the assessment of any model of Lake Ontario must consist of essentially three steps dealing, respectively, with seasonal time scales, time variations of a decade or more, and spatial distributions. The seasonal simulation would concentrate on kinetic interactions and it would require a high-resolution data set for at least one complete year. The long-term study must concentrate on loading of nutrients and interchanges at the sediment-water interface. The data base for this study must cover a period longer than the retention time but the time-resolution can be relatively coarse. The spatial simulation study should be concerned with gradients and interactions between different volume elements of the lake and therefore requires a data base with a high spatial resolution.

The present report will address these three aspects of the Lake Ontario simulation problem. In each case, the discussion will start with a description of the available data base, followed by an analysis of typical models in ascending order of complexity. The seasonal study as well as the spatial simulations utilize the data base obtained during the 1972 International Field Year on the Great Lakes (IFYGL). The long-term analysis is based on all available surveillance data collected from 1966 to 1977. The model evaluations tend to be more diagnostic than prognostic in nature and an effort will be made to illustrate the potential and the limitations of different methodologies by considering their basic underlying principles rather than arcane formulations.

1.2 Modeling Principles

A model is a conceptual analog of certain rather universal traits of observed entities. Thus, the modeling of an ecosystem requires knowledge of the real system, obtained with experiments, and its

abstraction within a mathematical framework. However, a model which must be capable of accounting for all the input-output behaviour of the real system and be valid in all allowable experimental frames can never be fully known (Zeigler, 1976). This model, which Zeigler calls the *Base Model*, would be very complex and require a great number of computational resources, so that it would be almost impossible to simulate. As for ecosystems, the base model could never be fully known because of the complexity of the system and the impossibility to obtain all the necessary information. However, given an experimental frame of current interest, a modeler is likely to find it possible to construct a relatively simple model that will be valid in that frame. This is a *Lumped Model*: it is the experimental image of the real system with components lumped together and simplified interactions (Zeigler, 1976). This definition of model implies that the modeler has a large impact on model construction, and that given several modelers, their conceptualizations would be different. Each model may emphasize different aspects of the real system but reflect its basic structure. Moreover, Zeigler (1976) and Cale and Odell (1978) have shown that error is inherent in any dynamic aggregate regardless of how the aggregate was created. The mere fact that we must use lumped models implies a source of error: when this fact is coupled with the realization of the modeler's influence, then we must conclude that a model is not as perfect as it is believed to be.

Even so, the system approach is quite common in sciences as diverse as Biology, Physics and Sociology. This is because we have the evidence that certain system properties do not depend on the specific nature of the individual system but they are valid for systems of different nature: sophisticated procedures developed for the analysis of complex systems, mainly electrical, can now be applied to ecological systems whose analytical methodology is far less advanced. The quantitative formalism of a model allows the presentation and verification of hypotheses in a way that it is not otherwise possible. In this sense, system-theoretical arguments pertain to, and have predictive value, inasmuch as general structures are concerned (Bertalanffy, 1972). We take the *holistic* view that system properties are more, and different from, what can be found from the analysis of the system parts. Indeed, these system properties

depend on the interaction of the system parts, or components, among themselves and with the environment (defined as everything outside of the system of interest). The important point, therefore, is the good conceptualization of the units of functional interest (components). Mathematically, this corresponds to the building of a lumped model, with its functional units called compartments. This is where system theory and ecological principles interact to produce a good model. To make advances in ecosystem ecology, we must understand ecosystem level behaviour and laws; we must be able to specify organisms, level dynamics and finally identify the statistical formalisms connecting the two.

A model should therefore be cautiously formulated to include all available information, consisting of data as well as knowledge of ecological processes. The approach usually taken by lake ecosystem modelers is to develop a model in state space. The components of the lumped model, also called compartments, are the state variables. These variables describe observable and unobservable ecological components. Their behaviour depends only upon their present state and the inputs from the environment at that time. As such, the models are *memory-less* (no time delays are included) and *non-anticipatory* (the system does not anticipate future inputs). Since the lake behaves as a system, each state variable influences all others directly or indirectly. Relationships between variables are the most important in determining the system behaviour. There is a *causal* relationship among the state variables.

Formally the model is set up as a system of ordinary, or partial, linear, or nonlinear, differential, or difference, equations. Each equation represents the behaviour of a state variable (or compartment). Thus, each compartment is modeled by a theoretically derived mechanistic model. Random (stochastic) influences are usually not included for the modeling *per se*, but may be used during model *verification* (testing that the model behaves as expected) and *validation* (testing that the model describes some experimental observations). The simulation is accomplished numerically by solving the equations on a computer. Analytical solution of the equations is usually not possible because of the model complexity which makes the solution mathematically

intractable. Thus, the five elements that are necessary for modelling and simulation are:

- The Real System
- The Experimental Frame
- The Base Model
- The Lumped Model
- The Computer.

Once these five elements are present and a goal for the simulation exercise has been set, then we face the problem of testing that the lumped model is an adequate representation of the real system and it abides by the hypotheses that have been formulated. Stages of analysis are commonly employed in system modeling. They are the verification and validation stages.

Model Verification and Calibration

During this stage of model testing, it is important to check if the model behaves as expected on the basis of theoretical considerations. In the first instance, this stage is not concerned with a specific set of data but rather with a general pattern of observed behaviour of a lake. For example, phytoplankton is expected to grow in spring and summer, while soluble reactive phosphorus is being utilized. The model should be in equilibrium; no wild oscillations should be observed which lead to the extinction of one or more components. The ecosystem is quite stable, and so the model should be. Model verification was defined by Mirham (1972): "The model's responses are compared with those which would be anticipated if indeed the model's structure was prepared as intended." Thus, this stage consists of debugging tests which are designed to locate logical faults in the model's structure. The model is then calibrated by comparison with a set of observations from the particular system under consideration.

Model Validation

This stage is concerned with establishing the verisimilitude of the responses from the verified model by comparison with independent sets of observations, either from the same lake under different conditions

or from a different lake (Mirham, 1972). A complete validation could be accomplished if concomitant experiments on the model and on the real system were made. However, in many instances, this experimentation is not feasible, as for example, producing a strong perturbation in the loadings into Lake Ontario. This means that only a partial validation can be done with the available observations, and therefore modelers should be aware of the consequences that will probably follow from a haphazardly constructed and invalidated simulation model. Another factor that must be considered is whether it is appropriate to compare the response arising from a deterministic model with a set of corresponding observations made on a complex, stochastic system (e.g., a lake).

Chapter 2

SEASONAL ANALYSIS AND SIMULATION

2.1 Biochemical Observations (IFYGL)

During the period April 1972 to March 1973, the most comprehensive chemical, physical, and biological study ever undertaken in the history of Lake Ontario was implemented as a joint program by Canada and the United States of America. For the purposes of this chapter of the report, three components of the biology-chemistry program will be discussed.

Biochemical Data

The primary data set that is used in this investigation was obtained from a program entitled "Ontario Organic Particle Study" (OOPS), which assessed 32 stations in the lake on nine surveys covering the period considered in this chapter, April 72 to March 73. A second phase of the OOPS program consisted of two time-series stations, one nearshore and one open water. Samples were obtained every four hours for 48 hours at 5-m intervals to a depth of 20 m, and at 40-m intervals to the lake bottom. Analysis and interpretation (Stadelmann and Fraser, 1974) consisted of vertical linear interpolation of transects across the lake, followed by horizontal interpolation, to yield mass contents by segment and thus volume-weighted concentrations for individual parameters.

Nutrients under study consisted of three phosphorus forms - total phosphorus, total filtered phosphorus, and soluble reactive phosphorus; and four species of nitrogen - total particulate nitrogen, ammonia nitrogen, nitrate plus nitrite nitrogen, and total filtered nitrogen. Particulate organic carbon, chlorophyll a, primary production, phytoplankton, zooplankton, and ATP analyses were also major parameters under study. Details of this latter group of data can be found in the following: Stadelmann and Munawar (1974); Vollenweider, Munawar, and Stadelmann (1974).

Interface areas, layer volumes, and other dimensions of Lake Ontario are given in Table 2.1.1. Volume-weighted lake-wide means of the OOPS data are presented in Table 2.1.2 for three layers, - 0-20 m,

20-40 m, and 40 m-bottom. Volume-weighted mean values for the whole lake are presented in Table 2.1.3. Figure 2.1.1 shows the OOPS station pattern, while Figures 2.1.2-4 display the data of Table 2.1.2. In these figures the upper layer is denoted by circles, the middle layer by triangles and the bottom layer by squares.

TABLE 2.1.1: *Lake Ontario dimensions*

Areas ($10^{10}m^2$)		Volumes ($10^{10}m^3$)	
Surface	1.85	0 - 20 m	34.8
20 m	1.61	20 - 40 m	29.6
40 m	1.35	40 m - bottom	101.3
		Total	165.7

Length: 300 km Width: 70 km Maximum depth: 230 m

Typical thermocline depth: 15 - 20 m
Niagara River - St. Lawrence flow: $22.10^{10}m^3$/year

TABLE 2.1.3: *Whole lake contents (10^3 tons)*

	Apr 72 10-14	May 72 23-27	Jun 72 19-23	Jul 72 17-21	Sep 72 5-9	Oct 72 17-21	Nov 72 20-23	Jan 73 9-12	Mar 73 6-8
SRP	23.0	20.5	15.9	15.6	14.8	16.8	17.8	24.7	24.9
SOP	6.2	7.0	8.6	8.3	8.7	7.0	9.8	9.2	9.7
TPP	8.7	7.9	9.4	7.9	9.1	6.4	6.6	5.3	5.0
Total P	37.9	35.4	34.0	31.8	32.6	30.2	34.2	39.2	39.5
$NO_2 + NO_3$	387	389	369	329	346	335	406	338	424
NH_3	9	9	15	35	14	21	15	14	12
SON	199	218	186	282	128	291	85	390	166
TPN	49	53	76	89	69	55	33	33	37
Total N	644	669	646	735	557	702	539	775	639

TABLE 2.1.2: Mean Concentrations by Layers (µg/ℓ)

		10-14 APR 72	23-27 MAY 72	19-23 JUN 72	17-21 JUL 72	5-9 SEP 72	17-21 OCT 72	20-23 NOV 72	9-12 JAN 73	6-8 MAR 73
SRP	0-20 m	12.0	10.1	4.8	1.9	1.5	5.1	7.7	13.9	13.9
	20-40 m	12.7	11.2	7.8	5.6	5.9	5.7	8.2	14.2	14.3
	40-bottom	14.4	13.1	11.4	12.7	12.0	12.7	12.1	15.0	15.1
SOP		3.8	4.8	6.4	8.2	5.8	5.0	5.9	6.1	6.2
		3.7	4.6	5.1	5.3	4.5	4.7	5.7	5.8	5.8
		3.6	3.7	4.7	3.6	5.1	3.7	5.8	5.1	5.6
TPP		7.3	6.2	9.4	8.6	9.8	5.7	4.4	4.5	4.0
		6.1	5.1	6.1	5.1	4.7	5.1	4.2	3.9	3.6
		4.1	4.0	4.1	3.3	4.1	2.8	3.7	2.4	2.4
$NO_2 + NO_3$		233	217	143	44	48	151	207	209	254
		231	227	213	182	194	161	213	203	249
		227	236	245	248	259	224	259	196	251
NH_3		7.0	5.6	7.0	21.0	13.2	16.5	8.8	8.3	7.8
		4.9	5.8	10.8	25.8	10.2	15.2	10.0	10.0	6.8
		5.0	5.0	8.6	18.8	6.3	10.5	8.1	7.8	7.0
SON		115	125	120	173	118	170	48	231	104
		118	127	112	155	82	186	52	237	103
		119	130	106	169	61	170	50	229	94
TPN		39	43	95	121	88	47	26	20	20
		34	34	49	52	37	41	23	20	28
		24	27	27	30	26	25	16	19	21
TPC		225	232	499	607	619	357	192	166	139
		200	186	271	290	256	314	175	157	135
		173	151	158	200	208	221	140	147	109
Chl a	0-20 m	2.9	3.4	5.0	5.7	4.8	3.0	1.9	.9	1.6
	20-40 m	2.7	3.0	2.7	2.8	1.3	2.6	1.6	.8	1.5
Zoopl	0-50 m	5	8	19	223	152	79	43	20	11

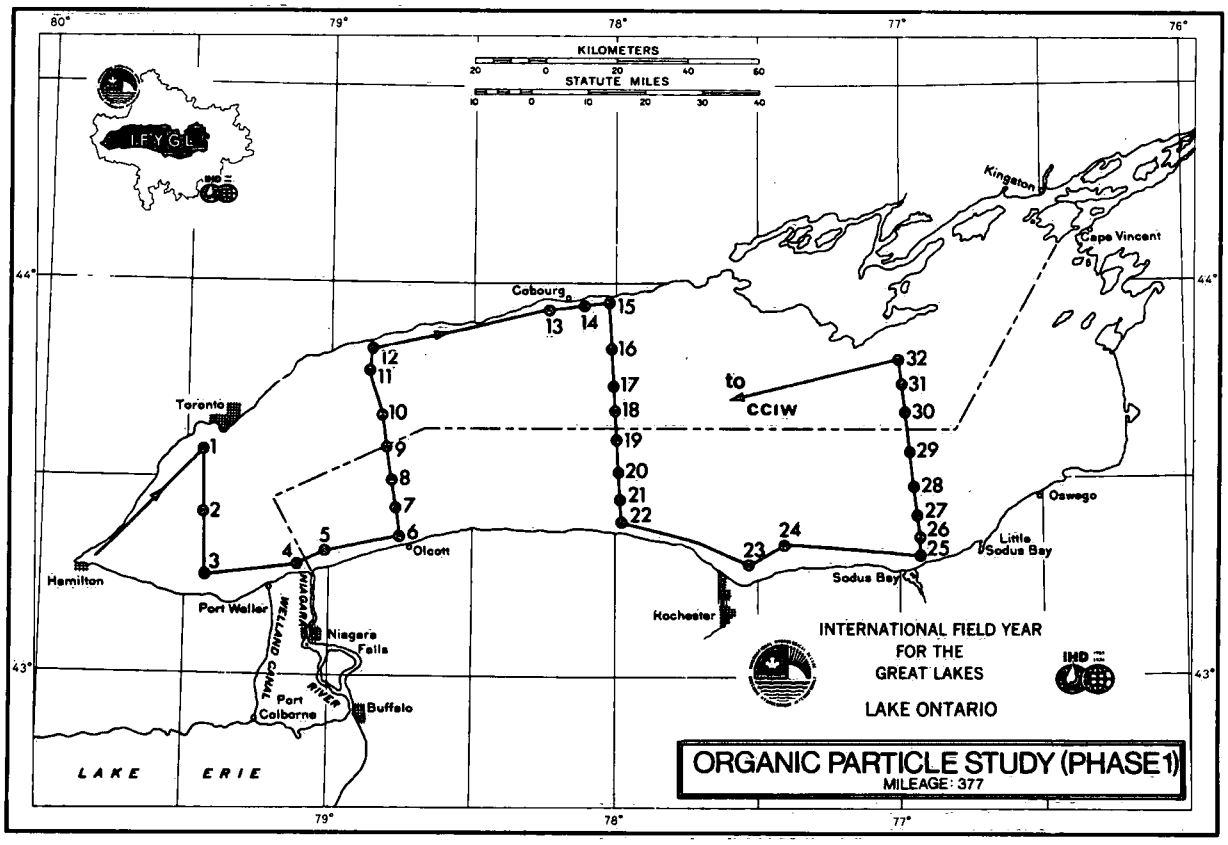

Figure 2.1.1 OOPS station pattern in Lake Ontario

As part of the nine OOPS cruises, zooplankton samples were collected at 32 stations by vertical hauls with a towed net, 40 cm in diameter at the mouth, two metres long, constructed of 64 (aperture) Nitex screening (Watson, 1978). Samples were taken to a depth of 50 m in deep water and to two metres from the bottom in shallower water. Species composition and abundance were estimated from subsamples and the values were converted to water column concentrations as numbers per volume. Numbers were converted to biomass as dry weight per volume by estimating specific weights of individual organisms. The total zooplankton biomass, averaged over the whole lake, is included in Table 2.1.2 and Figure 2.1.4, in units of mg dry weight/m^3. The detailed data set may be obtained from Dr. N. Watson at CCIW. To convert biomass dry weight to carbon, Watson *et al* (1975) derived a conversion factor of 0.41.

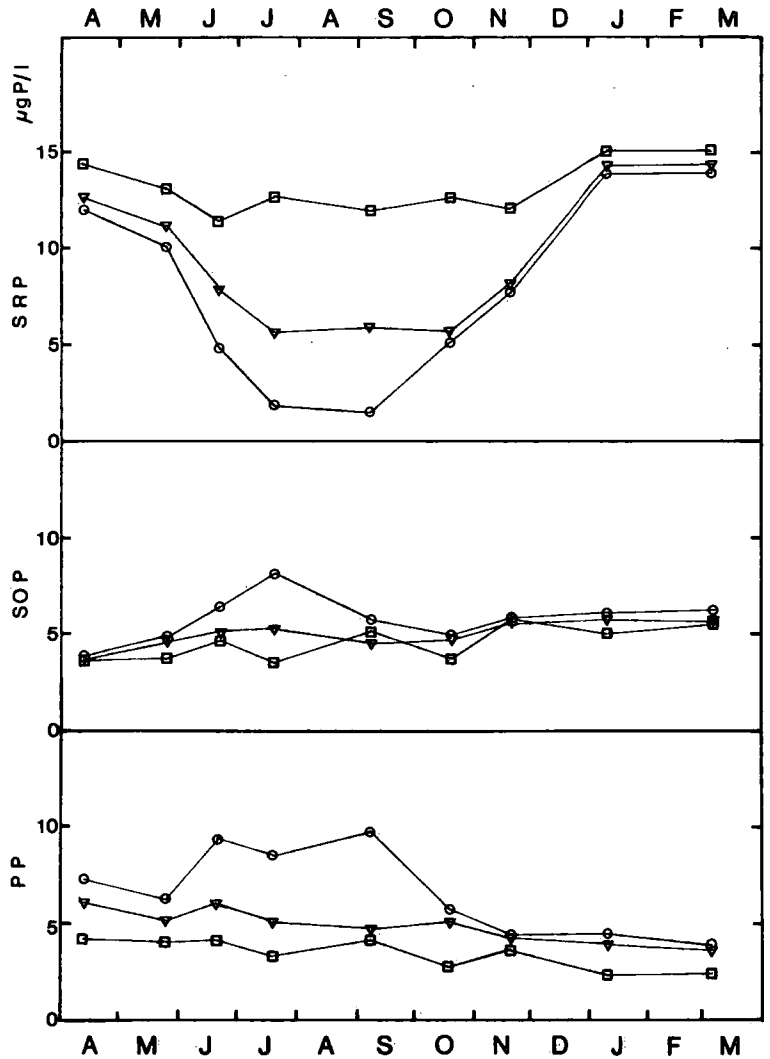

Figure 2.1.2 Mean concentrations of soluble reactive phosphorus (SRP), soluble organic phosphorus (SOP), particulate phosphorus (PP), by layers. Concentrations are µg P/ℓ. Circles denote 0-20 m; triangles, 20-40 m; and squares, 40 m to bottom.

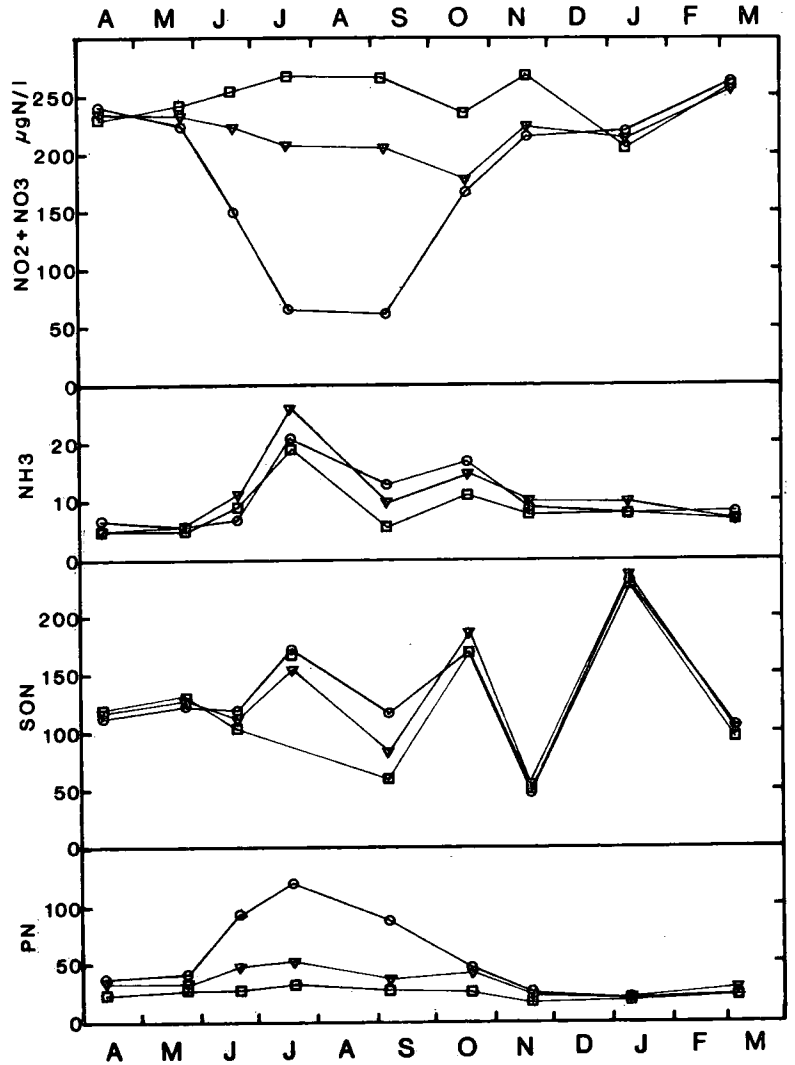

Figure 2.1.3 Mean concentrations of nitrite plus nitrate (NO_2 + NO_3), ammonia (NH_3), soluble organic nitrogen (SON) and particulate nitrogen (PN); µg N/ℓ.

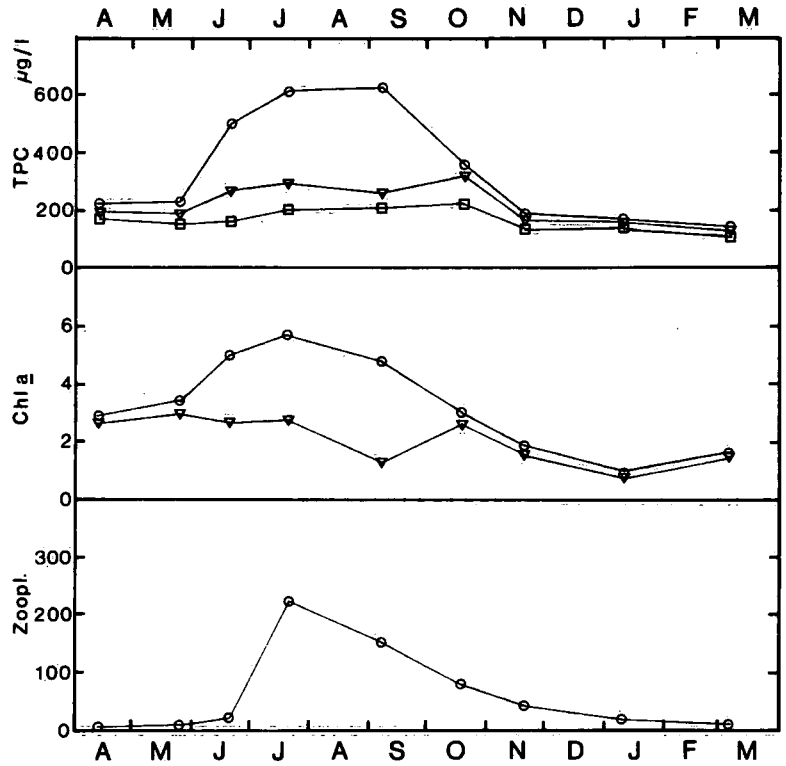

Figure 2.1.4 Top: total particulate carbon (TPC) in µg C/ℓ, as in Fig. 2.1.2. Middle; chlorophyll a in µg/ℓ for 0-20 m (circles) and 20-40 m (triangles). Bottom; zooplankton, 0-50 m, in µg dry weight/ℓ.

Nutrient Loadings

A comprehensive study of major component loadings from all sources was undertaken during the IFYGL. Data were gathered by the U.S. Environmental Protection Agency and the Ontario Ministry of the Environment. A study including the major and minor tributary sources (Casey and Salbach, 1974) provided preliminary loading information which was subsequently detailed by Fraser, Casey and Clark (1977). Total phosphorus loadings were estimated to be 49.6 t/day as the mean monthly figure for the period April 1972 to March 1976. Loading information of this type for the following parameters - total phosphorus, soluble reactive phosphorus, soluble organic phosphorus, particulate phosphorus, total nitrogen, filtered nitrate plus nitrite, filtered ammonia, total organic nitrogen, and total organic carbon - are detailed in Tables 2.1.4-6.

TABLE 2.1.4 Monthly Mean and Mean Monthly Loadings to Lake Ontario (t/D)

	Soluble Reactive P			Soluble Organic P			Particulate P			Total Phosphorus		
MONTH	GROSS INPUT	ST. LAWR. OUTPUT	NET LOAD	GROSS INPUT	ST. LAWR. OUTPUT	NET LOAD	GROSS INPUT	ST. LAWR. OUTPUT	NET LOAD	GROSS INPUT	ST. LAWR. OUTPUT	NET LOAD
APR 72	-	-	-	-	-	-	-	-	-	57.2	20.7	36.5
MAY	12.9	2.4	10.5	-	11.5	-	-	5.9	-	42.1	19.8	22.3
JUN	14.1	3.5	10.6	-	8.9	-	-	9.3	-	53.8	21.7	32.1
JUL	12.7	8.1	4.6	7.0	13.8	-6.8	28.4	5.2	23.2	48.1	27.1	21.0
AUG	10.9	4.5	6.4	12.1	11.4	0.7	17.8	17.7	0.1	40.8	33.6	7.2
SEP	10.3	1.9	8.4	2.7	12.8	-10.1	20.8	7.6	13.2	33.8	22.3	11.5
OCT	11.7	1.8	9.9	6.6	14.3	-7.7	16.2	0.8	15.4	34.5	16.9	17.6
NOV	15.1	2.1	13.0	2.6	10.9	-8.3	29.3	2.8	26.4	47.0	15.8	31.2
DEC	21.3	4.1	17.2	12.5	13.2	-0.7	35.0	-4.0	39.0	68.8	13.3	55.5
JAN 73	16.6	4.1	12.5	25.4	6.2	19.2	6.1	2.6	3.5	48.1	12.9	35.2
FEB	14.9	6.5	8.4	15.2	8.4	6.8	19.6	5.5	14.1	49.7	20.4	29.3
MAR	19.2	9.3	9.9	-	16.5	-	-	-0.4	-	70.7	25.4	45.3
MEAN	14.5	4.4	10.1	10.5	11.6	-0.9	21.7	4.8	16.9	49.6	20.8	28.7

TABLE 2.1.5 Monthly Mean and Mean Monthly Loadings to Lake Ontario (t/D)

	Nitrate Plus Nitrite			Filtered Ammonia			Total Organic Nitrogen			Total Nitrogen		
MONTH	GROSS INPUT	ST. LAWR. OUTPUT	NET LOAD	GROSS INPUT	ST. LAWR. OUTPUT	NET LOAD	GROSS INPUT	ST. LAWR. OUTPUT	NET LOAD	GROSS INPUT	ST. LAWR. OUTPUT	NET LOAD
APR 72	273.6	100.0	173.6	114.4	3.3	111.1	197.0	95.1	101.9	584.9	198.4	386.5
MAY	246.8	158.5	88.3	95.8	4.4	91.4	176.5	90.8	85.7	519.1	253.7	265.4
JUN	345.1	82.6	262.5	134.8	12.5	122.3	167.1	76.1	91.0	577.5	171.2	406.3
JUL	257.0	222.5	34.5	103.7	29.2	74.5	176.1	168.8	7.3	536.8	420.5	116.3
AUG	180.6	169.7	10.9	98.8	32.8	66.0	171.4	120.4	51.0	450.8	322.9	127.9
SEP	91.1	30.0	61.1	78.0	13.0	65.0	151.6	198.3	-46.7	320.6	241.3	79.3
OCT	117.3	60.3	57.0	86.9	11.3	75.6	124.9	186.6	-61.7	329.1	258.2	70.9
NOV	233.7	90.9	142.8	170.6	11.1	159.5	125.4	106.4	19.0	529.7	208.4	321.3
DEC	283.3	108.2	175.1	126.7	13.0	113.7	207.5	93.3	114.2	617.5	214.5	403.0
JAN 73	287.9	136.2	151.7	97.4	19.2	78.2	156.6	79.9	76.7	542.9	235.3	307.6
FEB	251.5	181.7	69.8	83.2	26.5	56.7	175.6	103.6	72.0	510.3	311.8	198.5
MAR	355.7	258.4	97.3	126.3	36.4	89.9	199.2	96.0	103.2	681.2	390.8	290.4
MEAN	243.6	133.3	110.4	109.7	17.7	92.0	169.1	117.9	51.1	516.7	268.9	247.8

TABLE 2.1.6: *Total organic carbon; Monthly mean loadings to Lake Ontario (tons/day)*

Year	Month	Gross Input	St. Lawrence Output	Net Load
1972	Apr	3673.5	1666.8	2006.7
	May	3954.0	1921.0	2033.0
	Jun	3931.8	2603.9	327.9
	Jul	3111.6	1894.4	1217.2
	Aug	3791.1	2232.8	1558.3
	Sep	3217.7	3319.9	-102.2
	Oct	3276.9	3562.1	-285.2
	Nov	3623.8	1935.0	1688.8
	Dec	4096.6	813.2	3283.4
1973	Jan	3067.5	651.3	2416.2
	Feb	2848.1	1001.9	1846.2
	Mar	3860.0	641.8	3218.2
	Mean	3454.4	1853.7	1600.7

The loading figures are compiled for direct municipal and industrial sources, major and minor tributaries including the Niagara River, as well as atmospheric precipitation and deposition. Consideration was also given to inputs from shore erosion and from groundwater, but the latter were not considered to be significant.

Materials Balance

A major component of the lake assessment program during IFYGL was the development of a materials balance (Fraser, Casey and Clark, 1977). The strategy developed for the materials balance program consisted of 11 major cruises (seven by U.S. ships and four by Canadian ships). On the cruises which involved Canadian vessels the standard analysis procedures used were those used in the U.S. program. The station distribution consisted of 105 open lake stations spanning the entire lake. Samples were obtained at depths of 5, 10, 15, 20, 25, 30, 40, 50, 100, 150, and 200 metres at all stations qualified by the bathymetry.

Over the same period of time the previously discussed OOPS cruises, specifically designed to identify limnological processes in the lake, were undertaken by the CCIW on the Canadian vessel,

M.V. Martin Karlsen. The chemical analysis procedures used for these cruises are fully documented in two publications, Traversy (1971), and Philbert and Traversy (1973) and will not be elaborated further here. While the primary purpose of these cruises was not the collection of data for use in the materials balance calculations, circumstances related to the quality of the U.S. data necessitated the extensive use of this Canadian data set.

A materials balance for a water body requires an assessment of the inputs and outputs, and the storage within the system for specified variables. The differences between the content of the lake at the beginning and end of any time period (one year in this case) is directly related to gains to and loss from the system. The inputs to the system are tributary inflow, direct municipal and industrial input, atmospheric input, groundwater inflow, and sediment resuspension. The outputs are outflowing streams, evaporation and sedimentation.

A materials balance can be used also to indicate the reliability of sampling regimes and representative qualities of the data. Evaluation of the primary data set produced from the 11 U.S. materials balance cruises has uncovered several severe problems in data quality. Although the analytical procedures followed are those widely accepted by the scientific community, there are indications that certain measurements are in error.

Robertson *et al.* (1974) have examined the chemical reliability of laboratories participating in the IFYGL program. Their findings indicated that the three prime laboratories contributing to this study produced statistically significant differences in results for 50% of the parameters when analyzing aliquots of the same standard sample. A similar test using aliquots of a sample of water from Lake Ontario showed significant differences among the three laboratories for 66.7% of the measurements. Robertson *et al.* conclude that a "substantial bias is usually introduced into data sets if they are composed of results from more than one laboratory".

Another study (Boyd and Eadie, 1977) examined the quality of data for 12 parameters sampled during the open lake phase of the study. On the basis of statistical tests and comparisons with data from CCIW,

they concluded that large parts of the U.S. IFYGL chemical data set were of poor quality. Their analyses revealed that only data for total organic carbon, one out of twelve parameters assessed, was usable in its present form. Total filtered ammonia, filtered nitrate plus nitrite, total phosphorus, total calcium, and soluble reactive silicate were "usable with some editing". Total alkalinity, pH, total Kjeldahl nitrogen, and total filtered phosphorus were "marginally useful after editing". Soluble reactive phosphorus and filtered sulphate were deemed "suspect".

In addition to these evaluations, there are internal inconsistencies in the data set which point to its own unreliability. In the case of the total filtered phosphorus, the reported value is frequently greater than the value of total phosphorus reported for the same sample. Similarly, values for total filtered ammonia were at times greater than the values for total Kjeldahl nitrogen, which represents organic nitrogen plus ammonia. This kind of discrepancy is indicative of analytical error or contamination.

A procedural problem which was discovered during the evaluation of the data involved the method of sample preparation for the analysis of soluble reactive phosphorus. The documented method used involved shipboard filtering followed by freezing of the filtrate and transport to the shore laboratory for analysis. The freezing of reactive phosphorus samples for later analysis produces a concentration result approximately 25% below the concentration obtained if the analysis is done immediately after sample acquisition (Philbert, 1973).

The data obtained from the seven (OOPS) Canadian lake process cruises did not suffer from the data quality problems encountered on the materials balance cruises and therefore, although the station distribution was somewhat weak for whole lake integration, the data have been used to form the basis of the balance.

Examination of the behaviour of the data and balance components and consideration of previous discussion related to data quality and associated seasonal variance led to the decision to reject the EPA data set and to substitute the Canadian process-oriented data sets (OOPS) for the computation of the empirical content figures in five out of the eight balance parameters. The three parameters for which U.S. data were used

are: total Kjeldahl nitrogen, total organic nitrogen, and total organic carbon. Of these three, total organic carbon yielded favourable results and did not appear to have data quality problems. The other two parameters were not considered to be fully reliable from a data quality standpoint, but current information from the Canadian sources was not available for comparison. Total Kjeldahl nitrogen and TON were therefore not assessed.

Thus, for the purposes of providing detailed loadings input information for the models the entire joint Canadian/U.S. data set is employed. However, the seasonal variations in lake conditions upon which verification studies are based rely almost singularly upon the Canadian process study data obtained under the OOPS strategy.

As an example of the results obtained from the development of the materials balance the case for total phosphorus is cited. The concentration of total phosphorus in the water column is of particular importance to biological systems in Lake Ontario. Large-scale remedial programs for phosphorus loading abatement are in place in the Lower Lakes basins for the purpose of controlling the excessive development of phytoplankton. Over the balance period for Canadian data (April 10, 1972 - April 10, 1973) the empirical content of total phosphorus (as P) increased by 5,650 metric tons. Over this same period the computed content, based on net loading increased by 10,550 metric tons (P). The balance yields a difference at the end of the period of 4,900 metric tons (P), which indicates a net storage of approximately 10% (Figure 2.1.5). Worthy of note is the parallel increase in both the computed and empirical content from December 1972 to April 1973, which implies an equilibrium situation between loading and lake content during the winter and spring for total phosphorus. The concurrent U.S. total phosphorus data produce lower values for content and become variable in the winter period, a situation most probably due to sample storage procedures and associated quality assurance problems.

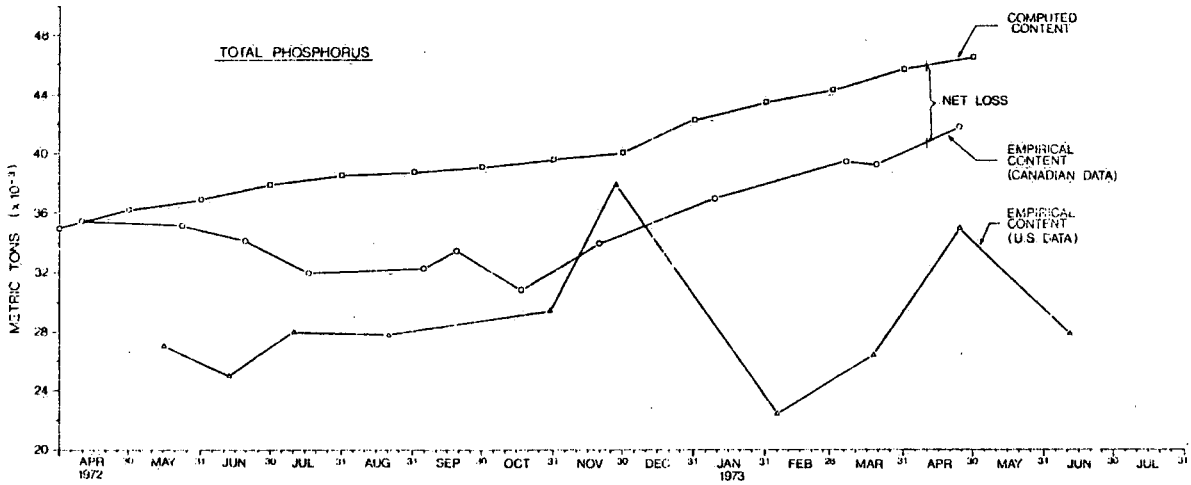

Figure 2.1.5 Lake content of total phosphorus observed by ship surveys ("empirical content") and carbon computed from loading data ("computed content).

2.2 Temperatures and Vertical Mixing

Temperatures

Throughout the 1972-73 field year (IFYGL), lakewide temperature measurements were made in Lake Ontario by ship surveys at weekly intervals. During each survey, EBT (electronic bathythermograph) profiles were taken in about 100 stations distributed evenly over the lake. All the EBT profiles taken during the 60-hour survey period were assumed to apply to a central time (centre of gravity of sampling times plotted along a time axis). Heat contents were computed for specified layers and zones by an algorithm which takes into account the horizontal distribution of sampling points and the depths of the profiles (Boyce *et al.* 1977). The corresponding temperatures represent weighted means of measurements at station locations. Figure 2.2.1 shows lake-wide mean temperatures during the period April 72-March 73 for three layers, 0-20 m (solid line), 20-40 m (dashed curve), and 40 m-bottom (dot-dash). The corresponding numerical values are presented in Table 2.2.1, where the first column indicates days reckoned from January 1, 1972. The data have been slightly smoothed in time by weighting adjacent cruises by the factors .25, .50, .25.

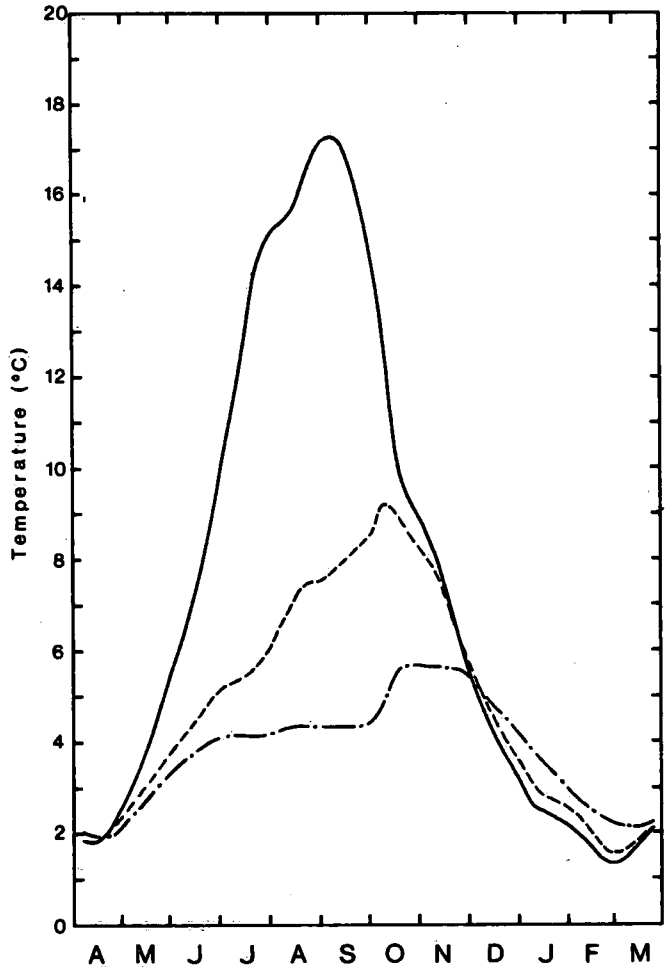

Figure 2.2.1 Temperatures, April 72 to March 73, for three layers, 0-20 m (solid line); 20-40 m (dashed); and 40 m-bottom (dot-dash).

Vertical Mixing

It is known that vertical mixing of water masses is enhanced by wind forcing, whereas stratification tends to inhibit mixing processes. Indeed, Kullenberg *et al.*(1973) found that it was quite possible to formulate vertical diffusion of materials as a function of temperature, wind and currents. For the spatial scales considered at present, vertical mass exchanges can be readily estimated from the heat budgets presented by Boyce *et al.*(1977). First, vertical heat fluxes through any imaginary level below the surface are deduced from heat content changes between consecutive ship surveys. Next, these fluxes are related to vertical temperature gradients to estimate exchanges of water masses or equivalent diffusion coefficients.

TABLE 2.2.1

Week	T(°C) 0	T(°C) 20	T(°C) B	E(m/day) 20 m	T(°C) 0	T(°C) 20	T(°C) 40	T(°C) B	E(m/day) 20 m	E(m/day) 40 m
96 - 102	1.9	2.0			1.9	1.9	2.0			
103 - 109	1.8	1.8			1.8	1.8	1.8			
110 - 116	2.1	1.9			2.1	2.0	1.9			
117 - 123	2.5	2.2			2.5	2.3	2.1			
124 - 130	2.9	2.4		5.52	2.9	2.6	2.3			
131 - 137	3.4	2.6		4.11	3.4	2.9	2.6		5.83	
138 - 144	4.1	2.9		3.14	4.1	3.2	2.9		3.89	
145 - 151	5.0	3.3		1.94	5.0	3.5	3.2		2.28	
152 - 158	5.8	3.5		1.19	5.8	3.9	3.4		1.41	4.76
159 - 165	6.6	3.7		0.80	6.6	4.2	3.6		0.96	3.07
166 - 172	7.5	3.9		0.69	7.5	4.5	3.8		0.82	2.74
173 - 179	8.6	4.2		0.56	8.6	4.9	4.0		0.67	1.94
180 - 186	9.8	4.3		0.20	9.8	5.2	4.1		0.24	0.57
187 - 193	11.3	4.4		0.00	11.3	5.3	4.1		0.00	0.00
194 - 200	12.9	4.4		0.02	12.9	5.4	4.1		0.02	0.00
201 - 207	14.2	4.4		0.08	14.2	5.6	4.1		0.09	0.08
208 - 214	15.0	4.5		0.15	15.0	5.9	4.1		0.17	0.31
215 - 221	15.3	4.7		0.22	15.3	6.4	4.2		0.26	0.50
222 - 228	15.5	4.9		0.20	15.5	6.9	4.3		0.24	0.35
229 - 235	15.9	5.0		0.07	15.9	7.3	4.3		0.08	0.02
236 - 242	16.7	5.0		0.00	16.7	7.5	4.3		0.00	0.00
243 - 249	17.2	5.0		0.00	17.2	7.5	4.3		0.00	0.00
250 - 256	17.3	5.1		0.07	17.3	7.7	4.3		0.08	0.07
257 - 263	17.0	5.1		0.09	17.0	8.0	4.3		0.12	0.02
264 - 270	16.3	5.2		0.00	16.3	8.2	4.3		0.00	0.00
271 - 277	15.3	5.3		0.25	15.3	8.5	4.3		0.36	0.36
278 - 284	13.6	5.7		0.84	13.6	9.0	4.7		1.44	1.41
285 - 291	11.4	6.2		0.90	11.4	9.2	5.3		2.14	1.67
292 - 298	9.8	6.4		0.00	9.8	8.8	5.7			0.45
299 - 305	9.2	6.3		0.00	9.2	8.4	5.7			0.00
306 - 312	8.8	6.2		0.00	8.8	8.1	5.6			0.00
313 - 319	8.2	6.1		0.00	8.2	7.8	5.6			0.26
320 - 326	7.4	6.0		0.00	7.4	7.1	5.6			0.22
327 - 333	6.5	5.8			6.5	6.4	5.6			
334 - 340	5.6	5.5			5.6	5.7	5.5			
341 - 347	4.9	5.1			4.9	5.1	5.2			
348 - 354	4.2	4.7			4.2	4.5	4.8			
355 - 361	3.8	4.4			3.8	4.1	4.5			
362 - 368	3.4	4.1		3.11	3.4	3.7	4.3		6.52	2.98
369 - 375	2.8	3.9		3.28	2.8	3.3	4.1		8.27	3.03
376 - 382	2.5	3.5		3.70	2.5	2.9	3.7		9.18	5.12
383 - 389	2.4	3.2		3.65	2.4	2.8	3.4		7.73	6.12
390 - 396	2.3	3.0		3.22	2.3	2.6	3.1		6.20	5.00
397 - 403	2.1	2.8		2.88	2.1	2.5	2.9		5.47	4.45
404 - 410	1.9	2.6		3.00	1.9	2.3	2.7		5.71	4.25
411 - 417	1.6	2.4		3.42	1.6	1.9	2.5		7.38	3.87
418 - 424	1.3	2.2		2.36	1.3	1.6	2.3		6.35	2.36
425 - 431	1.3	2.1			1.3	1.5	2.2			
432 - 438	1.5	2.1			1.5	1.7	2.2			
439 - 445	1.8	2.2			1.8	1.9	2.2			
446 - 452	2.0	2.2			2.0	2.0	2.3			
453 - 459	2.2	2.3			2.2	2.2	2.4			

It is not feasible to estimate exchange coefficients from heat budgets during unstable conditions, because the rapid rate of the convection process prevents the formation of significant temperature gradients. Fortunately, however, such conditions can be taken to result in complete mixing for the present purposes and hence it is only necessary to determine when instability occurs. At the start of the present calculations (April 72), the temperatures throughout the lake were approximately two degrees centigrade and surface heating resulted in unstable stratification until the temperature approached the value corresponding to maximum density (four degrees). Thus, at any point in the lake, a column of water was taken to be fully mixed from the bottom up to the highest level where the temperature was below this threshold value. The onset of fall overturning was defined by a reversal from downward to upward heat fluxes. In that case the water column was assumed to be fully mixed from the surface down to the lowest layer for which the heat flux was upward. As a result, stratification proceeds to ever-increasing depths in spring, with a similar behaviour during the overturning process in autumn.

Exchange Coefficients

Figure 2.2.2 presents downward heat fluxes per unit area at depths of 20 and 40 metres, together with the corresponding exchange coefficients, E, for a three-layer and a two-layer model, respectively. The latter are also shown in Table 2.2.1.

These calculations were done in the following manner. Consider a layer of water of volume V and average temperature T, bounded by two permeable interfaces. Let A_1 and A_2 be the areas of the upper and lower interface and F_1 and F_2 the downward heat fluxes per unit area at the respective levels. The heat balance equation of the layer is then

$$\frac{d}{dt}(TV) = F_1A_1 - F_2A_2 \qquad (2.2.1)$$

If t is given in days, T in degrees, V in m^3 and A in m^2, then the "heat" content is defined in deg. m^3 and the fluxes are in units of deg. m/day.

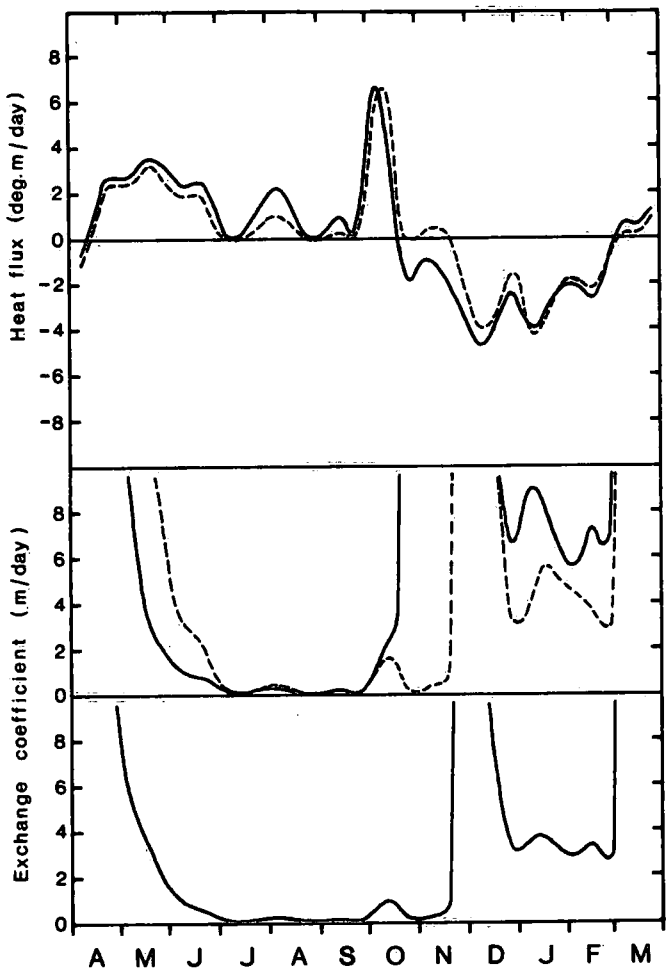

Figure 2.2.2 Top: downward heat flux per unit area at depths of 20 m and 40 m. Below: corresponding mass exchange coefficients for three-layer model (middle), and two-layer model (bottom). Solid lines represent the 20-m level and dashed lines the 40-m level. (See Table 2.2.1).

To convert to calories, both sides of the equation can be multiplied by the product of water density and specific heat, but this would only complicate the present calculations.

The left-hand side of (2.2.1) can be determined from weekly heat contents by layers. If it is assumed that there is no heat flux through the bottom, then the flux through the first interface above the bottom follows from (2.2.1) as it is applied to the lowest layer. The flux at the second level from the bottom follows then from the balance equation for the next layer and so on. The solid line at the top of Figure 2.2.2

shows the computed flux at 20 m, while the dashed line represents the flux at 40 m.

The mixing parameter can be defined in different ways such as a large-scale analogue of the molecular diffusion coefficient or a volume exchange per unit area. Since the present parameters will be used to estimate vertical mixing of chemical variables, it does not really matter which formulation is selected as long as the same convention is followed later on. Thus, we define the exchange coefficient, E, as the flux across an interface F, divided by the temperature difference between the two adjacent layers ΔT; that is

$$E = F/\Delta T \tag{2.2.2}$$

This coefficient has dimensions of a velocity (m/day) and its value depends on the layer structure adopted for the calculation. Table 2.2.1 presents the values of this parameter for a three-layer and a two-layer model, respectively. The three-layer results are displayed in the middle of Figure 2.2.2, the two-layer results at the bottom. The solid lines represent the 20-m level, the dashed line refers to 40 m. The following comments may be made concerning these results.

As mentioned before, the above expression cannot be used when ΔT approaches zero or when the flux is against the temperature gradient. These cases may be taken to represent complete mixing and therefore the corresponding coefficient should be assigned some appropriate value. In this case, a value of 10 m/day has been taken as an arbitrary upper limit. This is not meant to imply that all computed values below this limit are physically meaningful. For instance, the temperature differences during winter are so small that the numerical values of the exchange coefficients are quite uncertain. Thus they are included in the table mostly to illustrate the qualitative effects of inverse stratification.

The choice of the upper limit to the mixing coefficient is intimately connected with computational aspects of predictive models. To illustrate this, let us consider a two-layer model of Lake Ontario with subscript e denoting the epilimnion and h denoting the hypolimnion. Now (2.2.1) can be applied to each layer, whereby the left-hand side is

expressed in finite-difference form. If we ignore surface fluxes of heat and use a prime to denote the new temperature after time step Δt, then from (2.2.1)

$$T_e' = T_e - \Delta t.\ F.\ A/V_e \qquad T_h' = T_h + \Delta t.\ F.\ A/V_h \tag{2.2.3}$$

where F and A refer to the interface. Full mixing will be achieved in a single time step if $T_e' = T_h'$, that is

$$\Delta t.\ F.\ A \left(\frac{1}{V_e} + \frac{1}{V_h}\right) = T_e - T_h \tag{2.2.4}$$

Thus, with (2.2.2), the full mixing condition becomes

$$\Delta t.\ E = \frac{V_e\ V_h}{A(V_e + V_h)} \approx \Delta Z_e \frac{V_h}{V_e + V_h} \tag{2.2.5}$$

Substituting appropriate values for Lake Ontario with a thermocline depth of some 20 metres, we find that the right-hand side of (2.2.5) is about 17 metres. On the other hand, for two adjacent layers of 20 m depth each, the value is 10 metres. Consequently, if we compute vertical mass exchanges with a time step of one day, an exchange coefficient of 10 m/day will result in instantaneous mixing. If the model time step were one week, the upper limit would be about 2 m/day. In effect, we will see in the following that the maximum values may be considerably below these technical upper bounds because even during mixing episodes there are noticeable vertical gradients of some nutrients in Lake Ontario.

As a final remark, it may be pointed out that the seasonal variations of the exchange coefficient are in perfect agreement with the nutrient observations shown in Section 2.1. Thus, the concentrations of the upper two layers become the same when the exchange coefficient at 20 m becomes indeterminate, but the gradients between the lower layers persist for at least another month. In this connection, it may be noted that the exchange coefficient for the two-layer model during this

particular period cannot be assigned a value corresponding to full mixing, because this would lead to complete mixing of the whole lake instead of the upper 40 metres only. Instead, the values obtained at the 40-m level of the three-layer model are probably a better approximation, if the coefficients are used in a predictive model. Examples of such predictions will be shown in Section 4.4.

Alternative Mixing Calculations

While the foregoing model leads to estimates of vertical mixing coefficients at any arbitrary interface, the most interesting question relates to the value of this parameter at the thermocline during the stratified season. The definition of thermocline depth necessitates a certain departure from objectivity. In this case we have sought to determine the isothermal surface which best coincides with the region of strongest density gradient (Boyce, 1978). We have taken EBT profiles for each cruise in digital form, sought the points on each profile where the density gradients were largest (exclusive of transients), and determined the temperature class into which each point fell. A histogram of relative frequency with which each temperature class is involved with the region of strongest gradient helps to define the "best" isothermal surface.

Figure 2.2.3 presents the large-scale vertical eddy conductivity at the level of maximum stability (thermocline) for the stratified season (June to December 1972) in Lake Ontario. The eddy conductivity, K, is defined as the vertical heat flux divided by the vertical temperature gradient, i.e.,

$$K = \frac{F}{\partial T/\partial Z} \qquad (2.2.6)$$

Missing values in Figure 2.2.3 indicate apparent negative conductivities caused by advective (reversible) transports. Boyce (1978) has related K to environmental parameters such as wind stress, stability of the water column, etc. The results are inconclusive with the exception of the observation that the wind stress parameter which best correlates with K_V is the peak eight hourly averaged wind stress within the cruise interval.

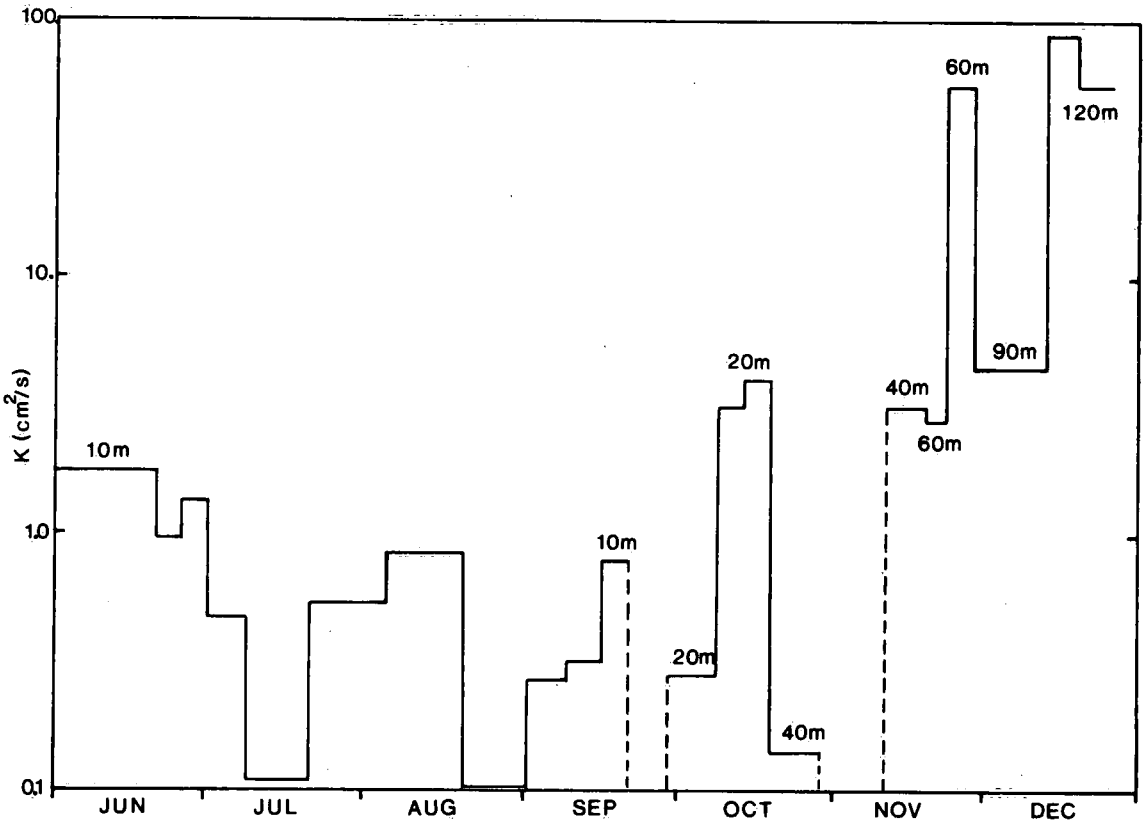

Figure 2.2.3 Vertical eddy conductivity at the level of maximum stability (thermocline), June to December, 1972.

Short strong wind impulses convey energy most efficiently to the surface current, and this we believe is the principal source of turbulent mixing energy at depth.

All the above computations of vertical mixing based on systems of horizontal layers are somewhat artificial because level surfaces are not surfaces of constant properties in a large lake. Furthermore, heat fluxes across fixed surfaces also take place due to changes in heat distribution (advection) and such fluxes cannot be parameterized in terms of mean gradients and diffusion coefficients. The result is as often as not, a meaningless negative eddy conductivity.

An alternative method of computing vertical transports has been suggested by Sweers (1969). In this scheme, the transport equation for heat is integrated through a subvolume of the lake comprising all the water having temperatures greater than or equal to a reference temperature θ_1. A stable thermal structure is assumed (monotonic mean temperature profile) as shown in Figure 2.2.4. The lower boundary of the subvolume is

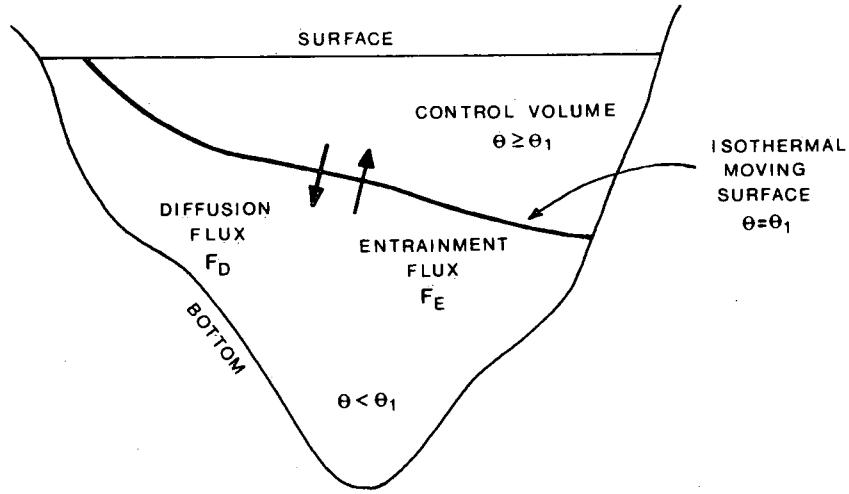

Figure 2.2.4 Sketch of diffusion/entrainment model.

the isothermal surface $\theta = \theta_1$. Large-scale motions are assumed to be parallel to surfaces of constant density/temperature hence the integrated transport equations retain terms expressing the storage of heat within the subvolume and its flux across the surfaces. The equation may be written

$$\underset{(1)}{\frac{1}{\rho C_p}\frac{\partial}{\partial t}\begin{bmatrix}\text{Heat content of}\\ \text{subvolume } \theta > \theta_1\end{bmatrix}} = \underset{(2)}{\theta_1 \frac{\partial}{\partial t}\begin{bmatrix}\text{Volume of}\\ \text{subvolume } \theta > \theta_1\end{bmatrix}}$$

$$- \underset{(3)}{\begin{bmatrix}\text{Total diffusive flux outward}\\ \text{across sfc } \theta = \theta_1\end{bmatrix}} - \underset{(4)}{\begin{bmatrix}\text{Net sfc heat flux across}\\ \text{upper sfc having } \theta_s > \theta_1\end{bmatrix}}$$

Terms 1, 2 and 4 can be measured; term 3 is evaluated as a residual. The ratio of term 3 to term 2 has special interest, since we anticipate it will be a minimum in the thermocline region. Moreover, the relative magnitude of the two terms should also indicate which of the two parameterizations of turbulent transport, eddy diffusivity or entrainment velocity, is most appropriate. Figure 2.2.5 is a diagram of the mean depth of selected isothermal surfaces as a function of time from July to October, 1972.

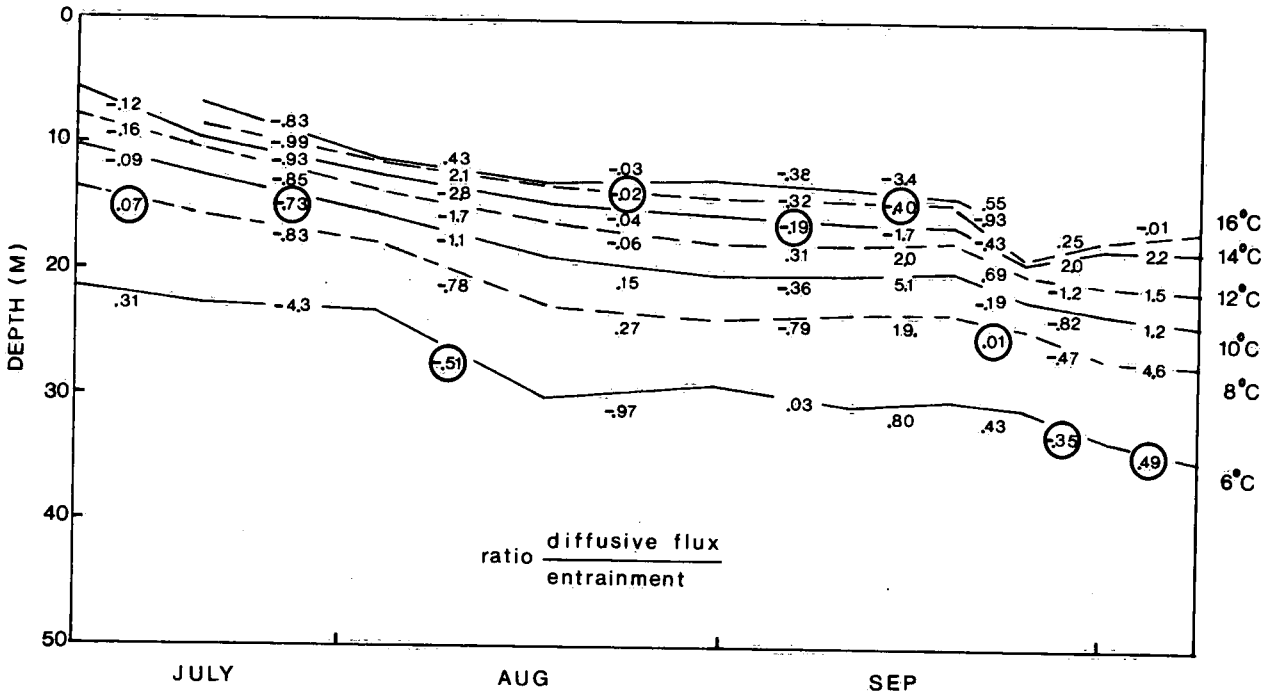

Figure 2.2.5 Mean depths of selected isothermal surfaces (temperatures denoted on the right), July to October 1972. Numbers in the figure denote ratio of downward diffusive transport of heat to the upward transport by entrainment. Circles mark maximum values.

The ratio of downward diffusive transport to upward transport of heat by entrainment is indicated by the numbers on the diagram. A mid-thermocline minimum is taken as evidence of a "diffusion floor".

Efforts to make the measured entrainment velocities fit laboratory models of entrainment strongly suggest that local wind stress (expressed as a friction velocity W_*) is not the most useful parameter. The entrainment or diffusion process seems more directly related to the velocity scale associated with the near surface currents.

Parameterizations of Large-Scale Processes

Two numbers relating to the energetics of lake circulation are simply calculated from the temperature distribution data, the baseline reference potential energy (RPE), and the available potential energy (APE) of the thermal stratification. The concept of APE is often used in the analysis of oceanic eddies wherein the difference in density profiles inside and outside the eddy is used to compute a potential energy which is theoretically "available" to fuel horizontal motion as the eddy

runs down. The reference baseline potential energy can be defined by $gM\overline{Z}$ where $\overline{Z}$ is the vertical distance of the centre of mass of the water column above a reference level, M is the mass of the water column (usually between two fixed levels) and g is the acceleration due to gravity. In the case of an oceanic eddy, the reference potential energy is defined in terms of the density profile obtained in a zone of presumed no motion relative to the eddy. In the lake we must take into account the closed nature of the basin; the reference state of the lake is that with all isothermal surfaces horizontal, a statically stable density profile, and the distribution of temperature with lake volume (conservation of heat) conserved. To compute this state, we calculate the volume of the lake occupied by a number of temperature classes, arrange their classes in order of increasing density, and then using the hypsometric curve for the basin, compute the depths of the surface separating the temperature classes. The change in potential energy from this state and that with the same mass/heat but with centre of mass of the centroid of the basin is a measure of the minimum amount of energy needed to mix the basin to vertical homogeneity. The variation of RPE and APE from May through December 1972 is shown in Figure 2.2.6.

Note the steady build and decay of RPE (one notable exception), while APE term is much more variable, being linked to winds and thermal stratification. A very simple dynamic model of this behaviour is proposed.

$$\frac{dP}{dt} = -\frac{P}{\tau} + \rho W_*^3(D^2) \qquad (2.2.7)$$

where ρW_*^3 = work/unit area/unit time done by wind

D = diameter typical of lake

τ = time scale $\simeq D/C$

c = internal wave speed

The model is not expected to work in spring and fall (large changes in RPE) but might have some validity in summer (provided the wind is not too strong - no violent mixing).

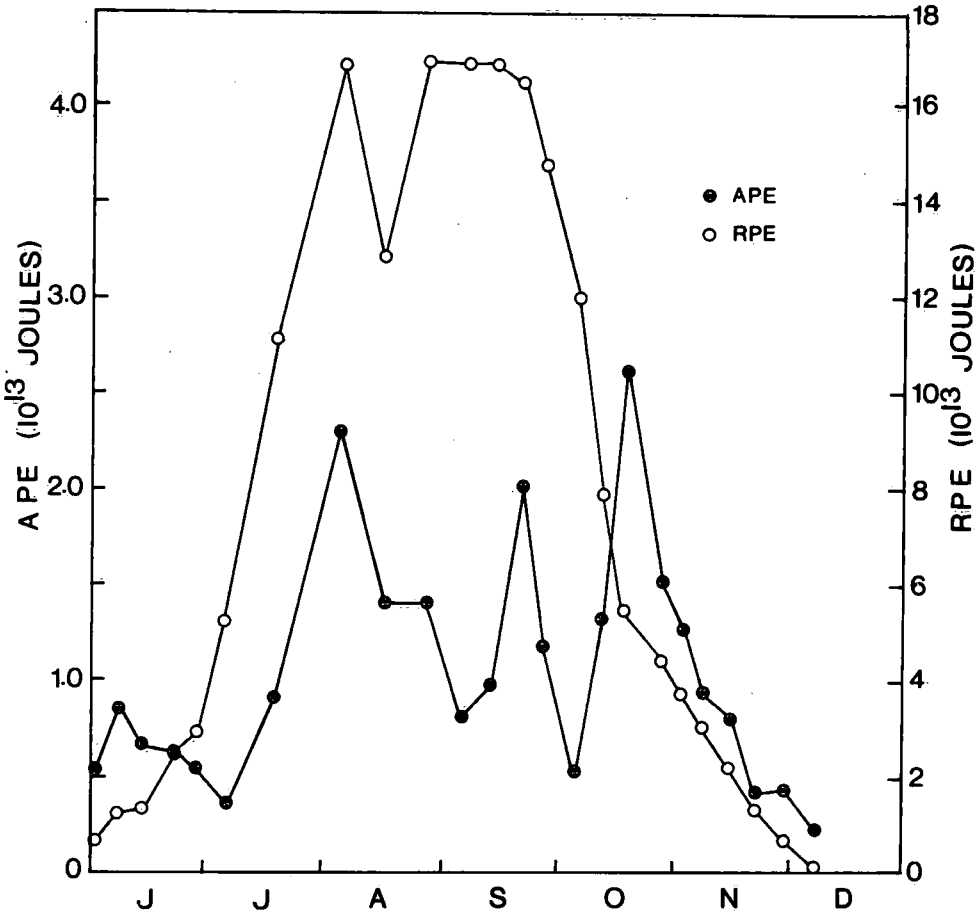

Figure 2.2.6 Reference potential energy (RPE) and available potential energy (APE), May through December, 1972.

A linear regression of the data cast in the form of the above model shows marginal statistical significance. The time scale is of the order of six days.

Accuracy of Heat Content Estimates

Boyce *et al.*(1977) have estimated the accuracy of the heat content computations which constitute the basis for the results presented in this chapter. The error band was estimated on the basis of a simple model

$$E = \frac{E_0(t)}{\sqrt{N}} + kT$$

where $E_0(t)$ = confidence limit for vertical integral of a single profile; includes instrument error and internal wave effects which are proportional to stratification.

N = number of stations.

T = duration of cruise.

k = taken to be small fraction of mean heat flux during cruise interval. (20%)

N & T related by ship's speed taking into account size of basin and time on station.

This model illustrates the necessity of a trade-off between the number of stations and the speed of execution of survey. Given speed of ship, station time and area of basin, a minimum E is found for certain $N = N_{opt}$ (Boyce *et al.* 1977). The model also illustrates the desirability of obtaining good estimates for the E_0 term, in particular for the contribution of internal waves seen as a high frequency noise contaminating the seasonal lake-wide pattern (Table 2.2.2). Figure 2.2.7 presents error estimates for lake-wide heat fluxes at the surface of Lake Ontario between consecutive cruises.

TABLE 2.2.2: *Sources of presumed random errors in heat content computations. Values expressed are the standard deviation from the mean of 100 stations.*

Source of error	Standard Deviation (cal/cm^2)	
	Summer Full Stratification	Winter Negligible Stratification
Internal Waves	± 132	± 50
Instrument Errors	± 200	± 100
Digitization of Temperature	± 50	± 25
Computation of Heat Content	± 160	± 100
Total (Root Sum of Squares)	± 290 cal/cm^2	± 150 cal/cm^2

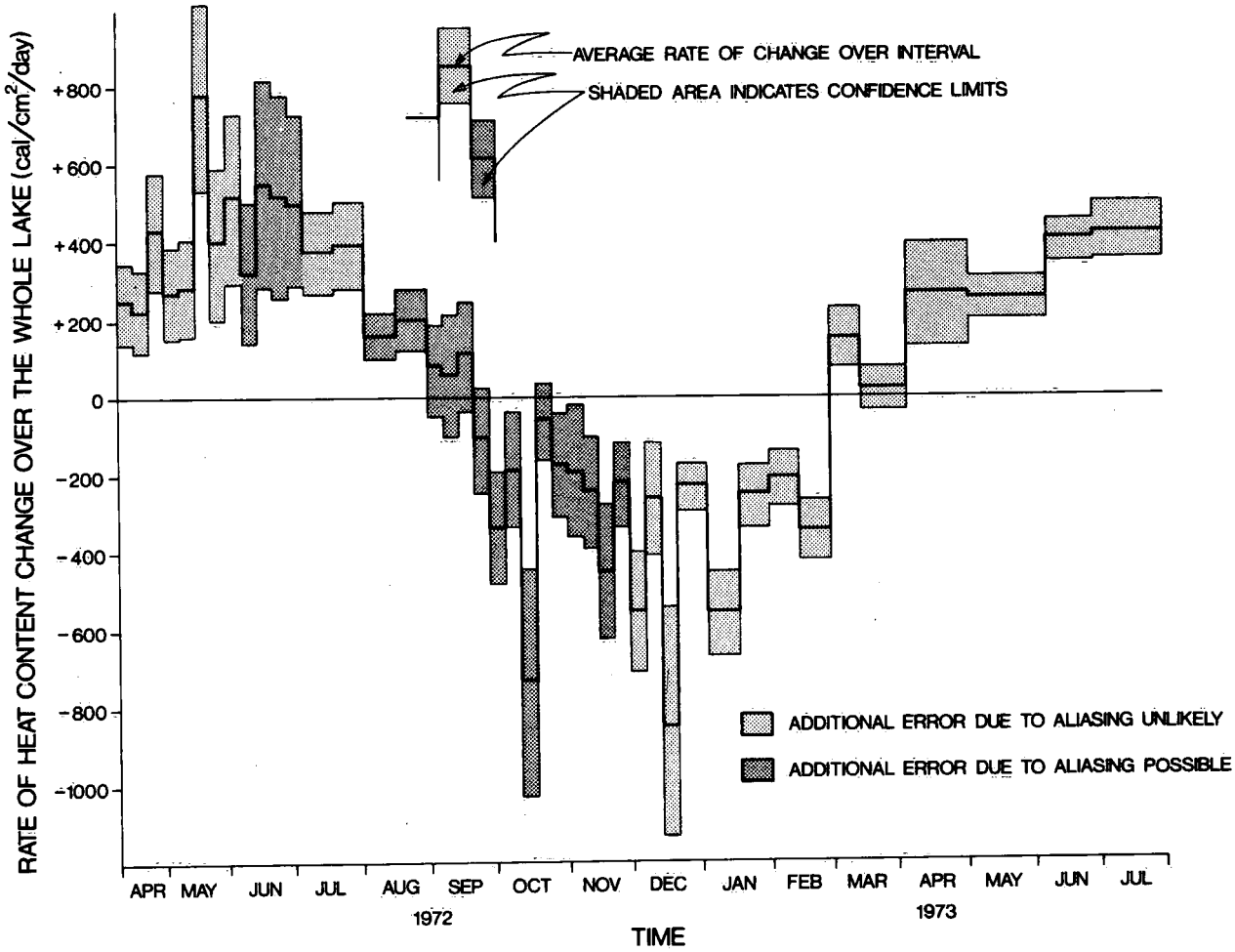

Figure 2.2.7 Error estimates for surface heat fluxes computed during IFYGL.

An alternate estimate of the accuracy of heat content measurements may be obtained by direct comparison with observed heat fluxes at the surface. During IFYGL, Lake Ontario surface fluxes of latent and sensible heat were measured, together with net radiation fluxes. Figure 2.2.8 compares the sum of these surface fluxes (circles) with the corresponding values obtained from changes in heat content between consecutive cruises (solid line). Figures 2.2.7 and 2.2.8 both suggest that estimates of heat fluxes from heat content measurements are surrounded by considerable uncertainty, even for the present high-resolution data base.

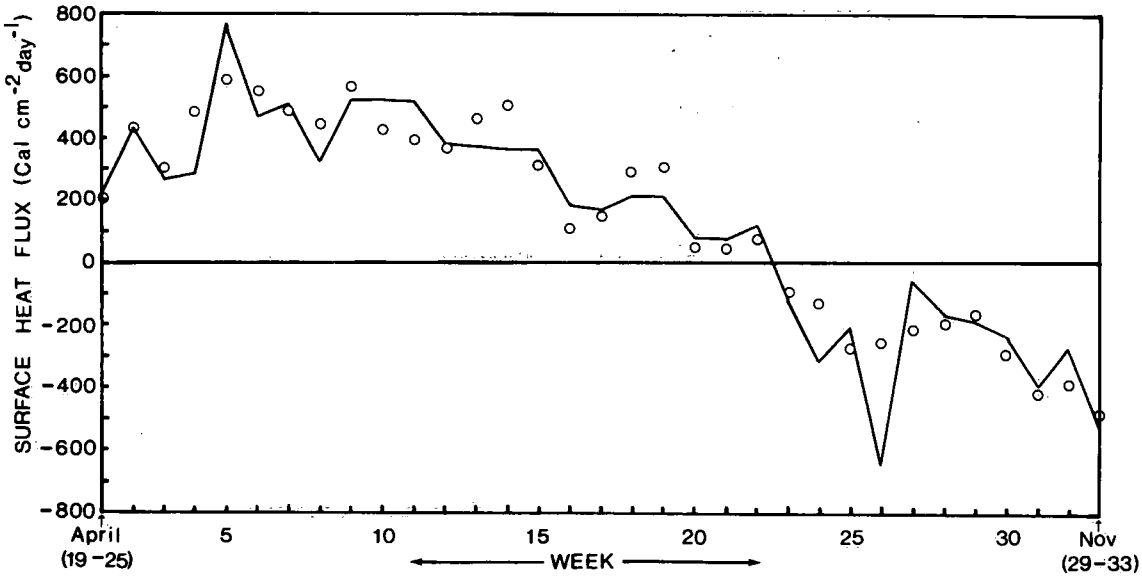

Figure 2.2.8 Measured surface fluxes (radiation, latent and sensible heat) denoted by circles, compared with fluxes computed from heat budgets (solid line), April to November, 1972.

2.3 Light and Primary Production

Radiation Measurements

Solar radiation fluxes were measured at eight stations on the perimeter of Lake Ontario, plus a few meteorological buoys on the lake (Davies and Schertzer, 1974). Daily mean values were interpolated to a 5-km grid covering the whole lake and then averaged over all grid points. The upper part of Figure 2.3.1 shows weekly ranges (vertical bars) and weekly means (black circles) of this lake-wide radiation during IFYGL. To estimate hourly radiation fluxes from daily mean values, a normalized distribution of radiation over a day was derived for each month on the basis of measurements at Burlington, Scarborough, Trenton, and Kingston. These distributions are shown in Table 2.3.1.

Optical measurements were taken on a number of ship cruises carried out during the 1972 Field Year on Lake Ontario (Thomson *et al.* 1974). A spectrometer was used to measure downwelling irradiance of sunlight in the 400-700 nm band and the resulting transmission curves permit estimates of extinction coefficients to be made. Where extinction coefficients are available only for the 500-nm wavelength, mean coefficients for the photosynthetic band were obtained by recourse to the

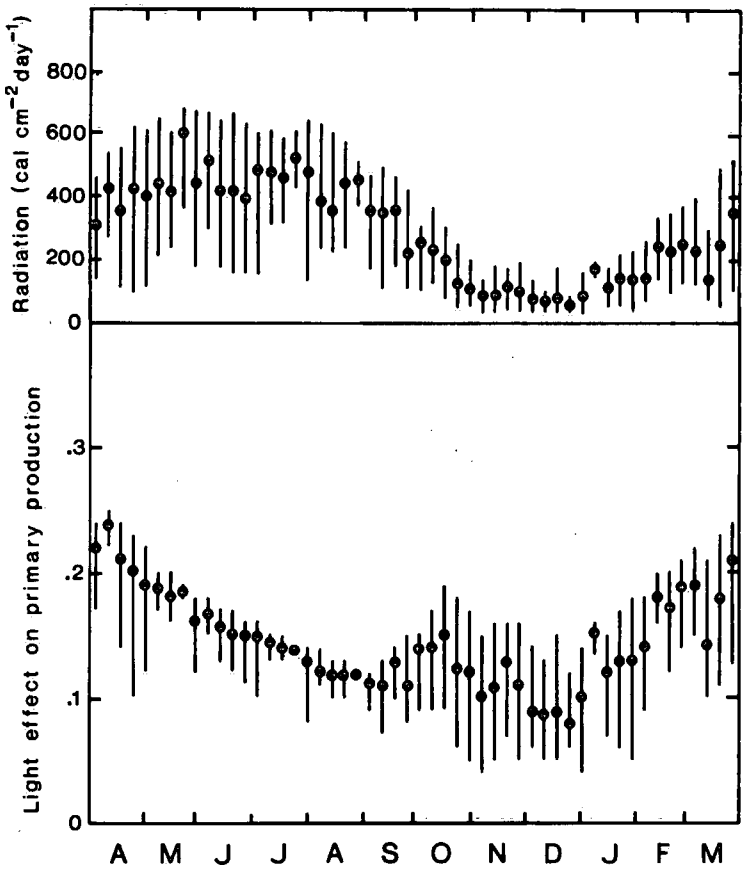

Figure 2.3.1 (top) Surface radiation during IFYGL year, weekly means and ranges. (bottom) Light effect on primary production, weekly means and ranges.

TABLE 2.3.1: *Hourly distribution of solar radiation (%) and mean extinction coefficient $\bar{\varepsilon}$ for Lake Ontario by months*

Month	Hour	6	7	8	9	10	11	12	13	14	15	16	17	18	19	$\bar{\varepsilon}$
Jan				1	5	10	15	18	18	15	11	6	1			.25
Feb				2	7	11	14	16	16	14	11	7	2			.25
Mar			1	3	8	11	13	15	14	13	11	7	3	1		.25
Apr		1	2	5	8	10	12	13	12	11	10	8	5	2	1	.30
May		1	3	5	8	10	11	12	12	11	10	8	5	3	1	.35
Jun		1	3	6	8	9	11	12	11	11	10	8	6	3	1	.40
Jul		1	3	6	8	10	12	12	12	11	9	7	5	3	1	.45
Aug		1	3	6	8	10	12	12	12	12	9	7	5	2	1	.50
Sep			2	4	7	10	12	14	14	12	11	8	4	2		.50
Oct			1	2	7	11	14	15	15	13	11	7	3	1		.25
Nov				1	6	11	16	18	17	15	10	5	1			.25
Dec				1	5	10	16	19	19	15	10	4	1			.25

linear relationship presented by Thomson *et al.* (1974). The measured light extinction can be related to algal self-shading and the resulting relationships can be incorporated in a photosynthesis model. This type of analysis will be carried out in Chapter 3.1 dealing with long-term observations on Lake Ontario. The present seasonal simulations (and the three-dimensional considerations of Chapters 4.1-4) rely on observed extinction coefficients which implicitly incorporate the self-shading effect. Lake-wide mean extinction coefficients for each month during IFYGL are shown in the last column of Table 2.3.1.

Surface radiation fluxes and extinction coefficients can be combined to estimate radiation as a function of depth. In turn, this must be related to the optimum light intensity for phytoplankton growth. Effects of light on photosynthesis have been reviewed by Vollenweider (1970) and Platt *et al.* (1975). A convenient formula was suggested by Steele (1965), namely, $r = R \exp(1 - R)$ where r is the relative photosynthesis and R is the solar radiation in the photosynthetic wave band expressed as a fraction of the saturation light intensity. In a homogeneous layer of water, the light intensity decreases with depth as $R = R_t \exp(-\varepsilon z)$ where R_t is the incident radiation at the top of the layer and ε is the extinction coefficient. Thus, Steele's function can be integrated immediately to give the depth-averaged relative photosynthesis for a layer

$$\rho = \frac{1}{\varepsilon\delta}(e^{1-R_b} - e^{1-R_t})$$

where R_b is the radiation passing through the bottom of the layer and δ is the layer thickness.

The light effect, ρ, was computed at hourly intervals from the IFYGL data base and then averaged over each day. It was estimated that 6% of the incoming radiation is reflected and that 48% of the net radiation is contained in the photosynthetically active 400-700 nm band. The saturation light intensity, referred to this band, was taken to be 4.75 cal/cm^2/hr by recourse to the light-effect curves presented by Stadelmann *et al.* (1974). The bottom of Figure 2.3.1 shows weekly ranges and means of the computed light effect averaged over the upper 20 metres

of Lake Ontario. Note that the depth here is purely a computational device and has no physical meaning like the euphotic depth or the compensation depth. In first approximation, the light effect, ρ, is inversely proportional to the layer depth and also, as seen in Figure 2.3.1, to the light extinction.

Primary Production Measurements

Primary production measurements were carried out at an inshore and an offshore station in Lake Ontario as the second phase of each OOPS cruise (Stadelmann *et al.* 1974). The stations were shown as station 11 and station 19, respectively, in Figure 2.1.1. Photosynthetic rates were measured approximately six times a day at eight levels down to 20 m. Daily carbon uptake rates per unit area were computed by integrating observations over the depth of the euphotic zone and averaging over a day. Vertical profiles of temperature and relevant biochemical variables were obtained six times daily and were also integrated over a day to obtain daily averages. Continuous surface radiation measurements were taken in the wavelength band 400-700 nm, and extinction coefficients were obtained from measured transmission curves as a function of depth (Thomson *et al.* 1974).

In conjunction with the primary production measurements, taxonomic identification of phytoplankton and biomass computations were carried out for the same stations (Munawar *et al.* 1974). Samples were collected by an 0-10 m integrating sampler at 10 a.m. on two consecutive days for each station and each cruise. For each species, cell volume was estimated and converted to biomass fresh weight. According to Munawar (pers. comm.) biomass carbon can be estimated to be some 8-12% of biomass weight.

Table 2.3.2 presents daily averages of some of the above variables for the upper 20 metres of stations 11 and 19. Included are the light effect (ρ) defined above, temperature (T), soluble reactive phosphorus (P), ammonia plus nitrite plus nitrate (N), chlorophyll a (A), algal biomass fresh weight (B), and observed primary production (G). The last two columns give computed primary production values as discussed in the following.

TABLE 2.3.2: *Daily mean values, 0-20 m, at stations 11 and 19, of light effect on primary production (ρ), temperature (T), soluble reactive phosphorus (P), ammonia plus nitrate plus nitrite (N), chlorophyll a (A), algal biomass fresh weight (B), observed primary production and computed primary production based on chlorophyll a (A) and biomass (B), respectively. Primary production, μg C/ℓ/day.*

Date			ρ	T	P	N	A	B	Prim. Prod., μg C/ℓ/day		
Yr	Mo	Day		°C	μg/ℓ	μg/ℓ	μg/ℓ	mg/ℓ	Obs.	Computed	
Station 11											
72	4	20	0.23	2.2	10.9	245.	2.75	1.13	35.7	31.6	41.4
72	4	21	0.25	2.1	11.9	238.	2.75	1.00	35.7	34.1	39.6
72	6	1	0.11	6.1	4.6	177.	5.20	2.03	42.0	37.2	44.6
72	6	2	0.19	6.8	3.4	157.	6.80	1.52	87.7	88.0	60.1
72	6	27	0.16	8.5	1.8	110.	5.70	2.43	84.6	69.7	89.3
72	6	28	0.16	9.1	1.6	104.	6.50	2.16	100.2	82.8	82.2
72	7	27	0.17	8.1	2.1	96.	4.75	2.72	73.9	60.1	103.8
72	7	28	0.17	8.7	1.4	92.	4.75	1.52	56.2	62.6	60.1
72	9	14	0.10	13.2	1.0	110.	2.65	.82	49.5	27.8	24.8
72	9	15	0.10	12.3	0.9	109.	3.35	1.60	59.7	33.1	45.9
72	10	26	0.16	8.4	4.5	193.	3.75	.74	33.0	45.5	27.0
72	10	27	0.16	8.1	5.2	179.	3.75	.76	28.5	44.6	27.3
72	11	30	0.11	5.8	8.5	243.	1.85	.60	13.7	13.0	13.0
72	12	1	0.11	5.5	8.9	254.	1.35	.19	8.3	9.3	4.0
73	3	13	0.18	1.1	14.1	262.	1.55	.21	11.3	12.9	5.6
73	3	14	0.08	1.1	15.0	273.	1.60	.21	6.0	5.9	2.5
Station 19											
72	4	18	0.27	1.5	13.5	255.	1.55	.60	19.0	19.9	24.8
72	4	19	0.16	1.7	12.8	254.	1.30	.59	13.7	10.0	14.6
72	5	30	0.18	3.0	14.3	265.	1.80	.32	13.9	17.1	9.6
72	5	31	0.23	3.0	14.5	266.	1.60	.30	23.5	19.4	11.5
72	6	29	0.23	5.6	9.5	243.	1.25	.50	22.3	18.1	22.3
72	6	30	0.12	5.5	9.3	236.	2.40	.60	23.4	18.0	13.9
72	7	25	0.15	13.2	2.3	57.	5.05	1.05	62.1	79.6	47.6
72	7	26	0.15	14.5	1.5	46.	3.70	1.23	57.8	63.7	60.1
72	9	12	0.11	16.0	1.0	60.	5.15	1.73	72.2	71.9	67.7
72	9	13	0.11	16.4	1.1	59.	3.65	1.51	44.7	52.4	60.5
72	10	24	0.05	7.1	5.2	209.	3.65	.44	13.1	12.7	4.7
72	10	25	0.10	6.8	5.3	203.	3.90	.92	17.2	26.6	19.1
72	11	28	0.06	5.7	9.2	227.	1.40	.25	5.0	5.3	2.9
73	1	19	0.06	3.1	13.6	223.	0.85	.31	2.9	2.7	3.1
73	3	15	0.20	1.9	15.5	291.	1.25	.18	9.7	12.2	5.6
73	3	16	0.17	1.9	14.3	272.	1.35	.40	11.9	11.2	10.6

Primary Production Model

Since primary production measurements are available only for the two stations 11 and 19, it will be necessary to correlate them with local biochemical and physical variables so that primary productivity for different times and locations can be estimated from the data in Chapters 2.1-3. As data are more readily available for Chl a than for biomass, the former is preferred as an indicator of phytoplankton. The other independent variables are taken to be ρ, T, P and N (i.e., light, temperature, and nutrients) listed in Table 2.3.2. Our aim is to derive an empirical regression model for algal growth, G, by considering observed primary production as the dependent variable. With reference to typical formulations for phytoplankton growth (see, e.g., DiToro *et al.* 1971) we postulate a relationship of the following form

$$G = C_1 A^{C_2} \rho^{C_3} (C_4)^T f(P, N) \qquad (2.3.1)$$

where f(P,N) represents nutrient limitation effects. Taking the log of the above, we have

$$\log G = \log C_1 + C_2 \log A + C_3 \log \rho + (\log C_4)T + \log f \qquad (2.3.2)$$

which is taken as the basis for our regression analysis.

The steps for constructing the regression equation are as follows:

(1) Correlate the dependent variable, log G, with each of the independent variables;

(2) Choose the variable with the highest correlation to be the first to enter the regression equation;

(3) Estimate the values of log G, using the derived regression equation, and calculate the residual, which is the difference between the observed value of log G and its estimated value;

(4) Correlate the residual with all the independent variables and choose the variable with the highest correlation with the residual to be the second variable to enter the regression equation;

(5) Repeat steps (3) and (4) to include the other variables in the equation.

The above procedure was applied to the data from stations 11 and 19 separately, as well as to the combined data set. For the nearshore station 11, the highest correlation, 0.90, is found between log G and log A. The regression equation between log G and log A explains 83 percent of the total variability in the primary production data. This equation is

$$y = 1.74 + 1.51 \log A$$

where y is the estimated value of log G. The residual is then calculated as

$$R = \log G - Y$$

and correlated with the rest of the variables. The results of this calculation are given in the first column for station 11 in Table 2.3.3. The maximum correlation is found with the temperature, namely, 0.41. The regression equation is then recalculated using log A and T as the independent variables. The result explains 87 percent of the total variation, which means that temperature explains 24 percent of the residual variation. The new regression equation is

$$y = 1.60 + 1.33 \log A + 0.053\ T$$

Repeating the above process identifies light as the next important variable as seen in the second column of station 11 in Table 2.3.3. The total explained variation when A, T, and ρ are included is 93 percent, i.e., 46 percent of the residual variation is explained by the light.

TABLE 2.3.3: *Correlation between the residual and each independent variable in regression analysis for primary production*

Variable	Station 11			Station 19		
Residual	1.00	1.00	1.00	1.00	1.00	1.00
A	-0.08	-0.06	<0.01	0.18	0.46	<0.01
ρ	0.22	0.56	<0.01	0.76	-0.02	0.01
T	0.41	<0.01	<0.01	<0.01	<0.01	<0.01
P	-0.31	-0.13	-0.16	0.02	-0.17	-0.04
N	-0.37	-0.01	-0.02	-0.01	0.03	0.02

The regression equation is now

$$y = 3.28 + 1.00 \log A + 0.097\ T + 0.82 \log \rho \qquad (2.33)$$

The next variable to enter the regression is phosphorus (see third column of station 11 in Table 2.3.3), but the amount of explained variation increases by less than 0.8 percent and hence the contributions from the nutrients are not significant.

For the mid-lake station 19, the temperature is found to be the primary variable, explaining 55 percent of the total variation. The regression equation is

$$y = 2.10 + 0.122\ T$$

The light is next, as shown in the first column of station 19 in Table 2.3.3. The amount of explained variation is now 87 percent and the regression equation is

$$y = 3.99 + 0.146\ T + 1.01 \log \rho$$

The next column of Table 2.3.3 shows that chlorophyll is the third variable, increasing the explained variation to 96 percent of the total. The equation is now

$$y = 3.87 + 0.074\ T + 1.01 \log \rho + 0.80 \log A \qquad (2.3.4)$$

Again, phosphorus is the next variable, but since it shows an increase in explained variation of less than 0.5 percent it is not significant. Thus it is concluded that almost all the variation in the data can be explained in terms of the physical variables (light and temperature) and chlorophyll.

If it is assumed that primary production can be modelled as a function of ρ, T, and A, then the next step is to find out if the equations (2.3.3-4) for the two stations are the same in a statistical sense. A regression equation was fitted to the combined data set with the result

$$y = 3.76 + 0.94 \log A + 0.98 \log \rho + 0.075\ T \qquad (2.3.5)$$

which explains 93 percent of the variation. This equation can be regarded as a weighted regression equation representing the individual equations (2.3.3-4) if these two equations are equal in a statistical sense. The statistic for testing the equality of (2.3.3) and (2.3.4) has an F distribution with four and 24 degrees of freedom. The observed value is found to be 1.877, which is not statistically significant at the 10 percent level. Hence, the two regression equations (2.3.3-4) are equal and can be combined into Equation (2.3.5) for the total data set.

By comparing Equations (2.3.2) and (2.3.5) it is now a simple matter to compute the coefficients C_1 - C_4 in our empirical phytoplankton model (2.3.1). Since the exponents of A and ρ are close to unity, it is of interest to test the significance of the deviation from unity. The 95 percent confidence intervals for the model parameters have been computed and are given in Table 2.3.4. It is seen that the intervals for the exponents of A and ρ (i.e., the coefficients of log A and log ρ in the regression equation) include the value 1.0 and hence we can simplify the model in this regard. The corresponding values of the other

coefficients may be found by regressing log ($G/A\rho$) against T with the results shown at the bottom of Table 2.3.4. Thus, our empirical primary production model is

$$G = 43.\ A.\ \rho.\ (1.07)^T \qquad (2.3.6)$$

where A is expressed in units of μg Chl a and G in μg carbon per day, both referred to the upper 20 m layer. Assuming that the optimal temperature for photosynthesis is about 20°C, the maximum gross production rate according to (2.3.6) would be 175 g C/g Chl a per day.

TABLE 2.3.4: *Estimated values of constants in Equation (2.3.1)*

	C_2	C_3	C_4	C_1 (g C/g Chl a/day)
Best Estimate	0.94	0.98	1.077	42.8
95% Confidence Interval	1.16 0.73	1.22 0.75	1.109 1.047	69.9 26.2
Approximation	1.0	1.0	1.073	43.1

The estimated temperature dependence is seen to be quite close to the value found by Eppley (1972). The growth rate coefficient, C_1, may be further adjusted by regressing computed versus observed primary production and requiring that the slope of the maximum likelihood estimate (Kendall and Stuart, 1970) be equal to unity. The resulting rate constant is about 45 g C/g Chl a/day. Using the observed carbon to chlorophyll ratio of 100 (Stadelmann and Munawar, 1974), the rate constant is about .43 per day, which will be used in the following simulations. Primary production values computed from (2.3.6) are shown in Table 2.3.2 in the column following observed values. The same values are also plotted in Figure 2.3.2 where a triangle represents the first day of each cruise and a circle represents the second day. A similar regression analysis was carried out with phytoplankton being represented by algal biomass instead of chlorophyll. The temperature coefficient was found to be about the same and the growth rate was 0.14 g C/dry weight/day. The resulting computed primary production values are entered in the last column of Table 2.3.2.

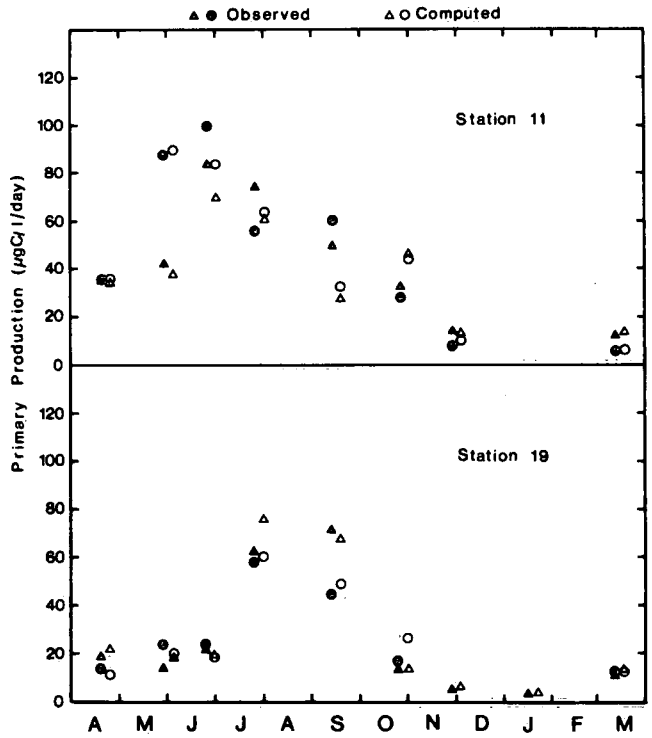

Figure 2.3.2 Observed and computed primary production. Triangles represent the first day, circles the second day, of each cruise.

Effects of Nutrients

Since the previous analysis would suggest that the immediate effects of nutrients on primary production are insignificant compared to effects of light and temperature, it is worthwhile to consider this matter in more detail, in particular because any dynamic plankton model must obviously include a nutrient limitation effect to prevent continued growth after depletion of the nutrient pool. Thus we will now include a phosphorus limitation effect in the growth formulation (2.3.6), using the familiar half-saturation concept, such that the equation becomes

$$G_A = C_A \, A \, \rho \, (C_T)^T \frac{P}{P + C_P} \, . \qquad (2.3.6.a)$$

In this section, statistical methods for fitting the above model are developed. These include the estimation of the unknown parameters; the derivation of confidence intervals; and checking the compatability of the model with the data.

In order to use the statistical methods Equation (2.3.6a) is modified to the stochastic form

$$G_A = C_A \, A \, \rho \, C_T^{\,T} \frac{P}{P + C_p} e^{\varepsilon} \tag{2.3.7}$$

where ε is a random variable which is assumed to be normally distributed with mean 0 and variance σ^2. Dividing both sides of Equation (2.3.7) by $A \rho P$ and taking logarithms gives

$$Y = \alpha_o + \alpha_1(T-\overline{T}) - \ln (P + C_p) + \varepsilon \tag{2.3.8}$$

where $Y = \ln \{G_A/A\rho P\}$, $\quad \alpha_o = \ln \{C_A \, C_T^{\,\overline{T}}\}$

$\overline{T}$ is the mean of the temperature, and $\alpha_1 = \ln C_T$. A set of n observations is available on each variable given in Equation (2.3.7) and it is required to estimate the unknown parameters C_A, C_T, C_p. The methods of least squares (or equivalently the method of maximum likelihood) has the maximum efficiency under model (2.3.8). This method takes as estimates for α_o, α_1 and C_p the values $\hat{\alpha}_o$, $\hat{\alpha}_1$, $\hat{C}_p$ which minimize the residual sum of squares $S(\alpha_o, \alpha_1, C_p)$, where

$$S(\alpha_o, \alpha_1, C_p) = \sum_{i=1}^{n} \{Y_i - \alpha_o - \alpha_1 (T_i - \overline{T}) + \ln (P_i + C_p)\}^2$$

The estimates are the values of α_o, α_1 and C_p which satisfy the three equations.

$$\frac{\partial S}{\partial \alpha_o} = 0 \tag{2.3.9.a}$$

$$\frac{\partial S}{\partial \alpha_1} = 0 \tag{2.3.9.b}$$

$$\frac{\partial S}{\partial C_p} = 0 \tag{2.3.9.c}$$

Equation (2.3.9.a) gives $\hat{\alpha}_o\ (C_p) = \sum_{i=1}^{n} \left\{Y_i + \ln\ (P_i + C_p)\right\}/n$,

while Equation (2.3.9.b) produces

$$\hat{\alpha}_1\ (C_p) = \left[\sum_{i=1}^{n} (T_i - \overline{T})\ \left\{Y_i + \ln\ (P_i + C_p)\right\}\right] \Big/ \sum_{i=1}^{n} (T_i - \overline{T})^2.$$

Substituting $\hat{\alpha}_o\ (C_p)$ and $\hat{\alpha}_1\ (C_p)$ in (2.3.9.c), the following equation is obtained

$$\sum_{i=1}^{n} \frac{Y_i}{P_i + C_p} - \hat{\alpha}_o \sum_{i=1}^{n} \frac{1}{P_i + C_p} - \hat{\alpha}_1 \sum_{i=1}^{n} \frac{T_i - \overline{T}}{P_i + C_p} + \sum_{i=1}^{n} \frac{\ln\ (P_i + C_p)}{P_i + C_p} = 0 \tag{2.3.9.d}$$

The least-squares estimate of C_p, $\hat{C}_p$, can be obtained graphically by plotting the left-hand side of Equation (2.3.9.d) vs. C_p and taking the value $\hat{C}_p$ as the point for which the function intercepts the C_p axes.

Another approach for obtaining the least squares estimate as well as deriving the confidence interval for C_p can be easily developed by noting that: (1) the residual sum of squares, $S\ (\hat{\alpha}_o,\ \hat{\alpha}_1,\ \hat{C}_p)$, calculated from (2.3.8) follows approximately a $\chi^2_{n-3}\ \alpha^2$ distribution (a χ^2 distribution with (n-3) degrees of freedom); (2) when assuming that C_p is known in (2.3.8), the statistic $S\ \left\{\hat{\alpha}_o(C_p),\ \hat{\alpha},\ (C_p),\ C_p\right\}/\alpha^2$ follows

a $\chi^2_{n-2}\sigma^2$ distribution; and (3) then the statistic

$$D(C_p) = \frac{S\{\hat{\alpha}_o(C_p), \hat{\alpha}_1(C_p), C_p\} - S\{\hat{\alpha}_o, \hat{\alpha}_1, \hat{C}_p\}}{S\{\hat{\alpha}_o, \hat{\alpha}_1, \hat{C}_p\}/(n-3)} \qquad (2.3.10)$$

has an F-distribution with 1 and (n-3) degrees of freedom. Equation (2.3.10) can be used to derive a confidence interval for C_p. To illustrate that, consider that the interest is to obtain $(1-\alpha)$ confidence interval for C_ρ, where $0 \le \alpha \le 1$. From the table of the F-distribution, we can obtain the value of F, say δ_α, which corresponds to a tail area equal to α. Then all the values of C_ρ must satisfy the inequality

$$S\{\hat{\alpha}_o(C_p), \hat{\alpha}_1(C_p), C_p\} \le (1 + \frac{\delta\alpha}{n-3})\, S(\hat{\alpha}_o, \hat{\alpha}_1, \hat{C}_p). \qquad (2.3.11)$$

This equation can be solved graphically. Also, confidence intervals can be obtained for α_o and α_1 if we ignore the fluctuations in $\hat{C}_p$. These are given by

$$\hat{\alpha}_o - t_{(n-3)} \sqrt{\frac{S(\hat{\alpha}_o, \hat{\alpha}_1, \hat{C}_p)}{n(n-3)}} \le \alpha_o \le \hat{\alpha}_o + t_{(n-3)} \sqrt{\frac{S(\hat{\alpha}_o, \hat{\alpha}_1, \hat{C}_p)}{n(n-3)}}$$

(2.3.12.a)

and

$$\hat{\alpha}_1 - t_{(n-3)} \sqrt{\frac{S(\hat{\alpha}_o, \hat{\alpha}_1, \hat{C}_p)}{n\,\Sigma(T_i-\bar{T})^2}} \le \alpha_1 \le \hat{\alpha}_1 + t_{(n-3)} \sqrt{\frac{S(\hat{\alpha}_o, \hat{\alpha}_1, \hat{C}_p)}{n\,\Sigma(T_i-\bar{T})^2}}$$

(2.3.12.b)

The methods given above are applied here using the data available from stations 11 and 19. Figure 2.3.3 displays the 99% and 95% confidence intervals for C_p for station 11, station 19 and stations 11 and 19 combined, respectively. For station 11, it is clear that only

negative values are included in the confidence interval. These confidence intervals suggest values for C_p in the intervals (-0.78, -0.27) and (-0.72, -0.385) for the 99% and 95% confidence intervals, respectively. On the other hand, the corresponding intervals for station 19 include positive as well as negative values. The intervals are (-0.9, >10.0) and (-0.8, 2.3). The intervals based on stations 11 and 19 combined are negative and are (-0.73, -0.28) and (-0.69, -0.285).

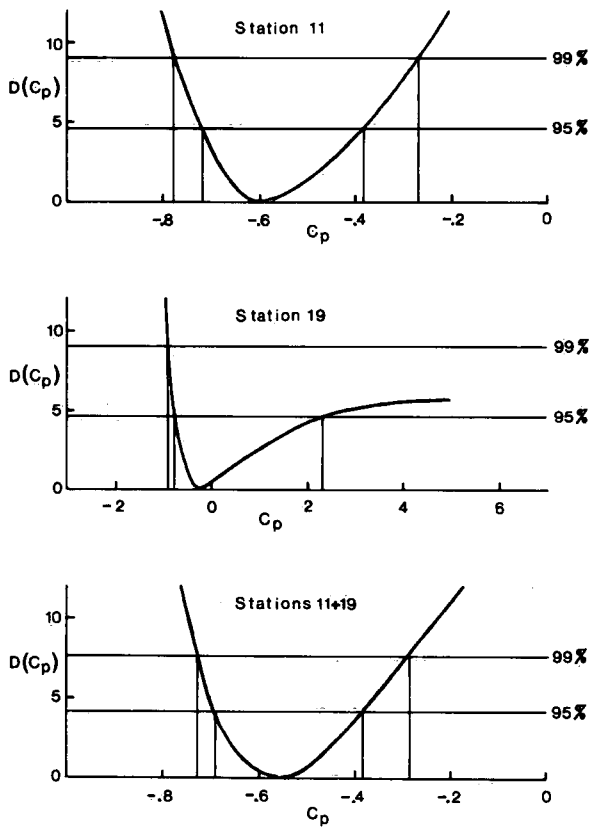

Figure 2.3.3 Statistical parameter $D(C_p)$ defined by Equation (2.3.10) and the 99% and 95% confidence intervals for C_p.

Table 2.3.5 summarizes the least-squares estimates of the unknown parameters α_0, α_1, and c_p. All the estimates of c_p are seen to be negative. Since c_p represents the half-saturation constant in the primary production model (2.3.6a) which was fitted to the present data set, such negative values are not admissible. Hence, the statistical analysis does not

support this conventional formulation of nutrient effects on plankton growth. This is not to say that there is no cause-effect relationship between nutrients and primary production (in fact we know there is), but this analysis fails to pinpoint any such relationship. Apparently, it is obscured by effects of physical parameters or, perhaps, the relationship is not instantaneous but involves a time-lag effect. Furthermore, as pointed out by Simons (1976b), it is possible to obtain a quite acceptable fit of (2.3.6a) to the present data set by assigning *a priori* a positive value to the half-saturation constant, c_p. Since nutrient concentrations are inversely correlated with temperature, the temperature coefficient, c_τ, must then be taken to be greater than the value 1.07 found above, in order to offset the phosphorus effect. It is felt, therefore, that the formula (2.3.6a) is acceptable to approximate nutrient effects in the following experiments with dynamic plankton models which, for reasons mentioned earlier, must incorporate some form of nutrient limitation. However, it is important to keep in mind that the present data base cannot be used to validate any such primary production model, since the statistical analysis suggests that the best model is one without instantaneous nutrient effects.

TABLE 2.3.5: *The least-squares estimates of the parameters of model (2.3.8)*

Parameters	Station 11	Station 19	Stations 11+19
$\hat{\alpha}_0$	3.98	4.12	4.01
$\hat{\alpha}_1$	0.0261	0.0406	0.0206
$\hat{c}_p$	-0.604	-0.240	-0.550

2.4 Dynamic Phosphorus Models

The simplest way to conceptualize the response of a lake to external loadings is to construct a budget model or "input-output" model. Vollenweider (1969, 1975) has extensively discussed the application of

mass balance principles to idealized lakes with quasi-homogeneous nutrient concentrations. This results in a formulation of total nutrient concentration as a function of loading rates and specific lake parameters. By recourse to observed correlations between nutrient concentrations at spring overturn and biomass in summer, such models can be used to make rough predictions of the trophic state of a lake. In particular, the time-independent steady-state solutions of such input-output models constitute the theoretical background for Vollenweider's loading plots, which display the degree of eutrophication in terms of total phosphorus loading, lake depth, and hydraulic retention time.

The continuity equation for a substance like total phosphorus may be written as

$$\frac{dM}{dt} = I - O - S \qquad (2.4.1)$$

where the left-hand side represents the time rate of change of the total mass of the nutrient contained in the lake, I is the total external input to the lake, O is the loss by river outflow, and S is the net amount disappearing into the sediments. This equation can be solved for a given loading, provided that the last two terms are expressed in terms of the nutrient concentration itself. In the simplest case, the lake is considered as a mixed reactor and both loss terms are taken to be proportional to M. The resulting solution illustrates many of the basic aspects of the response of a lake to nutrient inputs (Vollenweider, 1969, 1975). This matter will be the subject of a later section of this Report dealing with long-term simulations.

A total nutrient budget model has two major shortcomings. In the first place, the net sedimentation term is usually not directly proportional to the total nutrient concentration. Instead, one would expect sedimentation to be a function of the organic fraction, which may vary considerably as a function of time. The counteracting effects of resuspension from the sediments and phosphorus release under anaerobic conditions are even more complicated. The second major problem is associated with spatial variations and in particular the vertical gradients during summer stratification. The first step towards a more realistic

model is to take these factors into account by dividing the lake into two layers and separating the total nutrient into two components (O'Melia, 1972; Imboden, 1974). This is the simplest seasonal model consisting of four mass balance equations, one for each component and each compartment. The introduction of additional processes and parameters into the model is more troublesome than the fact that the number of equations has increased.

In a total nutrient budget model the only two parameters are the effective retention time and the net sedimentation rate. By dividing the lake into layers, it becomes necessary to prescribe the exchange between the layers and thus to simulate another physical process. Similarly, separation of the total nutrient into components requires a model for the kinetic interactions between them. In effect, these two steps constitute the basic distinction between a simple nutrient budget model and a sophisticated dynamic plankton model. All further refinements in terms of spatial distributions as well as biological reactions, are rather straightforward extensions of the same principles. It is for that reason that a detailed analysis of this kind of model follows. The nutrient selected for this discussion is phosphorus because of the general association of this nutrient with eutrophication problems in the Great Lakes.

Consider then two phosphorus components, say, soluble orthophosphate (SRP) and organic phosphorus (OP), the latter defined as total phosphorus (TP) minus the former. Let M denote the total mass (metric tons) of any one of these components contained in either of two layers, the upper one denoted by subscript 1, the lower one by subscript 2. Further, let the processes affecting the time rate of change of M be denoted by the following symbols (metric tons/day):

L: Net loading = external inputs minus river outflow (I-O)

S: Net effect of sedimentation and resuspension (positive upward)

D: Diffusive exchange from lower to upper layer

B: Biological transformation from organic to inorganic phosphorus

Note that all upward mass exchanges are defined to be positive. For example, a positive value of S means that resuspension exceeds settling. Also, a positive value of B represents a gain of SRP, i.e., nutrient regeneration exceeds uptake. This somewhat unusual convention will be seen to be convenient when the SRP-budget for the upper layer is considered.

If it is assumed that sedimentation is restricted to the organic component and that the reduction of horizontal area between the surface and thermocline level is negligible, the mass balance equations are

$$\frac{d}{dt} M_1(SRP) = L(SRP) + D(SRP) + B_1(SRP, OP) \tag{2.4.2}$$

$$\frac{d}{dt} M_2(SRP) = -D(SRP) + B_2(SRP, OP) \tag{2.4.3}$$

$$\frac{d}{dt} M_1(OP) = L(OP) + D(OP) + S_1(OP) - B_1(SRP, OP) \tag{2.4.4}$$

$$\frac{d}{dt} M_2(OP) = -D(OP) - S_1(OP) + S_2(OP) - B_2(SRP, OP). \tag{2.4.5}$$

Naturally, the biological exchange, B, disappears if the equations for SRP and OP are added together, with the following result

$$\frac{d}{dt} M_1(TP) = L(TP) + D(TP) + S_1(OP) \tag{2.4.6}$$

$$\frac{d}{dt} M_2(TP) = -D(TP) - S_1(OP) + S_2(OP) \tag{2.4.7}$$

where obviously $L(TP) = L(SRP) + L(OP)$ and $D(TP) = D(SRP) + D(OP)$. Similarly, the diffusive exchange, D, and the sedimentation, S_1, through the thermocline drop out if the equations for both layers are taken together. For the case of TP, the resulting equation reduces to (2.4.1).

At this point there are essentially two different ways in which to proceed. The first one is a budget procedure whereby the left-hand sides of the equations as well as the loadings and diffusive fluxes are computed from a given data set, whereupon the terms B and S follow from the above equations. Having obtained the latter as functions of time, one then compares these to environmental conditions and model variables in order to estimate functional relationships. The second method is based on the assumption that the kinetic functions are known from previous

investigations and it remains only to "fine-tune" the rate coefficients. The latter is done by trial and error, usually by a combination of subjective judgment and objective mathematical techniques, until one finds an optimal set of coefficients which minimizes the least-squares differences between computed and observed values of the variables. In a way, the choice between the two different procedures depends on one's confidence in the data base because the budget method implies a higher degree of accuracy of the individual data points than the optimization techniques. The two methods will now be illustrated by applying them in turn to the same data set.

Budget Computations

The calculations will be based on the IFYGL phosphorus observations presented in Section 2.1, with the assumption that the 20-m level approximates the mean thermocline position. The data base for two layers and two components corresponding to the above equations is obtained by averaging the observed values for the second and third layer and by adding the soluble organic and particulate components. Now the data points are connected by some form of interpolation, either by straight lines or a more pleasing curve such as a "cubic spline" or a "local procedure" fit (Reinsch, 1967; Akima, 1970). By recourse to the exchange coefficients presented in Table 2.2.1, weekly values of diffusive fluxes across the thermocline can be computed as the product of vertical phosphorus gradients and mixing coefficients. When these results are combined with the time rates of change of the interpolated concentration data and with interpolated loadings from Table 2.1.4, the biological interactions, B, follow from Equations (2.4.2-3) and the net sedimentation, S, from Equations (2.4.6-7). The set of equations for OP will be automatically satisfied.

The derivatives of the interpolated data curves - and therefore the resulting B and S - are in general not smooth functions of time. In the simplest case of linear interpolation, the derivatives are constant between consecutive cruises and B and S will be actually discontinuous at the time of each cruise. To make the resulting time series look more attractive, some form of subjective smoothing can be applied. In this case, the time series for B and S were smoothed to eliminate periods less than one month. For consistence, the original "first-guess" interpolated

curves must now be corrected to satisfy Equations (2.4.2-7). Thus, the equations are solved by step-wise forward integration, using the known values of loading, L, uptake, B, and sedimentation, S, and re-computing the diffusion from exchange coefficients and vertical gradients. The resulting curves for SRP, OP, and TP will no longer pass exactly through the original data points, the "error" being a function of the degree of smoothing applied to the series of B and S.

The results of these computations are presented here for the special case where all variables are assumed to be exactly periodic over a one-year time span. The upper half of Figure 2.4.1 shows the individual rate terms appearing in the SRP-balance equations for the upper layer alone as well as for the whole lake. The dashed line indicates the net rate of change and the dot-dash line represents the net loading including, in case of the upper layer, upward mixing across the thermocline. The solid line shows the biological transformation from organic to inorganic phosphorus as computed in the above-described iterative fashion. The lower half of Figure 2.4.1 presents the corresponding time variations of the inorganic component for both layers, together with the observations indicated by circles (0-20 metres) and squares (20 m-bottom). The two vertical lines in the upper part of the figure delineate the stratification period as determined from the heat flux computations. Outside this period, the vertical exchange coefficients are to some extent arbitrary. On the basis of considerations presented in the following, it was estimated that the "effective" exchange coefficient had a maximum value of about 2 m/day. It should be borne in mind, however, that for the upper layer only the parts of the curves between the vertical lines can be unambiguously determined. This restriction does, of course, not apply to the results for the whole lake.

Figure 2.4.2 shows the corresponding results for the total phosphorus balance with the solid lines now representing the net effect of sedimentation and resuspension. The latter is obtained from the total phosphorus budgets and, by virtue of our assumption regarding sedimentation, is identical to the net sedimentation effect in the organic phosphorus balance. The lower half of the figure presents the time variations of total phosphorus for both layers with observations for 0-20 m indicated by

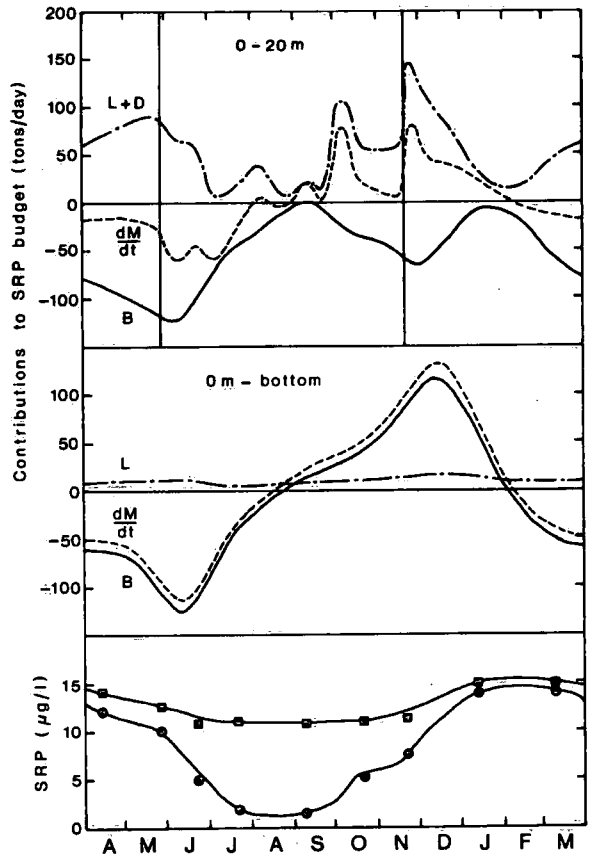

Figure 2.4.1 Contributions to mass balance of soluble reactive phosphorus (SRP) in epilimnion (top) and in the whole lake (middle) April 1972 to March 1973. L = net loading, D = diffusive flux, B = net biological effect, dM/dt = total rate of change. (Bottom) Associated concentrations of SRP and measured values for epilimnion (circles) and hypolimnion (squares).

circles and data for 20 m-bottom denoted by squares. Again, the exchanges across the thermocline during the winter season cannot be uniquely determined, but this does not affect the sedimentation estimates at the sediment-water interface represented by the solid line in the middle diagram.

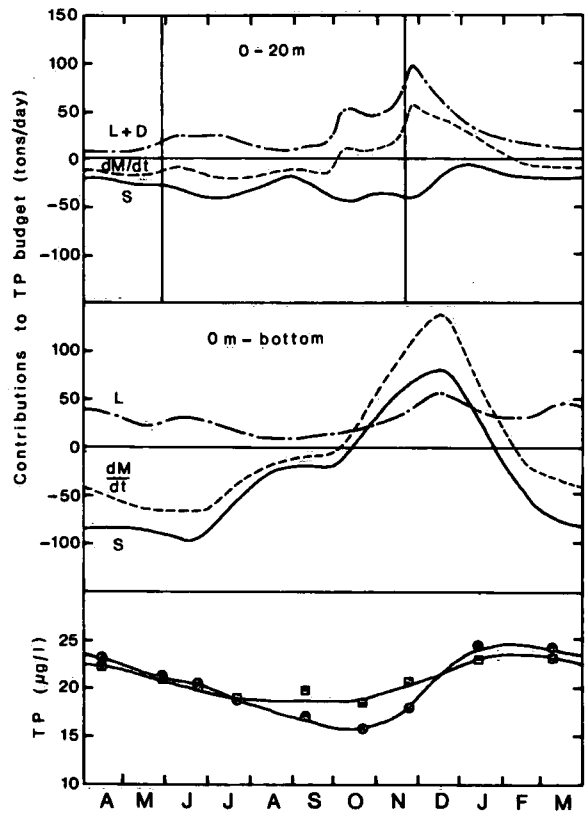

Figure 2.4.2 Same as Figure 2.4.1, except for total phosphorus. S = net effect of sedimentation.

It is logical to ask what these computations have accomplished. Certainly, in a predictive sense, nothing has been gained because the problem has simply been shifted from predicting variables to estimating biological transformations and sedimentation effects. But this is not to say that there is nothing to be learned from it. Take, for example, the nutrient uptake curves shown by the solid lines in the upper half of Figure 2.4.1. These results may be compared with observed concentrations of soluble and particulate phosphorus to try and formulate functional relationships. Especially if it is assumed that a fairly accurate primary production model is already available, this would lead to an estimate of total nutrient regeneration and hence to a model of net production.

Similarly, the sedimentation curves in Figure 2.4.2 may be related to the time-dependent values of organic phosphorus. It follows immediately then, that the highly variable sedimentation at the bottom is

not simply proportional to the nearly constant concentration of organic matter in the overlying water. If anything, the sedimentation curve shows a strong correlation with the biological transformation in the previous figure. This is not surprising since the larger part of the total phosphorus variation is apparently due to the inorganic component. Thus, the same variation is interpreted as biological in Equations (2.4.2-3) and as a result of settling in Equations (2.4.6-7). The obvious conclusion is that either the data are in error, or the hypothesis that sedimentation and resuspension affect only organic phosphorus is wrong, or finally the sedimentation coefficient varies from large positive to large negative values. Clearly, the next step is to quantify these qualitative conclusions.

Parameter Estimates

In order to convert the budget equations (2.4.2-7) into a predictive model, it is necessary to express the biological conversion, B, and the sedimentation term, S, in terms of the state variables themselves. It is understood that the diffusion term, D, is already formulated as the product of vertical gradients and exchange coefficients defined in Section 2.1. In the most simple terms, the biological transformations can be visualized as the net result of nutrient uptake by primary production and nutrient regeneration by direct respiration or through any intermediate biological process. It has been shown in Section 2.3 that the carbon uptake can be modeled reasonably well in terms of phytoplankton carbon and light and temperature. Since the observations of Section 2.1 indicate that the phosphorus-to-carbon ratio of organic material decreases by a factor two from winter to summer, the uptake of inorganic phosphorus will not be a constant fraction of the carbon uptake. In first approximation, however, this effect would cancel out if one expresses phosphorus uptake as a function of particulate phosphorus instead of carbon.

This leads to the problem of defining the particulate phosphorus component as a fraction of the total organic component utilized in the present model. For that purpose, these two phosphorus components for the three layers and the nine cruises presented in Section 2.1, are correlated

with each other in Figure 2.4.3. Also included is a straight line representing the relationship

$$PP = OP - 5. \qquad (\mu g/\ell) \qquad (2.4.8)$$

which seems to be a sufficiently accurate approximation for the present purpose. In essence, this is equivalent to Imboden's procedure of disregarding the dissolved organic component (Imboden, 1974; Imboden and Gachter, 1978). For easy reference, the bottom of Figure 2.4.3 shows the interpolated values of organic phosphorus computed as the difference between TP and SRP presented in Figures 2.4.1-2.

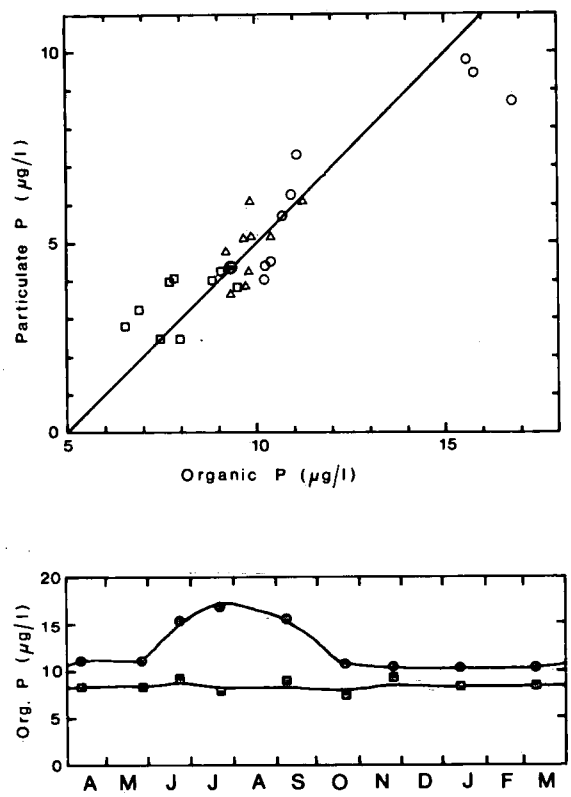

Figure 2.4.3 (Top) Observed particulate phosphorus *versus* total organic phosphorus for three layers and nine cruises of Figure 2.1.2, using the same symbols. (Bottom) Total organic phosphorus obtained as a difference between the total phosphorus of Figure 2.4.3 and SRP of Figure 2.4.2.

A second problem is the half-saturation constant for phosphorus uptake. Although the analysis of Section 2.3 did not confirm the expected effects of nutrient limitation, some effect of this type must be included to prevent the model from taking up SRP after the nutrient pool has been completely depleted. There are two simple ways of doing this. The first one is the conventional method of formulating primary production as a function of SRP but keeping regeneration independent of SRP. The second one would be to reverse this assumption. Once the photosynthesis formula has been adapted, the SRP uptake as a function of time follows immediately from observed values of all variables entering into this formulation. The nutrient regeneration can then be determined as the difference between this curve and the net biological conversions shown in Figure 2.4.1. This was done here for the upper layer during the stratified season.

First it is assumed that the half-saturation constant has a small but non-zero value, say, 0.5 μg P/ℓ. Hence, by reference to Section 2.3, the daily nutrient uptake by photosynthesis for a volume V equals

$$U = .43\ (1.07)^T\ \rho\ \frac{SRP}{SRP + .5}\ (OP - 5.)V \qquad (2.4.9)$$

Assuming that the temperature dependence of the regeneration process is of the same form, the following estimate was obtained for this term

$$R = .04\ (1.07)^T\ (OP - 5.)V \qquad (2.4.10)$$

By contrast, if it is assumed that the uptake by photosynthesis is formulated as follows

$$U = .43\ (1.07)^T\ \rho\ (OP - 5.)V \qquad (2.4.9a)$$

the corresponding formula for respiration may be written

$$R = .04\ (1.07)^{T}\ \frac{SRP + .5}{SRP}\ (OP - 5.)V \qquad (2.4.10a)$$

The latter differs from the former in postulating that low nutrient concentrations do not inhibit primary production but rather require a faster regeneration of nutrients. It should be realized that although the second formulation of biological activity is conceptually quite different from the first, the mathematical difference in net uptake (U - R) is simply a factor (SRP + 0.5)/SRP.

To illustrate the effects of the above formulations without confusing the picture by extraneous influences, a prediction may be made of the inorganic component in the upper layer only, after substituting (2.4.9-10) into (2.4.2). The previously interpolated observed SRP-values in the lower layer are used to evaluate the diffusion term and the observed organic phosphorus in the upper layer is entered in the Equations (2.4.9-10). The solid line in the upper half of Figure 2.4.4 shows the SRP curves computed from (2.4.9-10), the dashed line shows the results obtained from (2.4.9a-10a). The centre part of Figure 2.4.4 presents the corresponding net biological transformations, B, together with the gross uptake U. In keeping with the earlier sign convention, biological transformation from organic to inorganic phosphorus is counted positive, hence B = R - U, and uptake results in a loss of SRP and therefore is plotted against the negative part of the vertical coordinate. These results illustrate quite clearly that one can accommodate a wide range of primary production formulations in a model as long as there are additional degrees of freedom to "play with", in this case the uncertainty associated with respiration and other forms of nutrient regeneration.

A similar experiment can be carried out in regard to the sedimentation term. In this case, the organic component may be predicted from Equations (2.4.4-5) while utilizing the previously determined biological terms shown in Figure 2.4.1. Assuming that sedimentation may be formulated as the product of a constant settling velocity, W, and the concentration of

particulate phosphorus in the overlying water, the sedimentation term can be written

$$S = -W.A(OP - 5.) \qquad (2.4.11)$$

where A represents the surface of the lake. By trial and error, it is found that the solutions for both layers are periodic for W_1 = .2 m/day for the upper layer and W_2 = .4 m/day for the bottom layer. The solutions for the organic phosphorus component are shown at the bottom of Figure 2.4.4, together with the observed values. These results illustrate the dangers in fitting a model to simulate summer biomass. In this case, one would probably invoke a higher settling coefficient to reduce the error during the stratified season, with the result that the model would not be periodic anymore and hence would predict a different long-term response to loading.

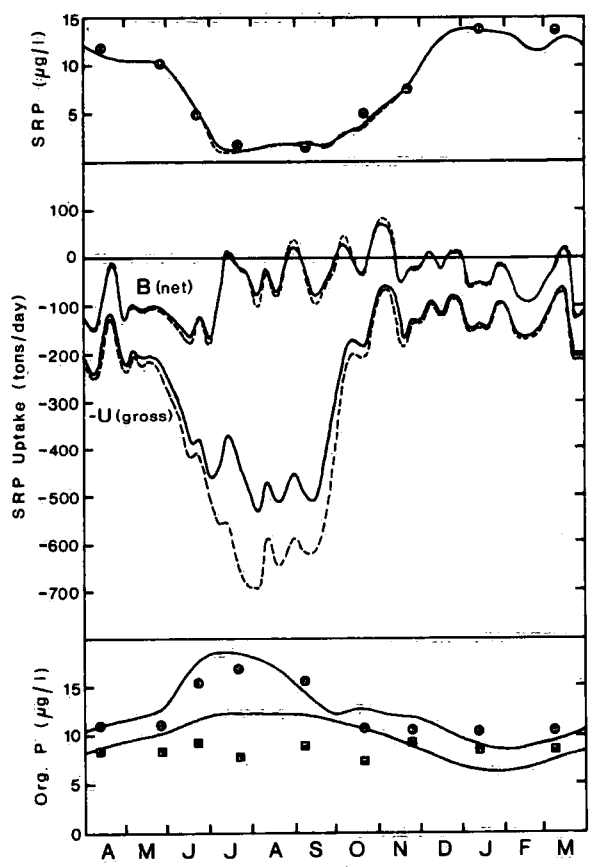

Figure 2.4.4 (Top) Observed concentrations (circles) of soluble reactive phosphorus (SRP) in epilimnion compared with simulations based on Equations (2.4.9-10) and (2.4.9a-10a), denoted by solid and dashed lines, respectively. (Middle) Corresponding net biological transformations from organic to inorganic phosphorus (B) and gross nutrient uptake (U). (Bottom) Observed concentrations of total organic phosphorus for epilimnion (circles) and hypolimnion (squares) compared with simulations based on (2.4.11).

Optimization Techniques

The foregoing has shown that the budget method allows us to partition the rate of change of a nutrient into contributions from separate effects such as sedimentation and net uptake, whereupon the latter may be correlated with the system variables to estimate functional relationships. Alternatively, the trial-and-error method described above may be replaced by a more rigorous mathematical method such as an optimization technique. Given a specific formulation for each kinetic process, this technique searches for the set of coefficients that minimizes the least-squares errors between the data and the model results. The advantage of this method is that it allows for a simultaneous fit of all model variables.

Consider again the mass balance equations (2.4.2-5) and substitute the following kinetic expressions similar to (2.4.9-11).

$$B_1(SRP,OP) = -\ .43(1.07)^T\ \rho\ \frac{SRP_1}{SRP_1+.5}\ (OP_1-5)V_1 + k_1(1.07)^T\ (OP_1-5)V_1 \tag{2.4.12}$$

$$B_2(SRP,OP) = k_2(1.07)^T\ (OP_2-5)V_2 \tag{2.4.13}$$

$$S_1(OP) = -\ k_3A_1(OP_1-5) \tag{2.4.14}$$

$$S_2(OP) = -\ k_4A_2(OP_2-5) \tag{2.4.15}$$

The problem is to determine the values of the constants k_1 to k_4 which give the best fit to the observations. Stated in the most general terms, the system may be written in vector for

$$\frac{d\vec{M}}{dt} = f(t, \vec{M}, \vec{k}) \tag{2.4.16}$$

where $\vec{M} \equiv (M_1(t), M_2(t), M_3(t), M_4(t))$ and $\vec{k} \equiv (k_1, k_2, k_3, k_4)$.

The nonlinear system (2.4.16) can be solved for the solution vector M by appropriate numerical integration procedures (Dahlquist, 1974), if $\vec{k}$ is given. Suppose there is a set of observed values, $\vec{M}^*$, at some time intervals, t_j, $j = 1, 2, \ldots, J$ and, assume, for the sake of simplicity that intervals are regular: i.e., $t_j - t_{j-1} = \Delta t$. These values may be from direct observation or from interpolation, for which some measure of the variances are known. Then, it is possible to construct the error vector, $\vec{\eta}$, by considering the errors at these points:

$$\eta_{ij} \equiv M^*_i(t_j) - M_i(t_j) \equiv M^*_{ij} - M_{ij}, \; i=1, \ldots, 4; \; j=1, 2, \ldots, J, \text{ i.e.,}$$

$$\vec{\eta} = \vec{M}^* - \vec{M} \tag{2.4.17}$$

The least-squares error, E, is defined as:

$$E \equiv \sum_{i=1}^{4} \sum_{j=1}^{J} \| \eta_{ij} \|_W^2 \, \Delta t \tag{2.4.18}$$

where $\|\eta_{ij}\|_W^2 = \vec{\eta}^T W \vec{\eta}$ and W is a 4xJ weighting matrix in the present case. Obviously the weights used in W can be related to the variances in $\vec{M}^*$. Thus, the problem is precisely: to find the optimal $\vec{k}$ which minimizes E.

There is a general class of methods that can solve this problem, namely the gradient method, as represented by the following algorithm:

$$\vec{k}_{m+1} = \vec{k}_m - \gamma R \vec{g} \tag{2.4.19}$$

where $\vec{k}_m$ is the mth iterate of $\vec{k}$, γ is a scalar step length, R is some positive definite matrix, and $\vec{g} \equiv \partial E / \partial \vec{k}$ is the gradient vector. The main difference among the methods that belong to this class is in the choice of R, such as:

$$R \equiv I \qquad \text{(Steepest Descent Method)} \tag{2.4.19a}$$

$$R \equiv [\partial^2 \vec{E}/\partial \vec{k}^2]^{-1} \qquad \text{(Newton-Ralphson Method)} \qquad (2.4.19b)$$

$$R \equiv [(\partial \vec{M}/\partial \vec{k})^T \, W \, (\partial \vec{M}/\partial \vec{k}) + \alpha I]^{-1}$$

$$\text{(Marquardt's Method)} \qquad (2.4.19c)$$

where I is the identity matrix and α is a scalar. Briefly, the steepest descent method uses the gradient itself as the direction for searching the optimal $\vec{k}$, which converges quite fast at the beginning, but rather slowly when it approaches the minimal E. The Newton-Ralphson Method assumes the direction as given by the second-order approximation of the Taylor's Series, and converges quadratically in the neighbourhood of minimum E, but it may not converge outside this neighbourhood. The Marquardt algorithm (Marquardt, 1963) is a combination of the two methods, but retains their good convergency property, by a systematic choice of α. Thus, for large α, the algorithm resembles the steepest descent, and for small α, the Newton-Ralphson. All these three methods have been tested; the Marquardt's algorithm is found to be the most reliable, and is used to identify the k's in Equations (2.4.12-15). Figure 2.4.5 shows a typical example of using this method for Equations (2.4.12-15) in the test of possible lower layer uptake rate (see later in three-layer results). While the meaning and the values of the constants involved need further explanation, it is at least clear here that the method can converge to a good fit (solid lines) from a rather bad guess (dotted line) in four iterative steps. The following is a more detailed account of the automatic fitting of the two-layer model.

In order to apply the Marquardt's algorithm, we need some initial approximation of the k's and definition of the weighting matrix, W. Fortunately, we have already a very close estimate of the constants from the computations by the budget method. As for the weights, the simplest procedure is to assume that the measurements of all the phosphorus constituents have similar errors and uniform weights can be used in the algorithm. If this is assumed, we would obtain the best overall fit, but there is no guarantee that the model will be periodic. Therefore, another possibility is to use uniform weights for the major part of the year, say,

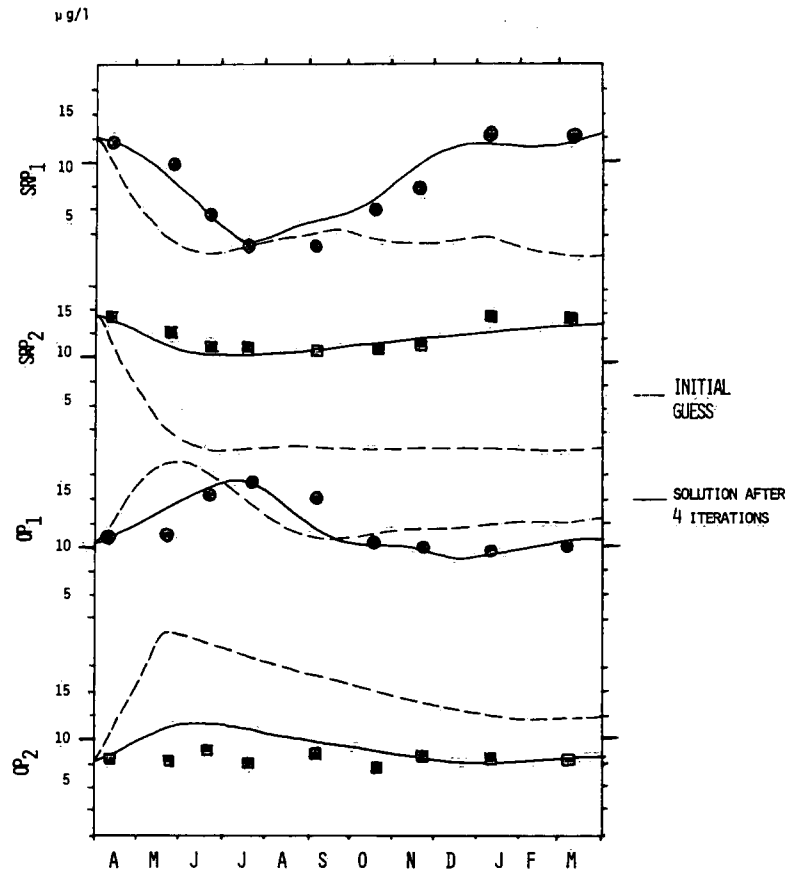

Figure 2.4.5 Convergence of Marquardt optimization procedure for two-layer, two-component phosphorus model.

the first ten months, and to double the weighting for the remaining two months. Since the data for all the constituents show reasonable periodicity (Figure 2.4.1-4), the latter type of weighting should result in a rather periodic model. It should not be misinterpreted to mean that we have more confidence in the data during the last two months, but rather it should be considered as a technique to ensure some degree of periodicity in each of the model variables. The results of these two cases are summarized in Figure 2.4.6. The algorithm found that k_1 = .043 per day, k_2 = .0065 per day, k_3 = .10 m/day and k_4 = .65 m/day for the first case (dashed lines), and k_1 = .043 per day, k_2 = .0065 per day, k_3 = .20 m/day and k_4 = .40 m/day for the second case (solid lines). It is interesting to see that the regeneration rate is about an order of magnitude lower in the hypolimnion than in the epilimnion, even after the temperature correction. The

sedimentation rates are similar to those used in most models but much lower than those measured in laboratory experiments with algae (Scavia *et al.* 1976). At first glance the two simulation results do not differ substantially from one another in terms of overall fit. However, the difference is large in terms of periodicity. This can be expressed as the relative difference between final concentration and initial concentration. For the first (non-periodic) case, it averages about 15%; for the second (near-periodic) case, it is about 2% in each of SRP_1, SRP_2, OP_1 and OP_2.

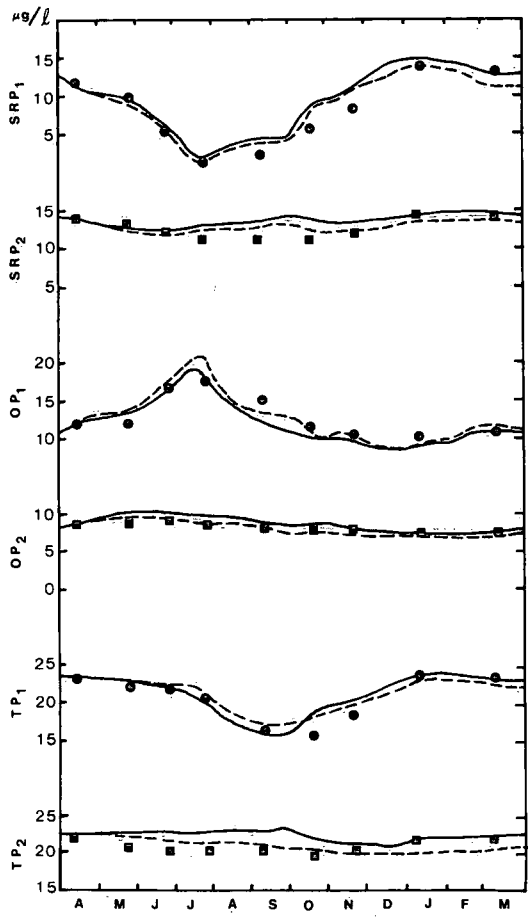

Figure 2.4.6 Observed values of soluble reactive phosphorus (SRP), total phosphorus (TP) and organic phosphorus (OP = TP - SRP) in epilimnion (circles) and hypolimnion (squares) compared with simulations using rate coefficients estimated by optimization techniques. Dashed lines represent solutions with best overall fit; solid lines represent periodic solutions.

To summarize, we may obtain a model with a set of optimal coefficients which fits the observed/interpolated IFYGL data in the least-squares sense with any desired degree of periodicity over one seasonal cycle. This enables one to investigate the long-term response of the lake to phosphorus loading, without any unknown imbalances in the seasonal model. We have presented two types of methods for decomposing and identifying the meaningful components in the phosphorus cycle based on different levels of confidence in the data. The first method is the budget method, which places almost total confidence in the data. The second method is the optimization method, which allows analytical and statistical errors in the data, but tries to make the best use of the data set.

Three-Layer Model

The preceding two-layer analysis of the phosphorus budget describes only part of what happens during the annual cycle of phosphorus components in Lake Ontario. More insight can be gained by considering a higher vertical resolution such as the three-layer observations presented in Figure 2.1.2. It is seen immediately from these data that the vertical structure of the lake is poorly described by a two-layer model. In effect, the intermediate layer between 20 and 40 metres, although previously included in the lower layer, appears to be closer to the upper layer in regard to its seasonal variations. In physical terms, this is a quite interesting problem because one generally tends to think of a lake as consisting of two layers separated by a thermocline, which in the case of Lake Ontario is situated well above the 20-m level during the summer. It is thus worthwhile to study this phenomenon in more detail.

In the first place, it is noted that all the nutrient data (Figures 2.1.2-4) and the temperature observations (Figure 2.2.1) are consistent with regard to the effects of stratification on vertical mixing during the fall season. The first major storms in October increase the depth of the upper mixed layer such that the upper model layer (0-20 m) and the next layer (20-40 m) merge together and, from that time onwards, behave as one. In a model with fixed layer depths, this process appears as full mixing at the intermediate (20-m) level as shown in Figure 2.2.2, but this is clearly not equivalent to deep mixing extending to the bottom. The latter does not occur until early December when nutrient concentrations

and temperatures in all layers are seen to become uniform. To model this particular aspect of the stratification cycle with a two-layer model, it would be obviously necessary to allow for a deepening upper layer depth, which is not a very desirable proposition from the viewpoint of routine data processing. The alternatives are to invoke complete mixing of the two-layer model if the full mixing criterion is met at the 20-m level, or to reduce artificially the mixing at the 20-m level until deep mixing occurs. The latter course of action was taken in the foregoing analysis because it naturally produces a more realistic upper layer solution.

A second point to be noted is the remarkable difference in behaviour in early spring between phosphorus (Figure 2.1.2) and the other variables (Figures 2.1.3-4 and Figure 2.2.1). As expected, the temperature of the intermediate layer rises very slowly because, as mentioned before, this layer is well below the seasonal thermocline. The nitrogen and carbon concentrations in this layer are consistent with this physical picture, but the same is not true for phosphorus. A similar discrepancy shows up at individual stations and it appears to be a crucial aspect of the phosphorus cycle. To illustrate this point we will consider the three-layer phosphorus budget following the same procedure as outlined for the two-layer model.

Figure 2.4.7 shows the SRP budgets for three layers, 0-20 m, 20-40 m, and 40 m-bottom, together with the corresponding seasonal variations of concentrations. As in Figure 2.4.1, the solid lines represent conversions to or from organic matter, the dash-dot lines represent net effects of vertical mixing, and the dashed lines show the net rates of change. Note that the curves for the three layers must add up to the corresponding curve for the whole lake shown in the middle panel of Figure 2.4.1. Again, the vertical lines indicate the beginning and end of the stratified season. Outside these lines the computations are somewhat ambiguous because mass exchanges can only be estimated by indirect methods.

Concentrating on the stratified season, we note that the nutrient uptake in the upper layer is confined to the spring season. The uptake in late summer shown at the top of Figure 2.4.1 is apparently a spurious result of the two-layer formulation as expected from the above discussion. There are now some indications of uptake in the second layer during this season, but this would disappear if the mixing between this layer and the

lower layer were slightly reduced. The major "biological" process in late summer is apparently the production of SRP in the bottom layer. This of course, is only true for the net conversions between organic and inorganic phosphorus. The individual biological processes in the epilimnion are far more dynamic than in the hypolimnion, as we have seen before.

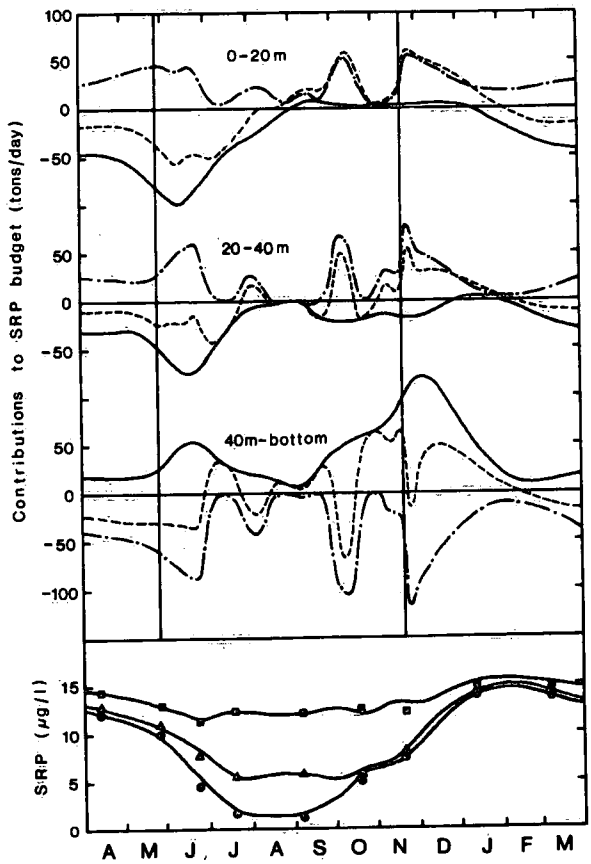

Figure 2.4.7 Same as Figure 2.4.1 but for a three-layer model. Dashed lines represent total rate of change; dash-dot lines show vertical exchange, including (in upper layer) net loading; solid lines represent net biological effect.

In spring and early summer, the results for the upper layer are consistent with the two-layer results, as they should be because the upper mixed layer is shallower than 20 metres. However, the breakdown of the lower layer into an intermediate layer and a bottom layer, shows that there

is considerable uptake of SRP in the 20-40 m layer. In principle, this could be a result of erroneous mixing estimates but the following argument shows that it is not. Suppose that the uptake were zero in this layer, then there would have to be a net loss by mixing because Figure 2.1.2 shows that the concentration in this layer drops quite substantially in early spring. Since the gradient of SRP across the 40-m level is at least of the same magnitude as that across 20 m, such a loss by mixing could only be possible if the exchange coefficient at 20 m exceeds the mixing at 40 m. This, however, is contrary to the evidence presented by all other variables which indicate a level of increased gradients and reduced mixing (thermocline) around 20 m. It must be concluded, therefore, that there is substantial uptake of SRP in the intermediate layer.

It does not appear useful to predict the response of a lake to changing phosphorus loadings by dynamical models unless such processes are fully understood and simulated. After all, it is the ability to simulate this type of process that sets a dynamical model apart from simple *static* considerations. It is not enough for a model to simulate that SRP drops to a value of 2 μg/ℓ in summer, the question is *how* it gets to that point. A similar argument can be made regarding sedimentation. We have seen that we can get a reasonable simulation by invoking some net sedimentation coefficient. If indeed it turns out that this sedimentation is made up of time-varying and counteracting effects of sedimentation and resuspension, then the latter does not qualify as a *dynamic* simulation in the true sense of the word.

2.5 Plankton Models

All models of Lake Ontario have more or less the same features, but as indicated above, their conceptualization depends on the modeler's point of view. Thus, some models may have more variables and others fewer. Relationships among compartments may be formalized differently, but given the paucity and scatter of the data, most models are able to give an adequate representation of the phenomena involved. This happens also because physical factors play a major part, much larger than in models of small lakes or reservoirs.

A number of aquatic plankton models are available in the literature, ranging from very simple models such as Steele's (1974) to multi-component systems described by Park (1974). Thomann *et al.*(1974) modified the dynamic phytoplankton model of DiToro *et al.*(1971) to simulate the seasonal cycle in Lake Ontario. Chen *et al.*(1975) adopted a version of Chen and Orlob's (1975) Lake Washington model to simulate the three-dimensional nutrient-plankton interactions in Lake Ontario during IFYGL. Scavia *et al.*(1976) formulated a seasonal Lake Ontario plankton model concentrating on the interactions of various phytoplankton and zooplankton species. Before turning to a discussion of our own experiments, it is perhaps useful to summarize the basic properties of the above models.

Manhattan Model

Thomann *et al.*(1974) were the first to apply a fairly complete dynamic plankton model to Lake Ontario. The variables considered in the model are phosphate, nitrate, ammonia, non-living organic nitrogen and phosphorus, phytoplankton, and zooplankton separated into herbivores and carnivores. Photosynthesis is formulated according to Equation (6a) of Chapter 2.3, including the limiting effects of nitrogen as well as phosphorus. Grazing by zooplankton is proportional to the product of predator and prey. Dead organic matter originates from algal losses, zooplankton death, and the undigested portion of grazing. Decomposition of organic components to nutrients is simulated by first order reaction kinetics. All rate coefficients are proportional to temperature. The coefficients were adjusted by simulating a typical seasonal cycle derived from 1966-1970 surveillance data on Lake Ontario.

The Manhattan model was programmed at CCIW for use in the three-dimensional IFYGL simulations discussed by Simons (1976b). While the model appeared to reproduce the earlier data reasonably well, the agreement with the IFYGL data presented in Chapter 2.1 was rather unsatisfactory. In this context, it is to be realized that the physical effects (radiation, temperature, mixing) were based on IFYGL observations (Chapters 2.2-3) and thus different from the corresponding data used by Thomann *et al.* It is of little interest to analyze the model behaviour in more detail because we understand that the original authors are presently re-evaluating the model in light of the IFYGL data. It may be useful to point out, however, that

this type of model does not incorporate any mechanisms to deal with the phosphorus budget problems outlined in the previous section. Thus phosphorus uptake is essentially confined to the upper mixed layer and sedimentation is more or less uniform in time.

Scavia Model

The Scavia *et al.*(1976) model includes essentially the same nutrient-plankton interactions as the Manhattan model, but the phytoplankton-zooplankton interactions are treated in more detail. Phytoplankton is broken down into small and large diatoms and small and large non-diatoms. Zooplankton compartments include small and large cladocerans, copepods, rotifers, and carnivores. Another feature of the model is an attempt to simulate the sinking of detritus and phytoplankton by a detailed time-and-species-dependent formulation of settling rates. As a result, small phytoplankton groups reach much higher spring peaks in the model solutions than the larger species.

Again, the Scavia model was programmed at CCIW on the basis of information presented in the technical report by Scavia *et al.*(1976). The model was run with the physical data presented in Chapters 2.2-3, whereas the settling calculation was simplified to take into account only effects of size distributions. We understand that the original model has been undergoing substantial changes, so it is of little interest to compare these simulations with the original ones.

Typical Plankton Model Solutions

The above plankton models can be expanded to include more compartments, such as the model applied to Lake Ontario by Chen *et al.* (1975). In regard to basic nutrient-plankton interactions, however, the models are reasonably similar. To put the following discussion in a better perspective, it may be useful to illustrate some typical solutions from these first-generation Lake Ontario models. As an example, we take a model having the following variables: Soluble reactive phosphorus, nitrite and nitrate, ammonia, soluble organic nitrogen, detritus, small ($< 20\ \mu$) and large ($> 20\ \mu$) phytoplankton, cladocerans, copepods, and carnivores. We take the appropriate kinetic coefficients from the report by Scavia *et al.*(1976), so there is no need to reproduce them here. Note

however, that the complete Scavia model incorporates additional components, so the following results should not be construed as a measure of the performance of that model. By recourse to the phosphorus simulations in Chapter 2.4, we specify the settling velocities for detritus and large phytoplankton to vary from .30 in the upper layer to .45 in the bottom layer of a three-layer model. Sedimentation velocities of small phytoplankton are assumed to be one-third of the above. The model is run with the light, temperature, and mixing data presented in Chapters 2.2-3, and nutrient loadings are based on the data of Chapter 2.1.

Figure 2.5.1.a shows model solutions of SRP, NO_3, and NH_3, for the three model layers, together with the corresponding observations from Chapter 2.1. For our purpose, the interesting aspect of the solutions is the similarity between SRP and NO_3 in the model as contrasted with the observed difference in behaviour. Thus, the current type of model cannot account for the uptake of SRP below the thermocline. Also, like the Manhattan model, the model over-predicts ammonia. Figure 2.5.1.b shows computed and observed values of the different plankton groups in the upper layers, again indicating interesting discrepancies. It is to be expected that further experimentation with these models will lead to a better agreement with the data base. It should be borne in mind, however, that this does not necessarily add to our predictive ability although it may attest to the ingenuity of mathematical modelers.

As a further extension of our discussion of the phosphorus balance in the previous chapter, we computed a nutrient balance for a one-year run of the present model, starting from the first OOPS cruise and using observed net loads to the lake (see Chapter 2.4). The results are presented in Table 2.5.1. It is seen that, although the model appears to simulate the basic seasonal variations of the primary nutrients, the solutions are far removed from equilibrium. Assuming that we want to construct a model in balance with the loading, then the total P and N balance is about right (± 10% of net loading), but there is not enough uptake of SRP, NO_3, and especially NH3, to make up for the loss of particulate P and N by sedimentation. Note that only 20% of the net loading of SRP is converted to organic forms, while the net uptake of inorganic nitrogen is actually negative and hence could never balance the loading. While the actual

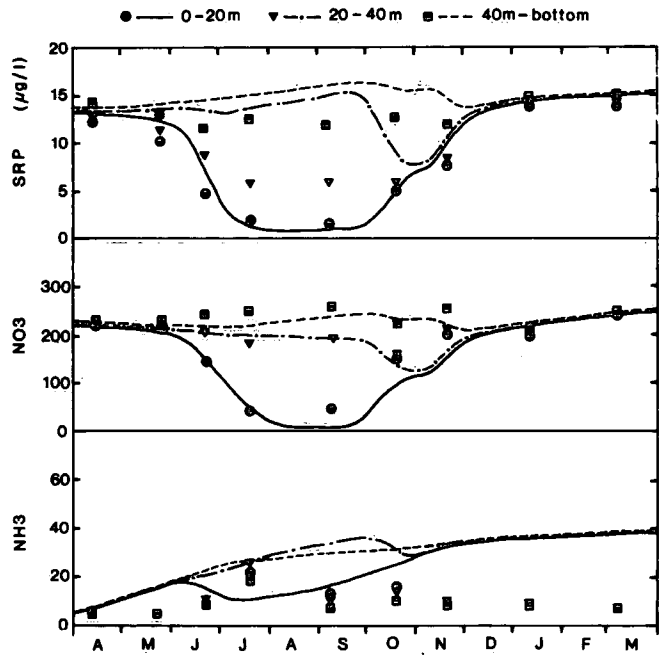

Figure 2.5.1.a Comparison of simulations by three-layer plankton model with observations for SRP, NO_3 and NH_3.

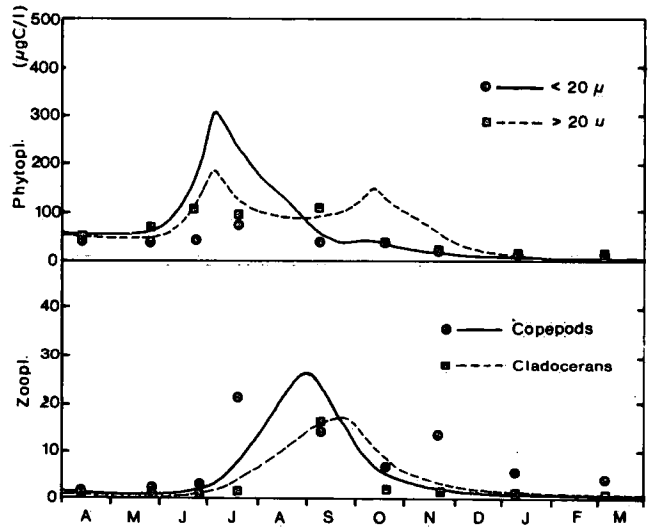

Figure 2.5.1.b Comparison of simulations by three-layer plankton model with observations; phytoplankton and zooplankton in the epilimnion.

numbers naturally differ for various models, this example indicates the problems facing us if we want to use models of plankton cycles for predictive purposes.

TABLE 2.5.1: *Budgets of variables in modified Scavia model, Apr 72-Mar 73*

Parameter	Kinetics	Net Loading	Sedimentation	Net Change
SRP	-2.1	10.1	0.	8.0
PP (.024 PC)	2.1	17.5	-31.5	-11.9
Total P	0.	27.6	-31.5	-3.9
NO_3	-35	110	0	75
NH_3	51	91	0	142
SON	-32	-70	0	-102
PN (.18 PC)	16	131	-236	-89
Total N	0	262	-236	26
PC	88	728	-1312	-496

Halfon's Model

An example of a somewhat different plankton model is the one developed by Halfon at CCIW, reflecting some of the more recent development in ecological modeling (Bierman, 1976; Jorgensen, 1976; Parnas and Cohen, 1976). The essential difference from the foregoing models is that luxury uptake and storage of nutrients in the cell are explicitly simulated. The model also incorporates a different concept of nutrient uptake and respiration.

The model is made up of nine state variables. Four of these can be measured or estimated: phytoplankton carbon, detrital carbon, soluble reactive phosphorus (SRP) and soluble organic phosphorus (SOP). The other five are latent, i.e., unobservable and unmeasurable by current methodologies. They are phytoplankton phosphorus with fast and slow metabolism, respectively, zooplankton carbon and phosphorus, and detrital phosphorus. The model also has two outputs which are linear combinations of state variables, namely, particulate phosphorus and total filtered (soluble) phosphorus. These again can be compared with measurements. The model

structure is shown in Figure 2.5.2; the mathematical formulations are presented in Table 2.5.2. The latter are based on the following concepts: carbon and phosphorus interact with each other in the cells. However, phosphorus uptake and release rates are higher than carbon rates. Turnover time of phosphorus in a lake ranges between four minutes and 12 hours. Phosphorus limitation may be felt on the algal cell not as a decrease in growth, but as increase in respiration: a response to a state of stress. This has been found in laboratory cultures by Humphrey (1973). When these observations are included in the model, the ratio of carbon to phosphorus may change in time according to the algal state. The other hypothesis included in the model is that the algal cell stores phosphorus when environmental conditions are good and the cells are growing. This phosphorus is used up when phosphorus in the cell decreases and a stress situation may occur. The mathematical formulation of this process follows the theoretical ideas formulated by Parnas and Cohen (1976). The first assumption is that storage occurs only when phosphorus in the cell is greater than is needed for growth and there is a possibility of shortage in the future. The second assumption is that storage is utilized only when a short period of starvation is expected so that it is optimal for the cell growth to have additional phosphorus available. In this instance, this period is September to November, when lake circulation brings back into the epilimnion SRP which can be readily utilized by the cells.

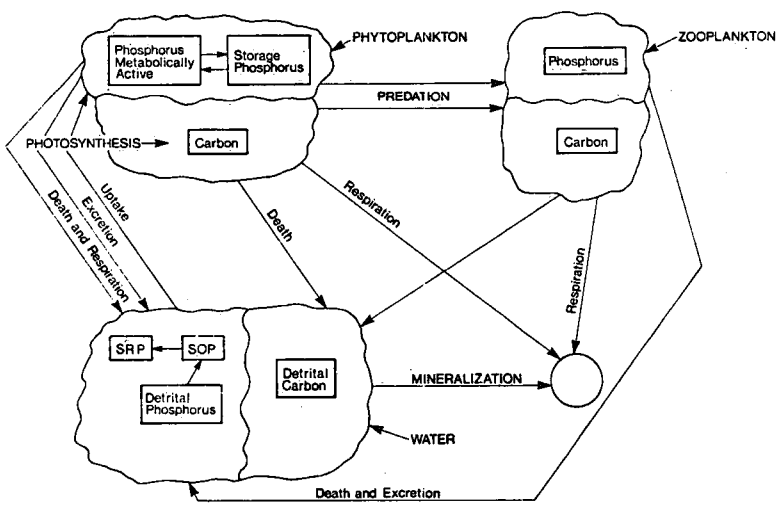

Figure 2.5.2 Conceptual model structure.

TABLE 2.5.2: *Mathematical model of Lake Ontario*

STATE VARIABLES		OBSERVABILITY
X_1	Phosphorus in algal cells ($\mu g\ P\ \ell^{-1}$)	Unobservable
X_2	SRP ($\mu g\ P\ \ell^{-1}$)	Observable
X_3	Carbon in algal cells ($\mu g\ C\ \ell^{-1}$)	Unobservable
X_4	Phosphorus storage in algal cells	Unobservable
X_5	Carbon in zooplankton ($\mu g\ C\ \ell^{-1}$)	Unobservable
X_6	Phosphorus in zooplankton ($\mu g\ P\ \ell^{-1}$)	Unobservable
X_7	Detrital carbon ($\mu g\ C\ \ell^{-1}$)	Unobservable
X_8	Detrital phosphorus ($\mu g\ P\ \ell^{-1}$)	Unobservable
X_9	SOP ($\mu g\ P\ \ell^{-1}$)	Observable

OUTPUTS

$Y_1 = X_1 + X_6 + X_8$	Particulate Phosphorus ($\mu g\ P\ \ell^{-1}$)	Observable
$Y_2 = X_2 + X_9$	Soluble Phosphorus ($\mu g\ P\ \ell^{-1}$)	Observable

INPUTS

Z_1	Water temperature (^oC)
Z_2	Light extinction coefficient (m^{-1})
Z_3	Solar radiation (Langleys day^{-1})
Z_4	Day length (fraction)

COEFFICIENTS

P_{max}	Maximum uptake of SRP ($\mu g\ \ell^{-1} day^{-1}$)
a's	Rate constants (day^{-1})
k's	Concentrations ($\mu g\ \ell^{-1}$)

TABLE 2.5.2: (Cont'd)

RELEASE OF PHOSPHORUS DURING GROWTH

$$g = 1.059^{z_1} \frac{x_1}{k_2 + x_1}$$

ZOOPLANKTON PREDATION ON PHYTOPLANKTON

$$p_1 = (a_1 f_1 + a_2 f_2) x_1 x_5 / (k_3 + x_3)$$

$$p_2 = (a_1 f_1 + a_2 f_2) x_3 x_5 / (k_3 + x_3)$$

RATE OF PHOSPHORUS STORAGE OR RELEASE FROM STORAGE

$$s = x_4(1-x_4) \qquad 0 \leq x_4 \leq 1$$

TEMPERATURE EFFECTS

$$f_1 = z_1/20$$

$$f_2 = 20/z_1$$

PHOTOSYNTHESIS

$$u = \rho(z_3, z_2, z_4) \qquad 1.059^{z_1}$$

RESPIRATION

$$r = 1.059^{z_1}/(1.059^{z_1} + x_1/k_4)$$

TABLE 2.5.2: (Cont'd)

MODEL EQUATIONS

$$\frac{dx_1}{dt} = P_{max}\left(\frac{x_2}{k_2 + x_2} - g - sgn(\frac{dx_1}{dt})\ s\ g\right) - p_1 - a_{91}\ f_2\ x_1$$

$$\frac{dx_2}{dt} = P_{max}\left(g - \frac{x_2}{k_2 + x_2}\right) + a_{29}\ x_9 + a_{25}\ f_1\ x_6$$

$$\frac{dx_3}{dt} = a_0\ (u - r)x_3 - a_{72}\ f_2\ x_3 - P_2$$

$$\frac{dx_4}{dt} = sgn(\frac{dx_1}{dt})\ s\ g$$

$$\frac{dx_5}{dt} = P_2 - a_{25}\ f_1\ x_5 - a_{75}\ x_5^2/k_5$$

$$\frac{dx_6}{dt} = P_1 - a_{25}\ f_1\ x_6 - a_{75}\ x_6^2/k_6$$

$$\frac{dx_7}{dt} = a_{72}\ f_2\ x_3 - a_{97}\ f_2\ x_7 + a_{75}\ x_5^2/k_5$$

$$\frac{dx_8}{dt} = a_{75}\ x_6^2/k_6 - a_{97}\ f_2\ x_8$$

$$\frac{dx_9}{dt} = a_{97}\ f_2\ x_8 + a_{91}\ f_2\ x_1 - a_{29}\ x_9$$

Zooplankton is made up of two compartments, one describing the carbon, and one describing the phosphorus in the animals. Again, these compartments are decoupled but they behave similarly because the uptake and release functions are the same. Zooplankton is not subdivided into species because of the lack of information at the level required by the model. However, to take into account the fact that different species behave in a different manner, two terms describe the feeding upon phytoplankton. The grazing terms of zooplankton were derived as follows: grazing depends upon the phytoplankton and zooplankton biomass (carbon). At high phytoplankton densities grazing levels off. This is expressed with a Michaelis-Menten function. Thus zooplankton grazing rate (carbon) is

$$p_i(C) = K_2 \frac{\text{phyto (C) zoo (C)}}{k_3 + \text{phyto (C)}} f_i(z_3)$$

where f_i (z_3), $i = 1, 2$, is a function of temperature. Phosphorus concentrations within phytoplankton and zooplankton cells are also affected by this grazing and the amount of phosphorus that transfers from phytoplankton to zooplankton is $p_i(C) \frac{\text{phyto (P)}}{\text{phyto (C)}}$, where phyto (P)/phyto (C) is a time varying ratio of circulations. Thus

$$p_i(P) = K_2 \frac{\text{phyto (P) phyto (C) zoo (C)}}{\text{phyto (C) } (k_3 + \text{phyto (C)})} f_i(z_3)$$

$$= K_2 \frac{\text{phyto (P) zoo (C)}}{k_3 + \text{phyto (C)}} f_i(z_3).$$

Detritus (carbon and phosphorus) receives inputs from the environment as well as from dead algae and zooplankton. Bacterial action is implicitly described by the solution of particulate phosphorus into soluble organic phosphorus (SOP). Soluble organic phosphorus receives phosphorus also from algae and zooplankton and releases phosphorus to the inorganic pool, thus completing the cycle. Phosphorus thus cycles through the system and influences the plankton in a feedback mode.

Results of a simulation run of the model are presented in Figures 2.5.3-2.5.5. The first two figures show model variables which can be compared with measurements, soluble and particulate phosphorus (Figure 2.5.3) and soluble reactive and soluble organic phosphorus (Figure 2.5.4). As shown in Table 2.5.2, the first two model outputs are linear combinations of a number of state variables which, individually, may not be observable.

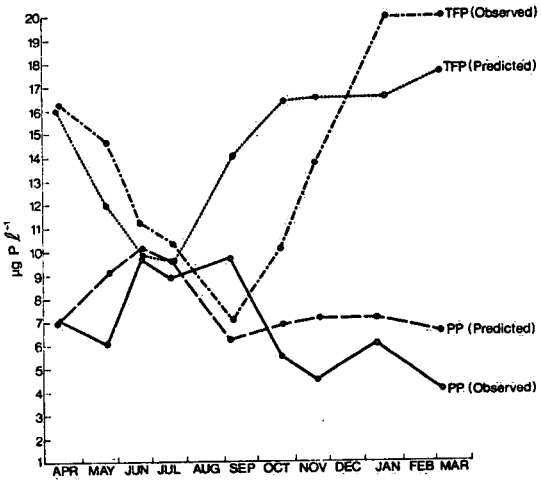

Figure 2.5.3 Observations and model simulations of observable variables. TFP is total filtered phosphorus, (soluble) and PP is particulate phosphorus. Results for the first layer, top 20 metres.

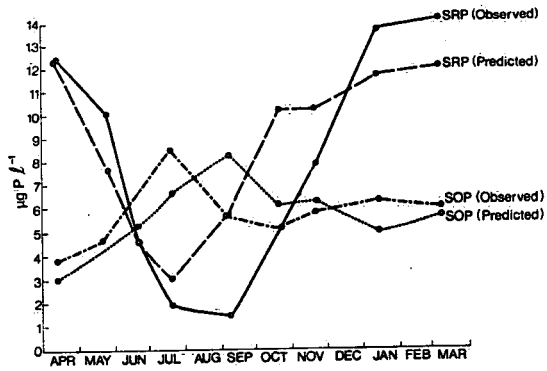

Figure 2.5.4 Observations and model simulations of observable variables. SRP is soluble reactive phosphorus and SOP is soluble organic phosphorus. Results for the first layer, top 20 metres.

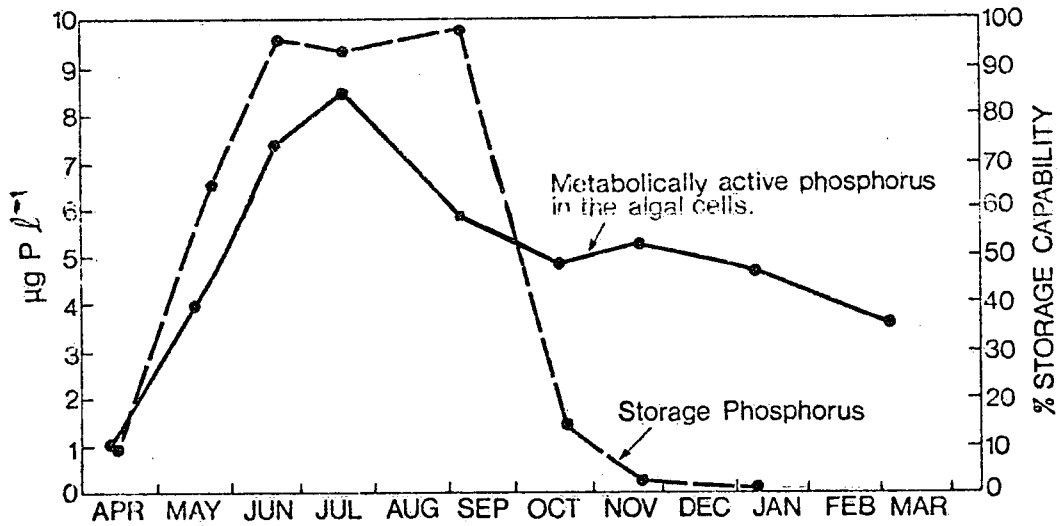

Figure 2.5.5 Model simulations of metabolically active phosphorus and storage phosphorus in phytoplankton.

One of the advantages of the state space approach is that we have some information on the internal dynamics of the system. One of the most evident and interesting features of the model is that soluble organic phosphorus (SOP) has very slow kinetics compared with other chemical forms of phosphorus. Soluble reactive phosphorus (SRP) is taken up and released in a time of the order of magnitude of minutes. SOP, instead, has a turnover time of the order of months. Indeed, a small amount of phosphorus goes through the SOP form; most phosphorus circulates only between plankton and water. Thus, for a successful modeling of a seasonal cycle SOP need not be included in the model structure. However, the long turnover time of SOP may be important for long-term simulations and should therefore be included in a detailed model. This inclusion, however, is not a simple thing to accomplish. SOP is a refractory form of phosphorus and its formation and metabolism are still obscure. The quantification of its dynamics is therefore subject to errors. The one-year fit may be good (Figure 2.5.4), but a wrong formulation may lead to disastrous long-term conclusions. A model without an SOP compartment would probably behave better, but could we call it an adequate model? Successive aggregations of the model compartments would produce more abstract models which can be compared with one another for adequacy. The theory of this approach is well developed (Zeigler, 1976; Halfon and Reggiani, 1978). The problems

are with the lack of understanding of biological processes. In this regard, collaboration with field ecologists is imperative.

Figure 2.5.5 shows the hypothetical behaviour of the metabolically slow phosphorus or storage form in phytoplankton cells. The model shows that this form of phosphorus is accumulated in the cells between April and June: 94% of storage capability is utilized. High reserves are kept until September, and indeed these reserves are even slightly increased between July and September, when SRP concentration in the water is rapidly falling, and other forms of phosphorus available to the cell for growth are also decreasing. Only when SRP is really low, but the cells can still grow because of good environmental conditions (optimal light and temperature), the storage is rapidly utilized and in about a month, reserves fall from 98% to 15%. The rest is utilized in October and November. In the meantime, the phosphorus within the cells which is metabolically active remains quite stable, in spite of large changes in SRP and storage. The algae show a homeostatic mechanism.

Inference

Even if we could say that a model is validated, we are still left with the problem of predicting the long-term behaviour of a lake. One option is to use a partially validated model that describes the seasonal cycle of biological, physical and chemical variables. As mentioned previously (Section 2.4), several models can describe the seasonal behaviour over a year. This does not mean that they are validated, since we lack information on the model validity under different conditions, for example, increased or decreased loadings. Another hazardous aspect of time extrapolation is that solar irradiance and lake temperature are stochastic inputs which can be predicted only with a margin of uncertainty. Models are very sensitive to these inputs, so that prediction over more than a few years is unreliable. This conclusion is not encouraging, since we expect to see variations in the state of the lake, in this case, Ontario, only over a long span, say 10 to 20 years.

Our conclusion is, therefore, that the immediate rewards of seasonal model studies must be sought not so much in the use of such models for long-term predictions, but rather as a means of testing hypotheses set up by field ecologists. If field work and the development

of systems models proceed together, they can be used to test respective results. When we have developed a satisfactory model structure which is acceptable to field ecologists and which produces a set of behaviours totally acceptable, then we can say that these hypotheses are likely correct. Over the long run, given this better understanding of the lake processes, coupled with a more definite knowledge of loadings to the lake, we ought to be able to reduce the range of uncertainty of our models.

Chapter 3

LONG-TERM ANALYSIS AND SIMULATION

3.1 Physical and Biochemical Observations, 1966-1977

Temperature

The water quality concerns addressed in this report are dependent upon the thermal characteristics of Lake Ontario which influence the rates of chemical and biological processes and current patterns. A first approximation of the temperature regime of the lake for the years 1966-1977 is discussed.

Temperature from 181 synoptic surveys, conducted by the Canada Centre for Inland Waters, forms the basis from which the long-term estimates of the thermal characteristics of Lake Ontario can be deduced. For most years, intensive measurements of temperature and other physical and biochemical parameters were observed throughout the regular field period April through November. Extrapolation of temperatures to winter months is possible by reference to measurements conducted for seven of the twelve years which included observations in this interval.

Profiles of lake temperature were determined from bathythermograph (BT) prior to 1972 and from electronic bathythermograph (EBT) thereafter. Calibration of instrumentation is done routinely before and after the field program. Periodic checks of calibration for BT were done by comparison to a reference temperature, and for EBT, this is done internally. Intercomparison of measurement systems showed comparable results and, on this basis, data are considered reliable.

Synoptic cruise patterns and station locations varied considerably, especially prior to 1972, but in general, network densities were of the order of one station per 200 km^2. The effect of varying cruise patterns and station locations on the reliability or comparability of results from year to year has not been evaluated.

Continuous analogue traces of temperature versus depth have been processed by digitizing to a maximum of nine appropriate points which conserve the predominant features of the temperature profile. This is done for each station and cruise. Using these data and a knowledge of the

lake bathymetry, values are area and volume weighted by a procedure similar to the Theisson polygon approach utilizing 2 km grid squares.

For the purposes of the water quality models discussed elsewhere in this report, the thermal characteristics of Lake Ontario are described for three distinct layers. Seasonal cycles of the lakewide mean temperature for layers 0-20 m, 20-40 m and 40-225 m are depicted in Figures 3.1.1 (a-l) for individual years. These include surface temperature (0m), which has been determined from the values given by the air-borne thermometry program of the Atmospheric Environment Service (AES, 1977). Monthly means for all layers (Table 3.1.1) have been determined by hand integrating interpolated layer temperatures. The interpolation for each layer was done through lakewide mean temperatures plotted at the cruise midpoints. In general, cruises were completed within a period of one week and this tends to reduce aliasing effects. Long-term means shown in Table 3.1.2 have been determined by interpolation using all 181 cruise data extending from 1966-1977. Mean lake temperature has also been included.

The long-term means (Figure 3.1.2) show a well-defined seasonal pattern for each layer. For Lake Ontario, thermal stratification is established at mid-April and a return to homothermy is expected in early December. Maximum mean surface temperature (0m) approaches 20°C near the end of July, while the long-term maximum for the 0-20 m layer occurs approximately one month later and prior to the maximum lake temperature, which is directly proportional to lake heat content. The time progression and consequent lag in seasonal temperature maximums is clearly illustrated for each layer.

As indicated previously, the annual thermal characteristics for each layer have been deduced by interpolation through mean lakewide temperatures plotted at the cruise mid-point. In most instances, cruises were of sufficient frequency that this technique allows for reasonable assessment of the annual seasonal trends. Cruises during IFYGL were initiated at one to two week periods, while those for other years occurred at approximately two to four week intervals. Exceptions were year 1971 and the latter half of 1973 in which very few field programs were initiated. Layer temperatures in these years have been subjectively determined with

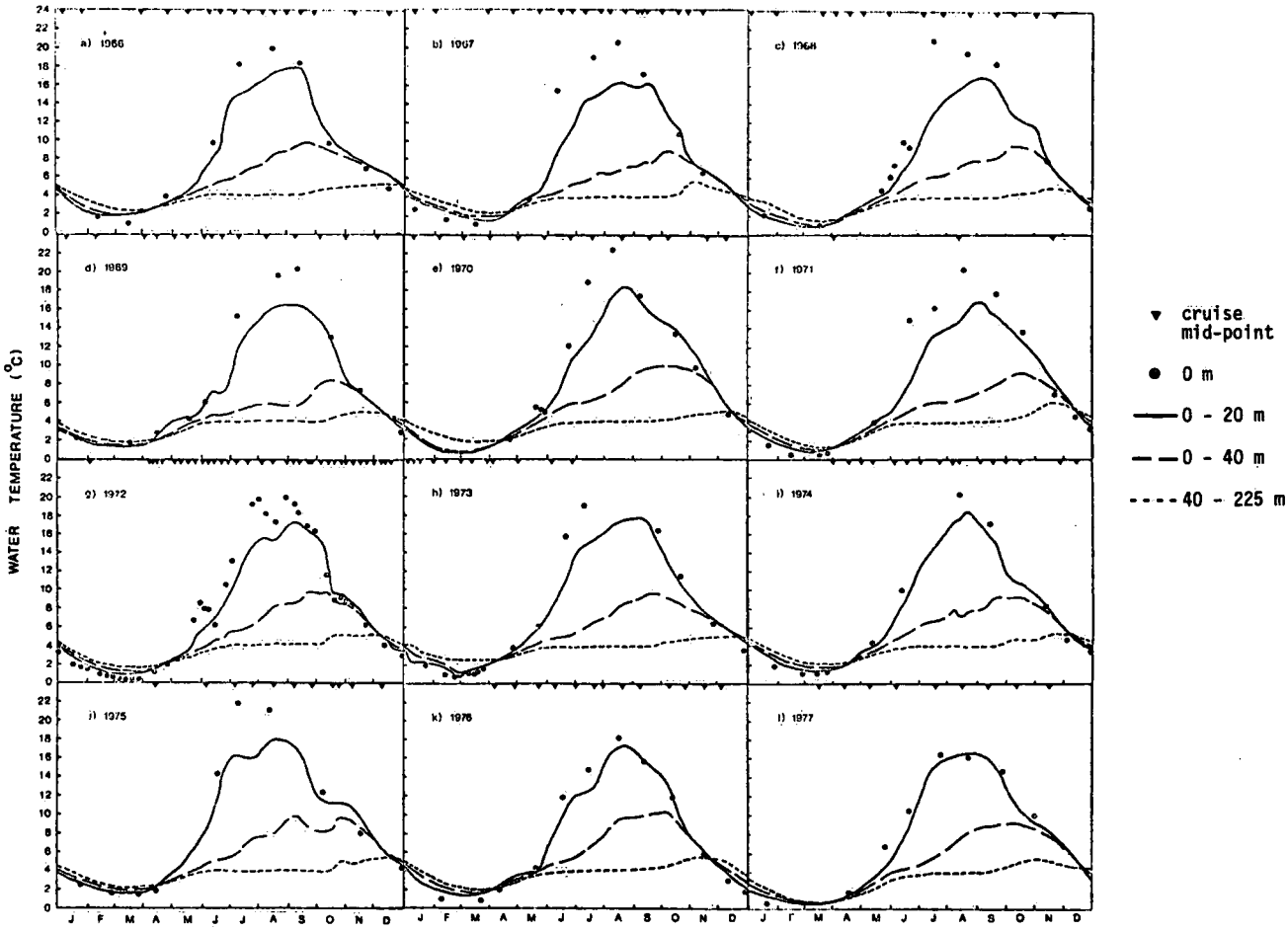

Figure 3.1.1 Seasonal cycles of the lakewide mean temperature, 1966-77.

TABLE 3.1.1: *Monthly mean water temperature in Lake Ontario 1966-77. (1, 0-20 m; 2, 20-40 m; 3, 40-225 m)*

		J	F	M	A	M	J	J	A	S	O	N	D
66	1	3.3	2.0	1.9	2.7	4.4	9.1	15.2	17.1	16.7	10.7	7.8	6.1
	2	3.7	2.3	1.9	2.6	3.9	5.1	6.4	7.9	9.5	9.9	7.5	6.1
	3	4.3	3.0	2.3	2.6	3.4	4.1	4.0	4.1	4.1	4.7	5.0	5.2
67	1	3.5	2.4	1.7	2.1	4.2	9.5	14.5	15.9	15.7	11.8	7.0	4.8
	2	3.7	2.7	1.8	2.0	3.6	4.7	5.9	6.8	7.7	8.5	6.9	4.9
	3	4.2	3.2	2.4	2.4	3.3	3.9	4.0	4.0	4.0	4.6	5.3	4.4
68	1	2.2	1.3	1.0	2.1	3.9	7.3	12.7	15.9	16.5	12.6	8.6	4.7
	2	2.7	1.7	1.1	2.0	3.6	5.0	6.2	7.3	8.1	9.4	7.6	4.7
	3	3.6	2.3	1.5	2.0	3.0	3.9	4.0	4.0	4.1	4.4	4.9	4.5
69	1	2.3	1.4	1.3	2.5	4.3	7.0	12.9	16.0	16.1	12.6	7.1	4.7
	2	2.6	1.6	1.5	2.1	3.6	4.6	5.3	5.7	6.3	8.2	6.9	4.7
	3	3.0	2.1	1.8	2.1	3.1	3.9	3.9	4.0	4.0	4.3	4.9	4.7
70	1	2.2	0.7	0.8	0.9	4.1	8.1	15.1	17.7	16.1	13.7	9.9	5.2
	2	2.4	0.9	0.9	0.9	3.5	5.3	6.2	7.7	9.7	9.8	8.8	5.2
	3	3.3	2.3	1.8	0.9	2.9	3.7	3.9	3.9	4.0	4.3	4.7	4.9
71	1	2.6	1.2	0.8	2.2	3.9	7.5	12.8	15.4	15.8	13.0	9.2	5.4
	2	3.0	1.6	1.1	2.0	3.4	4.9	6.0	6.5	7.8	9.0	8.0	5.4
	3	3.6	2.0	1.4	2.0	3.1	3.9	4.0	4.0	4.1	4.4	5.7	5.4
72	1	2.9	1.4	0.9	1.7	3.6	7.2	13.0	15.7	16.7	11.7	7.7	4.6
	2	3.2	1.7	1.3	1.7	3.0	4.5	5.7	7.8	9.1	9.1	7.4	4.6
	3	3.5	2.1	1.7	1.8	2.7	3.6	4.0	4.1	4.1	4.7	5.0	4.7
73	1	2.5	1.6	1.6	2.8	5.1	10.1	14.1	17.2	16.9	11.9	7.9	5.6
	2	3.0	1.9	1.7	2.7	3.9	5.0	6.2	9.5	9.3	8.9	7.4	5.7
	3	3.6	2.7	2.5	2.7	3.5	3.9	3.9	4.0	4.0	4.6	4.9	5.0
74	1	3.4	1.9	1.5	2.4	4.3	8.1	14.3	17.6	15.4	10.7	7.9	4.7
	2	3.6	2.3	1.8	2.3	3.7	5.3	6.6	7.6	8.7	9.0	7.5	4.9
	3	4.0	2.7	2.1	2.3	3.3	3.9	4.0	3.9	4.1	4.6	5.0	4.9
75	1	3.0	1.9	1.6	2.4	5.3	11.5	16.1	17.6	15.3	11.3	9.9	5.9
	2	3.4	2.4	2.0	2.4	3.7	5.0	6.6	8.3	9.2	8.8	8.7	5.9
	3	3.7	2.6	2.2	2.4	3.3	3.9	3.9	3.9	4.0	4.5	4.9	5.3
76	1	3.1	1.7	1.4	2.6	4.1	9.5	12.9	16.9	15.5	11.0	6.1	4.3
	2	3.7	2.2	1.7	2.5	3.7	4.9	6.6	8.2	10.0	9.3	6.3	3.9
	3	4.1	2.4	2.1	2.4	3.4	3.9	4.0	4.0	4.2	4.8	5.3	3.3
77	1	1.6	0.8	0.6	1.4	3.6	8.0	14.7	16.4	15.6	10.7	8.3	5.4
	2	2.1	1.1	9.7	1.3	2.9	4.3	5.3	7.6	8.9	9.1	7.9	5.4
	3	2.5	1.2	0.7	1.2	2.3	3.4	3.8	3.9	4.1	5.0	5.1	4.5

reference to trends in long-term means and by extrapolation with reference to surface temperature (0m) values given by the infrared thermometry technique (AES, 1977) in comparison to other years.

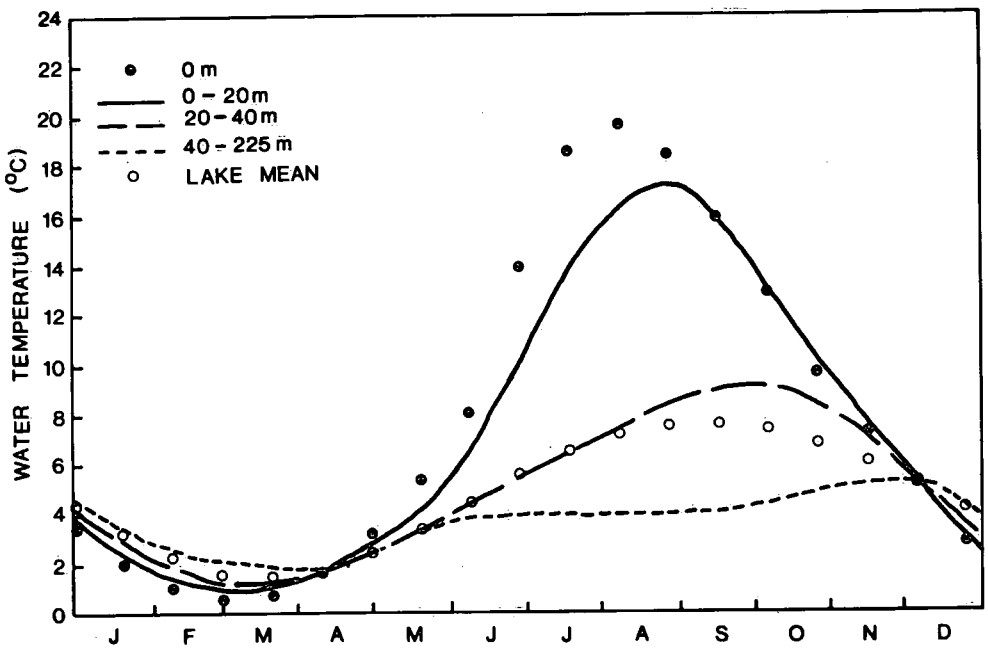

Figure 3.1.2 Long-term mean of seasonal temperature cycle (1966-77).

TABLE 3.1.2: *Long-term mean lakewide temperature for Lake Ontario 1966-77*

Layer	J	F	M	A	M	J	J	A	S	O	N	D	Mean
0 m	2.4	0.9	0.8	2.0	5.1	10.4	17.7	19.1	16.0	10.9	7.2	4.1	8.1
0 - 20 m	2.8	1.3	1.0	2.0	3.9	7.7	13.1	16.7	15.9	11.8	7.9	4.2	7.4
20 - 40 m	3.2	1.7	1.2	1.9	3.2	4.6	6.4	7.9	8.8	8.8	7.1	4.4	5.0
40 - 225 m	3.7	2.4	1.9	1.9	3.0	3.9	4.0	4.0	4.1	4.5	5.1	4.7	3.6
Lake Mean	3.6	2.1	1.5	1.9	3.2	4.7	6.4	7.3	7.5	7.1	6.1	4.7	4.7

The annual variability in temperature is substantially more pronounced for the surface water layers, as they respond to short-term meteorological fluctuations - being especially evident at 0 m (Figure 3.1.1). Conversely, values at 20-40 m and 40-225 m show relatively small deviation from long-term means, and consequently, subjective extrapolations in 1971 and 1973 for these layers may be considered reasonable. Figure 3.1.3 shows layer temperature ranges from all cruise data conducted from 1966-1977. In general, these would tend to indicate that for years 1971 and 1973, extrapolations with little or no data can result in large errors primarily in the surface layers 0 m and 0-20 m. For the layer 0-20 m, a maximum error of 3-4°C can result. However, it is assumed that with reference to long-term means and measured surface temperatures reasonable approximations are made for the 0-20 m layer for those years.

Incoming Global Radiation

Incoming global radiation (280-2800 nm) was measured at shoreline meteorological stations and at buoy locations in Lake Ontario (Figure 3.1.4). Observations were conducted using Eppley or Kipp pyranometers and were recorded on analogue strip chart, integrator tape or magnetic tape. Continuous measurements at all sites were integrated over hourly intervals and formed into daily totals. Instrument calibration and maintenance is conducted routinely by supervising agencies. Analysis of recorded observations during IFYGL (Davies and Schertzer, 1974) indicated no significant systematic or recording errors in the global radiation flux during IFYGL and, as such, it is assumed that all measurements from the same supervisory agencies are reliable.

The record of observation for each station (Table 3.1.3) illustrates a dearth of direct measurements for most years except during the period 1972-73 which corresponds to the intensive monitoring during the IFYGL program. This lack of spatial resolution in most years necessitates the inclusion of supplementary computation of flux estimates using other meteorological data. The paucity of direct measurements is such that the only readily available long-term global radiation observations are those at CCIW.

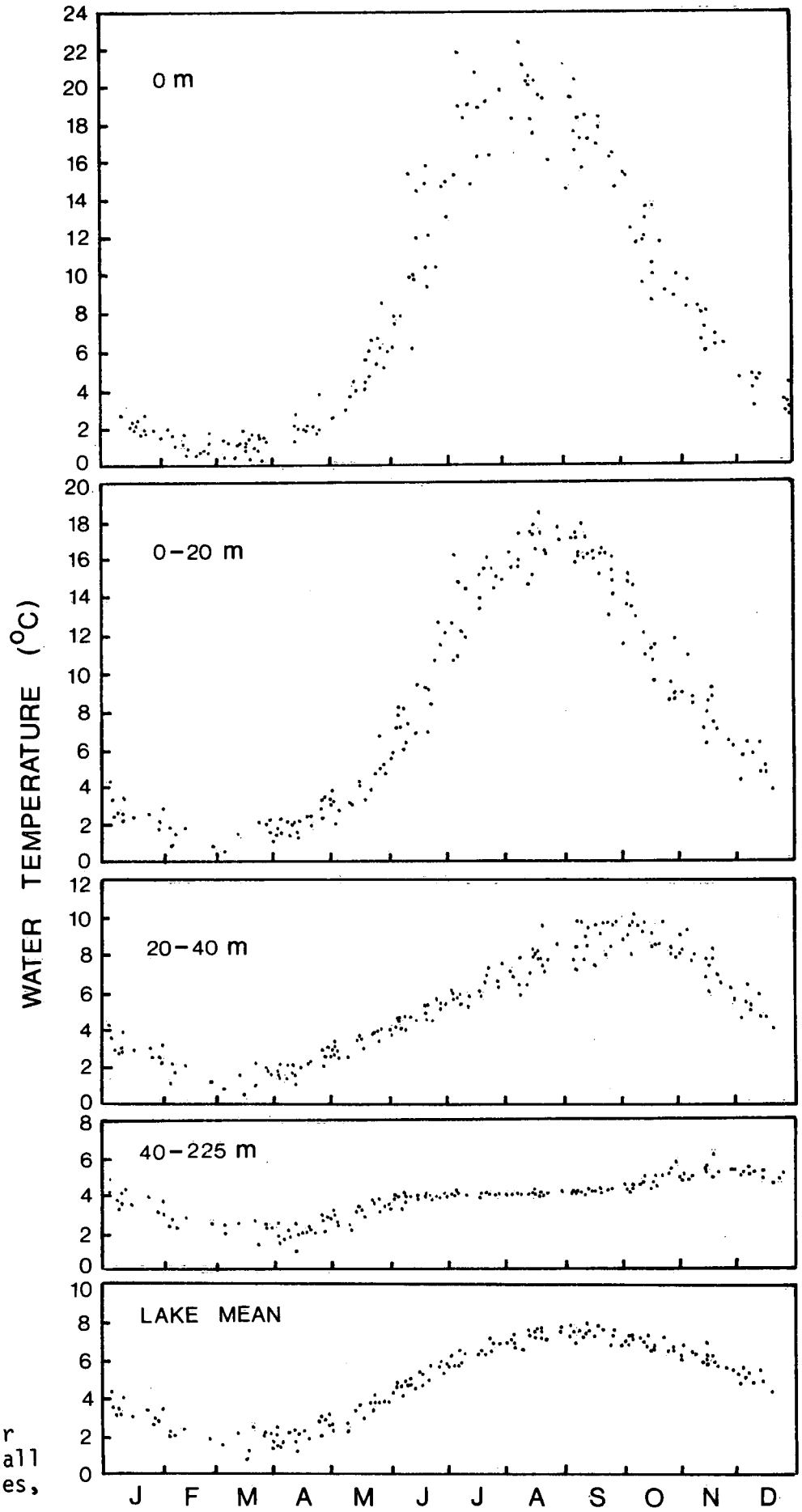

Figure 3.1.3 Layer temperatures from all surveillance cruises, 1966-77.

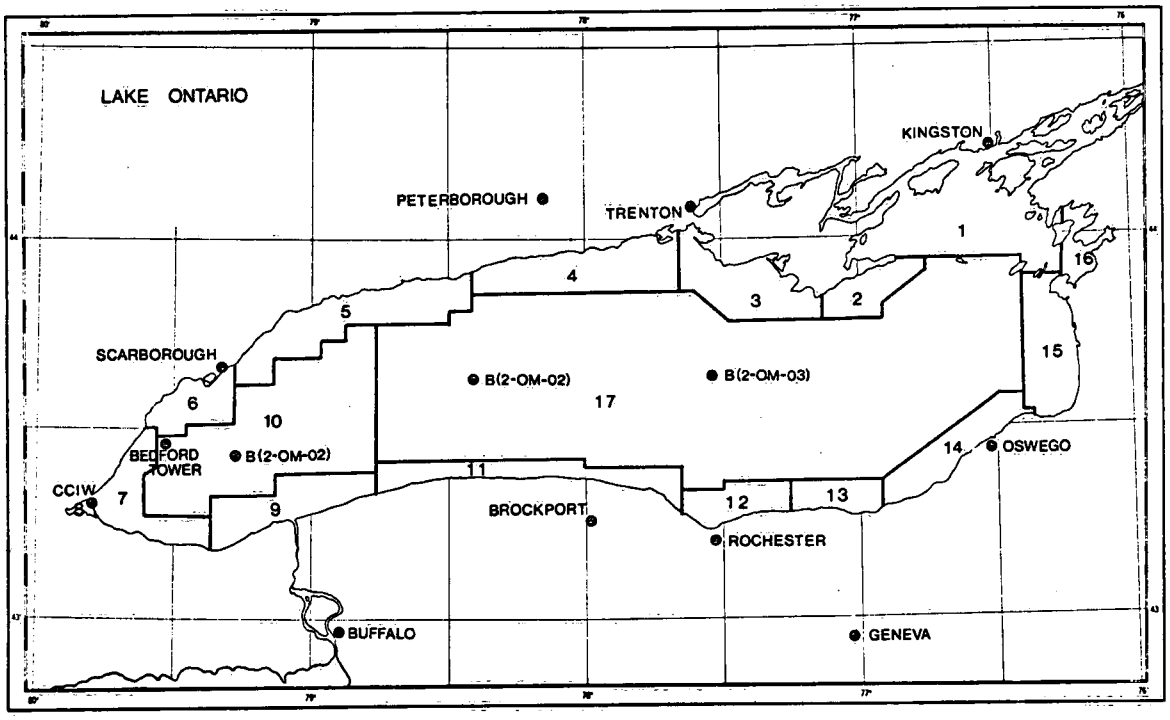

Figure 3.1.4 Location of shoreline and buoy meteorological stations in Lake Ontario.

TABLE 3.1.3: *Computation of lake-wide mean global radiation; availability of yearly data. X = global radiation, Y = sunshine hours.*

Station	'66	'67	'68	'69	'70	'71	'72	'73	'74	'75	'76
Canadian:											
CCIW			Y	XY	XY	XY	XY	XY	XY	XY	XY
Scarborough	Y	Y	Y	Y	Y	Y	XY	XY	Y	Y	Y
Peterborough							X	X			
Trenton							X	X			
Kingston			Y	Y	Y	Y	XY	XY	Y	Y	Y
Buoy (2-Om-02)							X	X			
Buoy (2-Om-07)							X	X			
Buoy (2-Om-10)							X	X			
Bedford Tower							X				
United States:											
Brockport							X	X			
Geneva							X	X			
Buffalo		Y	Y	Y	Y	Y	Y	Y	Y	Y	Y
Rochester		Y	Y	Y	Y	Y	Y	Y	Y	Y	Y
Oswego								X			

Consequently, the global radiation climatology for Lake Ontario for the years 1966-76 was achieved by augmenting direct observations with estimates using relationships of sunshine duration to global radiation (Mateer, 1955; Angstrom, 1956). Such observations have been used successfully on other Great Lakes investigations involving energy budget computations (Bolsenga, 1975; Schertzer, 1977). Daily values of sunshine duration and radiation at CCIW, Scarborough and Kingston observed during IFYGL were used to derive linear regression equations of the following form:

$$K\downarrow I_0 \cos Z = a + b\,[Sm/Sp]$$

where
- $K\downarrow$ = global radiation
- $I_0 \cos Z$ = extraterrestrial radiation
- I_0 = solar constant (1.94 cal cm^{-2} min^{-1})
- Z = solar zenith angle
- Sm = measured sunshine (hours and tenths)
- Sp = potential sunshine (hours and tenths)
- a, b = constants.

Regression statistics given in Table 3.1.4 show good correspondence between the radiation and sunshine observations ($r = .95$) for all three stations for very large sample sizes. The resulting regression coefficients were used to form daily global radiation estimates for the stations lacking direct observations. The mean of the coefficients at CCIW, Scarborough and Kingston were applied to the long-term sunshine records at Rochester and Buffalo to give some measure of control on the American portion of the lake, especially for years other than during IFYGL.

TABLE 3.1.4: *Regression coefficients for the correlation of* $K\downarrow/I_0 \cos Z$ vs Sm/Sp

	Observations	Y-Intercept	Slope	Correlation Coefficient
CCIW/Mt. Hope	407	0.17	0.62	0.95
Scarborough	440	0.19	0.63	0.94
Kingston	385	0.20	0.57	0.94
Rochester/Buffalo		0.19	0.60	

Daily lakewide mean global radiation was computed as the arithmetic mean of individual station values. Table 3.1.5 shows a summary of weekly lakewide means for the years 1966-1976 including the long-term mean. Weekly deviations from the long-term mean for each year are shown in Figure 3.1.5, together with the long-term mean.

Mean incoming global radiation for Lake Ontario ranges from approximately 100 cal cm^{-2} day^{-1} in winter months to 500 cal cm^{-2} day^{-1} in summer. Weekly deviations from the long-term mean show winter values as low as 50 cal cm^{-2} day^{-1} and summer maximums to 700 cal cm^{-2} day^{-1}. On a day to day basis, the magnitude of the global radiation flux can vary considerably, largely due to the attenuating effect of cloud cover. The largest summer income of global radiation occurred in 1966 while the least was in 1976.

For the purposes of phytoplankton modeling, the incident lakewide mean global radiation is reduced to approximate the photosynthetically active wavelengths (PHAR) considered here as 400-700 nm. Experimental evidence indicates that the proportion of PHAR in measured global solar radiation is relatively constant at 44-53 percent depending on the degree of cloudiness (Sauberer, 1962). A further reduction of the incident flux at the surface is due to surface reflection with monthly means ranging from 8% in summer to a mean of 16% in winter (Davies and Schertzer, 1974).

Light Extinction

The availability of photosynthetically active radiation (PHAR) within the water column is a requisite for establishing the magnitude of primary production (Talling, 1965). The distribution of the downwelling light with depth is dependent on the surface irradiance intensity and the rate of attenuation of the light flux. The diminution of light intensity for PHAR (considered here as wavelengths 400-700 nm), between two irradiances at the surface I_o and at some depth I_Z is given by

$$I_Z = I_o e^{-\alpha m}$$

in which α is the vertical extinction coefficient and m is the thickness of the layer of water in metres. The vertical extinction coefficient

TABLE 3.1.5: *Weekly mean global radiation 1966-76*

Weeks*	'66	'67	'68	'69	'70	'71	'72	'73	'74	'75	'76	Mean
1-7	119	106	111	118	128	114	118	128	119	113	115	117
8-14	133	99	135	117	138	115	146	153	135	100	133	128
15-21	101	149	130	133	140	147	136	132	91	120	142	129
22-28	151	92	118	169	101	150	124	103	128	115	110	124
29-35	123	144	135	106	152	167	172	144	147	170	153	147
36-42	199	194	182	216	154	127	236	199	188	143	141	180
43-49	208	223	225	256	244	162	143	257	228	117	156	202
50-56	201	198	308	164	263	122	205	210	201	153	192	202
57-63	244	209	229	252	185	227	169	225	163	222	160	208
64-70	226	247	252	303	312	202	279	218	264	218	208	248
71-77	345	258	237	264	321	272	156	137	287	297	233	255
78-84	186	275	218	247	249	309	241	322	304	203	278	258
85-91	335	320	377	276	309	299	406	293	234	308	260	311
92-98	275	328	378	360	366	385	312	252	282	257	376	325
99-105	355	339	432	503	451	416	435	494	311	429	455	411
106-112	389	321	414	344	368	425	350	416	448	426	422	393
113-119	299	432	372	351	459	285	430	338	407	399	281	368
120-126	387	362	328	520	402	367	398	302	388	324	417	382
127-133	473	325	417	304	355	413	439	342	286	526	384	388
134-140	424	428	323	395	407	540	422	382	485	477	324	419
141-147	638	492	446	496	381	373	609	354	409	493	399	463
148-154	502	550	270	454	487	514	456	415	474	429	402	450
155-161	547	452	601	450	563	528	518	533	482	427	589	517
162-168	587	491	414	448	455	500	414	488	394	473	457	466
169-175	665	502	466	328	463	548	424	428	415	556	383	467
176-182	706	463	294	510	455	494	396	497	441	592	386	476
183-189	621	423	494	538	487	550	496	555	524	549	396	512
190-196	609	339	657	541	384	532	476	483	566	455	387	485
197-203	584	425	517	447	429	498	466	534	527	467	471	488
204-210	467	446	513	393	508	450	520	436	351	515	501	464
211-217	590	469	548	470	490	439	482	424	394	466	445	574
218-224	448	426	463	474	545	529	390	450	464	448	332	452
225-231	481	437	474	442	434	503	353	425	487	412	399	441
232-238	422	391	353	553	437	378	454	350	457	313	523	421
239-245	488	360	463	411	394	328	467	418	290	301	338	387
246-252	397	414	385	341	318	319	351	450	370	390	436	379
253-259	447	452	350	333	303	227	346	330	302	297	351	340
260-266	300	316	375	310	282	248	361	297	282	221	228	293
267-273	250	230	259	201	277	252	222	296	269	239	289	253
274-280	301	325	266	216	247	277	254	251	254	304	331	275
281-287	252	200	271	260	163	196	227	292	204	168	223	223
288-294	184	167	262	186	214	274	199	216	255	137	176	206
295-301	323	179	169	180	172	153	117	232	292	259	196	207
302-308	172	153	212	158	102	229	107	111	115	148	156	151
309-315	89	112	120	91	142	152	85	134	118	172	127	126
316-322	121	111	79	128	86	123	94	90	116	139	194	116
323-329	172	114	104	147	128	106	118	116	102	122	106	121
330-336	77	134	76	89	94	99	92	85	124	67	87	93
337-343	89	97	80	114	91	72	70	84	116	100	106	93
344-350	99	81	122	71	65	108	65	91	68	71	129	88
351-357	93	100	108	93	61	103	70	90	100	87	95	91
358-364	72	113	97	115	121	72	55	86	89	80	104	91

* Weeks = days of the year.

characterizes the attenuation of light with vertical depth. Under cloudless conditions direct beam irradiance at the surface is considerable. The vertical extinction coefficient is computed accounting for refraction and solar elevation and has units of m^{-1}.

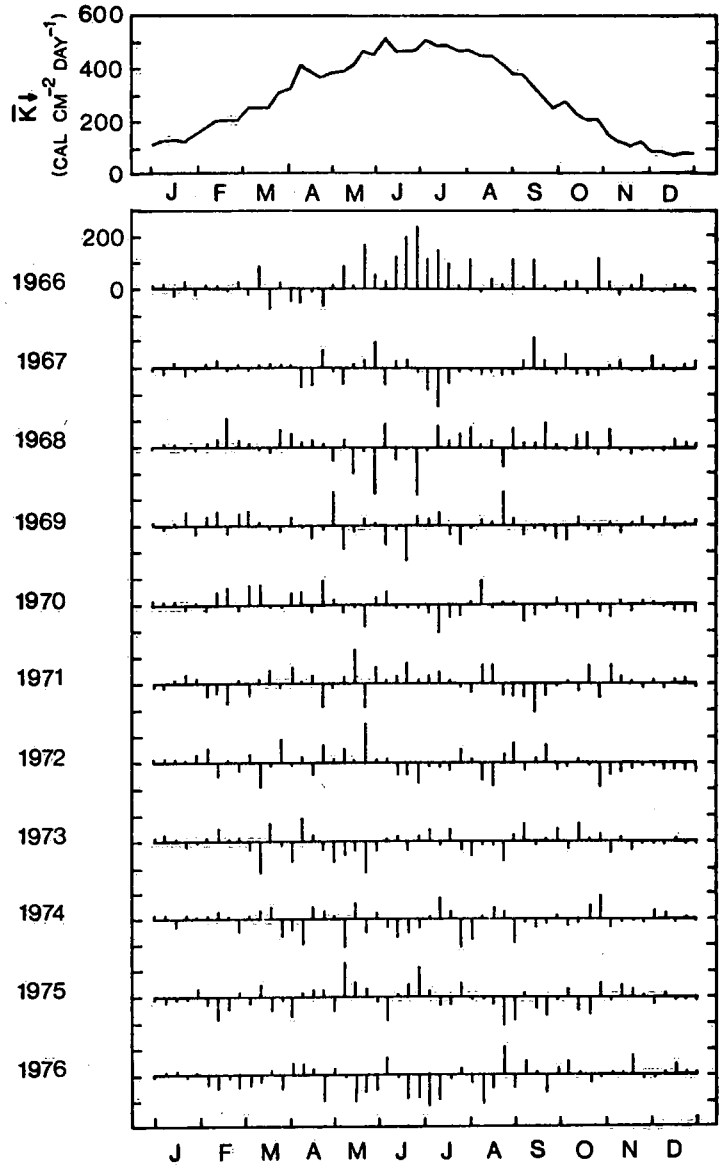

Figure 3.1.5 Long-term mean of seasonal radiation cycle, 1966-77, and weekly deviations from the mean for each year.

The relative transparency of the lake to light transmission is dependent on the concentrations of organic dissolved materials and organic and inorganic suspended particulates which are spatially variable. Consequently, the magnitude of the mean vertical extinction coefficient is affected by such limnological factors as upwelling, currents, coastal erosion, stratification and biological growth cycle. Temperature and depth figure prominently in the regulation of these influences on light attenuation.

Measurements relating to water transparency were observed on 181 synoptic cruises on Lake Ontario from 1966-1977 by the use of the spectrometer, transmissometer and Secchi disc. Mean vertical extinction coefficients can be determined directly from irradiance measurements observed at depth by spectrometer, but these measurements are extremely time consuming and were conducted on only a few cruises (June and August, 1974). Conversely, Secchi depth (S, 30-cm disc) was observed on all cruises; the percentage transmittance (T) of a collimated beam of light over a 1-m or 0.25-m path length using a transmissometer was measured from 1974 to 1977. In the period 1974-1977, transmissometer measurements were more numerous and more spatially representative of the lakewide condition than those of the Secchi disc. Observations were conducted by technical personnel from CCIW and calibration procedures and operational methods were strictly adhered to. As indicated previously, measurements were conducted at a grid of stations over the lake which varied considerably, especially prior to 1973. In general, optical network densities were of the order 1 per 300 km^2. The effect of varying station location from cruise to cruise on the comparability of results has not been evaluated.

Spectrometer measurements conducted at a total of 32 stations during June and August, 1974 were used to compute a mean vertical extinction coefficient (MVEC) per metre for each station location. The parameter was derived statistically employing the successive technique of Vollenweider (1955)

$$\bar{\alpha} = \frac{1}{n} \sum_{i=1} \left[\frac{1}{m}(\ln I_o - \ln I_Z)\right]_i$$

where n denotes the number of successive layers of water under consideration between observations. Mean vertical extinction coefficients computed from spectrometer measurements were then regressed against the beam attenuation coefficient (ln 1/T) and also against the inverse of Secchi depth (1/S). Regressions were derived for observations at corresponding locations for all cruise data (Table 3.1.6). Some variance in the correlation is probably due to the differing wavelength intervals of measurement between the instruments, variable depths of observations at corresponding stations and the different abilities of the instruments for measuring light attenuation due to adsorption and scattering. Whereas the spectrometer data are a measure of light attenuation due primarily to absorption, beam transmittance is a measure of both absorption and scattering of light between source and receptor over a known path (Jerlov, 1968; Thomson and Jerome, 1973). Secchi disc depth is affected by light attenuation due to absorption and scattering but gives only a rough approximation of extinction coefficient over an extremely wide spectral range (Strickland, 1958; Tyler, 1968).

TABLE 3.1.6: *Regression statistics for the correlation of mean vertical extinction coefficient ($\alpha\lambda$ 400-700 nm) with beam attenuation (ln 1/T) and inverse Secchi disc depth (1/S) for Lake Ontario*

	y-intercept	Slope	Correlation Coefficient
α vs ln.1/T	0.05	0.20	0.90
α vs 1/S	0.23	0.59	0.77

Since regressions between MVEC determined from spectrometer and 1/S and ln 1/T could only be determined from limited data in June and August, 1974, the applicability of the relationships to other months could not be statistically tested. However, correlations conducted using June or August data independently showed that relationships using Secchi disc are relatively insensitive to seasonal changes, while the change in regression constants using the transmissometer were significant. This implies that the absolute values of MVEC determined from the two

relationships may not be directly comparable for very high or low values, although trends will be similar. Further examination of this problem is required to determine reliable monthly estimates of this parameter. In Table 3.1.7 "a" shows the lakewide average MVEC and associated statistics for Lake Ontario during 1972. These indicate that MVEC can vary considerably - primarily due to nearshore and midlake differences. Section "b" shows a comparison between monthly means from the present computations using lakewide values and earlier estimates listed in Table 2.3.1 from which the model was calibrated. In the present computations, monthly averages of MVEC (Table 3.1.8) were derived by graphical integration through values plotted at cruise midpoints (Figure 3.1.6). For periods between field programs (e.g., winter), MVEC is estimated by forcing a smooth interpolation through appropriate minimas determined from nearest limited winter observations. In the earlier case, summer values were derived from essentially midlake observations and winter values were estimated by extrapolation from these. As indicated in Table 3.1.7, summer estimates of MVEC in both cases are in very good agreement, while those in winter show substantial differences. It will be seen in Chapter 3.4 that the typical plankton model is very sensitive to values of light extinction.

TABLE 3.1.7: *Comparison of mean vertical extinction coefficient (MVEC) derived for Lake Ontario 1972*

a) Cruise Mid-point	MVEC	N	SD	Max	Min
April 13	.35	158	.08	.82	.28
April 26	.35	41	.10	.82	.28
May 07	.36	97	.10	.82	.28
June 01	.40	103	.12	.82	.28
June 25	.39	47	.07	.52	.29
July 23	.44	48	.15	1.41	.35
Sept 15	.48	91	.06	.62	.38
Oct 16	.38	64	.03	.47	.31
Dec 06	.39	71	.11	.82	.29

b) Table Number	J	F	M	A	M	J	J	A	S	O	N	D
2.3.1	.25	.25	.25	.30	.35	.40	.45	.50	.50	.25	.25	.25
3.1.8	.34	.34	.35	.38	.39	.42	.45	.45	.46	.41	.39	.40

TABLE 3.1.8: *Estimates of the monthly mean vertical extinction coefficient, MVEC, (λ 400-700 nm) for Lake Ontario 1966-77*

	J	F	M	A	M	J	J	A	S	O	N	D
'66	.34^{E}	.34^{E}	.34^{E}	.34^{E}	.35^{E}	.38	.40	.42	.39	.35^{E}	.34^{E}	.34^{E}
'67	.34^{E}	.35^{E}	.36^{E}	.36^{E}	.39^{E}	.41	.43	.43	.39	.37	.34^{E}	.34^{E}
'68	.34^{E}	.34^{E}	.34^{E}	.35^{E}	.36	.43	.50	.43	.40	.38	.37	.36^{E}
'69	.34^{E}	.34^{E}	.35^{E}	.36	.39	.43	.45	.44	.43	.41	.37	.35
'70	.34	.35	.37	.38	.37	.39	.44	.51	.42	.38	.37	.39
'71	.35^{E}	.35^{E}	.37^{E}	.38^{E}	.38^{E}	.41^{E}	.41^{E}	.45^{E}	.56^{E}	.42^{E}	.37^{E}	.35^{E}
'72	.34^{E}	.34^{E}	.35	.38	.39	.42	.45	.45	.46	.41	.39	.40
'73	.40	.40	.42	.41	.45	.46	.48^{E}	.48^{E}	.46^{E}	.41^{E}	.36^{E}	.33^{E}
'74	.29^{E}	.29^{E}	.30^{E}	.32	.36	.46	.50	.61	.47	.36	.32	.30
'75	.29^{E}	.29^{E}	.30^{E}	.33	.43	.52	.54	.57	.43	.40	.38	.33
'76	.31^{E}	30^{E}	.32^{E}	.36	.37	.37	.38	.41	.33	.30	.25	.26
'77	.25^{E}	.22^{E}	.23^{E}	.27	.31	.32	.34	.37	.33	.33	.31	.28

Estimates of the MVEC are plotted for years 1966 to 1977 on Figure 3.1.6 . Values for 1966 to 1973 are determined using extinction derived from Secchi disc observations, while those derived for the period 1974 to 1977 are based on transmissometer measurements. As indicated previously, these values represent a first approximation of lakewide average MVEC.

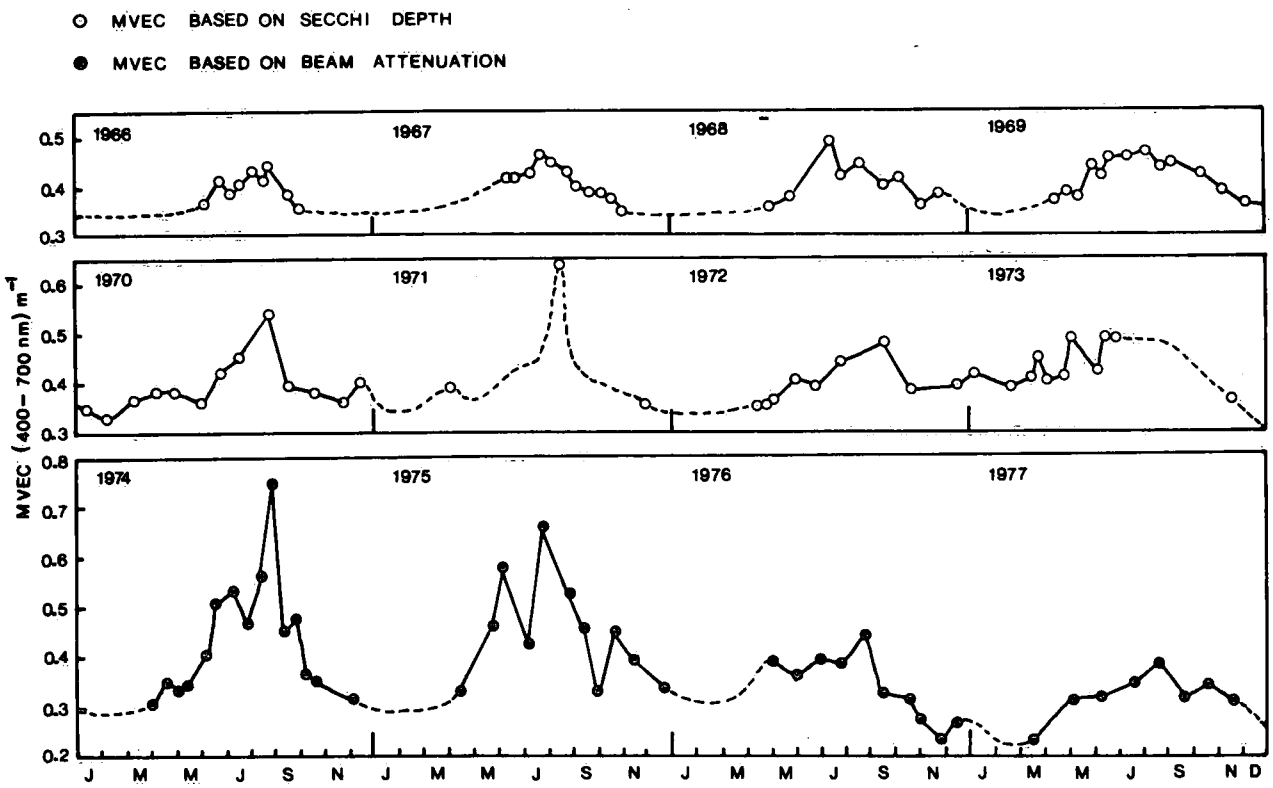

Figure 3.1.6 Light extinction coefficients, 1966-77.

Nutrients

Nutrient data are available for 65 synoptic surveys conducted by the Canada Centre for Inland Waters between 1967 and 1977. Synoptic cruise patterns and station locations varied considerably, especially prior to 1972, with network densities ranging from one station per 200 km^2 to one station per 400 km^2. In addition, the number of depths sampled at each station varied from 1 to 18, with the average ranging from four to six depths. Fortunately, sample handling, preservation and analysis techniques have remained fairly consistent for the 12-year period even though considerable improvement in analytical methods has occurred. The effects of varying cruise patterns and station locations on the reliability or comparability of results from year to year has not been evaluated. However, it has been shown by El-Shaarawi and Kwiatkowski (1978) that spatial variation in Lake Ontario on any one cruise is less than 1/60th the temporal variation over one year.

All data were processed and edited in a consistent fashion before statistical and other calculations were performed. Lake Ontario was divided into 17 "quasi-homogeneous" regions based on results of the statistical analysis of El-Shaarawi and Kwiatkowski (1978). These zones were outlined before in Figure 3.1.4. Mean concentrations were obtained by zones and layers for all variables. The measured values were volume and area weighted by a procedure similar to the Theisson polygon approach utilizing 2 km grid squares. To give an indication of the available nutrient data, lake-wide volume-weighted mean concentrations for three layers, 0-20 m, 20-40 m, and 40 m-bottom, are presented in Tables 3.1.9 to 3.1.17. Some of these data are depicted in Figures 3.1.7 to 3.1.10. A further discussion of the nutrient data is deferred to Chapter 3.3.

3.2 Nutrient Loadings to Lake Ontario

Introduction

The biological activity in a lake and thus the trophic status of a lake are closely tied to the loading of nutrients to that lake. The load of input nutrients and the internally recycled nutrients are potentially available for biologic activity. Large lakes, especially those the size of the Great Lakes, do not respond instantaneously to changes in nutrient loadings. The time lag between the change in loading and the lake's response towards a new equilibrium state can easily be in the order of several years.

It is for this reason that long-term modeling studies require a long-term data base with which to evaluate the predictive capacity of the model. This data set should cover a period at least equal to the retention time of the lake, which in the case of Lake Ontario is approximately 10 years.

However, it is also useful to examine the short-term cycle of loadings to the lake. Nearshore waters probably react to changes in loading much more rapidly than does the water of the open lake.

The purpose of this study was to provide an estimate of the yearly loadings to Lake Ontario for the period of record from 1967 to 1976.

TABLE 3.1.9: *Soluble reactive phosphorus*, µg P/ℓ

DATE	0 m-20 m	20 m-40 m	40 m-bottom	0 m-bottom
1967				
June 12-17				
June 25-29				
July 10-13				
July 25-30				
Aug. 7-10				
Aug. 21-25				
Sept. 16-21				
Oct. 1-6				
Oct. 17-21				
Oct. 28- Nov 2				
1968				
Apr. 29-May 1	12.2	13.2	14.3	13.7
May 27-30	7.3	8.2	9.2	8.6
July 2-6	5.9	6.7	10.6	9.0
Oct. 5-8	5.8	9.1	15.6	12.4
Oct. 27-31	5.7	8.9	18.2	14.1
Nov. 18-22	2.1	2.3	2.8	2.6
1969				
Apr. 12-16	11.3	12.5	14.3	13.4
May 12-17	8.4	10.5	11.2	10.1
June 9-13	4.4	5.4	6.8	6.1
July 8-13	2.5	5.5	10.0	7.7
Aug. 5-10	4.5	8.3	14.0	11.0
Sept 4-9	2.5	5.6	9.5	7.4
Oct. 2-7	1.8	5.2	11.4	7.4
Oct 31-Nov 4	7.1	8.2	12.6	10.7
Dec 1-6	10.5	10.3	12.1	11.5
1970				
Jan. 6-12	13.2	13.5	14.4	14.0
Feb. 3-8	13.5	13.4	13.9	13.7
Mar. 3-8	12.0	12.5	13.4	12.9
1971				
Mar.30-Apr.3	12.3	13.0	13.8	13.3
Aug. 9-13	2.2	5.7	9.4	7.3
Nov. 15-19	6.3	7.9	13.9	11.3
1972				
Feb. 1-10				
Apr. 10-22	12.0	12.7	14.4	13.6
May 23-June 3	10.1	11.2	13.1	12.1
June 19-Jul.1	4.8	7.8	11.4	9.4
July 17-19	1.9	5.6	12.7	9.2
Sept. 5-16	1.5	5.9	12.0	8.7
Sept. 19-23	1.8	5.8	12.8	9.3
Oct. 17-28	5.1	5.7	12.7	9.9
Nov. 20-Dec 2	7.7	8.2	12.1	10.5
1973				
Jan.9-19	13.9	14.2	15.0	14.6
Mar. 6-17	13.9	14.3	15.1	14.7
Mar. 20-24	14.5	15.3	16.4	15.8
Apr. 24-28	12.0	14.4	16.4	15.1
Oct. 30-Nov. 3	7.1	7.8	13.1	10.9
Dec. 4-6	10.7	11.2	13.3	12.4
1974				
Apr. 1-4	14.1	14.8	15.6	15.2
July 2-5				
Aug. 12-16	1.6	3.6	8.8	6.4
Sept. 3-7				
Nov. 25-29				
1975				
Apr. 11-14	11.0	12.3	13.8	12.9
June 2-8	6.6	8.7	12.0	10.3
Sept. 2-15	8.2	8.7	13.7	11.7
1976				
Apr. 5-9	9.8	11.5	13.0	12.1
Apr. 26-30				
June 7-11	4.2	7.2	10.1	8.4
June 28-July 2				
July 27-31				
Aug. 17-21	2.4	6.1	13.2	9.7
Sept. 7-11				
Oct. 4-8				
Oct.25-29	5.2	5.7	11.9	9.4
Nov. 15-19				
Dec. 3-7				
1977				
Mar. 15-20	10.7	11.0	11.5	11.3
Apr. 12-15	7.8	8.5	10.0	9.3
May 9-13	7.2	8.8	9.2	8.4
June 6-10	4.8	6.7	8.6	7.5
July 18-23				
Aug. 15-19				
Sept. 9-16	1.5	4.4	11.9	8.5
Oct. 11-15				
Nov. 14-18				

TABLE 3.1.10: *Total filtered phosphorus* µg P/ℓ

DATE	0 m-20 m	20 m-40 m	40 m-bottom	0 m-bottom
1967				
June 12-17				
June 25-29				
July 10-13				
July 25-30				
Aug. 7-10				
Aug. 21-25				
Sept. 16-21				
Oct. 1-6				
Oct. 17-21				
Oct. 28- Nov 2				
1968				
Apr. 29-May 1				
May 27-30				
July 2-6				
Oct. 5-8				
Oct. 27-31				
Nov. 18-22				
1969				
Apr. 12-16				
May 12-17				
June 9-13				
July 8-13				
Aug. 5-10				
Sept 4-9				
Oct. 2-7				
Oct 31-Nov 4				
Dec 1-6				
1970				
Jan. 6-12				
Feb. 3-8				
Mar. 3-8				
1971				
Mar.30-Apr.3				
Aug. 9-13	10.9	14.9	18.6	16.4
Nov. 15-19	9.9	10.9	14.3	12.8
1972				
Feb. 1-10	6.2	6.2	6.1	6.1
Apr. 10-22	15.8	16.4	18.0	17.3
May 23-June 3	14.9	15.8	16.8	16.3
June 19-Jul.1	11.2	12.9	16.1	14.5
July 17-19	10.1	10.9	16.3	14.1
Sept. 5-16	7.3	10.4	17.1	13.9
Sept. 19-23	9.0	12.8	20.3	16.7
Oct. 17-28	10.1	10.4	16.4	14.0
Nov. 20-Dec 2	13.6	13.9	17.9	16.3
1973				
Jan.9-19	20.0	20.0	20.1	20.1
Mar. 6-17	20.1	20.0	20.7	20.4
Mar. 20-24	18.1	18.8	19.1	18.8
Apr. 24-28	18.8	20.7	20.3	21.1
Oct. 30-Nov. 3	13.8	14.3	19.9	17.7
Dec. 4-6	14.3	14.5	16.2	15.5
1974				
Apr. 1-4	19.1	19.6	20.7	20.2
July 2-5				
Aug. 12-16				
Sept. 3-7				
Nov. 25-29				
1975				
Apr. 11-14	14.3	15.3	16.7	16.0
June 2-8	9.4	11.2	14.0	12.6
Sept. 2-15	12.3	12.7	18.2	16.0
1976				
Apr. 5-9	15.7	17.2	20.8	19.1
Apr. 26-30				
June 7-11	13.1	15.9	18.1	16.7
June 28-July 2				
July 27-31				
Aug. 17-21	11.5	13.7	18.6	16.3
Sept. 7-11				
Oct. 4-8				
Oct.25-29	12.0	11.9	16.6	14.8
Nov. 15-19				
Dec. 3-7				
1977				
Mar. 15-20	17.5	17.8	16.6	14.8
Apr. 12-15	15.0	15.6	17.3	16.5
May 9-13	13.0	14.0	14.9	14.4
June 6-10	11.1	12.2	13.4	12.7
July 18-23				
Aug. 15-19				
Sept. 9-16	8.0	9.4	15.3	12.8
Oct. 11-15				
Nov. 14-18				

TABLE 3.1.11: *Total phosphorus* µg P/ℓ

DATE	0 m-20 m	20 m-40 m	40 m-bottom	0 m-bottom
1967				
June 12-17				
June 25-29				
July 10-13				
July 25-30				
Aug. 7-10				
Aug. 21-25				
Sept. 16-21	12.6	14.0	23.6	19.7
Oct. 1-6	17.6	17.2	19.2	18.5
Oct. 17-21				
Oct. 28- Nov 2	12.6	11.8	14.5	13.6
1968				
Apr. 29-May 1				
May 27-30				
July 2-6				
Oct. 5-8	15.6	16.8	20.8	19.0
Oct. 27-31				
Nov. 18-22	4.0	4.1	5.0	4.6
1969				
Apr. 12-16				
May 12-17	23.7	21.8	23.6	23.3
June 9-13	23.0	20.6	26.3	24.6
July 8-13	19.0	17.0	19.4	18.9
Aug. 5-10	17.9	18.6	24.0	21.8
Sept 4-9	19.9	17.6	21.4	20.4
Oct. 2-7	15.9	17.8	25.6	22.2
Oct 31-Nov 4	20.7	18.7	21.4	20.8
Dec 1-6	21.5	20.5	20.8	20.9
1970				
Jan. 6-12	20.4	19.7	18.2	18.9
Feb. 3-8	24.4	24.0	23.6	23.8
Mar. 3-8	23.2	22.4	21.8	22.2
1971				
Mar.30-Apr.3	24.9	24.5	26.1	25.6
Aug. 9-13	21.8	20.7	22.7	22.2
Nov. 15-19	13.1	13.9	16.8	15.5
1972				
Feb. 1-10	24.1	23.7	25.4	24.9
Apr. 10-22	23.1	22.5	22.1	22.4
May 23-June 3	21.1	20.9	20.8	20.9
June 19-Jul.1	20.6	19.0	20.2	20.1
July 17-19	18.7	16.0	19.6	18.8
Sept. 5-16	17.1	15.1	21.2	19.3
Sept. 19-23	17.9	18.7	23.3	21.4
Oct. 17-28	15.8	15.5	19.2	17.8
Nov. 20-Dec 2	18.0	18.1	21.6	20.2
1973				
Jan.9-19	24.5	23.9	22.5	23.2
Mar. 6-17	24.1	23.6	23.1	23.4
Mar. 20-24	25.4	24.1	22.3	23.3
Apr. 24-28	25.6	25.0	25.3	25.3
Oct. 30-Nov. 3	21.9	20.8	24.3	23.2
Dec. 4-6	18.5	18.3	18.7	18.6
1974				
Apr. 1-4	24.3	24.5	24.9	24.7
July 2-5	20.3	20.3	24.5	22.9
Aug. 12-16				
Sept. 3-7	22.1	21.7	26.3	24.6
Nov. 25-29	23.5	23.4	23.3	23.4
1975				
Apr. 11-14	22.0	21.3	20.8	21.2
June 2-8	17.1	18.0	18.7	18.3
Sept. 2-15	18.3	18.8	22.6	21.1
1976				
Apr. 5-9	22.5	22.1	21.8	22.0
Apr. 26-30	24.0	23.2	22.8	23.1
June 7-11	23.0	24.0	23.4	23.4
June 28-July 2	18.5	18.8	20.6	19.8
July 27-31	23.1	21.0	22.0	22.0
Aug. 17-21	22.5	20.6	22.3	22.1
Sept. 7-11	19.0	18.7	23.2	21.6
Oct. 4-8	18.3	18.6	20.8	19.9
Oct.25-29	18.3	17.7	20.6	19.6
Nov. 15-19	20.5	20.0	21.1	20.8
Dec. 3-7	19.6	18.8	19.2	19.2
1977				
Mar. 15-20	22.4	22.3	23.0	22.8
Apr. 12-15	21.8	21.1	21.5	21.5
May 9-13	19.6	19.7	19.8	19.7
June 6-10	20.2	19.6	19.7	19.8
July 18-23	17.9	18.4	20.4	19.5
Aug. 15-19	19.0	17.6	21.5	20.3
Sept. 9-16	15.0	14.1	19.0	17.3
Oct. 11-15	14.4	13.4	17.3	16.0
Nov. 14-18	14.8	13.7	16.7	15.8

TABLE 3.1.12: *Nitrate and nitrite* µg N/ℓ

DATE	0 m-20 m	20 m-40 m	40 m-bottom	0 m-bottom
1967				
June 12-17				
June 25-29				
July 10-13				
July 25-30				
Aug. 7-10				
Aug. 21-25				
Sept. 16-21				
Oct. 1-6				
Oct. 17-21				
Oct. 28- Nov 2				
1968				
Apr. 29-May 1	204.	216.	221.	216.
May 27-30	202.	217.	227.	220.
July 2-6	73.	156.	207.	170.
Oct. 5-8	105.	154.	205.	176.
Oct. 27-31	91.	140.	243.	194.
Nov. 18-22	196.	212.	260.	238.
1969				
Apr. 12-16	232.	234.	241.	238.
May 12-17	201.	214.	228.	220.
June 9-13	140.	195.	224.	202.
July 8-13	62.	173.	230.	186.
Aug. 5-10	46.	169.	262.	202.
Sept 4-9	53.	159.	256.	197.
Oct. 2-7	38.	136.	238.	180.
Oct 31-Nov 4	150.	168.	234.	205.
Dec 1-6	211.	215.	232.	225.
1970				
Jan. 6-12	227.	229.	239.	235.
Feb. 3-8	244.	242.	227.	233.
Mar. 3-8	239.	233.	230.	232.
1971				
Mar.30-Apr.3				
Aug. 9-13	56.	177.	229.	184.
Nov. 15-19	162.	190.	269.	233.
1972				
Feb. 1-10	215.	231.	231.	228.
Apr. 10-22	233.	231.	227.	229.
May 23-June 3	217.	227.	236.	230.
June 19-Jul.1	143.	213.	245.	218.
July 17-19	44.	182.	248.	194.
Sept. 5-16	48.	194.	259.	204.
Sept. 19-23	51.	141.	260.	196.
Oct. 17-28	151.	161.	224.	198.
Nov. 20-Dec 2	207.	213.	259.	240.
1973				
Jan.9-19	209.	203.	196.	200.
Mar. 6-17	254.	249.	251.	251.
Mar. 20-24	271.	273.	275.	273.
Apr. 24-28	243.	254.	260.	255.
Oct. 30-Nov. 3	192.	212.	269.	243.
Dec. 4-6	247.	251.	266.	260.
1974				
Apr. 1-4	286.	286.	285.	285.
July 2-5				
Aug. 12-16	77.	128.	179.	149.
Sept. 3-7				
Nov. 25-29				
1975				
Apr. 11-14	278.	283.	288.	285.
June 2-8	261.	275.	294.	284.
Sept. 2-15	266.	294.	323.	306.
1976				
Apr. 5-9	296.	303.	308.	305.
Apr. 26-30				
June 7-11	244.	287.	313.	295.
June 28-July 2				
July 27-31				
Aug. 17-21	114.	210.	315.	255.
Sept. 7-11				
Oct. 4-8				
Oct.25-29	238.	249.	318.	290.
Nov. 15-19				
Dec. 3-7				
1977				
Mar. 15-20	315.	317.	319.	318.
Apr. 12-15	296.	299.	304.	302.
May 9-13	287.	298.	309.	302.
June 6-10	256.	288.	304.	291.
July 18-23				
Aug. 15-19				
Sept. 9-16				
Oct. 11-15				
Nov. 14-18				

TABLE 3.1.13: *Ammonia* µg N/ℓ

DATE	0 m-20 m	20 m-40 m	40 m-bottom	0 m-bottom
1967				
June 12-17	12.	15.	15.	14.
June 25-29	31.	35.	31.	32.
July 10-13	48.	52.	46.	48.
July 25-30	27.	35.	26.	28.
Aug. 7-10	24.	24.	17.	20.
Aug. 21-25	40.	94.	60.	62.
Sept. 16-21	46.	48.	48.	48.
Oct. 1-6	49.	48.	48.	48.
Oct. 17-21	54.	45.	39.	43.
Oct. 28- Nov 2	28.	25.	34.	31.
1968				
Apr. 29-May 1				
May 27-30	11.	10.	10.	10.
July 2-6	36.	38.	39.	38.
Oct. 5-8	15.	12.	10.	11.
Oct. 27-31	45.	44.	36.	39.
Nov. 18-22	29.	25.	19.	22.
1969				
Apr. 12-16	13.	11.	11.	11.
May 12-17	22.	17.	13.	15.
June 9-13	27.	27.	19.	22.
July 8-13	30.	35.	34.	33.
Aug. 5-10	22.	26.	16.	20.
Sept 4-9	28.	24.	20.	22.
Oct. 2-7	24.	18.	13.	16.
Oct 31-Nov 4	24.	18.	13.	16.
Dec 1-6	16.	11.	10.	11.
1970				
Jan. 6-12	17.	14.	13.	14.
Feb. 3-8	22.	17.	14.	16.
Mar. 3-8	25.	20.	19.	20.
1971				
Mar.30-Apr.3	20.	17.	8.	12.
Aug. 9-13	16.	14.	6.	10.
Nov. 15-19	17.	14.	7.	11.
1972				
Feb. 1-10	28.	29.	29.	29.
Apr. 10-22	7.	5.	5.	5.
May 23-June 3	6.	6.	5.	5.
June 19-Jul.1	7.	11.	9.	9.
July 17-19	21.	26.	19.	21.
Sept. 5-16	13.	10.	6.	8.
Sept. 19-23	16.	13.	8.	11.
Oct. 17-28	17.	15.	11.	13.
Nov. 20-Dec 2	9.	10.	8.	9.

DATE	0 m-20 m	20 m-40 m	40 m-bottom	0 m-bottom
1973				
Jan.9-19	8.	10.	8.	8.
Mar. 6-17	8.	7.	7.	7.
Mar. 20-24	7.	6.	4.	5.
Apr. 24-28	5.	5.	5.	5.
Oct. 30-Nov. 3	19.	17.	10.	13.
Dec. 4-6	3.	3.	3.	3.
1974				
Apr. 1-4	5.	4.	3.	4.
July 2-5				
Aug. 12-16	19.	13.	6.	10.
Sept. 3-7	4.	3.	3.	3.
Nov. 25-29				
1975				
Apr. 11-14				
June 2-8				
Sept. 2-15				
1976				
Apr. 5-9	4.	3.	3.	3.
Apr. 26-30				
June 7-11	7.	8.	5.	6.
June 28-July 2				
July 27-31				
Aug. 17-21	14.	13.	3.	7.
Sept. 7-11				
Oct. 4-8				
Oct.25-29	11.	10.	5.	7.
Nov. 15-19				
Dec. 3-7				
1977				
Mar. 15-20	3.	3.	2.	3.
Apr. 12-15	4.	4.	4.	4.
May 9-13	5.	5.	5.	5.
June 6-10	5.	6.	6.	6.
July 18-23				
Aug. 15-19				
Sept. 9-16				
Oct. 11-15				
Nov. 14-18				

TABLE 3.1.14: *Total filtered nitrogen* µg N/ℓ

DATE	0 m-20 m	20 m-40 m	40 m-bottom	0 m-bottom
1967				
June 12-17				
June 25-29				
July 10-13				
July 25-30				
Aug. 7-10				
Aug. 21-25				
Sept. 16-21				
Oct. 1-6				
Oct. 17-21				
Oct. 28- Nov 2				
1968				
Apr. 29-May 1				
May 27-30				
July 2-6				
Oct. 5-8				
Oct. 27-31				
Nov. 18-22				
1969				
Apr. 12-16				
May 12-17				
June 9-13				
July 8-13				
Aug. 5-10				
Sept 4-9				
Oct. 2-7				
Oct 31-Nov 4				
Dec 1-6				
1970				
Jan. 6-12				
Feb. 3-8				
Mar. 3-8				
1971				
Mar.30-Apr.3				
Aug. 9-13				
Nov. 15-19	318.	334.	385.	362.
1972				
Feb. 1-10	376.	398.	387.	386.
Apr. 10-22	355.	354.	351.	352.
May 23-June 3	348.	360.	371.	364.
June 19-Jul.1	270.	336.	360.	337.
July 17-19	238.	363.	436.	382.
Sept. 5-16	179.	286.	326.	288.
Sept. 19-23	182.	262.	352.	301.
Oct. 17-28	337.	362.	404.	383.
Nov. 20-Dec 2	264.	275.	317.	300.

DATE	0 m-20 m	20 m-40 m	40 m-bottom	0 m-bottom
1973				
Jan.9-19	448.	450.	433.	439.
Mar. 6-17	366.	359.	352.	356.
Mar. 20-24	369.	353.	349.	354.
Apr. 24-28	367.	373.	376.	374.
Oct. 30-Nov. 3	372.	377.	411.	397.
Dec. 4-6	385.	394.	399.	395.
1974				
Apr. 1-4				
July 2-5				
Aug. 12-16				
Sept. 3-7				
Nov. 25-29				
1975				
Apr. 11-14	375.	374.	377.	376.
June 2-8	363.	370.	350.	369.
Sept. 2-15	413.	435.	460.	446.
1976				
Apr. 5-9	475.	478.	491.	486.
Apr. 26-30				
June 7-11	376.	410.	430.	414.
June 28-July 2				
July 27-31				
Aug. 17-21	284.	352.	419.	380.
Sept. 7-11				
Oct. 4-8				
Oct.25-29	407.	412.	456.	438.
Nov. 15-19				
Dec. 3-7				
1977				
Mar. 15-20	444.	447.	450.	448.
Apr. 12-15	435.	431.	436.	435.
May 9-13	430.	440.	458.	449.
June 6-10	409.	434.	445.	436.
July 18-23				
Aug. 15-19				
Sept. 9-16	241.	332.	432.	375.
Oct. 11-15				
Nov. 14-18				

TABLE 3.1.15: *Total particulate nitrogen* µg N/ℓ

DATE	0 m-20 m	20 m-40 m	40 m-bottom	0 m-bottom
1967				
June 12-17				
June 25-29				
July 10-13				
July 25-30				
Aug. 7-10				
Aug. 21-25				
Sept. 16-21				
Oct. 1-6				
Oct. 17-21				
Oct. 28- Nov 2				
1968				
Apr. 29-May 1				
May 27-30				
July 2-6				
Oct. 5-8				
Oct. 27-31				
Nov. 18-22				
1969				
Apr. 12-16				
May 12-17				
June 9-13				
July 8-13				
Aug. 5-10				
Sept 4-9				
Oct. 2-7				
Oct 31-Nov 4				
Dec 1-6				
1970				
Jan. 6-12				
Feb. 3-8				
Mar. 3-8				
1971				
Mar.30-Apr.3				
Aug. 9-13				
Nov. 15-19				
1972				
Feb. 1-10				
Apr. 10-22	39.	34.	24.	29.
May 23-June 3	43.	34.	27.	31.
June 19-Jul.1	95.	49.	27.	45.
July 17-19	121.	52.	30.	53.
Sept. 5-16	88.	37.	26.	41.
Sept. 19-23	74.	49.	41.	41.
Oct. 17-28	47.	41.	25.	32.
Nov. 20-Dec 2	26.	23.	16.	19.

DATE	0 m-20 m	20 m-40 m	40 m-bottom	0 m-bottom
1973				
Jan.9-19	20.	20.	19.	20.
Mar. 6-17	21.	28.	21.	22.
Mar. 20-24	39.	36.	30.	33.
Apr. 24-28	36.	30.	22.	26.
Oct. 30-Nov. 3	44.	36.	24.	30.
Dec. 4-6	21.	20.	14.	17.
1974				
Apr. 1-4				
July 2-5				
Aug. 12-16	87.	72.	56.	65.
Sept. 3-7				
Nov. 25-29				
1975				
Apr. 11-14				
June 2-8				
Sept. 2-15				
1976				
Apr. 5-9	18.	18.	16.	17.
Apr. 26-30				
June 7-11				
June 28-July 2				
July 27-31				
Aug. 17-21				
Sept. 7-11				
Oct. 4-8				
Oct.25-29				
Nov. 15-19				
Dec. 3-7				
1977				
Mar. 15-20				
Apr. 12-15				
May 9-13				
June 6-10				
July 18-23				
Aug. 15-19				
Sept. 9-16				
Oct. 11-15				
Nov. 14-18				

TABLE 3.1.16: *Particulate organic carbon* µg C/ℓ

DATE	0 m-20 m	20 m-40 m	40 m-bottom	0 m-bottom
1967				
June 12-17				
June 25-29				
July 10-13				
July 25-30				
Aug. 7-10				
Aug. 21-25				
Sept. 16-21				
Oct. 1-6				
Oct. 17-21				
Oct. 28- Nov 2				
1968				
Apr. 29-May 1				
May 27-30				
July 2-6				
Oct. 5-8				
Oct. 27-31				
Nov. 18-22				
1969				
Apr. 12-16				
May 12-17				
June 9-13				
July 8-13				
Aug. 5-10				
Sept 4-9				
Oct. 2-7				
Oct 31-Nov 4				
Dec 1-6				
1970				
Jan. 6-12				
Feb. 3-8				
Mar. 3-8				
1971				
Mar.30-Apr.3				
Aug. 9-13				
Nov. 15-19				
1972				
Feb. 1-10				
Apr. 10-22	225.	200.	173.	188.
May 23-June 3	232.	186.	151.	174.
June 19-Jul.1	499.	271.	158.	248.
July 17-19	607.	290.	200.	300.
Sept. 5-16	619.	256.	208.	300.
Sept. 19-23	528.	356.	213.	303.
Oct. 17-28	357.	314.	221.	265.
Nov. 20-Dec 2	192.	175.	140.	157.
1973				
Jan.9-19	166.	157.	147.	153.
Mar. 6-17	139.	135.	109.	120.
Mar. 20-24	232.	205.	136.	168.
Apr. 24-28	128.	103.	72.	89.
Oct. 30-Nov. 3	283.	229.	164.	200.
Dec. 4-6	149.	151.	119.	131.
1974				
Apr. 1-4				
July 2-5				
Aug. 12-16	474.	391.	307.	356.
Sept. 3-7				
Nov. 25-29				
1975				
Apr. 11-14				
June 2-8				
Sept. 2-15				
1976				
Apr. 5-9	165.	161.	146.	152.
Apr. 26-30				
June 7-11				
June 28-July 2				
July 27-31				
Aug. 17-21				
Sept. 7-11				
Oct. 4-8				
Oct.25-29				
Nov. 15-19				
Dec. 3-7				
1977				
Mar. 15-20				
Apr. 12-15				
May 9-13				
June 6-10				
July 18-23				
Aug. 15-19				
Sept. 9-16				
Oct. 11-15				
Nov. 14-18				

TABLE 3.1.17: *Chlorophyll-a* µg/ℓ

DATE	0 m-20 m	20 m-40 m	40 m-bottom	0 m-bottom
1967				
June 12-17				
June 25-29				
July 10-13				
July 25-30				
Aug. 7-10				
Aug. 21-25				
Sept. 16-21				
Oct. 1-6				
Oct. 17-21				
Oct. 28- Nov 2				
1968				
Apr. 29-May 1				
May 27-30				
July 2-6				
Oct. 5-8				
Oct. 27-31				
Nov. 18-22				
1969				
Apr. 12-16				
May 12-17				
June 9-13				
July 8-13				
Aug. 5-10				
Sept 4-9				
Oct. 2-7				
Oct 31-Nov 4				
Dec 1-6				
1970				
Jan. 6-12				
Feb. 3-8				
Mar. 3-8				
1971				
Mar.30-Apr.3				
Aug. 9-13				
Nov. 15-19				
1972				
Feb. 1-10				
Apr. 10-22	2.9	2.7		
May 23-June 3	3.4	3.0		
June 19-Jul.1	5.1	2.7		
July 17-19	5.7	2.8		
Sept. 5-16	4.8	1.3		
Sept. 19-23				
Oct. 17-28	3.0	2.6		
Nov. 20-Dec 2	1.9	1.6		
1973				
Jan.9-19	.9			
Mar. 6-17	1.6	1.5		
Mar. 20-24				
Apr. 24-28				
Oct. 30-Nov. 3				
Dec. 4-6				
1974				
Apr. 1-4				
July 2-5	5.5			
Aug. 12-16	4.2			
Sept. 3-7	4.3			
Nov. 25-29	5.6			
1975				
Apr. 11-14	2.5			
June 2-8	5.2			
Sept. 2-15	5.9			
1976				
Apr. 5-9	3.2			
Apr. 26-30	3.2			
June 7-11	5.1			
June 28-July 2	6.3			
July 27-31	6.2			
Aug. 17-21	4.7			
Sept. 7-11	6.4			
Oct. 4-8	8.8			
Oct.25-29	3.8			
Nov. 15-19	3.0			
Dec. 3-7	2.7			
1977				
Mar. 15-20	1.8			
Apr. 12-15	2.2			
May 9-13	3.5			
June 6-10	4.1			
July 18-23	5.0			
Aug. 15-19	4.2			
Sept. 9-16	4.5			
Oct. 11-15	3.4			
Nov. 14-18	2.6			

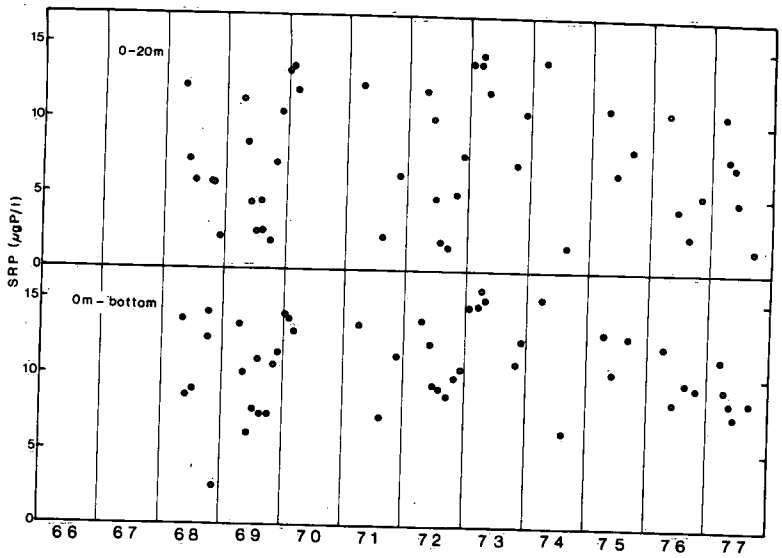

Figure 3.1.7 Chemical observations of soluble reactive phosphorus; all cruises, 1966-77.

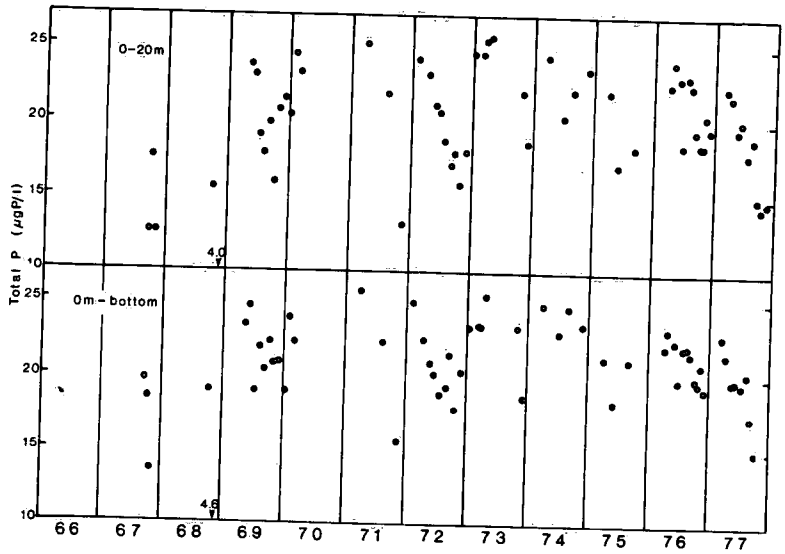

Figure 3.1.8 Chemical observations of total phosphorus; all cruises, 1966-77.

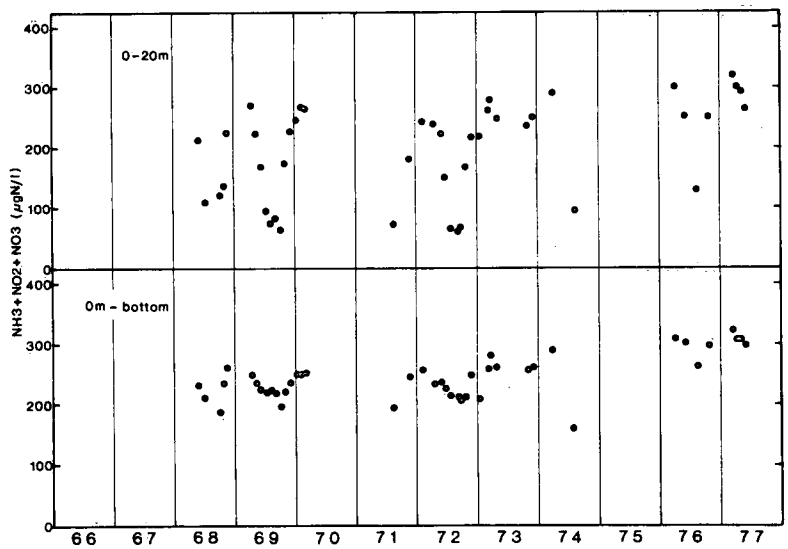

Figure 3.1.9 Chemical observations of NH_3 + NO_2 + NO_3; all cruises, 1966-77.

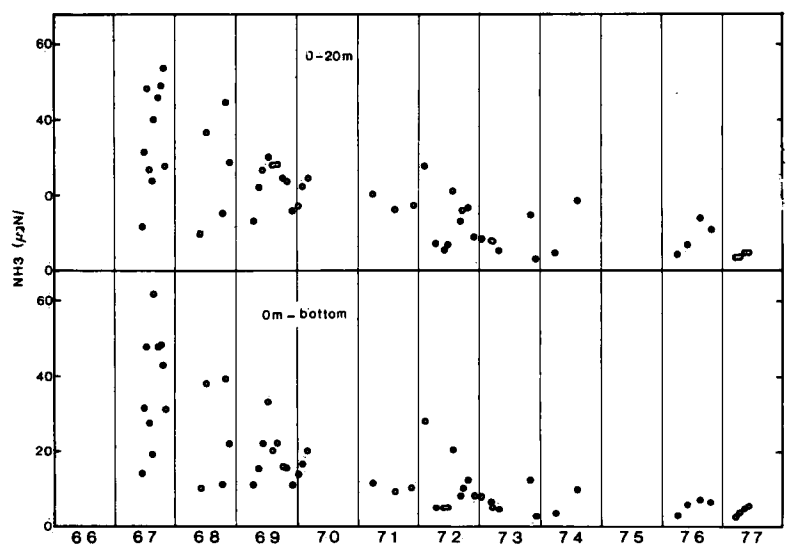

Figure 3.1.10 Chemical observations of NH_3; all cruises, 1966-77.

A monthly breakdown of these yearly loads was also performed whenever the existing data were sufficient. A complete summary of the results may be found in a report by Willson (1978).

Existing Estimates of Lake Ontario Loadings

Before discussing the data base and methods employed in this study, it is well to review the existing estimates of loadings to Lake Ontario.

The two existing sources of estimated loads to Lake Ontario are: the Great Lakes Water Quality Board reports and the loading estimates prepared by Hydroscience Inc. in 1976. Each of these sources will be discussed below.

Great Lakes Water Quality Board Reports

These reports, published in 1969, 1974, 1975, 1976, provide estimates of nutrient loadings to Lake Ontario only as a mean annual load. The 1969 report provided a detailed breakdown as to the sources of the load to the lake. This was not repeated until the 1976 report when loads from individual municipal plants and industries were reported. The data for these reports were summarized by the local jurisdictions (New York State for the U.S. side and the Province of Ontario for the Canadian side) and submitted to the International Joint Commission. There are two major problems with the estimates provided by these reports.

The first problem is that loads from municipal and industrial dischargers upstream from the tributary mouths were subtracted from the monitored tributary load to achieve an estimate of the true tributary load. This was done on the assumption that 100% of the added load appeared at the sampling point. This is probably not the case, and consequently the estimated tributary loading is too low. The second complication is that only 14 Canadian tributaries out of a total of 26 for which adequate data exist were included in these reports. No estimate for the remaining tributaries was provided until the 1976 report. Also, changes in the computational methods, discussed further below, changed the accuracy and confidence in the tributary loading estimates.

Hydroscience Report

The report to the International Joint Commission by Hydroscience Inc. (1976) contained a detailed yearly load estimate for the years 1967 to 1974. This data set also has inherent problems which reduce the accuracy and confidence of the reported loads.

The loading estimates were computed using the long-term mean nutrient concentration for the years 1967 to 1974 and the mean annual flow for each year using the formula

$$L = \overline{C}\,\overline{F} \qquad (3.2.1)$$

where L = mean annual load

$\overline{C}$ = long-term mean nutrient concentration

$\overline{F}$ = mean annual flow.

This would have the effect of smoothing out the effects of decreasing nutrient concentrations on the annual load, and this adds an undesired bias to the data.

The data from only five tributaries were used, two of which are Canadian (12 Mile Creek, Trent River) to provide the tributary loading estimate. The computed loads were then scaled up by 1.54 for total phosphorus and 1.38 for total nitrogen to account for the input from other tributaries. The upstream load from municipal and industrial sources was subtracted from the tributary load which again produces an estimate which is probably too low.

The rationale for using the Trent River as one of only two Canadian tributaries is questionable. The Trent River empties into the Bay of Quinte, which has its outflow at the extreme eastern end of the lake. It seems reasonable to assume that almost all of the nutrient load leaving the Bay of Quinte is flushed straight down the St. Lawrence River. Thus, the Trent would appear to be a very poor choice upon which to base a tributary loading estimate.

Computation Formulas

The simplest method of calculating loads is flow times concentration,

$$L = FC \tag{3.2.2}$$

where L = load

F = flow

C = concentration.

The use of this formula can introduce extreme bias into the results. In cases where sampling is not evenly distributed throughout the year, or when sampling is more frequent during high flow periods, the resultant data set is skewed. This departure from normality results in values which are biased, either inaccurately high or low, depending on the nature of the data.

The use of an unbiased ratio estimation (3.2.3) reduces this bias by including a variance term in the equation. The resultant computed load is, therefore, a more accurate estimate of the true load from the tributary.

For this reason the International Joint Commission adopted the use of Beale's unbiased ratio estimator in computing tributary loads in 1975, i.e.,

$$u_y = \mu_x \cdot \frac{m_y}{m_x} \cdot \frac{\left(1 + \frac{1}{n} \cdot \frac{S_{xy}}{m_y m_x}\right)}{\left(1 + \frac{1}{n} \cdot \frac{S_x^2}{m_x^2}\right)} \tag{3.2.3}$$

where μ_x = mean daily flow for the year

m_y = mean daily loading for the days concentrations were determined

m_x = mean daily flow for the days concentrations were determined

n = number of days concentrations were determined

$$S_{xy} = \frac{\sum_{i=1}^{n} X_i Y_i - n \cdot m_y \cdot m_x}{n-1}$$

$$S_x^2 = \frac{\sum_{i=1}^{n} X_i^2 - n \cdot m_x^2}{n-1}$$

and X_i and Y_i are the individual measured flow and calculated loading, respectively, for each day concentrations were determined.

It is felt that this is the best method presently available for calculating tributary loadings, with the exception of using the estimator within the strata of a stratified data set. The latter would allow a more accurate estimate to be made, but it is not always feasible or possible to obtain stratified data.

Present Study

This study was performed to produce a data set of historical loadings to Lake Ontario as well as provide a seasonal breakdown of the data.

The net load to a lake is equal to the inputs minus the outputs. The inputs into the lake come from: Tributaries, Direct Municipal, Direct Industrial, Atmospheric, Groundwater, Resuspension from Sediments. The outputs are: Outflow, Sedimentation. For the purposes of this study "net load" is defined as the difference between inputs and outflow, but excluding resuspension and sedimentation. Also, it was shown by Fraser *et al.* (1977) that the groundwater term is negligible when compared to the tributary inflow and thus was not considered further. Therefore, the net load to Lake Ontario is computed using the formula:

Net Load = Tributary Load + Direct Municipal Load +
Direct Industrial Load + Atmospheric Load +
Niagara River, - Outflow (St. Lawrence River)

Each of the above terms will be discussed further below. The net loads considered are for the parameters: total phosphorus, soluble reactive phosphorus (orthophosphate), total nitrogen, ammonia, nitrite + nitrate, and chloride, and were determined for the years 1967 to 1976.

It was decided to use the zones developed by the surveillance group at CCIW and to sum the loads from the various dischargers in each zone. These zones were shown previously in Figure 3.1.4. The present summary deals only with the whole lake load and the loads to Hamilton Bay (zone 8) and the Bay of Quinte (zone 1). The latter two were subtracted from the whole lake load to obtain the loading to the main body of the lake.

Hamilton Bay was not included in the lake load, as it acts as a giant settling pond. Several studies have been performed to determine the magnitude of the flux of nutrients out into Lake Ontario with the result that no statistically conclusive statements can be made regarding this flux.

The "main lake" loading estimates, summarized in Tables 3.2.1 to 3.2.6, do not include the zone 1 load due to the uncertainty involved in estimating how much the Bay of Quinte influences the open lake. The net loads to Lake Ontario were calculated by adding the zone 1 load to the "main lake" load before subtracting the St. Lawrence (outflow) load.

TABLE 3.2.1: *Estimated load of total phosphorus to Lake Ontario: metric tonnes*

Year	Zone 8 Load	Zone 1 Load	Load to Main Lake	Main Lake + Zone 1 Load	St. Lawrence Outflow	Net Load
1967	353	375	10 996	11 371	4 694	6 677
1968	498	389	13 173	13 562	7 119	6 443
1969	439	818	13 779	14 597	6 397	8 200
1970	394	322	13 452	13 774	5 032	8 742
1971	358	328	13 046	13 374	4 269	9 105
1972	375	468	13 093	13 561	5 394	8 167
1973	309	351	12 592	12 943	4 538	8 405
1974	255	377	11 158	11 535	5 274	6 261
1975	104	295	10 075	10 370	5 407	4 963
1976	91	351	9 355	9 706	4 545	5 161

TABLE 3.2.2: *Estimated load of soluble reactive phosphorus to Lake Ontario: metric tonnes*

Year	Zone 8 Load	Zone 1 Load	Load to Main Lake	Main Lake + Zone 1 Load	St. Lawrence Outflow	Net Load
1967	203	128	5 614	5 742		
1968	59	113	4 997	5 110	2 212	2 898
1969	59	141	5 551	5 692	2 327	3 365
1970	67	82	5 558	5 640	2 017	3 623
1971	61	71	4 528	4 599	3 845	754
1972	75	102	3 959	4 061	1 957	2 104
1973	67	99	4 049	4 148	1 580	2 568
1974	64	37	3 395	3 432	2 635	797
1975	42	25	3 631	3 656	944	2 712
1976	22	24	2 811	2 835		

TABLE 3.2.3: *Estimated load of total nitrogen to Lake Ontario: metric tonnes*

Year	Zone 8 Load	Zone 1 Load	Load to Main Lake	Main Lake + Zone 1 Load	St. Lawrence Outflow	Net Load
1967	15 018	8 171	87 641	95 812		
1968	4 816	5 857	162 189	168 046	81 745	86 301
1969	4 736	5 977	168 615	174 592	127 773	46 819
1970	4 714	4 345	171 237	175 582	130 416	45 166
1971	4 836	4 434	184 848	189 282	114 727	74 555
1972	5 033	8 823	207 092	215 915	103 216	112 699
1973	5 266	6 045	230 373	236 418	103 581	132 837
1974	5 360	6 014	220 217	226 231	103 839	122 392
1975	4 546					
1976	4 656					

TABLE 3.2.4: *Estimated load of ammonia to Lake Ontario: metric tonnes*

Year	Zone 8 Load	Zone 1 Load	Load to Main Lake	Main Lake + Zone 1 Load	St. Lawrence Outflow	Net Load
1967	155	1 332	43 368	44 700		
1968	162	666	36 924	37 590	16 691	20 899
1969	162	443	31 577	32 020	18 918	13 102
1970	157	316	30 286	30 602	18 335	12 267
1971	156	316	30 246	30 562	15 561	15 001
1972	169	420	25 788	26 208	7 262	18 946
1973	311	503	27 761	28 264	12 562	15 702
1974	318	417	31 877	32 294	10 838	21 456
1975					7 410	
1976	303				4 735	

TABLE 3.2.5: *Estimated load of nitrate + nitrite to Lake Ontario: metric tonnes*

Year	Zone 8 Load	Zone 1 Load	Load to Main Lake	Main Lake + Zone 1 Load	St. Lawrence Outflow	Net Load
1967	121	2 052	13 937	15 989		
1968	184	2 067	35 423	37 490	27 477	10 043
1969	144	785	33 326	34 111	47 733	-13 622
1970	176	718	35 908	36 626	56 381	-19 755
1971	252	848	38 977	39 825	23 684	16 141
1972	364	1 515	42 625	44 140	16 549	27 591
1973	446	1 438	63 731	65 169	21 202	43 967
1974	507	1 186	89 469	90 655	27 463	63 192
1975						
1976						

TABLE 3.2.6: *Estimated load of chloride to Lake Ontario: metric tonnes*

Year	Zone 8 Load	Zone 1 Load	Load to Main Lake	Main Lake + Zone 1 Load	St. Lawrence Outflow	Net Load
1967	9 370	90 393	6 143 152	6 233 545	5 201 569	1 031 976
1968	8 078	39 867	5 947 711	5 987 578	6 051 015	-63 437
1969	7 368	40 525	6 863 625	6 904 150	6 323 887	580 263
1970	7 872	38 647	6 640 548	6 679 195	6 171 557	507 638
1971	10 965	62 916	6 638 345	6 701 261	6 230 127	471 134
1972	12 198	61 545	6 748 472	6 810 017	6 626 253	183 764
1973	13 851	52 691	6 786 435	6 839 126	7 470 470	-631 344
1974	12 755	45 906	6 755 838	6 801 744	6 911 205	-109 461
1975						
1976						

Municipal and industrial loads from plants which discharge upstream from the tributary monitoring stations were not subtracted from the tributary load. This provided a value which was representative of the load which was actually discharged from the tributary mouth.

The Canadian tributary loads were calculated from Ontario Ministry of the Environment (MOE) data by Ongley (1974). This data set was provided by the Pollution from Land Use Activities Reference Group (PLUARG) Canadian Task Group D.

In this data set there was a total of 26 tributaries for which adequate flow and concentration data exists. Nine of these tributaries have flow gauges located close to the tributary mouth. The remaining 17 tributaries have flow gauges located upstream from the sampling sites. The flow was augmented using areal deposition rates to account for the downstream portion of the tributary. There are an additional 25 tributaries in this data set for which there is concentration data but no flow data. A regression of mean annual discharge on basin area (Ongley, 1974) showed that for Canadian tributaries to Lake Ontario, the mean annual discharge is proportional to the basin area. This allowed an annual load to be calculated; thus 51 tributaries were used to produce the estimate of Canadian tributary loading.

Although the loads were calculated using the monthly mean concentration times the monthly mean flow, the data was accepted as being a good estimate of the true load. A study performed by Gregor (1977) showed that there was no significant trend in differences between loads calculated using a ratio estimator and loads calculated using Ongley's (1974) method. It was felt that the observed differences were probably within the error associated with the two methods.

This data set covered the period of record from 1967 to 1974. The 1975 and 1976 data records were not available from the Ontario Ministry of the Environment at the time of this study. Accordingly, an estimate of the total phosphorus load for 1975 and 1976 was obtained from PLUARG. These estimates were based on a water year (October 1975 to October 1976), and after recalculation to the calendar year basis were used to estimate the 1975, 1976 tributary loading of total phosphorus.

The U.S. tributary loads were based on concentration data supplied by the New York State Department of Environmental Conservation, and daily flow records were obtained from the U.S. Geological Survey Water Resources Data Publications. Although data for only three tributaries were available it was felt that these would be adequate, since the same three tributaries have been used in other studies. A computer program developed by A.S. Fraser of CCIW was used to calculate the loads on a monthly and yearly basis using the ratio estimator.

The data set thus provided information for the years 1967 to 1976. An additional 1976 estimate was obtained from a report by Sonzogni *et al.* (1978), based on a water year. Sonzogni's values were compared with the computed calendar year estimated loads to obtain a conversion factor, and this factor was applied to the 1975, 1976 Canadian water year load estimates, above, to obtain estimates on the calendar year basis.

Municipal Loads

Direct municipal dischargers were defined as those which discharge either directly to Lake Ontario, to tributaries which are neither monitored nor tributary to a monitored tributary, or to monitored tributaries but discharged downstream from the monitoring station. A listing of direct municipal discharges was obtained from the 1976

Great Lakes Water Quality Board Remedial Programs Subcommittee report. This was checked against the list in the 1969 report and the list was amended accordingly.

Concentration data for all plants were obtained from the Ontario Ministry of the Environment. Flow data for the Ministry-operated plants, (8 of the 27 identified), were obtained from the individual plants.

Because instantaneous flow data at the time of sampling were not available and because municipal plant flows are highly variable, it was decided to use the monthly mean concentration values and the total flow values to compute total monthly loads. Data for periods where no flow data were available, either through lack of sampling or lack of records, were estimated by extrapolating the information from records for other years. The U.S. municipal data, both concentration and flow, were supplied by the New York State Department of Environmental Conservation. A total of 10 U.S. plants were identified and used in this study.

Industrial Loads

Direct industrial dischargers were defined to be those industries which discharge either directly to the lake, to tributaries which are neither monitored nor tributary to a monitored tributary, or to monitored tributaries but downstream from the monitoring station.

Canadian industrial data were generally unavailable from the monitoring agency (MOE). Some data for 1974 to 1976 were obtained from A. Sudar of CCIW. Additional data for this time period were obtained from the Great Lakes Water Quality Board Reports for 1974 to 1976. The 1969 Great Lakes Water Quality Board Report was used to obtain information for 1967, and information for the year 1968 was supplied by the MOE.

Data for missing years were estimated by extrapolation from the available information. As no information on seasonal loading was obtainable, the total yearly loads were divided by 12 to obtain a crude estimate of monthly loads. This was felt to be an acceptable method, since industrial dischargers were not expected to exhibit a pronounced seasonal cycle in discharge. A total of 36 industries were identified and used to make the estimate of industrial loading. The U.S. industrial data for the nine identified dischargers were supplied by the New York State Department of Environmental Conservation.

Atmospheric Loads

Estimation of atmospheric loading to Lake Ontario from both wet and dry deposition is extremely difficult due to the large number of error sources. Matheson (1974) discussed these error sources which included the problems of:

a) getting reproducible replicate samples
b) extrapolating the deposition on a small sampler area to the large lake area,
c) determining the representativeness of the sample station network, and
d) sample contamination from birds, insects, vegetable matter, etc.

Despite these many problems, reasonable estimates of atmospheric loading to Lake Ontario have been computed. A report by Elder *et al.* (1977) indicates that the best estimate of loading to Lake Ontario is a constant load over the past 10 years. A CCIW (1977) report shows that a linear least-squares fit of data from 1972 to 1976 again shows a trend of constant loading.

Estimated loads for total phosphorus, total nitrogen, and chloride were taken from the report by Elder *et al.* (1977). Analysis of data from Shiomi and Kuntz (1973) and CCIW atmospheric data allowed estimates of loads for soluble reactive phosphorus, ammonia, nitrite + nitrate to be made. No attempt was made to break these yearly values down into monthly loading estimates.

Niagara River

Concentration data taken by the MOE for the period 1967 to 1973 were supplied by PLUARG Canadian Task Group D. Additional data from 1969 to 1976 were supplied by the NYSDEC. Daily sample records for 1976 were supplied by C.H. Chan of CCIW. The flow records, taken at Queenston, were obtained from the Water Planning and Management Branch (Department of Fisheries and Environment).

Niagara Loading Estimate Problems

The Niagara River poses a unique problem in attempts to estimate loads to Lake Ontario. The load to the lake from this one source is so large in relation to all other sources that the confidence one has in the complete data set is closely linked to the confidence in the Niagara River data set (Sweers, 1969).

The problem of determining the number of samples which is required to obtain an efficient estimate of the material loadings was considered by El-Shaarawi and Whitney (1977). Those authors have applied time series methods and the principle of sampling technique, to arrive at a plan for sampling the phosphorus input from the Niagara River to Lake Ontario. The phosphorus data used were collected by the Water Quality Branch, and these data were of two types: (1) hourly samples were collected for four separate seven-day periods: August 12-18, 1975; November 22-28, 1975; February 11-17, 1976, and May 4-10, 1976. (2) daily samples were gathered between June to December 31, 1975. The flow rates data were measured at Queenston and were supplied by Water Planning and Management Branch (Department of Fisheries and Environment).

The hourly data and the daily data were analyzed separately because each set of data deals with different levels of variability. The steps of the analysis were:

(1) The application of the Box and Jenkins (1970) procedure for modeling time series data to obtain a model for the phosphorus concentration;

(2) The resulting phosphorus model was then combined with the flow rate data, which is assumed to be deterministic, to obtain an estimate for the loading;

(3) The variance of the loading was calculated under the three sampling designs: (a) simple random sample; (b) stratified; and (c) systematic. Comparison of the variances has shown that systematic plan was the best;

(4) Using the systematic plan, the number of samples required to estimate the mean phosphorus loads with a predefined precision with a specific confidence coefficient was determined. To be specific, let $d = \hat{X} - X$ be the minimum precision desirable in estimating the mean daily load

where $\hat{X}$ and X are the observed and the true mean loads, respectively. In El-Shaarawi and Whitney (1977), the relationship between the number of samples n and the absolute deviation $|d|$, was given.

Table 3.2.7 presents the mean daily loading $\bar{X}$ in metric tons, as taken from the extensive sampling, the absolute deviation $|d|/\bar{X}$ and the required sample size n for the hourly and the daily data under the 5% confidence coefficient. The table shows great variations in mean daily loading with the mean loading in May exceeding three times the corresponding value in August. The same relationship between the means was reflected in the absolute deviation, i.e., the maximum value of $|d|$ was obtained during May when the sample size is fixed. This suggests a corresponding relationship for the fluctuations and hence one needs different sample sizes for estimating the daily loadings with the same relative precision for different seasons. Sampling once a day (i.e., ignoring hourly variation) will produce an estimate which is subject to a maximum relative error of 0.09, 0.31, and 0.35 for August, February and May, respectively. On the other hand, sampling twice or three times a day will give relative maximum errors of 0.07 and 0.04 for August; 0.19 and 0.11 for February and 0.22 and 0.13 for May. If the hourly fluctuations were ignored, then it is required to sample once a month for the period of June 1 to December 31 to obtain an estimate with maximum relative precision 0.27, while twice and three times a month will produce an estimate with maximum precision of 0.16 and 0.06, respectively.

TABLE 3.2.7: *Mean T.P. load, absolute and relative precision and the corresponding sample size*

Period	Mean Daily Input in Metric Tons $\bar{X}$	d	$d\|\bar{X}$	*n	d	$d\|\bar{X}$	n	d	$d\|\bar{X}$	n
Aug. 12-18, 1975	7.68	0.65	0.09	7	0.51	0.07	14	0.33	0.04	21
Feb. 11-17, 1976	15.95	4.90	0.31	7	3.06	0.19	14	1.83	0.11	21
May 4-10, 1976	25.40	8.98	0.35	7	4.70	0.22	14	3.25	0.13	21
June 1-Dec. 31, 1975	13.03	3.52	0.27	6	2.08	0.16	12	0.86	0.06	36

*n = The number of samples required in the corresponding period.

A comparison of Table 3.2.8, which shows the number of samples in the data set, with Table 3.2.7, which shows the confidence limits associated with various sampling frequencies, illustrates the confidence which can be placed upon this particular data set.

TABLE 3.2.8: *Number of samples, n, in data set for Niagara River*

	February	May	Aug	June-Dec	Jan-Dec
1967		3	2	4	7
1968		1		2	4
1969		1	2	11	12
1970		1	2	12	14
1971		1	2	10	16
1972	1	3	2	17	24
1973	1	4	2	10	18
1974	1	1	1	7	12
1975	1	1	1	7	13
1976	4	5	5	31	55

St. Lawrence River

The flow data used were those measured at Cornwall by Water Surveys Canada. These values were converted to flows at Wolfe Island using the method determined by Casey and Salbach (1974). Concentration data for the North Channel were obtained from MOE data files. The South Channel data were obtained from the United States Geological Survey - Water Resources data for New York publications. The loads were computed using the ratio estimator equation (3.2.3).

Remarks on Tables 3.2.1 - 3.2.6

The values presented in these tables are preliminary estimates. They represent the best possible estimates using the presently available data set. As more data become available, these estimates will be updated. Final summaries will be presented by Willson (1978).

In particular, the following points should be noted. The 1975-1976 Canadian tributary data is not available at the present time, except for total phosphorus; thus no estimates are included for these years in Tables 3.2.2 to 3.2.6. Although the loading values presented

here are the best possible at the present time, they should not be considered as absolute. Further revisions of the provided data sets, inclusions of extra data, and changes in computation techniques could result in major revision to the loading estimates. Caution is, therefore, advised when the loadings are considered. It would be advisable to observe the trends in the loading values rather than the magnitude of the loads.

And finally, it may be seen that the present estimates for the years 1972-1973 are not the same as the IFYGL data presented in Chapter 2.1. Since the present study is not yet complete, it should not be concluded that the earlier data are wrong. By way of illustration, we may consider the total phosphorus loading for this period. This is done in Table 3.2.9. It is seen that the differences between the two estimates are largely due to the missing U.S. tributary data and the updated precipitation estimates.

TABLE 3.2.9: *Total phosphorus load to Lake Ontario in metric tonnes, Apr. 72 - March 73*
1 = IFYGL estimates (Chapter 2.1)
2 = estimates in this Chapter

	Apr - Dec 72		Jan - Mar 73		Apr 72 - Mar 73	
	1	2	1	2	1	2
Niagara River	5 445	5 907	2 130	2 121	7 575	8 028
U. S. major trib.	1 290	1 482	507	636	1 797	2 118
U. S. minor trib.	1 425	-	699	-	2 124	-
Canadian trib.	816	499	417	218	1 233	717
U. S. municip. + indust.	36	140	18	114	54	254
Can. municip. + indust.	2 067	1 581	855	620	2 922	2 201
Precipitation	1 713	354	429	108	2 142	462
Total inputs	12 792	9 963	5 055	3 817	17 847	13 780

3.3 Analysis of Long-Term Variations of Nutrients and Chlorophyll

Water samples have been collected routinely for at least 10 years from a number of stations in Lake Ontario, and analyzed to determine physical, chemical and biological characteristics. The basic objectives of this data collection were to describe the lake conditions on a year to year basis, to note the spatial and temporal changes in the water quality, and

to provide a continuing report and long-term trend information on water quality and eutrophication variables.

Since nutrient and plankton data on Lake Ontario are characterized by large variations in space as well as in time, a meaningful analysis of long-term trends must differentiate between different regions of the lake. As outlined at the end of Section 3.1, volume-weighted mean concentrations of all surveillance data between 1966 and 1977 are available for the 17 zones shown in Figure 3.1.4, which were defined on the basis of statistical investigations of spatial data variability. In the first part of this Section, these concentrations will be used to estimate trends for the major nutrients in Lake Ontario. The second part will be devoted to a detailed analysis of chlorophyll data.

To eliminate the seasonal and sampling variability, only data collected during the late winter (up to mid-April) isochemical period are used in the nutrient trend evaluation. Consequently, only 14 cruises can be utilized, all of them during the 1970-1977 period because prior to that no data were collected during winter.

Total Phosphorus

Volume-weighted mean total phosphorus concentrations in early spring are presented in Table 3.3.1. Area-weighted concentrations of total phosphorus in early spring are depicted in Figure 3.3.1 for zone 5 and for the whole lake (zone 25). Zone 5, the area east of Toronto, shows a systematic decrease of phosphorus concentrations, much more than appears in the whole lake. For each zone, a linear regression analysis was performed, together with an independent non-parametric test of rank correlation. The results are found in Table 3.3.2. Using both tests, there is a statistically provable decrease ($P < 5\%$) in the spring total P concentrations in zones 4, 5, 6 and 15. Both tests also indicate that the decreases observed in zones 1, 2, 3, 7, 12 and 13 and the lake as a whole are probable. Finally, the other five zones suggest that there exists a total P concentration decrease, but the decrease is not statistically provable.

It appears, therefore, that the combination of improved sewage treatment and the ban on phosphorus in detergents has resulted in a significant improvement in the concentration of total phosphorus in

offshore Lake Ontario, particularly in the region near Toronto, where the 1977 spring concentration has declined almost 35% from the 1970-1971 concentration.

TABLE 3.3.1: Volume-Weighted Mean Total Phosphorus, Lake Ontario, Early Spring - mg P/litre

ZONE	1970	1971	1972	1973	1974	1975	1976	1977
1	0.0245	0.0227	0.0257	0.0243	0.0220	0.0207	0.0229	0.0226
2	0.0248	0.0224	0.0254	0.0237	0.0220	0.0194	0.0229	0.0207
3	0.0219	0.0252	0.0245	0.0252	0.0218	0.0201	0.0222	0.0208
4	0.0238	0.0262	0.0248	0.0247	0.0218	0.0216	0.0211	0.0214
5	0.0264	0.0279	0.0273	0.0250	0.0237	0.0217	0.0227	0.0213
6	0.0318	0.0386	0.0250	0.0293	0.0300	0.0230	0.0231	0.0231
7	0.0275	0.0306	0.0229	0.0254	0.0221	0.0215	0.0229	0.0226
9	0.0273	0.0344	0.0268	0.0376	0.0277	0.0324	0.0241	0.0246
10	0.0223	0.0255	0.0238	0.0247	0.0244	0.0213	0.0253	0.0214
11	0.0230	0.0296	0.0241	0.0321	0.0355	0.0292	0.0231	0.0216
12	0.0257	0.0260	0.0248	0.0278	0.0228	0.0258	0.0299	0.0214
13	0.0239	0.0301	0.0234	0.0249	0.0222	0.0240	0.0210	0.0217
14	0.0239	0.0306	0.0226	0.0250	0.0218	0.0249	0.0241	0.0243
15	0.0248	0.0260	0.0247	0.0246	0.0218	0.0230	0.0213	0.0220
16	0.0247	0.0256	0.0254	0.0247	0.0220	0.0248	0.0238	0.0230
17	0.0223	0.0253	0.0229	0.0235	0.0246	0.0215	0.0219	0.0225
Whole Lake	0.0234	0.0273	0.0239	0.0248	0.0243	0.0222	0.0225	0.0222

TABLE 3.3.2: Statistical Analysis of Total Phosphorus Data of Table 3.3.1

	LINEAR REGRESSION METHODS			RANK CORRELATION METHODS	
ZONE	SLOPE OF REGRESSION LINE	(r^2) COEFFICIENT OF DETERMINATION	SCORE (S)	RANK CORRELATION COEFFICIENT ( )	PROBABILITY THAT CORRELATION IS RANDOM
1	- 0.00039	0.3446	12	- 0.4286	0.089
2	- 0.00055	0.4447	14	- 0.5000	0.054
3	- 0.00047	0.3306	10	- 0.3637	0.138
4	- 0.00065	0.6788	20	- 0.7143	0.0071
5	- 0.00095	0.8382	22	- 0.7857	0.0028
6	- 0.00171	0.5730	14	- 0.5092	0.054
7	- 0.00096	0.5446	14	- 0.5092	0.054
9	- 0.00087	0.1824	8	- 0.2857	0.199
10	- 0.00018	0.0672	4	- 0.1429	0.360
11	- 0.00028	0.0186	4	- 0.1429	0.360
12	- 0.00057	0.4317	12	- 0.4286	0.089
13	- 0.00074	0.4071	14	- 0.5000	0.054
14	- 0.00031	0.0823	2	- 0.0714	0.452
15	- 0.00061	0.7438	20	- 0.7143	0.0071
16	- 0.00030	0.3596	12	- 0.4364	0.089
17	- 0.00022	0.1695	6	- 0.2143	0.274
whole lake	- 0.00045	0.4198	12	- 0.4364	0.089

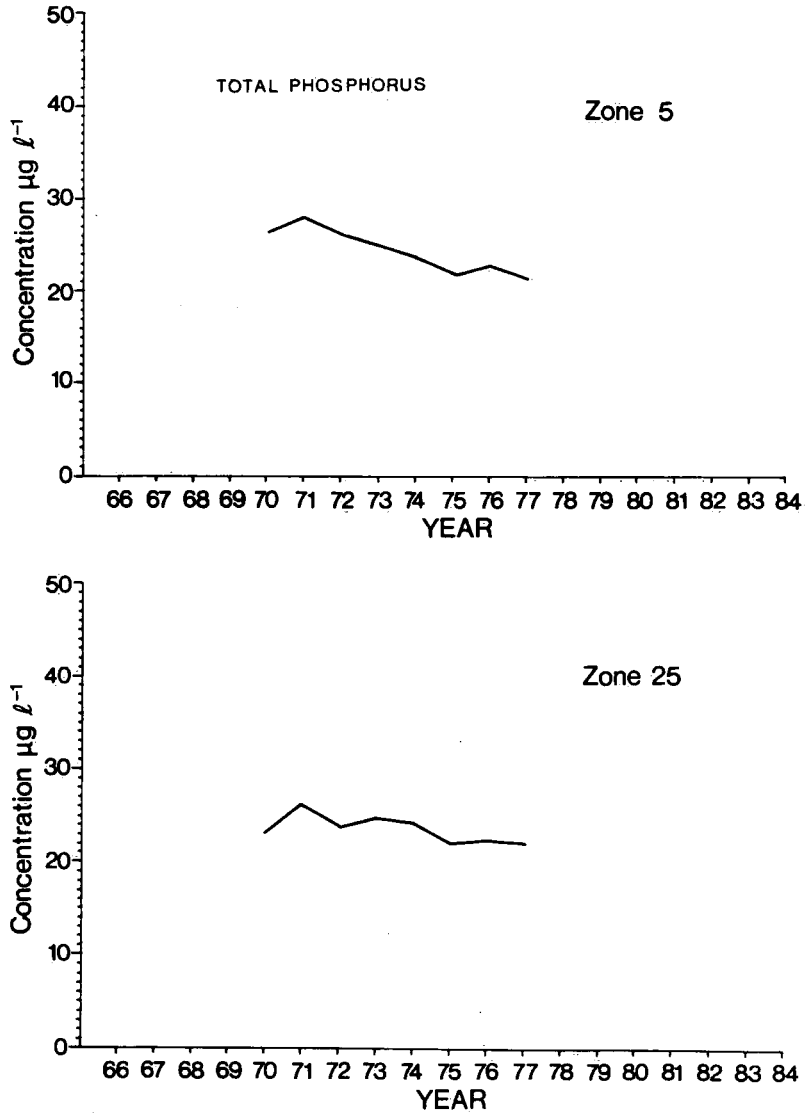

Figure 3.3.1 Area-weighted concentration of total phosphorus in early spring for two lake zones.

Nitrogen

In contrast with total phosphorus, the nitrogen content in Lake Ontario, as indicated by the spring concentration of filtered nitrate + nitrite, is increasing.

The same system of lake zones (Figure 3.1.4) and data analysis technique used to determine the total phosphorus trends was applied to the nitrate data. In this case, data from two depths (one metre and 40 metres) were used in the analysis (Tables 3.3.3 and 3.3.4). Statistical

summaries of the data are presented in Tables 3.3.5 and 3.3.6. Figure 3.3.2 illustrates typical nitrate variations for two zones in Lake Ontario and for the whole lake (zone 25). All concentrations refer to the 40-m depth.

TABLE 3.3.3: FILTERED NITRATE + NITRITE , Lake Ontario, Early Spring, 1-metre depth

mg N/litre

ZONE/YEAR	1967	1968	1969	1970	1971	1972	1973	1974	1975	1976	1977
1			0.1892	0.2256	0.2198	0.1731	0.2274	0.2820	0.2031	0.2456	0.3186
2			0.2146	0.2190	0.2452	0.1786	0.2325	0.2820	0.2200	0.2918	0.3166
3			0.1865	0.2235	0.2252	0.2031	0.2489	0.2774	0.2540	0.2574	0.3058
4			0.2127	0.2338	0.2282	0.2599	0.2657	0.2549	0.2727	0.2174	0.3015
5			0.2457	0.2662	0.2585	0.2359	0.2580	0.2806	0.2887	0.2858	0.3167
6			0.2471	0.2793	0.2682	0.2554	0.3151	0.3040	0.2937	0.3078	0.3265
7			0.2490	0.2965	0.2607	0.2405	0.2634	0.2910	0.2879	0.3084	0.3180
8			-	-	-	-	-	-	-	-	-
9			0.2118	0.2425	0.2463	0.1979	0.2619	0.3149	0.2892	0.3007	0.3065
10			0.2419	0.2583	0.2506	0.2386	0.2605	0.2966	0.2866	0.3038	0.3076
11			0.2400	0.2421	0.2548	0.1950	0.2494	0.2891	0.2804	0.3093	0.3028
12			0.2474	0.2486	0.2450	0.1850	0.2561	0.2889	0.2899	0.2960	0.3114
13			0.2355	0.2319	0.2416	0.2703	0.2473	0.2934	0.2890	0.2995	0.3181
14			0.2340	0.2528	0.2934	0.2550	0.2451	0.2928	0.3044	0.2964	0.3165
15			0.2422	0.2422	0.2573	0.1713	0.2406	0.2884	0.2571	0.3290	0.3180
16			0.2032	0.2267	0.2363	0.1725	0.2344	0.2820	0.4811	0.3197	0.3180
17			0.2391	0.2396	0.2601	0.2255	0.2453	0.2842	0.2797	0.2996	0.3159
WHOLE LAKE			0.2331	0.2438	0.2539	0.2217	0.2494	0.2860	0.2772	0.2937	0.3141

The data collected from the one-metre depth describe an increasing trend for the concentration of nitrate, although much more variation is associated with these data than with the data collected at the 40-metre depth. This variation in the surface water arises from annual changes in the time of the start of phytoplankton growth and the concentration of nitrate in these waters. For this reason, the 40-metre data have been used to describe the trend for nitrate in Lake Ontario.

TABLE 3.3.4: Filtered Nitrate + Nitrite, Lake Ontario, Early Spring, 40 metres depth

mg N/litre

ZONE/YEAR	1967	1968	1969	1970	1971	1972	1973	1974	1975	1976	1977
1			0.1839	0.2139	0.2042	0.2083	0.2404	0.2810	0.2048	0.2466	0.3216
2			0.2112	0.2120	0.2400	0.2106	0.2536	0.2810	0.2422	0.3226	0.3203
3			0.1783	0.2087	0.2545	0.2165	0.2315	0.2764	0.2601	0.3041	0.3125
4			0.2415	0.2196	0.2284	0.2698	0.2610	0.2534	0.2785	0.2555	0.3102
5			0.2395	0.2521	0.2207	0.2367	0.2588	0.2802	0.2903	0.3035	0.3187
6			0.2300	0.2705	0.2413	0.2590	0.2544	0.3033	0.2963	0.3092	0.3339
7			0.2478	0.2770	0.2778	0.2664	0.2664	0.2912	0.2960	0.3110	0.3448
8			-	-	-	-	-	-	-	-	-
9			0.2203	0.2457	0.2233	0.2189	0.2663	0.2987	0.2895	0.3041	0.3091
10			0.2351	0.2505	0.2298	0.2555	0.2565	0.2903	0.2883	0.3044	0.3095
11			0.2230	0.2430	0.2310	0.2324	0.2691	0.2866	0.2888	0.2965	0.3041
12			0.2457	0.2251	0.2300	0.1975	0.2635	0.2801	0.2846	0.3046	0.3269
13			0.2406	0.2404	0.2448	0.2706	0.2715	0.2875	0.2837	0.3098	0.3236
14			0.2419	0.2395	0.2470	0.2468	0.2665	0.2892	0.2892	0.3087	0.3235
15			0.2341	0.2267	0.2504	0.1985	0.2615	0.2875	0.2749	0.3242	0.3190
16			0.1982	0.2117	0.2182	0.1946	0.2521	0.2810	0.4557	0.3199	0.3190
17			0.2360	0.2315	0.2477	0.2244	0.2617	0.2849	0.2862	0.3083	0.3182
WHOLE LAKE			0.2357	0.2354	0.2437	0.2318	0.2608	0.2864	0.2872	0.3076	0.3173

From the data in Table 3.3.4, it was determined that the mean lakewide increase in nitrate concentration during the last nine years averaged 0.011 mg N ℓ^{-1} yr^{-1}. This is an average increase of 4% yr^{-1} in the total spring lakewide content of nitrate. The largest increase occurs in zone 16 (0.017 mg N ℓ^{-1} yr^{-1}), the smallest in zone 4 (0.008 mg N ℓ^{-1} yr^{-1}), but in every zone, there is less than a 1% chance that the observed trend is not real.

The cause or causes of the observed increase are not clear at the present time. The reason may be as simple as the fact that there are no controls on nitrogen inputs to Lake Ontario or it may be as complex as a change in the feeding habits of the Lake Ontario phytoplankton community.

TABLE 3.3.5: NITRATE IN LAKE ONTARIO, NINE YEAR TREND, 1 metre depth

ZONE	LINEAR REGRESSION METHODS		RANK CORRELATION METHODS		
	SLOPE OF REGRESSION LINE	COEFFICIENT OF DETERMINATION (r^2)	SCORE (S)	RANK CORRELATION COEFFICIENT ($_1$)	PROBABILITY THAT CORRELATION IS RANDOM
1	0.0062	0.2033	19 (8)	0.3571	0.0116
2	0.0084	0.3116	22 (8)	0.5714	0.0028
3	0.0118	0.7677	32	0.7778	0.00012
4	0.0065	0.3769	27	0.5000	0.0021
5	0.0075	0.6779	29	0.6111	0.00083
6	0.0084	0.6907	30	0.6667	0.00043
7	0.0069	0.4925	28	0.5556	0.0012
8	-	-	-	-	-
9	0.0126	0.6688	30	0.6667	0.00043
10	0.0088	0.7921	31	0.7222	0.00027
11	0.0100	0.5650	30	0.6667	0.00043
12	0.0099	0.4977	31	0.7222	0.00027
13	0.0109	0.8772	33	0.8333	0.000073
14	0.0087	0.6325	30	0.6667	0.00043
15	0.0101	0.3007	19 (8)	0.6910	0.0116
16	0.0155	0.5843	29	0.6111	0.00083
17	0.0098	0.7527	31	0.7222	0.00027
WHOLE LAKE	0.0097	0.7562	31	0.7222	0.00027

It is therefore recommended that this problem be addressed during the intensive surveillance of Lake Ontario during 1981 and 1982. It may be interesting to note that some plankton models of the type discussed in Chapter 2.3 would predict an increase in nitrogen for decreasing phosphorus loading, because there would be less phytoplankton growth and therefore less sedimentation of particulate nitrogen.

Chloride

For purposes of comparison with the nutrient trends described above, the same zonal analysis was undertaken with a conservative variable, namely filtered chloride. A chemical variable is considered conservative when its concentration in the lake varies directly with loadings and lake

TABLE 3.3.6: NITRATE IN LAKE ONTARIO, NINE YEAR TREND, 40 metres depth

ZONE	LINEAR REGRESSION METHODS		RANK CORRELATION METHODS		
	SLOPE OF RE-GRESSION LINE	COEFFICIENT OF DETERMINATION (r^2)	SCORE (S)	RANK CORRELATION COEFFICIENT (τ)	PROBABILITY THAT COR-RELATION IS RANDOM
1	0.0120	0.5655	29	0.6111	0.00083
2	0.0141	0.7573	30	0.6667	0.00043
3	0.0149	0.8350	33	0.8333	0.000073
4	0.0078	0.6099	28	0.5556	0.0012
5	0.0109	0.8067	32	0.7778	0.00012
6	0.0114	0.8089	31	0.7222	0.00028
7	0.0092	0.7692	31	0.8733	0.00028
8	-	-	-	-	-
9	0.0124	0.8035	31	0.7222	0.00028
10	0.0102	0.8784	33	0.8333	0.000073
11	0.0109	0.8902	34	0.8889	0.000025
12	0.0126	0.6947	31	0.7222	0.00028
13	0.0106	0.9425	34	0.8889	0.000025
14	0.0110	0.9281	33	0.9297	0.000073
15	0.0128	0.7017	30	0.6667	0.00043
16	0.0172	0.8750	30	0.6667	0.00043
17	0.0116	0.8560	32	0.7778	0.00012
WHOLE LAKE	0.0114	0.8916	32	0.7778	0.00012

volume, and inversely with lake discharge. It is, therefore, an ideal parameter with which to calculate chemical budgets or to trace chemically distinct water masses.

As pointed out in Volume 3 of the IJC Lower Lake Report of 1969, the chloride concentration in Lake Ontario had increased from 7 mg ℓ^{-1} in 1907 to 26 mg ℓ^{-1} in 1966. This is an annual rate of increase of 0.32 mg ℓ^{-1} yr^{-1}. The post 1966 data are summarized in Table 3.3.7 and the whole lake trend since this time is illustrated in Figure 3.3.3. It should be noted that after almost 60 years of increasing, the chloride concentration in Lake Ontario peaked in the period 1973-1974 at just less than 29 mg Cl ℓ^{-1}. For the last few years, the chloride concentration has been decreasing, and the concentration presently stands at 27.7 mg ℓ^{-1}.

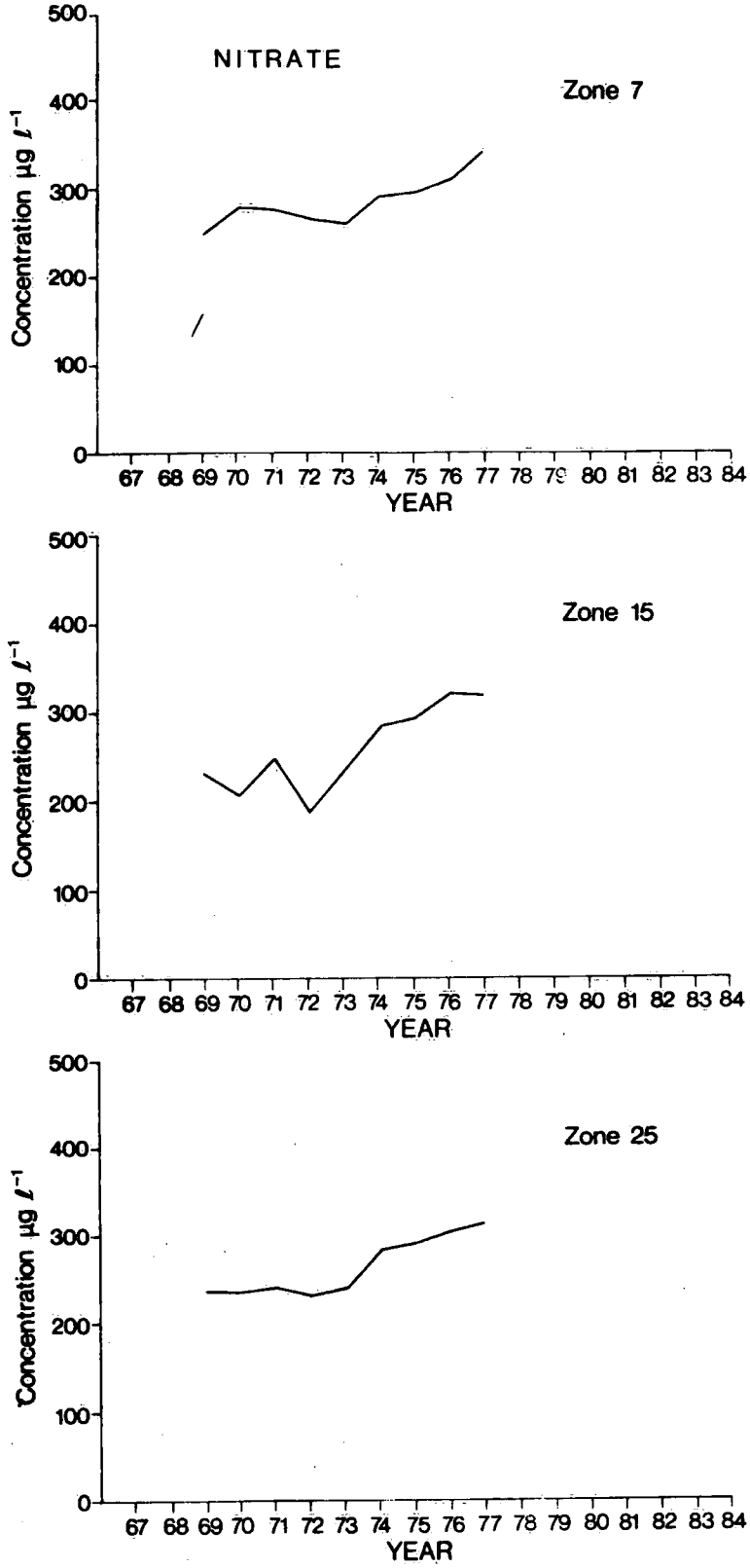

Figure 3.3.2 Volume-weighted concentration of nitrate in early spring, for two zones in Lake Ontario and for whole lake (zone 25). Concentrations are for the 40-m depth.

The long-term increase, recent maximization, and subsequent decrease in concentration reflect the conservative nature of this element in the lake system. The long-term concentration increase is primarily a result of an increase in chloride loadings to the lake, since lake volume has remained relatively (< 5% difference) constant. The loading increase was so prolonged and so large that a new input-output equilibrium took 56 years to achieve and did not occur until 1973-1974.

TABLE 3.3.7: *Volume-weighted mean chloride concentration for whole of Lake Ontario, 1966 - 1977*

Year	Mean Concentration of Filtered Chloride mg ℓ^{-1}
1966	26.2
1967	26.7
1968	27.3
1969	27.3
1970	no data collected
1971	28.5
1972	28.6
1973	28.8
1974	28.8
1975	28.3
1976	27.7
1977	27.7

Since 1974 chloride concentration in Lake Ontario has decreased, and the decrease is attributable mostly to increased water outflow from the lake. If the outflow volume had remained at its 1971 level, the chloride concentration in Lake Ontario would likely have remained near 29 mg ℓ^{-1}. However, the flow of water out of Lake Ontario was increased approximately 10% between 1972 and 1974 and has remained near this high level ever since. At the same time, inflow into the lake has decreased by about the same amount, although chloride input has not changed (Chan, pers. comm.).

Because approximately 16% of the total quantity of chloride in the lake is exchanged annually, a 10% net annual increase in outflow should result in an annual chloride decrease of 1.6% yr^{-1}. The observed

decrease of 4% in the chloride content of Lake Ontario over the last three years closely approaches the predicted decrease.

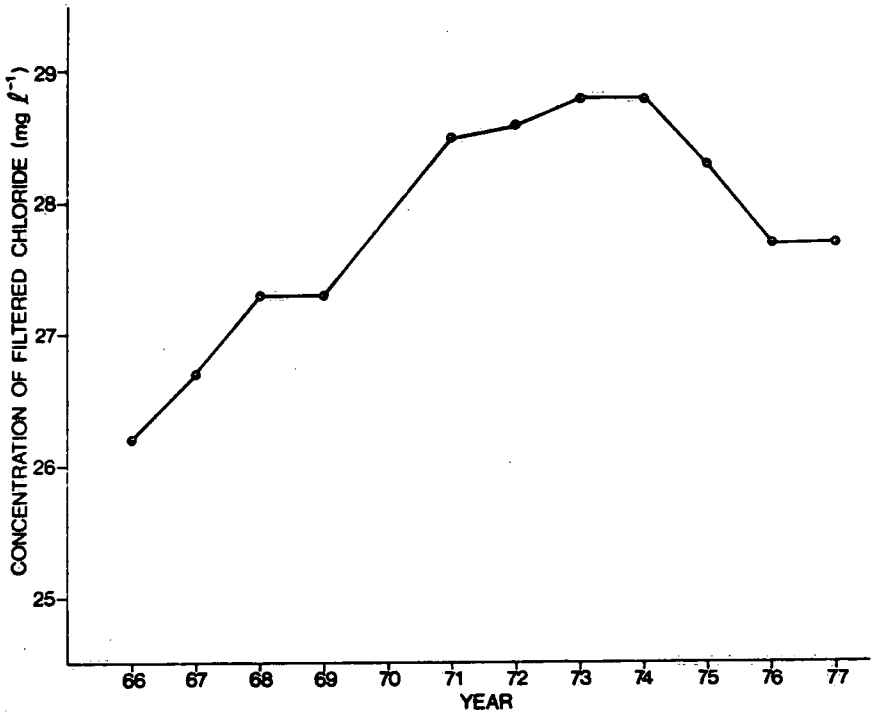

Figure 3.3.3 Trend of chloride concentration in Lake Ontario.

Chlorophyll

The chlorophyll a data available from Lake Ontario were collected during the years 1967-1977. In each of these years the sampling program consisted of a varying number of cruises, and during each cruise a number of stations were sampled. After 1973, the sampling technique used was an integrated sampler cast to 20 m, or 1 m off the bottom, whichever came first. Prior to 1974, a non-integrated method was used. This led us to analyze the data from 1967 to 1973 separately from the 1974 to 1976 data, and also because of the magnitude of the data, the analysis is restricted to the spring data only (March, April and May).

Statistical Analysis

The arithmetic mean, $\overline{X}(t)$, and the standard deviation, $S(t)$, were calculated for the chlorophyll a data obtained during each cruise. The variations of the values of $\overline{X}(t)$ within years gives the information about the seasonal cycle. Assuming that $\overline{X}(t)$ follow a normal distribution (which can be justified using the central limit theory) with mean $\mu(t)$ and variance $\sigma^2(t)/n$, where n is the number of sampling stations, then $\mu(t)$ and $\sigma(t)$ can be estimated by $\overline{X}(t)$ and $S(t)$, respectively. The statistic

$$D_i^2 = \sum_{j=1}^{K_1} \frac{n_{ij}}{S^2_{ij}} (\overline{X}_{ij} - \overline{X}_i)^2$$

has a χ^2 distribution with (k_i-1) degrees of freedoms, where K_i denotes the number of cruises conducted during the ith year (i=1, 2, ...,m), n_{ij} is the number of stations sampled during the jth cruise in the ith year, S_{ij}^2 and $\overline{X}_{ij}$ are the variance and the mean of the jth cruise in the ith year, and $\overline{X}_i$ is the mean of the ith year. This statistic can be used to test the significance of the seasonal cycle during the ith year. Applying this analysis to the data from 1967 to 1976, values of D_i^2 and the corresponding degrees of freedom are given in Table 3.3.8. Significant values of D_i^2 are marked by **. It is clear from the table that all the years have shown a very strong seasonal cycle with the exception of the 1971 data (which had data from only two cruises).

In order to determine the trend, in the presence of the seasonal cycle, it is first necessary to find the relationship between the mean $\overline{X}$ and the standard deviation S, and secondly, to divide the year into intervals such as seasons and determine the long-term variation in the mean of the season. Moreover, there are external non-controllable variable factors such as temperature and light for which allowance must be made before the long-term trend of chlorophyll a can be determined.

TABLE 3.3.8: *The Values of D^2 Calculated for the Years 1967 - 1976*

Years	Degrees of Freedom	D^2
1967	7	526.44**
1968	5	420.23**
1969	11	688.44**
1970	12	1290.85**
1971	1	2.49
1972	20	929.53**
1973	16	172.45**
1974	13	280.20**
1975	6	207.66**
1976	10	363.35**

** Significant at the 1% level.

The relation between the mean and the variance was found to be linear. Specifically it takes the form

$$S = \lambda \overline{X}$$

where λ is a constant. To transform the means into a scale such that the precision of the transformed means are equal, the following transformation is required

$$Z = \int \frac{d\overline{X}}{S} = \frac{1}{\lambda} \int \frac{d\overline{X}}{\overline{X}} = \frac{1}{\lambda} \ln\{\overline{X}\}.$$

The random variable Z is then taken to be normally distributed with mean $\ln \mu$ and variance σ^2/n where n is the number of samples entered in the calculation of $\overline{X}$.

Consider the model,

$$Z_{ij} = \alpha_i + B_0 T_{ij} + B_1 T_{ij}^2 + \rho_{ij} \ . \ . \ . \ , \qquad (3.3.1)$$

where Z_{ij} is the observed value of the random variable Z in the i<u>th</u> year and during the i<u>th</u> cruise, α_i is the effect of the i<u>th</u> year, B_0 and B_1 are

constants, T_{ij} is the observed temperature mean and e_{ij} is a random variable which is normally distributed with 0 mean and variance σ^2/n_{ij}. The inclusion of the temperature effect in the model will produce an adjusted mean for the season α_i (i.e., free from the temperature influence). Our interest is to test the hypothesis $\alpha_1 = \alpha_2 = \ldots = \alpha_n = \alpha$, which implies the absence of trend in the data. In addition, a test is conducted to see if the temperature effect should include the quadratic term.

When the above model was applied to the data during 1967-1973, testing for the inclusion of T_{ij}^2 in the model showed that it was not significant. Hence, the model was taken with the assumption that $B_1 \equiv 0$. The first row in Table 3.3.9a gives the least-squares estimate of the parameter of the model. To test whether there is a trend in the values Z_{ij}, an F statistic was calculated, which has four and 22 degrees of freedom, and found to be significant at the 5% and 1% levels. This indicates that during the period 1967 to 1973, there is statistical evidence indicating that the state of the lake has changed during spring. To determine whether two successive years show no significant differences, another F test was calculated for each four successive years. This test indicates that only 1968 and 1969 can be combined. The estimates of the parameters under the assumption of combining 1968 and 1969 are given in the 2nd row in Table 3.3.9a. The above results support the existence of trend in the data. The pattern of trend is the decrease in the chlorophyll a concentration.

TABLE 3.3.9a: *The least-squares estimates of the parameters of the model (1967 - 1973)*

	Years Effects						Temperature Effect
	1968	1969	1970	1971	1972	1973	B
The Estimates	1.220	0.881	1.193	-	0.977	0.607	0.0955
	1.042		1.175	-	0.964	0.598	0.1010

The same analysis was conducted for the 1974-1977 data. The results showed that the quadratic term was highly significant and hence it is necessary to include it in the regression equation. The estimates of the parameters of the model are given in the first row in Table 3.3.9b. A test of significance for the equality of years effects for the adjacent years have shown that the difference between 1975 and 1976 was not statistically significant. The parameters of the model under this assumption are given in the second row in Table 3.3.9b. It can be concluded from this table that a decrease in the chlorophyll a concentration is also found. In conclusion, the trend analysis has shown a continuing decline in the chlorophyll a concentration since 1972.

TABLE 3.3.9b: *The least-squares estimates of the parameters of the model (1974 - 1977)*

	Years Effects				Temperature Effect	
	1974	1975	1976	1977	B_0	B_1
The Estimates	0.988	0.645	0.681	0.5224	0.2726	-0.0154
	0.977	0.6597		0.514	0.2776	-0.0159

3.4 Long-Term Predictive Models

The response of a lake to external nutrient inputs may be simulated by recourse to mass balance principles (Vollenweider, 1969, 1975). It follows from such considerations that eutrophication should be a function of nutrient loading, lake configuration, and hydraulic flushing time. This leads to empirical loading plots which display the trophic state of different lakes in terms of the above characteristics (Vollenweider and Dillon, 1974). In first approximation, such plots may be used to predict the future state of a given lake for anticipated or postulated loading conditions. The problem is, of course, that loading plots presumably reflect steady state conditions and therefore give no information concerning the dynamic response of a lake to varying nutrient inputs. Thus, even if the loading plots were universally valid and therefore would accurately reflect the trophic state of the lake under the specified

(constant) loading conditions, they would not predict the time needed to achieve this steady state.

The main problem in predicting the future trophic state of a lake relates to the question of dynamic balance between present lake concentrations and nutrient loadings. If present nutrient inputs are balanced by the losses due to outflow and sedimentation, then the nutrient concentrations in the lake will increase with increasing loadings and decrease with decreasing inputs. However, if loadings have been increasing during the past years, it may be expected that the lake is currently not in equilibrium with the load and that the nutrient concentrations will continue to increase for some time if the loadings remain constant from this time onwards. Thus, the first step in constructing a long-term predictive model is to establish how far the actual lake is removed from dynamic equilibrium and to impose the same condition on the model.

How can we find out if the lake is presently in balance with the load and, if not, how close the lake approximates this condition? The error margin in the available data and short-term variations due to atmospheric influences are so large that a few years of observations cannot answer this question. If we had a universally valid loading plot or net sedimentation coefficient, then we could immediately compare observed with "predicted" average concentrations in the lake to find the answer. We might hope that a more complicated "process-model" could supply such sedimentation rates. As we have seen in Chapters 2.4-5, however, our current knowledge of various rate processes is so limited that we cannot come up with a unique model for a given lake. Besides, we have also seen that the rate coefficients themselves depend on our assumption regarding periodicity, i.e., whether the lake is in dynamic balance. Thus, the argument is completely circular. An example is the study of Thomann *et al.* (1976). One fits a model by simulating the short-term characteristics of a lake and then runs the model long-term to find that the model is not in balance with the loading and one intimates that the lake itself is not balanced. But in order to fit the seasonal model in the first place, it is essential to know whether the lake is presently in dynamic equilibrium or not. Once we know the present condition of the lake in relation to the equilibrium state, there is little doubt that we can find a set of kinetic coefficients to simulate the seasonal cycle.

At the present time, it appears that the only way to make long-term predictions for a lake such as Lake Ontario is to fit a model to long-term historical records. In effect, the record length should be of the same order as the hydraulic flushing time, that is about a decade for Lake Ontario. How complicated should such a model be? The answer is obviously that the model should not be more complicated than our understanding of the processes going on in the lake itself. A model with 10 rate coefficients, all of which are highly uncertain, has no greater predictive capability than a model which lumps all of these together in one big "unknown". Let us see then how the more fancy dynamic models compare with very simple loading models in predicting the future state of Lake Ontario.

Long-Term Response of Dynamic Models

Consider first the mass balance equation (2.4.1) for total phosphorus. Let the lake be completely mixed with mean concentration C, and assume that losses by sedimentation as well as outflow are proportional to this mean concentration. Then (2.4.1) may be divided by the total lake volume, V, to obtain

$$\frac{dC}{dt} = \ell - (q + k)C \qquad (3.4.1)$$

where $\ell = I/V$ = phosphorus input per volume per day
$q = Q/V$ = hydraulic flow divided by volume
k = net decay rate per day.

If all these parameters are constant, (3.4.1) may be solved to obtain

$$C = \frac{\ell}{q + k} + \left(C_o - \frac{\ell}{q + k}\right)e^{-(q + k)t} \qquad (3.4.2)$$

where C_o is the initial concentration for $t = 0$. The steady state or equilibrium concentration is clearly $C = \ell/(q + k)$.

Consider now the solution for parameter values corresponding to the data collected during 1972 on Lake Ontario. In contrast with Chapter 2.4, we now need estimates of gross nutrient inputs rather than

net loads. For a total phosphorus concentration of 22.5 mg/m^3 and a St. Lawrence outflow of $.612 \times 10^9$ m^3/day, the loss of phosphorus would be 14 tons/day. With a net loading of total phosphorus equal to 29 tons/day, the corresponding input would be 43 tons/day. The measured input reported in Chapter 2.1 is actually greater but for the estimates of Chapter 3.2 are close to this value. For our calculations we assume a gross input of total phosphorus equal to 40 tons/day. The values of the parameters are then ℓ = .02364 mg/m^3/day and q = .00036 per day. Thus, if the assumption is made that the observed initial total phosphorus concentration of 22.5 mg/m^3 is in balance with the loading, the sedimentation rate coefficient would have to be k = .0069 per day, about twice as large as the outflow coefficient q. The corresponding effective sedimentation velocity for total phosphorus would be .06 m/day.

Now let us reduce the total phosphorus loading by 10 tons/day. Based on the simple model (3.4.2), the lake will reach a new equilibrium concentration of 16.9 mg/m^3. The complete time-dependent solution (3.4.2) is $C = 16.9 + 5.6 \exp(-.383\ t)$ where t is time in years. This solution is shown by the dashed line in Figure 3.4.1a. This result may be compared with results from the two-component, two-layer phosphorus model of Chapter 2.4. First, the latter must be modified to compute net phosphorus loading on the basis of prescribed gross inputs and computed outflow, the latter obtained as the product of mean lake concentrations and known river flow. For a total phosphorus input of 40 tons/day, consisting of 15 tons/day of SRP and 25 tons/day of organic P, the optimal sedimentation coefficients are found to be slightly different from those in Chapter 2.4 where the net loading was prescribed. For a fit with uniform weights, the optimization procedure gives k_3 = .12 m/day, k_4 = .63 m/day, whereas for the periodic case k_3 = .18 m/day, k_4 = .37 m/day.

In Figure 3.4.1 "a" shows solutions obtained from the two-layer, two-component phosphorus model for the following loading cases.

1. SRP loading of 15 tons/day, organic P loading of 26 tons/day
2. SRP loading of 11.5 tons/day, organic P loading of 19.5 tons/day
3. SRP loading of 15 tons/day, organic P loading of 16 tons/day
4. SRP loading of 5 tons/day, organic P loading of 26 tons/day.

The curves in Figure 3.4.1a are identified by the case numbers. Case 1 is the equilibrium solution for this model; the other three cases all represent a reduction in phosphorus loading of 10 tons/day. It is interesting to see that the last solution is very similar to the prediction from the simple loading model (3.4.2).

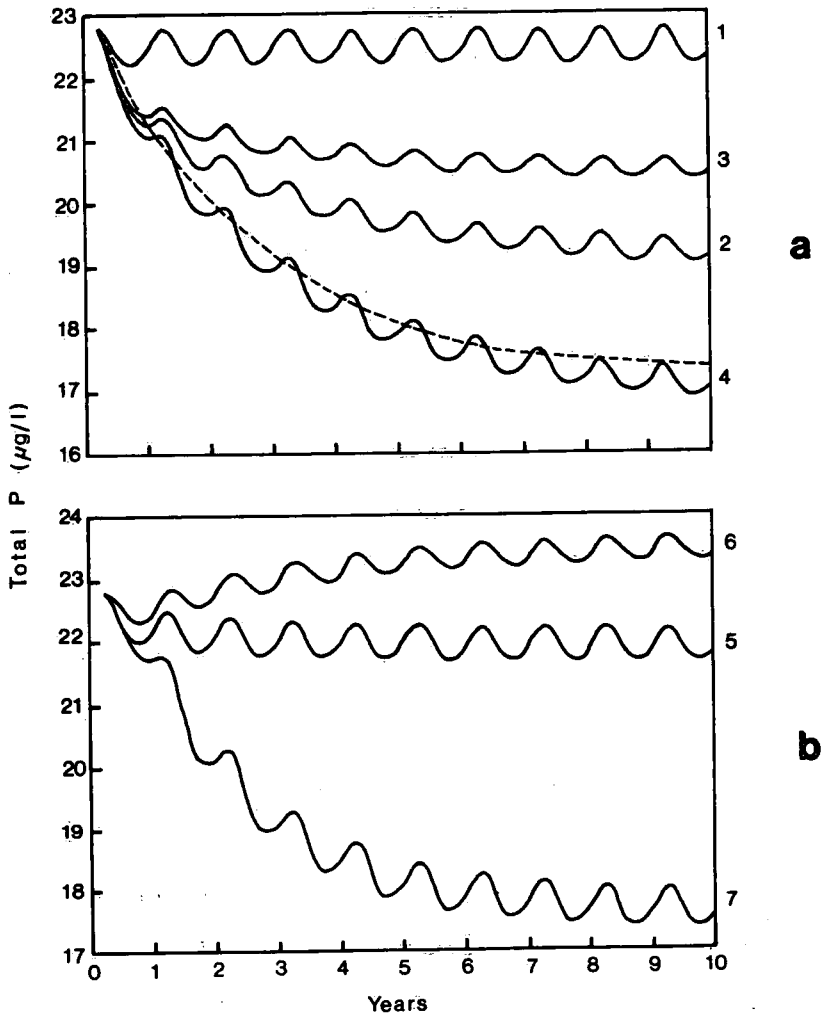

Figure 3.4.1 Long-term simulation of total phosphorus using the two-layer, two-component model of Chapter 2.4, under varying loading conditions (a), and for different rate coefficients (b) as described in text. (See legend for Table 3.4.1).

Since the above results represent the response to loading of one particular model with one particular set of coefficients, they should be compared with the sensitivity of the model to changes in parameters with the loading held constant. Examples of such experiments are shown in Figure 3.4.1b. The curve numbered 5 represents the solution of the two-layer, two-component model if the sedimentation velocities are increased by 10%. Solution 6 represents the case where the vertical mixing across the thermocline interface is doubled, and curve 7 is the solution for a reduction of nutrient regeneration coefficients by 10%. The various contributions to the phosphorus budget and the phosphorus concentrations after the model has reached a new dynamic equilibrium are shown in Table 3.4.1 for all the cases shown in Figure 3.4.1.

The above results illustrate some of the difficulties associated with long-term predictive application of dynamic models. Clearly, the uncertainty surrounding nutrient regeneration is much more than the 10% variation considered above. That is not to say that the possible error in the prediction is necessarily equivalent to a loading reduction of 10 tons/day as suggested by Figure 3.4.1. Naturally, a change of 10% in the respiration coefficient alone would cause the model to deviate considerably from the data used in the original "fitting" procedure. Thus, one would make changes in the other parameters to set things right again. However, it seems important to stress the fact that one cannot use models with so many degrees of freedom for predictive purposes. It is also evident that these problems are compounded, rather than alleviated, by more sophisticated models, at least until our scientific understanding of the various processes catches up with our modeling capability.

All the above applies to models which were forced to be initially in equilibrium with the loading by a judicious choice of rate coefficients and sedimentation parameters. This is not to imply that Lake Ontario approaches this condition, nor are any of the above results to be interpreted as actual predictions for this particular lake. On the contrary, the purpose was to illustrate the uncertainty surrounding any predictions based on mathematical models. This becomes even more evident if one realizes that the initially balanced models constitute only a small sub-set of a whole range of models with varying degrees of imbalance. An

example is the plankton model presented in Figure 2.5.1 and Table 2.5.2. This type of model will predict changes in the state of the lake even if the loading remains constant. The model presented by Thomann *et al.* (1974, 1976) belongs to this class. It may well be true that Lake Ontario is not in a state of dynamic equilibrium but a seasonal plankton simulation study is of no help in addressing that question.

TABLE 3.4.1 *Steady state solutions of dynamic phosphorus model of Ch. 2.4*

1. Original parameters. 2. Total P loading reduced by 10 t/d. 3. Org. P loading reduced by 10 t/d. 4. SRP loading reduced by 10 t/d. 5. Sedimentation velocities increased by 10%. 6. Mixing coefficients doubled. 7. Nutrient regeneration coefficients reduced by 10%. 8. Homogeneous input-output model. 9. Same as 8 with reduced loading.

	Input (t/d)	Outflow (t/d)	Sedim. (t/d)	Kinetics (t/d)	Equil. Conc. (mg/m^3)
SRP					
1	15.0	-5.5		-9.5	13.5
2	11.5	-4.7		-6.8	11.5
3	15.0	-5.6		-9.4	13.1
4	5.0	-3.4		-1.6	9.0
5	15.0	-5.5		-9.5	13.5
6	15.0	-6.9		-8.1	15.0
7	15.0	-2.8		-12.2	8.1
Org. P					
1	25.0	-7.9	-26.6	9.5	9.0
2	18.5	-6.6	-18.7	6.8	7.9
3	15.0	-6.5	-17.9	9.4	7.6
4	25.0	-6.6	-20.0	1.6	8.3
5	25.0	-7.5	-27.0	9.5	8.7
6	25.0	-7.3	-25.8	8.1	8.7
7	25.0	-7.9	-29.3	12.2	9.9
Total P					
1	40.0	-13.4	-26.6		22.5
2	30.0	-11.3	-18.7		19.4
3	30.0	-12.1	-17.9		20.7
4	30.0	-10.0	-20.0		17.3
5	40.0	-13.0	-27.0		22.2
6	40.0	-14.2	-25.8		23.7
7	40.0	-10.7	-29.3		18.0
8	40.0	-13.9	-26.1		22.5
9	30.0	-10.5	-19.5		16.9

Response to Long-Term Lake Ontario Data

After having considered the sensitivity and response of a typical dynamic phosphorus model in rather general terms, we should briefly evaluate the response of the same model to the actual changes in environmental conditions which occurred in the past years. In Chapter 3.1, we presented 12 years of physical and biochemical observations on Lake Ontario and in Chapter 3.2 we summarized preliminary findings of a survey of nutrient loadings for the same period. Let us now take the model of Chapter 2.4 with the above values of the sedimentation coefficients and subject it to these different effects. For instance, the physical effects give an indication of the sensitivity of the model to typical climatological variations. Naturally, the conclusions would apply only to this particular model, but it may be recalled that in this aspect the model is rather similar to most plankton models and therefore the results may have a somewhat general applicability.

With regard to the physical data, we may assume that temperature and radiation data presented in Chapter 3.1 are quite adequate for the present purpose. Vertical mixing coefficients were computed from these temperatures according to the method outlined in Chapter 2.2. A major problem, however, is caused by the uncertainty surrounding the extinction coefficients. As discussed in Chapter 3.1, there are large gaps in the data and, what is worse, results obtained by different measurement techniques may not be consistent. Furthermore, early estimates of extinction coefficients for IFYGL (Chapter 2.3), which were used in tuning the present model in Chapter 2.4, were subsequently thought to be too low, especially during winter, as can be seen from the more recent estimates in Chapter 3.1. Since this problem has not been resolved, we will simply utilize the extinction coefficients employed in the seasonal simulations of Chapter 2.4.

With regard to nutrient loading, available estimates from different sources also show considerable disparity, but the general trend of the phosphorus inputs over the last decade appears to be reasonably well established. Thus, phosphorus inputs apparently reached a peak around 1970 and steadily declined afterwards to a level of about three quarters of the peak value by the end of the period considered here. In

view of this qualitative information, the best procedure seems to be to postulate a simple linear decrease of phosphorus loading from the value of 40 tonnes/day in 1972, considered in the previous section, to a value of 30 tonnes/day in 1977. There is again a question as to the partition of this loading between the two components of the model. For simplicity, we will assume that the ratio of SRP input to total phosphorus input remains the same.

Using the above environmental conditions, we may run the model of the previous section with the two sets of coefficients, one set corresponding to the periodic solution, the other giving the best overall fit to the 1972 seasonal changes. The results are displayed in Figure 3.4.2 together with all available observations. The solid curves apply to the periodic model; the dashed curves represent the model with the best fit to the 1972 observations. Finally, the dash-dot curve shows the solution from the simple total phosphorus model under the same loading conditions.

Inspection of Figure 3.4.2 indicates that the periodic model provides a better overall fit to the long-term data base than the model with the best seasonal fit. This would support our earlier contention that it is advisable to impose certain conditions of periodicity or near-periodicity on seasonal model simulations, not because the lake is necessarily in balance with the loading but rather because slight deviations from periodic seasonal solutions lead to unrealistic long-term model responses. With regard to the correspondence between observations and model results displayed in Figure 3.4.2, it is seen that the seasonal variations of SRP are quite well simulated, but the large seasonal changes in total phosphorus for the whole lake are not seen in the model results. If these variations are real, they imply quite different formulations of sedimentation as noted in Chapter 2.4. Finally, it is noted that the total phosphorus simulations obtained from the two-layer, two-component model are quite similar to the results from the simple input-output model (3.4.1) and hence the two models would appear to have an equivalent predictive capability in terms of the overall response of a lake to changing loading conditions.

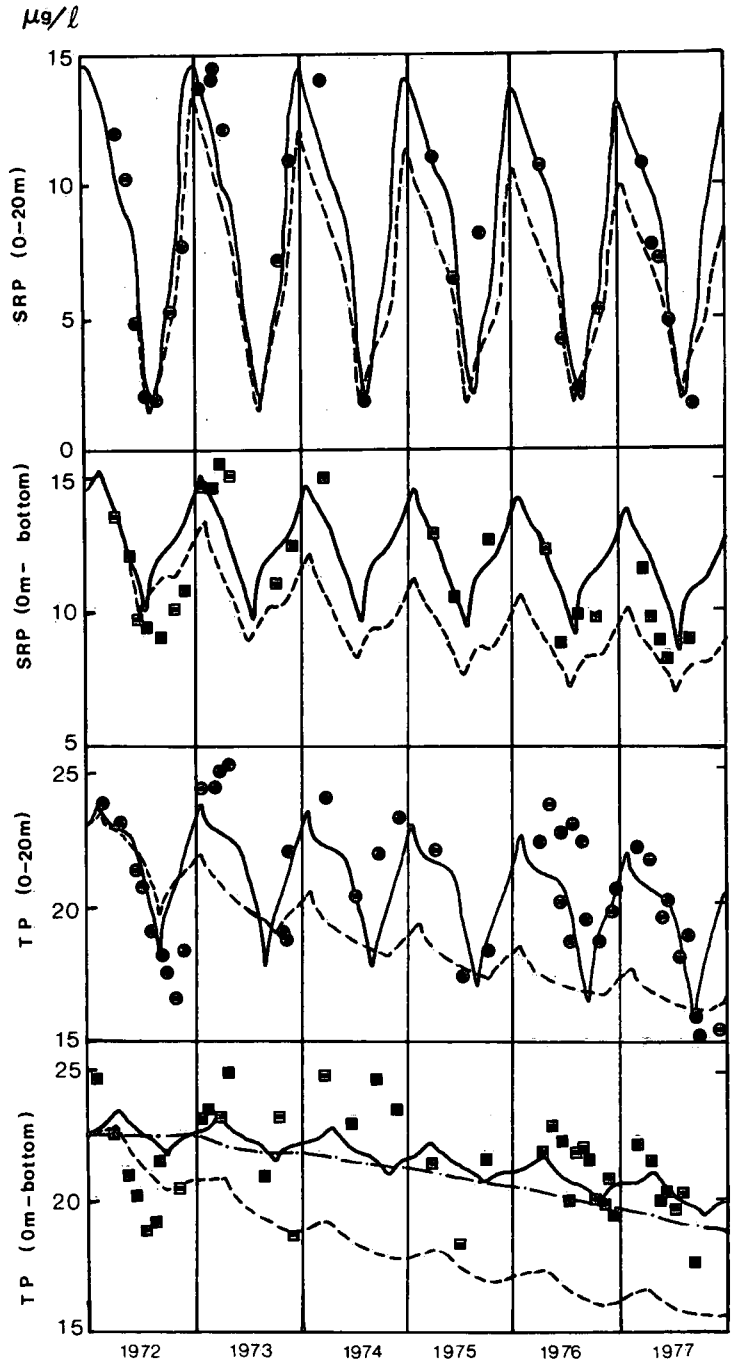

Figure 3.4.2 Long-term simulations for environmental conditions observed during 1972-1977 and for a linear approximation to observed decrease in phosphorus loading. Circles denote observations in epilimnion, squares represent whole lake, solid lines apply to periodic model for 1972, dashed lines represent model with best fit to 1972 seasonal variations, dash-dot line is solution from total phosphorus model.

Chapter 4

SPATIAL ANALYSIS AND SIMULATION

4.1 Three-Dimensional Data Base (1972)

The three-dimensional analysis presented in the present report is based on the physical and biological observations taken during IFYGL (1972). This data base consists of surface winds, temperatures, optical measurements, nutrient and biomass data, and external loadings to Lake Ontario. The data were interpolated in space and then averaged by zones and layers. For the processing of regular surveillance data, the lake was divided into 17 zones and 12 layers and a 2-km grid was used for interpolation. The same system of zones was also used for estimating nutrient loadings as discussed in Chapter 3.2. The outlines of these zones were shown previously in Figure 3.1.4. For the simulation experiments considered in the following, a different system of zones and layers was adopted. This was done to maintain continuity with earlier hydrodynamic and heat transport computations for Lake Ontario. In order to avoid confusion, all averages presented in this chapter will refer to the latter segmentation of the lake.

Figure 4.1.1 shows the 21 zones adopted for computing heat, nutrient, and biomass averages, together with the 5-km grid mesh used for hydrodynamic calculations. In the vertical, the lake is partitioned into four layers with horizontal interfaces at 10, 20, and 40 metres below the surface. The zone boundaries are based on the bathymetry of the lake such that the mean depth contour acts as the dividing line between shore zones and deep water. In addition to thermal considerations, the selection of this depth contour is inspired by an interesting aspect of wind-driven lake circulations. As explained by Bennett (1974), currents parallel to the mean depth contour will tend to be of opposite sign on either side of it, so that one would expect low tangential velocities along this contour. The east-west spacing between zone boundaries has been arbitrarily set equal to half a degree of longitude, that is, about 40 km.

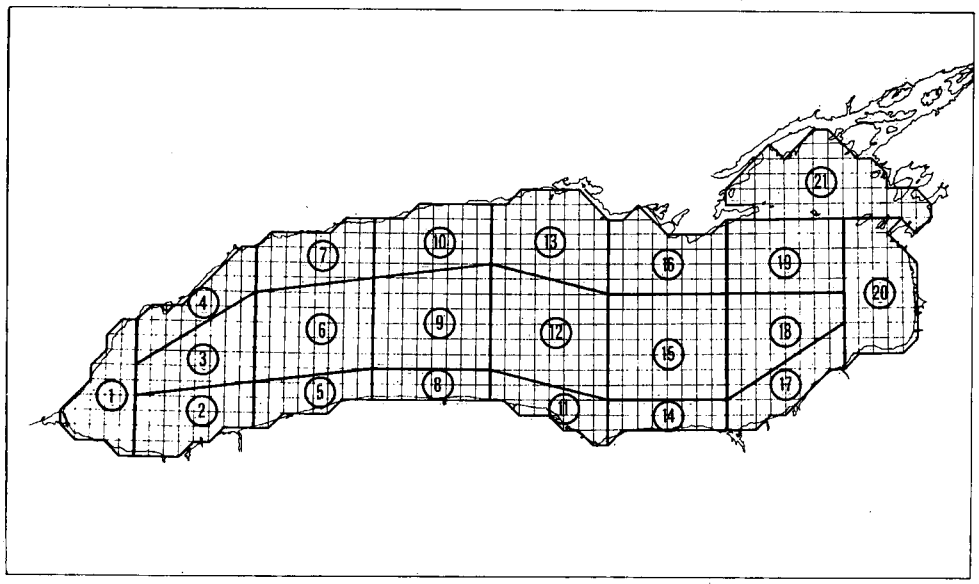

Figure 4.1.1 System of zones for computing heat and nutrient budgets, together with the 5 km grid mesh of the hydrodynamic model.

Biochemical Data

The biochemical data are based on the same 1972/1973 "Organic Particle Study" cruises discussed in Chapter 2.1. It may be recalled that the time interval between cruises ranged from four to six weeks for a total of nine surveys between April 1972 and March 1973. The first part of each cruise consisted of a lakewide survey of 32 stations, the second part concentrated on two selected stations, each of which was sampled six times a day over a two-day period. Sampling depths were at 5-m intervals down to 20 m and at 40-m intervals below. The data analysis consisted of vertical interpolation to 5-m intervals down to 100 m and at 25-m intervals from 100 m to the bottom, followed by horizontal interpolation to the 5-m grid of the hydrodynamic model at each of these levels. Mean concentrations for each volume element of the segmented lake were then obtained by averaging the appropriate grid point values.

Phosphorus measurements are available in the form of total phosphorus, soluble reactive phosphorus, and total filtered phosphorus. Nitrogen species are total particulate nitrogen, ammonia nitrogen, nitrite plus nitrate, and total filtered nitrogen. Additional biochemical variables include particulate organic carbon, chlorophyll a, and zooplankton biomass by species. It is beyond the scope of this report to

present a complete description of the three-dimensional nutrient and plankton distributions in Lake Ontario. Instead, we will confine ourselves to a limited set of observations which may serve to illustrate the following discussion. As will be seen, this discussion will concentrate on the horizontal variations in a lake, in contrast with the vertical gradients which were studied in Chapters 2.1-5. In particular, we will look at the zones surrounding the nearshore station 11 and the offshore station 19, which were sampled at least 12 times during each cruise.

Table 4.1.1 presents mean concentrations for the upper 20 metres of zone 7 along the north shore and zone 12 in the centre of the lake. The variables are soluble reactive phosphorus, soluble organic phosphorus, total particulate phosphorus, nitrite and nitrate, ammonia, soluble organic nitrogen, total particulate nitrogen, total particulate carbon, chlorophyll a, and total zooplankton biomass (dry weight), the latter based on a 50-m haul. The units are the same as in Chapter 2.1, i.e., μg/ℓ. Chl a and zooplankton biomass may be converted to living biomass carbon by multiplying the former by 35.0 and the latter by 0.45 on the basis of evidence presented in Chapters 2.1 and 2.3. Whereas Table 4.1.1 shows zone-averages - that is, spatial interpolations of single observations in more than one station - Table 4.1.2 presents two-day means of a dozen observations at four-hour intervals in the same location. This table refers to the upper layers (0-20 m) of stations 11 and 19, located in zones 7 and 12, respectively. Note that these observations lag behind by one week compared to the data presented in Table 4.1.1. An exception is zooplankton, which was taken from the regular cruises and therefore represents a single observation. The data of Table 4.1.1 are graphically displayed in the upper half of Figures 4.1.2-4; the data of Table 4.1.2 are presented in the lower parts of the same figures. In this context, it is also useful to recall our discussion of primary production measurements in Chapter 2.3. These observations were carried out at the same stations.

Nutrient loadings to Lake Ontario during the 1972 field year have been discussed in Chapter 2.1. For the present computations, spatial distributions of inputs were estimated from the report by Casey and Salbach (1974). Inputs from major rivers, municipalities, and industrial plants were assigned to the adjacent model zone. Loadings from minor

TABLE 4.1.1 Mean Concentrations for Zones 7 and 12, 0-20 m (μg/ℓ)

	Zone	10-14 APR 72	23-27 MAY 72	19-23 JUN 72	17-21 JUL 72	5-9 SEP 72	17-21 OCT 72	20-23 NOV 72	9-12 JAN 73	6-8 MAR 73
SRP	7	14.	4.9	1.4	2.0	1.6	12.1	6.8	13.9	13.8
	12	13.2	12.7	7.7	2.0	1.6	3.7	10.1	14.5	14.4
SOP	7	3.6	5.3	5.9	6.3	4.3	5.5	5.3	6.4	4.8
	12	3.3	3.0	6.2	9.3	5.7	5.0	5.7	5.0	6.4
TPP	7	5.9	9.6	11.2	8.6	6.0	3.6	4.9	4.3	3.7
	12	6.4	4.5	6.4	9.8	10.3	5.4	4.1	4.4	3.5
$NO_2 + NO_3$	7	263	172	113	66	103	255	173	227	245
	12	227	225	207	60	42	141	247	198	264
NH_3	7	5	6	5	12	16	14	5	9	8
	12	6	6	7	16	16	18	10	11	9
SON	7	126	87	84	-	117	114	86	288	-
	12	118	151	103	-	113	117	50	184	-
TPN	7	39	72	149	124	65	29	32	22	23
	12	36	31	45	139	83	48	22	21	17
TPC	7	221	390	795	673	430	206	219	168	140
	12	190	170	229	636	581	368	153	168	117
Chl *a*	7	2.2	5.0	7.8	5.9	3.9	1.2	2.4	0.9	1.6
	12	2.2	2.7	2.5	8.5	4.5	3.3	1.5	1.2	1.5
Zoopl. (0-50 m)	7	5	6	7	63	71	19	58	18	10
	12	7	6	12	62	162	62	28	17	10

TABLE 4.1.2 Two-day Means for Stations 11 and 19, 0-20 m (μg/ℓ)

		18-21 APR 72	30-31 MAY 72	27-30 JUN 72	25-28 JUL 72	12-15 SEP 72	24-27 OCT 72	28-30 NOV 72	16-19 JAN 73	13-16 MAR 7
SRP	Stat. 11*	11.4	4.0	1.7	1.7	.9	4.9	8.7	15.3	14.5
	19	13.2	14.4	9.4	1.9	1.0	5.2	8.8	14.0	14.9
SOP		3.2	5.8	5.4	4.8	5.8	8.9	8.3	4.1	4.9
		3.8	3.2	5.0	5.1	6.9	7.4	7.4	5.5	4.8
TPP		7.5	10.6	10.5	8.1	6.4	6.4	4.3	3.0	3.9
		5.5	3.0	7.5	9.9	6.3	5.1	3.4	2.7	4.0
$NO_2 + NO_3$		236	162	94	86	90	181	242	210	259
		249	260	235	31	49	200	216	210	274
NH_3		5	5	13	8	20	5	6	6	8
		5	5	4	21	11	7	9	5	8
SON		96	185	127	188	106	270	76	-	121
		91	125	118	141	103	248	75	-	95
TPN		33	71	124	94	66	45	25	22	30
		23	18	36	113	82	34	24	23	23
TPC		240	377	689	621	414	296	235	168	166
		140	115	273	638	579	234	193	161	149
Chl a		2.8	6.0	6.1	4.8	3.0	3.8	1.6	1.1	1.6
		1.4	1.7	1.8	4.4	4.4	3.8	1.4	.9	1.3
Zoopl. (0-50 m)		3	5	2	64	45	10	67	17	6
		6	7	10	47	100	30	.3	15	13

* Station 11 replaced by station 3 during January cruise

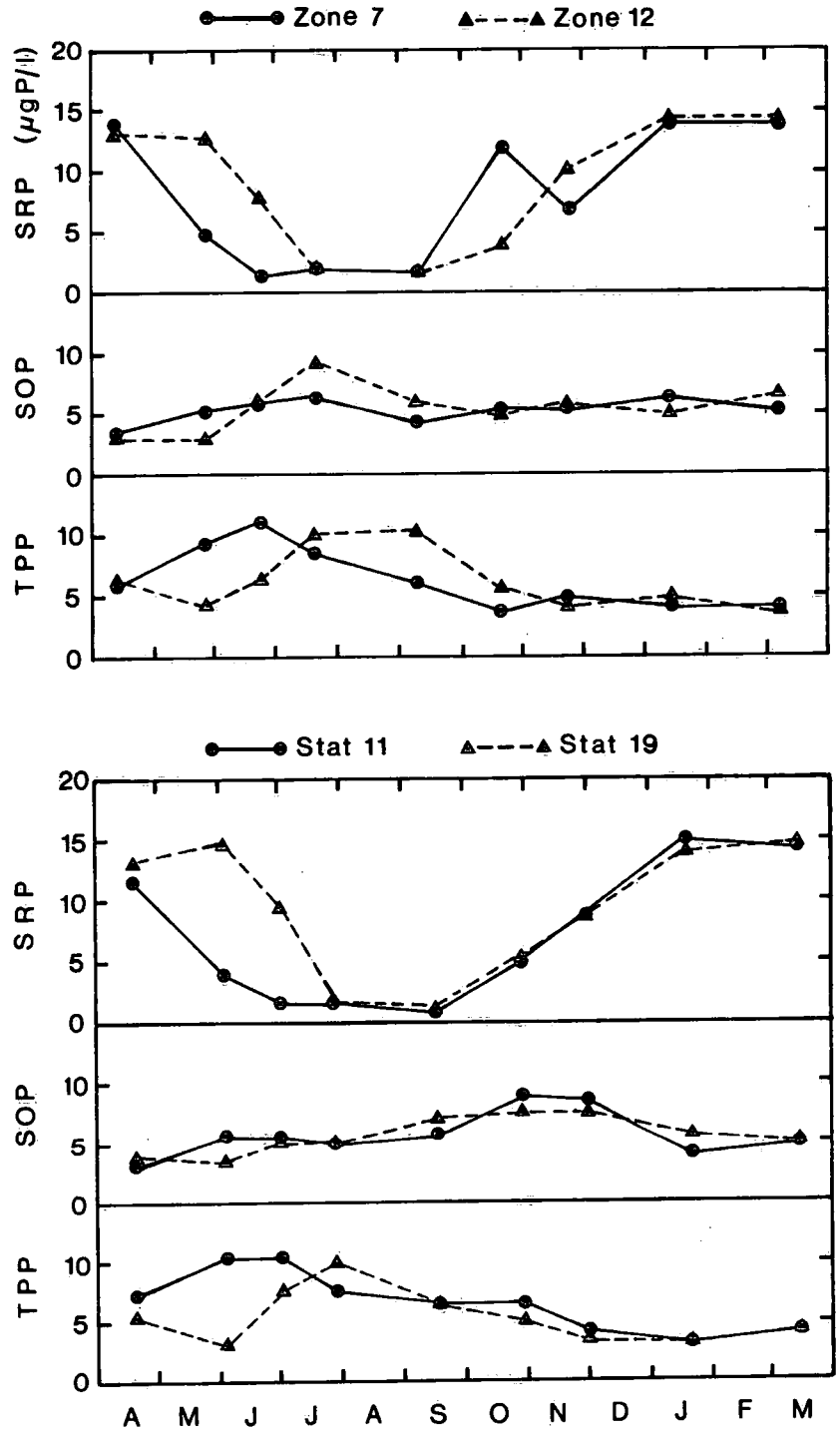

Figure 4.1.2 Concentrations of chemical variables in the epilimnion (0-20 m).

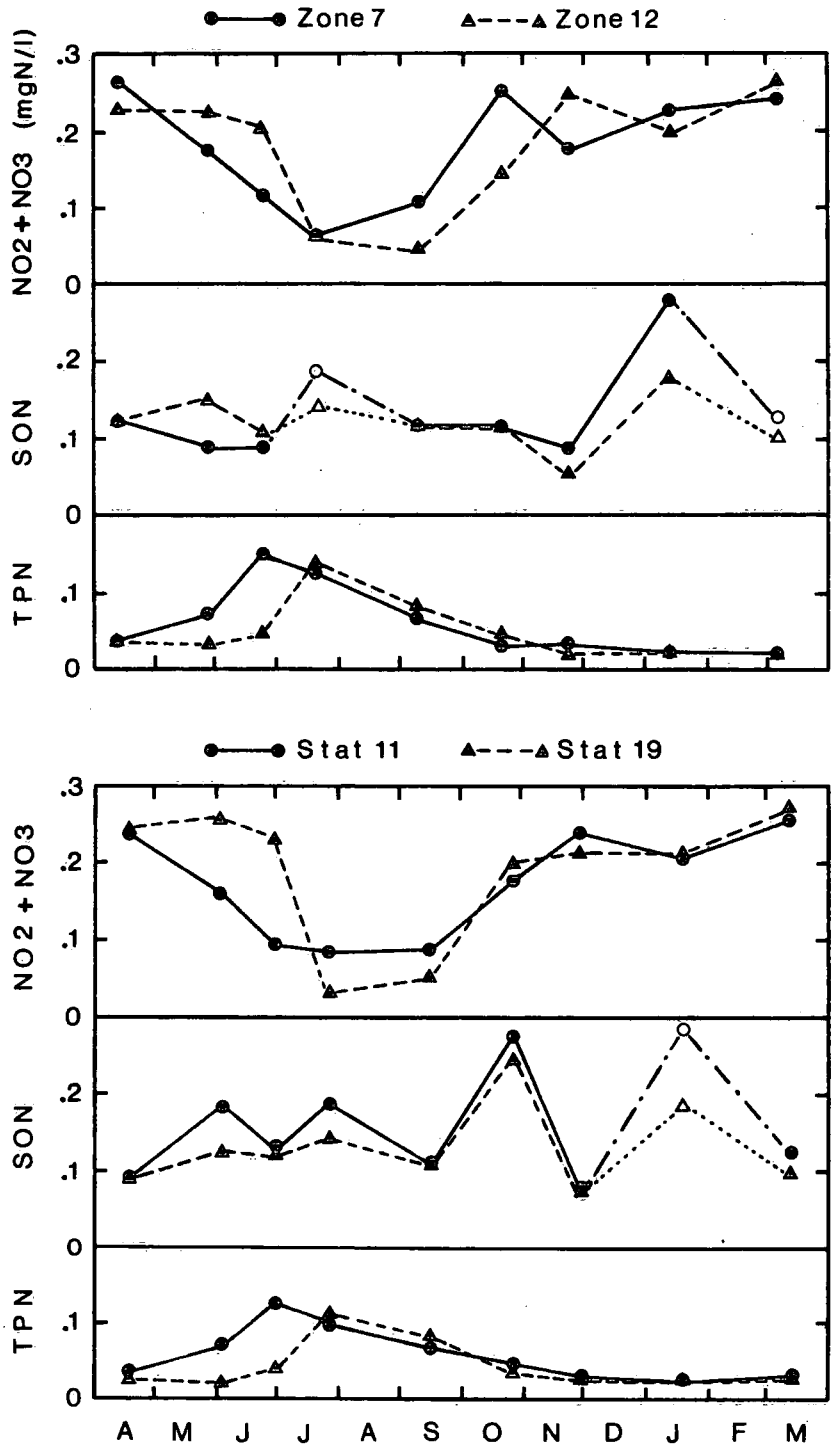

Figure 4.1.3 Concentrations of chemical variables in the epilimnion (0-20 m).

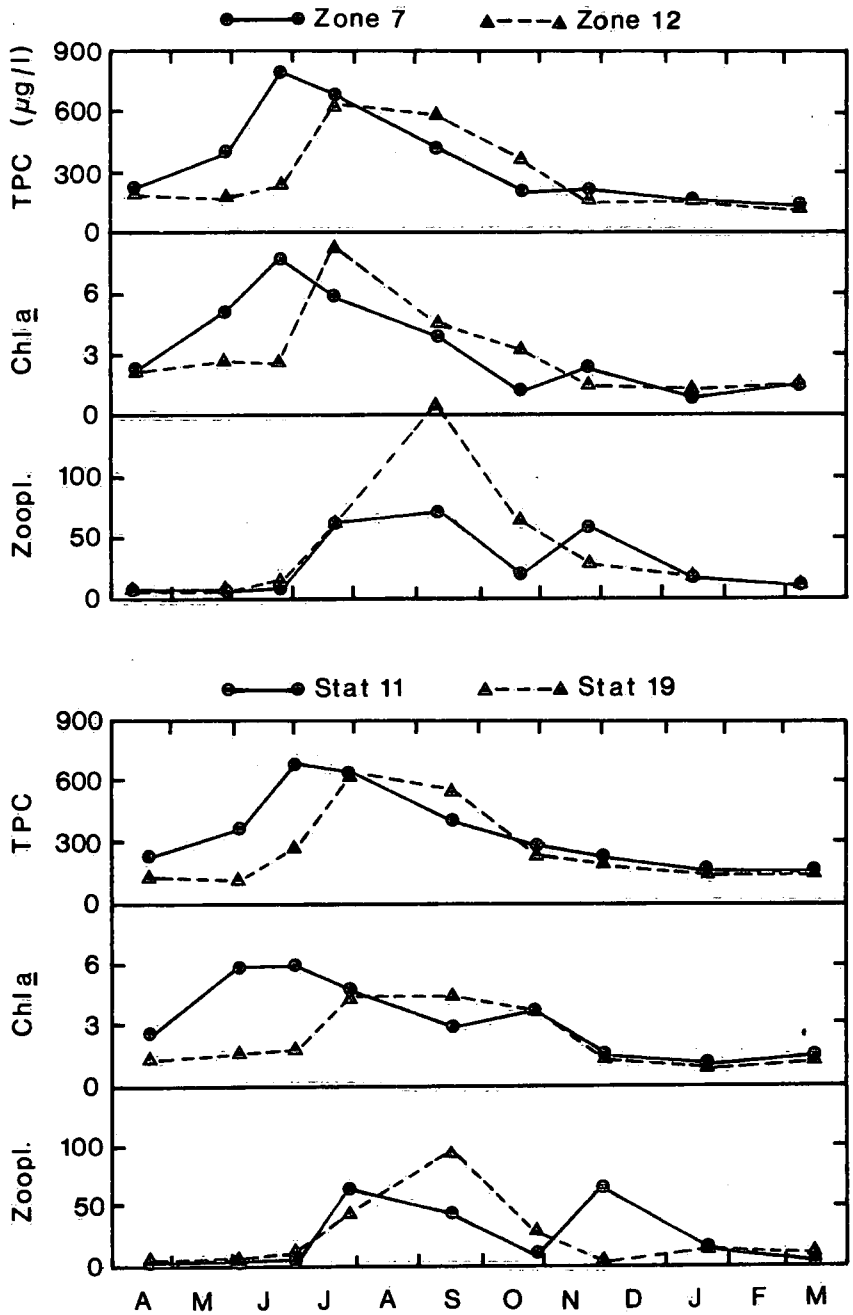

Figure 4.1.4 Concentrations of chemical variables in the epilimnion (0-20 m).

tributaries, precipitation, and groundwater, some 20% of the total, were distributed evenly over all zones. Since the information on time variations is not complete, the loadings were assumed to be constant in time. Effects of time variable loads are largely restricted to nearshore zones adjacent to major sources. The zones analyzed in the following are subjected to only minor direct loadings and the solutions are only weakly affected by the above assumption.

Physical Data

The processing of light and temperature observations during IFYGL and the subsequent estimation of vertical mixing, have been described in Chapters 2.2 and 2.3. In the present context, the same procedures were followed to obtain mean values for each zone and layer. Again, no attempt will be made to summarize these results, but the typical difference between a nearshore and a mid-lake zone is illustrated in Table 4.1.3 and Figure 4.1.5. The reader is referred to Chapter 2.2 for a discussion of the method by which these results were obtained and for a definition of this particular exchange coefficient, E. The relevant aspect of this comparison between zone 7 and zone 12 is the time lag of the stratification cycle. Typically, the suppression of vertical mixing occurs in north-shore zones about a month earlier than in deep water zones. It will be seen that this is the major reason for horizontal variations of simulated plankton blooms in the spring and early summer.

The essential difference between the data base required for the present study and the previous analyses in this report is the addition of large-scale water transports. During IFYGL currents were measured at up to 4 depths in some 10 to 20 stations distributed over Lake Ontario. The data coverage of this type of field program is usually not intended to satisfy the requirements of a spatial interpolation scheme, but rather to serve as a basis for verification of a hydrodynamic model. This chapter is devoted to a review of such hydrodynamic simulations carried out in conjunction with IFYGL. Since these models essentially compute the response of a lake to wind forcing, the required data consists of the spatial and temporal characteristics of the wind field over the lake. In addition, observed discharges from major rivers such as the Niagara River

are to be included, although their effects on water circulations in this lake are minor compared to the wind-driven transports.

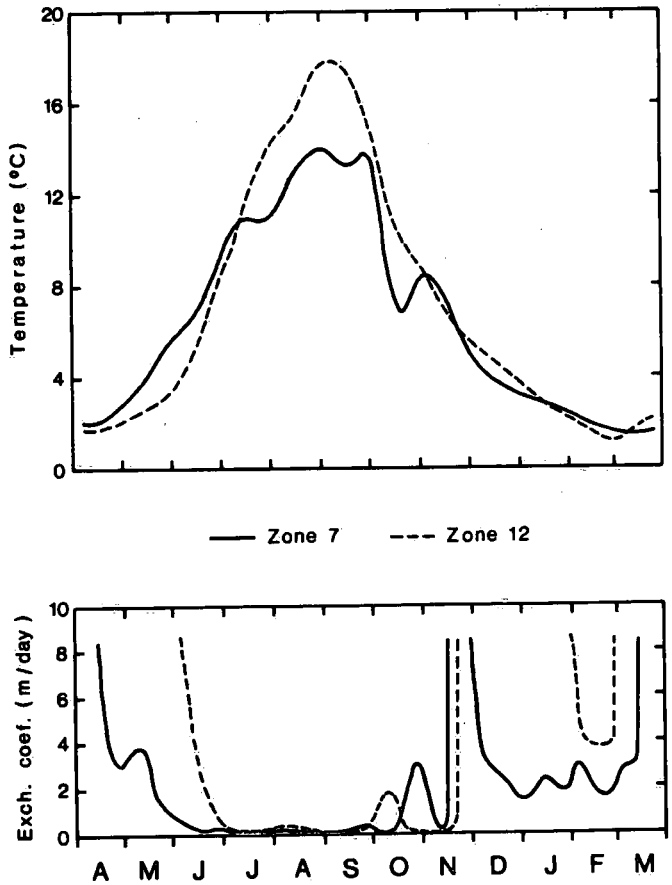

Figure 4.1.5 Temperature in upper layer, 0-20 m, and exchange coefficient at 20 m.

A meteorological buoy network was maintained on Lake Ontario from April through November, 1972. The present transport model utilized surface wind observations in 11 stations, most of them located in the north-western sector of the lake. Maps of wind stresses at the water surface were prepared at hourly intervals. Interpolation to grid points was carried out by weighting each station by the inverse of the square of the distance. The same horizontal interpolation scheme was also used for all other data.

TABLE 4.1.3: *Weekly values of temperature for two layers, 0-20 m and 20 m-bottom; and exchange coefficient at 20 m.*

	ZONE 7			ZONE 12		
	T(°C)		E(m/day)	T(°C)		E(m/day)
WEEK	0 - 20	- B	20 M	0 - 20	- B	20 M
96 - 102	2.1	2.1		1.8	1.9	
103 - 109	2.0	1.9		1.7	1.7	
110 - 116	2.2	1.9	3.41	1.8	1.8	
117 - 123	2.7	2.1	2.87	2.0	2.0	
124 - 130	3.1	2.5	3.76	2.3	2.2	
131 - 137	3.6	2.9	3.67	2.5	2.5	
138 - 144	4.3	3.2	1.77	2.8	2.7	
145 - 151	5.2	3.5	0.96	3.2	3.0	
152 - 158	5.9	3.8	0.73	3.6	3.3	
159 - 165	6.3	4.0	0.40	4.3	3.6	5.50
166 - 172	7.0	4.1	0.06	5.5	3.8	2.42
173 - 179	8.0	4.2	0.20	6.9	4.0	1.10
180 - 186	9.2	4.4	0.31	8.2	4.1	0.31
187 - 193	10.3	4.5	0.07	9.6	4.2	0.01
194 - 200	10.9	4.5	0.00	11.2	4.2	0.01
201 - 207	10.9	4.4	0.00	12.8	4.2	0.02
208 - 214	10.8	4.4	0.01	14.0	4.2	0.11
215 - 221	11.3	4.4	0.11	14.7	4.3	0.26
222 - 228	12.4	4.5	0.08	15.1	4.5	0.28
229 - 235	13.3	4.6	0.00	15.9	4.6	0.17
236 - 242	13.7	4.5	0.00	17.1	4.7	0.07
243 - 249	14.0	4.5	0.03	17.7	4.7	0.00
250 - 256	13.8	4.5	0.00	17.8	4.7	0.06
257 - 263	13.3	4.6	0.07	17.5	4.8	0.06
264 - 270	13.5	4.9	0.35	16.6	4.7	0.00
271 - 277	13.9	5.4	0.34	15.3	4.8	0.42
278 - 284	12.1	5.5	0.00	13.5	5.3	1.59
285 - 291	8.7	5.2	0.00	11.4	5.9	1.68
292 - 298	6.9	5.2	1.61	9.9	6.2	0.03
299 - 305	7.6	5.9	3.14	9.2	6.1	0.00
306 - 312	8.5	6.6	1.59	8.6	5.9	0.00
313 - 319	8.2	6.8	0.00	7.7	5.7	0.00
320 - 326	7.3	6.5		6.7	5.6	0.00
327 - 333	6.2	5.9		6.0	5.5	
334 - 340	5.1	5.2		5.5	5.3	
341 - 347	4.3	4.8	3.09	5.1	5.1	
348 - 354	3.8	4.5	2.67	4.7	4.7	
355 - 361	3.5	4.2	2.37	4.3	4.4	
362 - 368	3.3	4.0	1.43	3.9	4.2	
369 - 375	3.1	3.8	1.57	3.5	4.0	
376 - 382	2.8	3.6	2.46	3.0	3.5	
383 - 389	2.7	3.3	2.01	2.6	3.0	
390 - 396	2.6	3.1	1.77	2.3	2.6	
397 - 403	2.4	2.9	3.09	2.1	2.4	
404 - 410	2.0	2.6	2.71	1.8	2.3	3.92
411 - 417	1.7	2.4	1.60	1.5	2.1	3.90
418 - 424	1.6	2.2	1.64	1.1	2.0	3.83
425 - 431	1.5	2.0	2.91	1.1	2.0	
432 - 438	1.4	1.8	2.85	1.5	2.1	
439 - 445	1.4	1.7		1.9	2.2	
446 - 452	1.6	1.8		2.1	2.4	
453 - 459	1.8	1.9		2.3	2.4	

Interpolation of Current Meter Data

Although the resolution of the IFYGL current meter network is considered to be too coarse to allow for a spatial interpolation of the data without resorting to dynamical models, this is not necessarily true in other cases. Since the subject of hydrodynamic models is treated extensively in the following, it would seem appropriate to briefly discuss the problem of three-dimensional interpolation of observed currents. We will here summarize the principles of a method which, although not used in the following computations, was found to produce quite satisfactory results in closely related simulation studies. The method was originally developed for atmospheric wind interpolations by Sasaki (1970) and Sherman (1976).

Given a three-dimensional domain and a set of observed currents, it is possible to interpolate and extrapolate the flow field without satisfying the equation of continuity. Should continuity be desired, the interpolated/observed results must undergo some adjustment. There are many ways in which this adjustment can be achieved, but there is one that produces the least change according to the variational principle. Specifically, consider the following functional,

$$E(u, v, w, \lambda) = \iiint [w_1^2(v-v^o)^2 + w_2^2(w-w^o)^2 + w_3^2(w-w^o)^2 + \lambda(\frac{\partial u}{\partial x} + \frac{\partial v}{\partial y} + \frac{\partial w}{\partial z})]dxdydz \qquad (4.1.1)$$

where x, y, z are the coordinates; u, v, w are the adjusted velocity components in the x, y, z directions, respectively; u^o, v^o, w^o are the corresponding observed/interpolated variables; $\lambda(x, y, z)$ is the Lagrange multiplier; and w_1, w_2 and w_3 are weights which can be assigned according to the observational errors or statistical variances of the observed field. According to the variational principle, the extremal solution of the functional E minimizes the variance of the difference between the observed and adjusted variables subject to the constraint that it satisfies the continuity equation. This is given by the Euler-Lagrange equations

associated with Equation (4.1.1):

$$u = u^0 + \frac{1}{2w_1^2}\frac{\partial\lambda}{\partial y} \tag{4.1.2}$$

$$v = v^0 + \frac{1}{2w_2^2}\frac{\partial\lambda}{\partial y} \tag{4.1.3}$$

$$w = w^0 + \frac{1}{2w_3^2}\frac{\partial\lambda}{\partial z} \tag{4.1.4}$$

$$\frac{\partial u}{\partial x} + \frac{\partial v}{\partial y} + \frac{\partial w}{\partial z} = 0 \tag{4.1.5}$$

and appropriate boundary conditions. Note that Equation (4.1.5) is the continuity equation. In order to solve for u, v and w, Equations (4.1.2 - 4.1.4) are differentiated and substituted into Equation (4.1.5) to obtain an equation for λ first:

$$\frac{1}{w_1^2}\frac{\partial^2\lambda}{\partial x^2} + \frac{1}{w_2^2}\frac{\partial^2\lambda}{\partial y^2} + \frac{1}{w_3^2}\frac{\partial^2\lambda}{\partial_z^2} = 2\left(\frac{\partial u^0}{\partial x} + \frac{\partial y^0}{\partial y} + \frac{\partial x^0}{\partial x}\right) \tag{4.1.6}$$

This equation can be solved easily by either the successive over-relaxation method or the fast Poisson solvers. The values of u, v, w follow easily from Equations (4.1.2-4) and the λ's. The results are subject to the interpolation used and the weights assigned in the procedure. The choice of these reflects the extent to which the data can be adjusted in order to satisfy the continuity equation. For instance, if larger weights are placed on the observed velocities than the interpolated ones, the latter are subjected to more adjustment. It is possible to incorporate in the procedure irregular shore boundaries in the two-dimensional case and variable depths in the three-dimensional case. Numerical experiments on these and other aspects are under investigation

at CCIW (e.g., Dunbar, 1977). Figure 4.1.6 (a) and (b) show typical results of interpolated two-dimensional currents before and after applying the variational procedure, respectively, as compared with the observed values (thick arrows).

4.2 Hydrodynamic Simulations

In conjunction with the 1972 International Field Year on Lake Ontario, a comprehensive modeling program was initiated by the Canada Centre for Inland Waters with the goal of computing water levels, currents, temperatures, and the transport of dissolved or suspended materials in large lakes. The present section summarizes the principal results of the hydrodynamic simulations.

The modeling project was carried out in three phases. The first part was concerned with a systematic investigation and scrutiny of numerical techniques employed in the field of geophysical fluid dynamics and the development of a hierarchy of models describing the circulation of large lakes under various conditions. This model development and preliminary computations were described in three papers by Simons (1971, 1972, 1973a).

The second phase of the modeling program consisted of a verification study based on the abundance of observational data produced by IFYGL. In particular, two significant physical events were singled out during which the lake was subjected to strong atmospheric forcing. The first of these episodes was associated with tropical storm Agnes during June, 1972, when Lake Ontario was only weakly stratified. The second episode occurred in early August at the peak of the lake's stratification. The detailed procedures and results of these verification studies have been presented by Simons (1973b, 1974, 1975a).

The third phase dealt with long-term simulations of the physical characteristics of the lake with particular reference to the effects of hydrodynamic circulations on distributions of water quality parameters. The three-dimensional hydrodynamic model was run for the whole 1972 field year and the results were stored for subsequent use in ecosystem models. The computed currents were verified (Simons, 1976a) by comparing the

Fig. 4.1.6(a) Interpolated currents (→) *before* applying variational procedure. (➡) are observed currents.

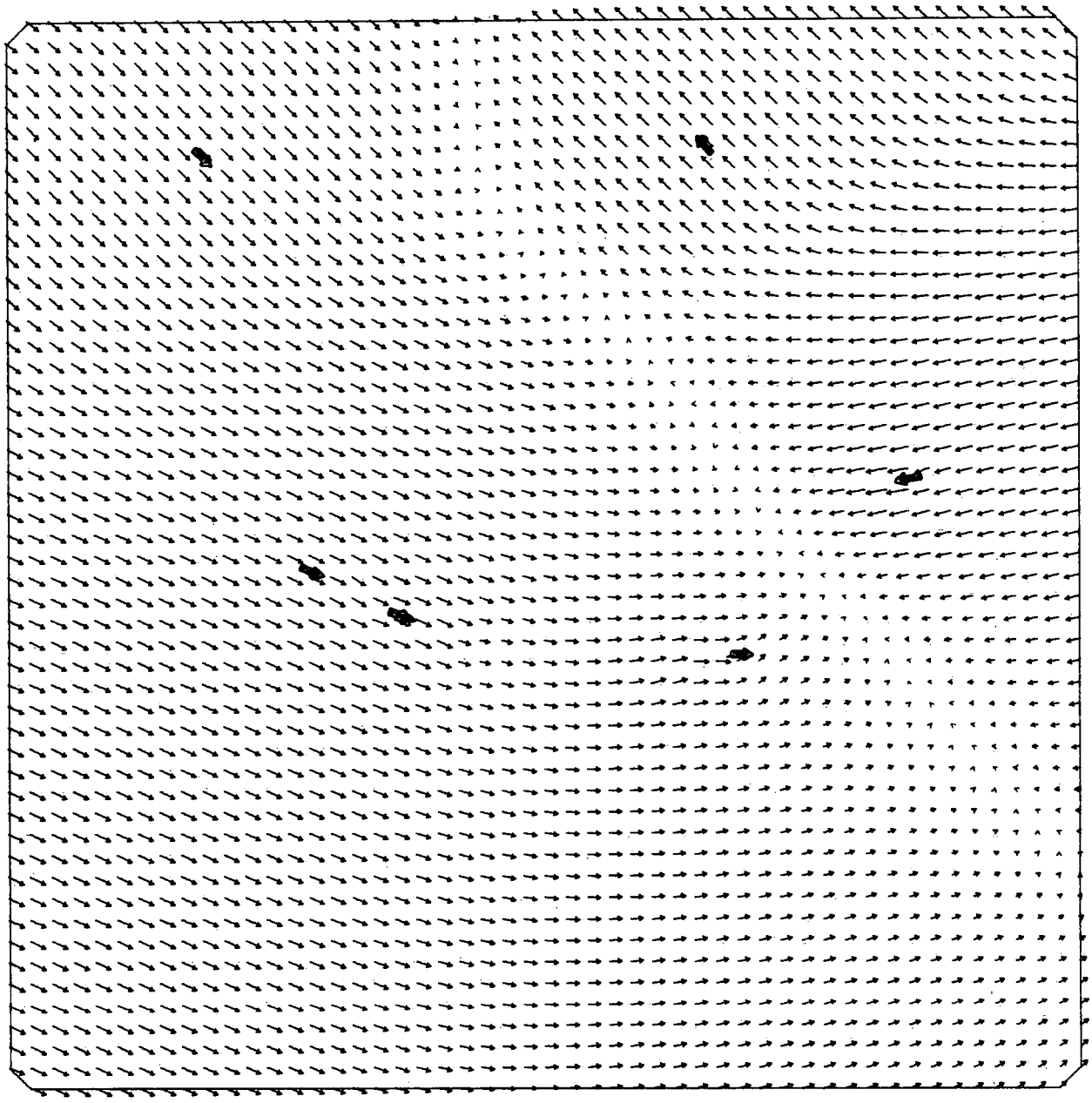

Fig. 4.1.6(b) Interpolated currents (→) *after* applying variational procedure. (⇒) are observed currents.

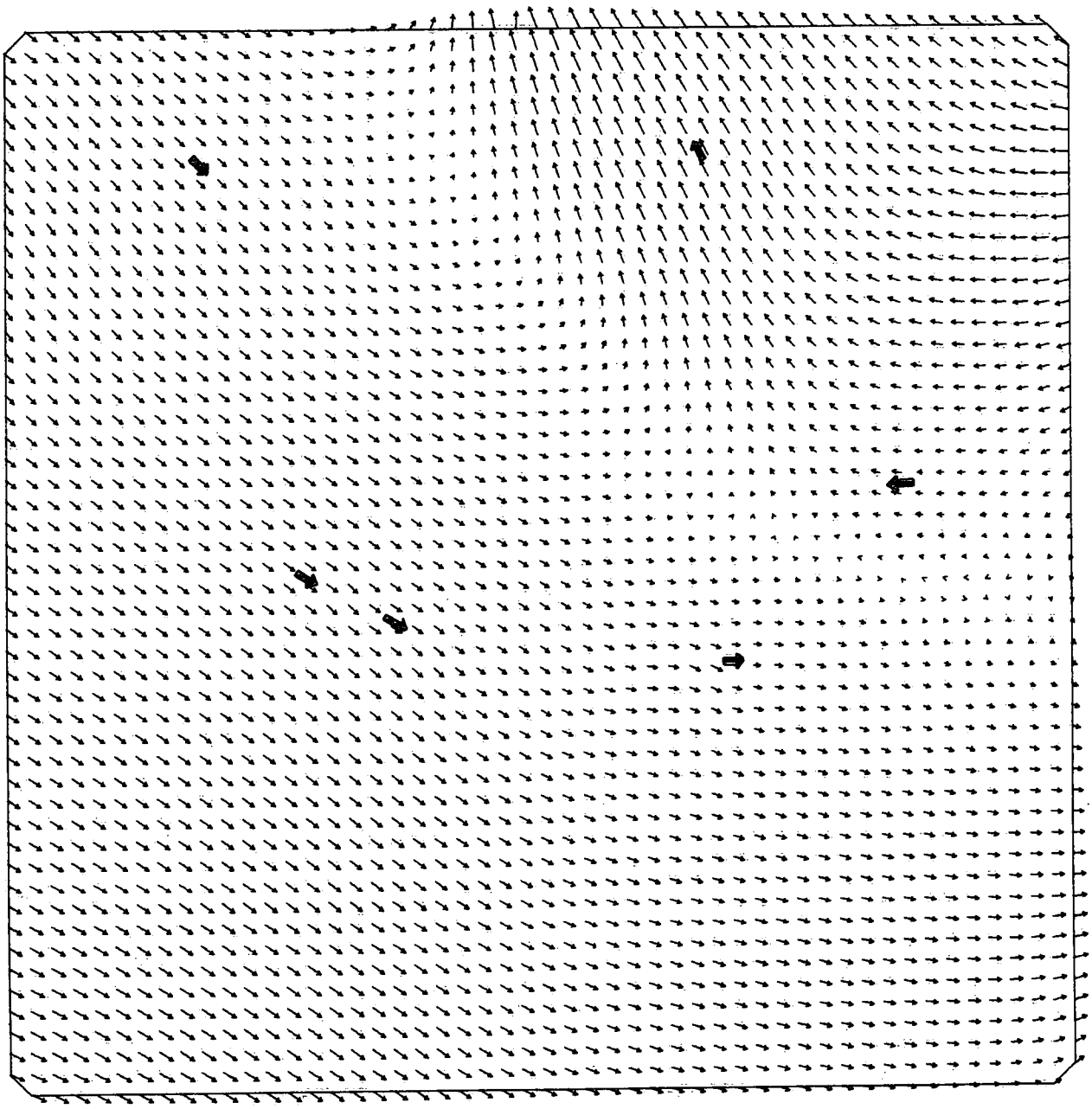

resulting heat transports with heat budgets prepared by Boyce (1978). A similar verification study was also carried out for Lake Erie by considering chloride distributions during 1970 (Lam and Simons, 1976). This interaction between hydrodynamic and water quality models will be dealt with in the next chapter.

Modeling Principles

The numerical model is based on the framework established by numerical weather prediction and storm surge forecasting. The underlying principle is that the dependent variables can be separated in large-scale organized flow, which can be treated deterministically, and smaller-scale quasi-random motions, which must be parameterized on the basis of statistical evidence. Such scale separation has not been established and in practice the grid resolution is selected on the basis of computer capabilities rather than physical considerations. The goal of the verification experiment is essentially to evaluate this separation hypothesis and the parameters involved.

With regard to the external mode (free surface and vertically integrated water transports) the model is quite similar to conventional storm surge models pioneered by Hansen (1956) and Platzman (1963). With regard to the internal mode (temperature variations and vertical profiles of currents) the model is based on the same principles as present oceanic models, which in turn have been derived from atmospheric models (Bryan, 1969). Thus the hydrostatic law is used throughout together with the Boussinesq approximation, and free convection associated with unstable stratification is simulated by instantaneous adjustment to neutral conditions. In view of the stratification cycle of the Great Lakes, the model was formulated so as to allow for a vertical structure in the form of fixed permeable levels as well as a system of layers of different densities separated by moving material interfaces (Simons, 1973a). The model version used for the Field Year studies employed permeable horizontal levels except for the free surface. Beyond the intersection of these levels with the bottom, the layers are bounded by the bottom; therefore, the thickness of any layer is, in principle, assumed to vary from point to point.

Since the hydrodynamical model equations in general form are well known, they will not be reproduced here. Essentially, the system of equations consists of two prognostic equations for the horizontal velocity components, one prognostic equation for the temperature, a diagnostic relationship between density and temperature, another diagnostic equation relating the pressure to the overlying water mass (hydrostatic law), and finally an equation expressing conservation of mass. The latter relates vertical transports to horizontal currents and appears in diagnostic or prognostic form depending on whether it is used to compute vertical velocities or surface displacements.

In view of the appearance of the major terms in the model equations the variables are distributed on a staggered grid in space and time. In a horizontal plane, the free surface, the vertical velocity, and the temperature are located at the centre of squares formed by the velocity component. In the vertical direction, temperature and currents are defined for layers, whereas vertical velocities, stresses, and heat fluxes are specified at interfaces. Central differences in time are employed for pressure-divergence terms and forward differences for friction-diffusion terms. Nonlinear terms in the temperature equation are treated by a Lax-Wendroff scheme. Effects of nonlinear terms in the equations of motion were evaluated in preliminary experiments but discarded in the verification studies since their effects appeared small compared to the effects of changing the values of adjustable model parameters within a range consistent with observations.

For the computations reported in this report, the horizontal grid spacing was 5 km, and the vertical resolution consisted of four layers separated by horizontal levels at 10, 20, and 40 metres below the surface, to approximate the location of current meters at 10, 15, 30 and 50 metres below the water surface. For purposes of time extrapolation the external and internal modes of the model are treated separately. Since the external gravity waves associated with the free surface tend to impose severe restrictions on the computational time step, the internal structure of the flow is computed after filtering out the effects of the free surface waves. This is accomplished by transforming the N layer equations into one equation for the vertical-mean flow and N-1 equations for vertical

shears of the currents. This means that the internal mode is modeled in the same way as in the usual "rigid-lid" models and, consequently, can be solved numerically with the same timestep as used in those models, say, up to one hour or so. All computations discussed here employed a timestep of 100 seconds for the external mode and a step of 15 minutes for the internal mode.

Typical Model Solutions

For relatively shallow water bodies with large depth variations, such as the Great Lakes, the bottom topography is a major factor governing the water circulation. A characteristic result is that a wind blowing parallel to the length axis of an elongated lake results in currents running with the wind near the shores and against the wind in deep water. This phenomenon can be explained by recognizing that the wind must move a much larger mass of water in the deep portions of the lake than in the shallow areas. Consequently, the shallow water acquires a greater velocity and the principle of mass conservation dictates a return flow in deep water. Figure 4.2.1a presents a cross section of Lake Ontario at a point approximately halfway down the length axis of the lake. The contours indicate a typical distribution of the component of the velocity in the direction of the wind, which is assumed to blow from the west. The thin horizontal lines mark the model layers used for this calculation. Bands of large surface velocities in the direction of the wind are observed nearshore, whereas the compensating return flow, indicated by negative contour values, consists of weak currents over the major portion of the cross section. This aspect of wind-driven lake circulations has been discussed in more detail by Bennett (1974).

In view of the large spatial dimensions of the Great Lakes, the Coriolis force is another parameter of major importance. Figure 4.2.1b shows the velocity component normal to the component shown in Figure 4.2.1a for the same wind forcing. The surface water shows the typical Ekman turning to the right of the wind, and the resulting pressure gradient returns the water at greater depths. Associated with these currents, upwelling occurs at the north shore and downwelling at the south shore, i.e., to the left and the right of the wind, respectively (Figure 4.2.1c).

When stratification is included in the model, this results in cooling of the lake at the north shore and warming at the south shore. This in turn leads to an additional baroclinic velocity component parallel to the wind as shown in Figure 4.2.1d. Such vertical shears of the currents can be related to horizontal temperature gradients by the so-called thermal wind relationship employed in meteorology. This means that the pressure gradients associated with the temperature gradients tend to be balanced by the Coriolis force. The total velocity component in the direction of the wind under stratified conditions is equal to the sum of Figures 4.2.1a and 4.2.1d.

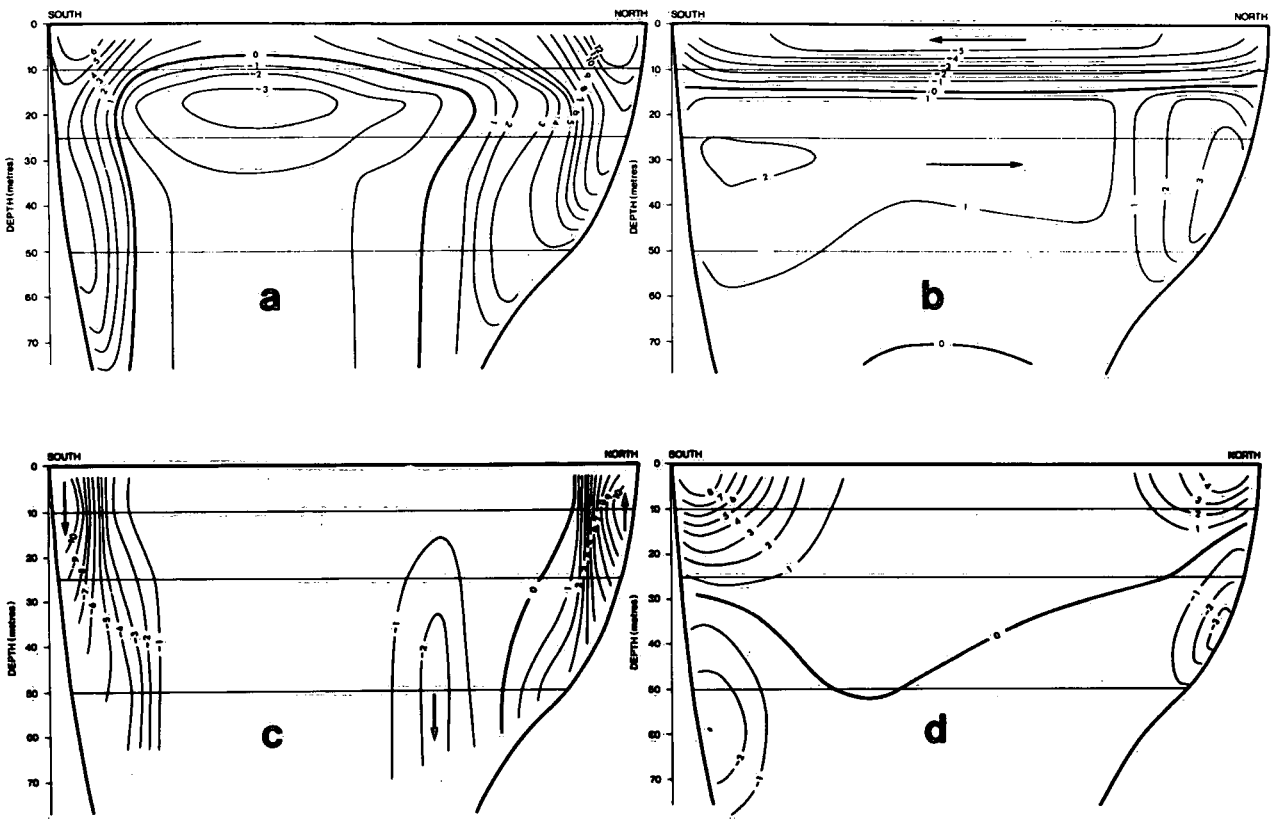

Figure 4.2.1 Currents computed in a cross section of Lake Ontario, halfway down its major axis, for an eastward surface wind: (a) eastward velocity component, without stratification; (b) northward velocity component; (c) vertical velocity component; (d) additional eastward velocity component resulting from temperature gradients.

A typical example of the horizontal velocity distribution is shown in Figure 4.2.2. These water transports were obtained by averaging the results of a model computation for actual winds from 20 April, 1971 to 14 May, 1971. The arrow outside the lake indicates the average wind for this period and the arrows within the lake represent vertically integrated velocities. Inflow and outflow from major rivers are included. Again this mean circulation pattern exhibits the nearshore currents in the direction of the wind compensated by return flow in deeper water. It will be clear that this holds interesting implications with regard to the dispersion of pollutants in a lake. This will be illustrated in Section 4.3.

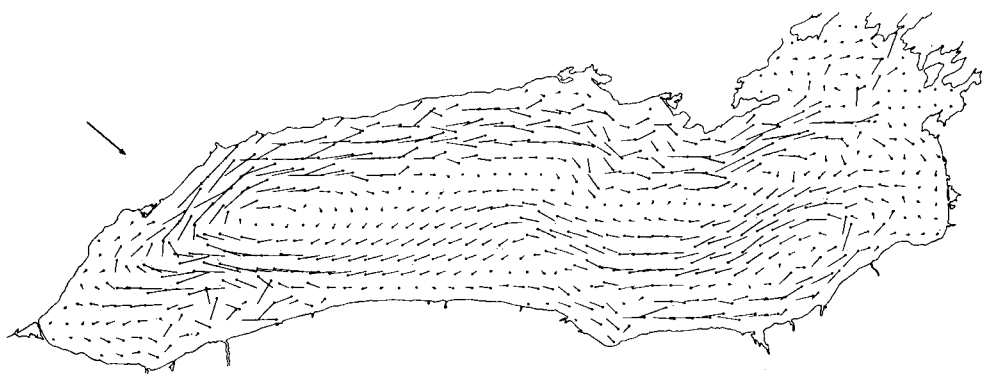

Figure 4.2.2 Computed vertically integrated transports in Lake Ontario, averaged over a 25-day period, 20 April to 14 May, 1971. Mean wind for the period is shown by the vector outside the lake.

Model Parameters

The model parameters essentially represent the effects of sub-grid-scale phenomena. In the momentum equations these parameters appear as surface wind stresses, interfacial shearing stresses, bottom friction, and horizontal diffusion terms. Similar parameters enter in the temperature equation. For the present calculations all sub-grid-scale diffusive fluxes were computed simply on the basis of the classical gradient diffusion concept. Wind and bottom stresses were computed on the basis of quadratic stress laws.

The primary objective of a verification study is to tune the model by establishing the range of numerical values of adjustable model

parameters. Among these, the most important is the surface stress which governs the transfer of energy from the wind to the lake. The wind stress coefficient over water has been the subject of numerous studies but it is still surrounded by uncertainty. One of the main problems is that the method used for estimating its value appears to affect the outcome. In particular, drag coefficients derived from atmospheric boundary layer measurements tend to be only half as large as those inferred from changes of water levels. Since the present model predicts surface elevations, the stress coefficient was estimated by comparison of observed and computed water levels on the perimeter of the lake. Extensive sets of data of this kind became available as a by-product when the model was run for the whole IFYGL period on Lake Ontario and a similar modeling program for the 1970 shipping season on Lake Erie. Statistical summaries of these results have been presented by Simons (1975b). The coefficient estimates appeared to average out to 1.85×10^{-3}, with typical values of 2.5×10^{-3} during stormy periods such as the two episodes selected for the IFYGL model verification study.

Figure 4.2.3 summarizes estimates of wind stress coefficients derived from numerical simulations covering the 1972 Field Year. The analysis was based on a comparison of observed and computed surface slopes between Burlington and Oswego. The data were divided into different classes in order to isolate effects of air-water stability. The stability parameter used is the familiar bulk Richardson number. Within each class, the correlations between observed and computed set-up were computed and the drag coefficient was estimated from the linear regression relationship.

The bottom stress is assumed to satisfy a similar law as the wind stress and thus it is taken to be proportional to the square of the bottom velocity. The coefficient was estimated from the decrease of observed kinetic energy after hurricane Agnes. On this basis the coefficient was set equal to the wind stress coefficient. A more crucial parameter is the vertical flux of momentum by small-scale eddies. According to the conventional gradient diffusion concept, this vertical flux is related to the velocity shear between layers through a diffusion coefficient. Now it appears that the vertical shear energy shows a maximum around the inertial frequency. Furthermore, it is common for the

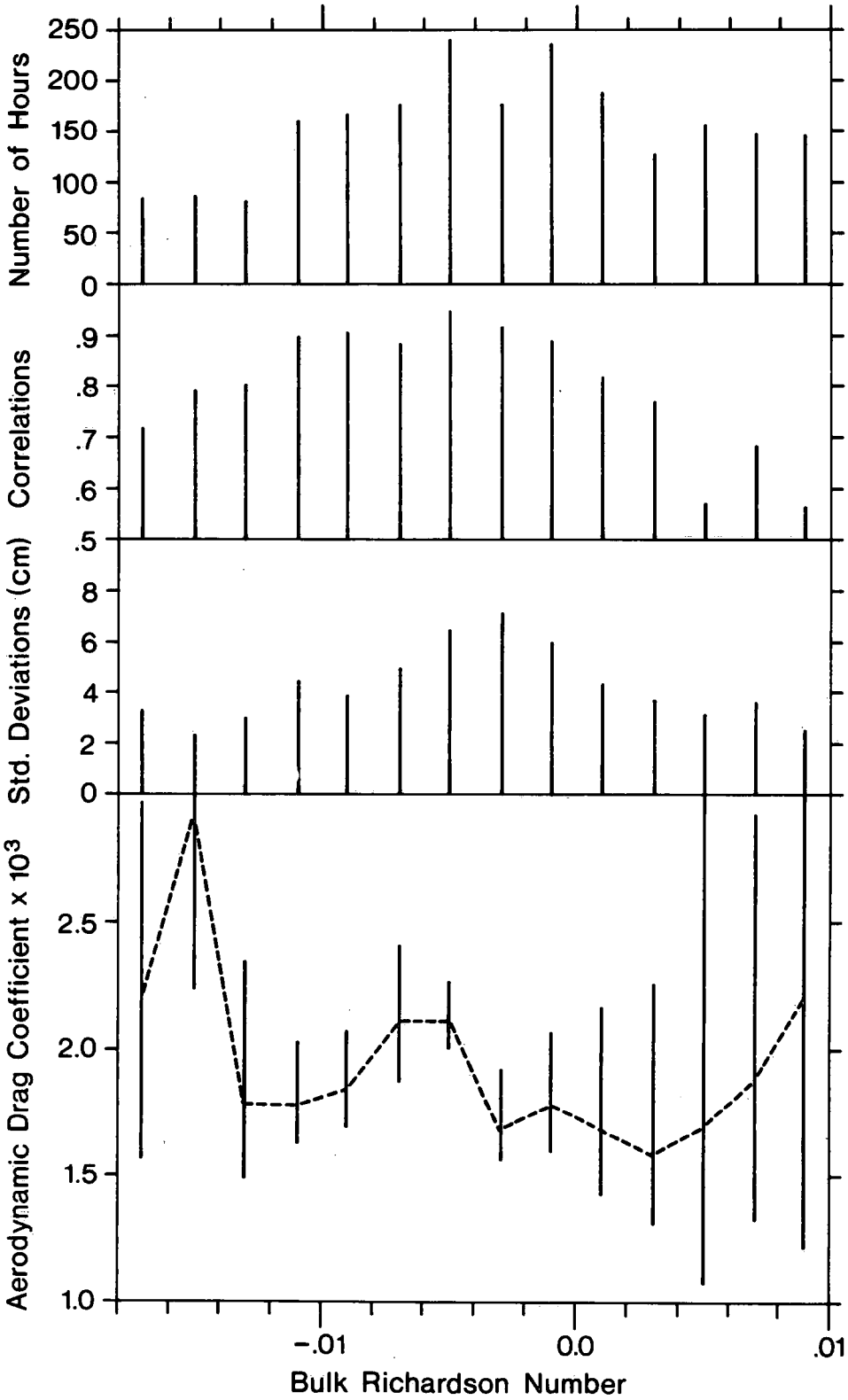

Figure 4.2.3 Correlation between observed and computed water set-up between ends of Lake Ontario, and the corresponding wind stress coefficients. Data and model results grouped according to atmospheric stability, measured by bulk Richardson number.

inertial rotations to attain a two-layer structure with the lower layer being exactly out of phase with regard to the upper layer. On the basis of the internal friction associated with this shearing motion, an estimate can be made of the decrease of shear kinetic energy and this can be compared with the observed decrease after a storm to estimate the vertical eddy diffusivity. In this manner, a typical value of 25 to 50 cm^2/sec was derived for the period of calm weather after hurricane Agnes (Simons, 1973a).

Diffusion coefficients, in particular vertical diffusion coefficients, depend on stratification as well as wind or velocity shears. A detailed investigation was made of the time history of the observed currents in one station of the lake during hurricane Agnes and a great number of computations were made to find the representation of vertical momentum fluxes that would produce the best simulation. It was found that good results could be obtained by making the vertical diffusion coefficient proportional to the wind stress with the coefficient of proportionality a function of the Richardson number. Figure 4.2.4 shows a comparison of observed and computed currents thus obtained for this particular station during and after hurricane Agnes. It can be seen that the model simulates the inertial oscillations after the storm in a satisfactory manner.

Model Verification Studies

The verification analysis with regard to lake currents was based on time series of computed and observed currents treated by digital filters. This makes it possible to evaluate the model performance for different time scales. The primary filter operation separated the spectrum at a frequency just below the inertial frequency. In addition, averages were computed for periods of the order of a few days, which are considered of interest in the framework of transports of material in a lake. Figure 4.2.5 shows observed and computed currents averaged over a period of three days coinciding with hurricane Agnes in June, 1972. The numbers 1 to 4 refer to depths of 10, 15, 30, and 50 metres, respectively. The wind was blowing from a north-easterly direction, thus causing a strong counterclockwise circulation, since the northern half of the lake is much shallower than the southern half. Aside from the bottom current in the station east of Toronto, there is a good agreement between observed and computed flow.

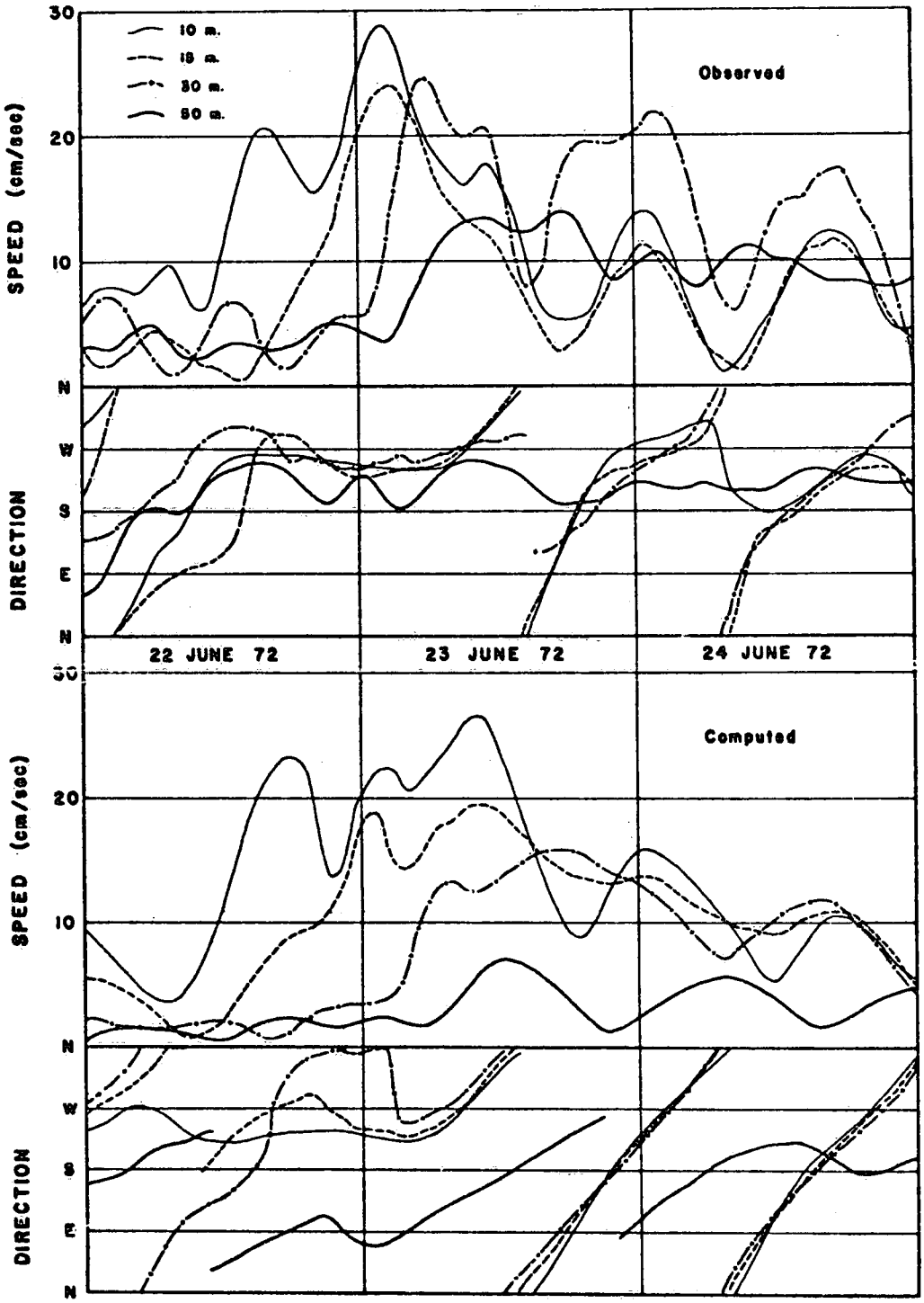

Figure 4.2.4 Observed and computed currents at four depths at one station, during storm Agnes in 1972.

STORM PERIOD AGNES

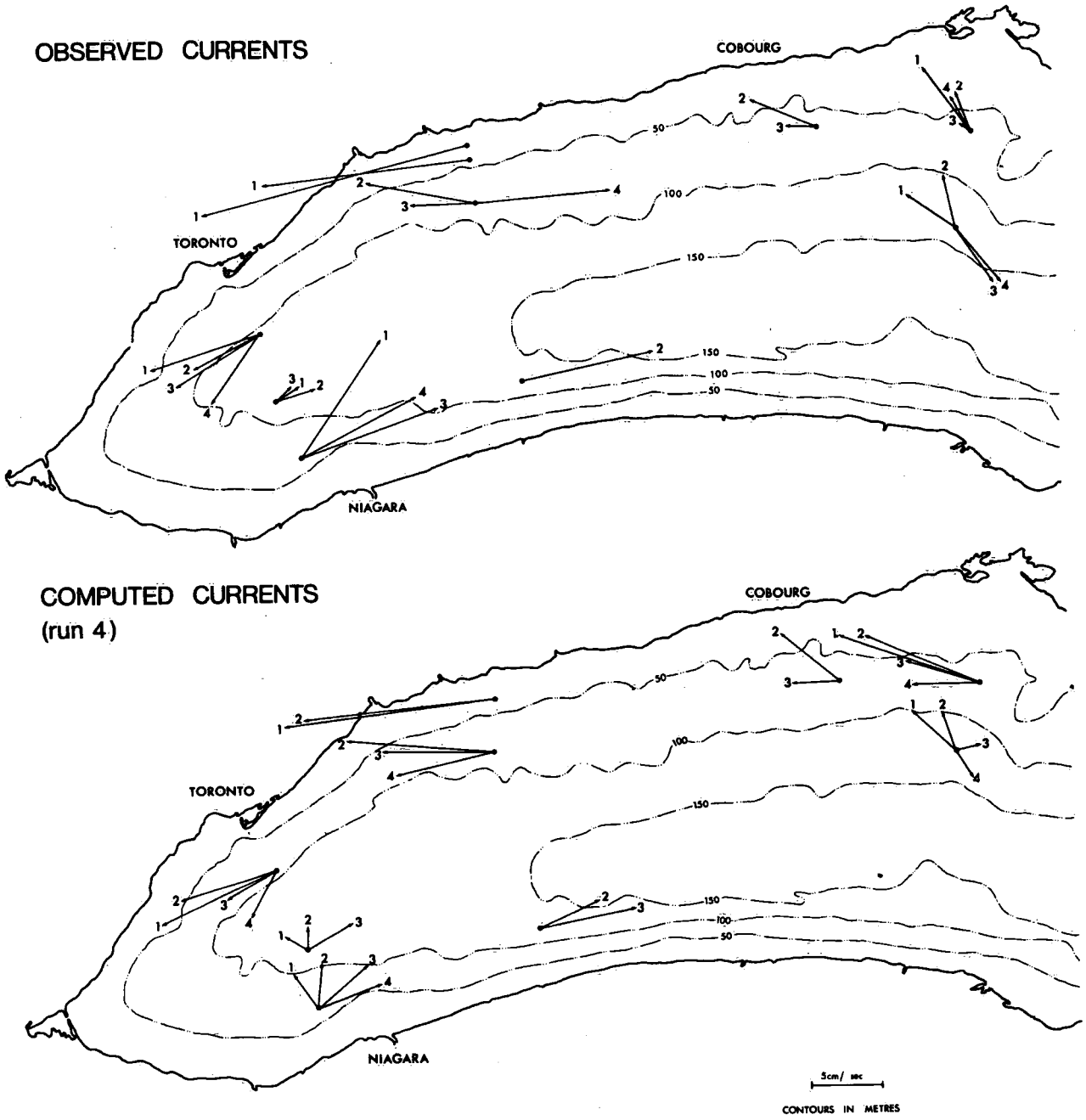

Figure 4.2.5 Observed and computed currents averaged over a three-day period, 22-24 June, 1972. Numbers 1 to 4 refer to depths of 10, 15, 30 and 50 m, respectively.

Time series of currents smoothed by the low-pass filter indicate a satisfactory correspondence of model results and observations, with regard to both current amplitudes and directions. For the stratified case study, the inclusion of baroclinic effects appears to improve the model simulations. This is illustrated in Figure 4.2.6 which presents results for two stations along the northern shore, computed with and without stratification. Although the differences between the homogeneous and stratified solution appear rather small at first glance, a synoptic view of the lakewide circulation shows that significant differences develop after the storm. It should be noted that such differences cannot be identified as purely baroclinic effects, since the corresponding vertical shears also cause indirect effects such as changes of bottom stresses.

In addition to water levels and currents, the model predicts lake temperatures. Initial temperature distributions throughout the lake were specified for each episode on the basis of ship cruises. The changes of temperature from one ship survey to the next were used for verification. Figure 4.2.7 shows computed and observed temperature changes for one model layer between two ship surveys in August. There is a general agreement with regard to apparent upwelling areas along the northern and eastern shores. It should be noted, however, that these results reflect the short-term response of the lake to a well-defined wind impulse. The verification of heat transport simulations presented in the following section shows that considerable errors can occur in long-term simulations. Many of these errors can be traced to insufficient model resolution, in particular in the nearshore area. Improvements in this direction have been suggested by Bennett (1977).

4.3 Transports of Heat and Nutrients

Large lakes may display significant spatial variations of temperature, nutrients and plankton. Pronounced examples are vertical gradients associated with the development of thermoclines and horizontal variations between shore zones and deep water. Conditions in such lakes can be properly simulated only by three-dimensional models. In its simplest form, a three-dimensional ecological model consists of a horizontal and vertical arrangement of volume elements within each of which

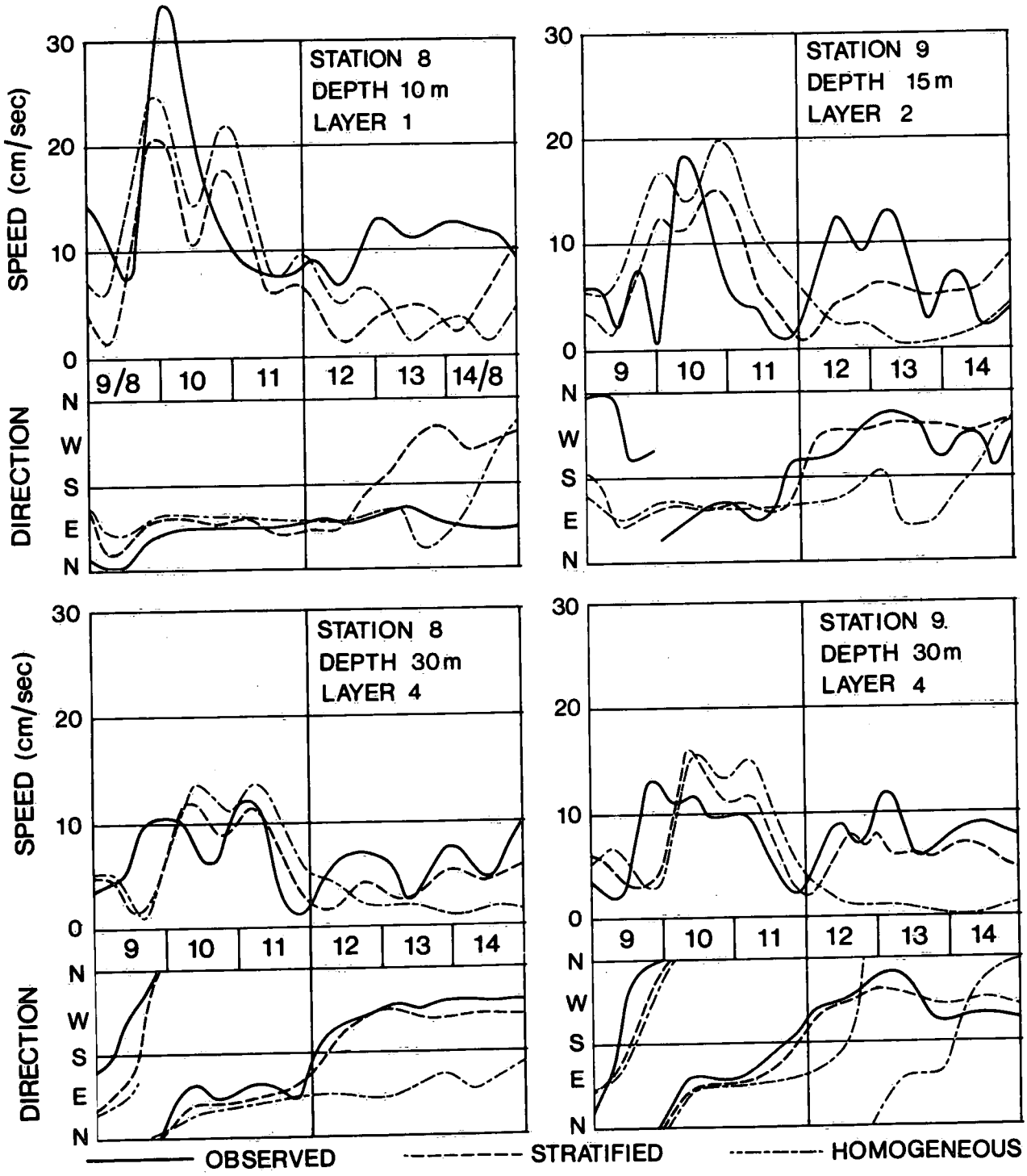

Figure 4.2.6 Observed and computed currents for homogeneous and stratified models. All time series are smoothed to remove periods less than the inertial period. Stations 8 and 9 are located along the north shore of Lake Ontario.

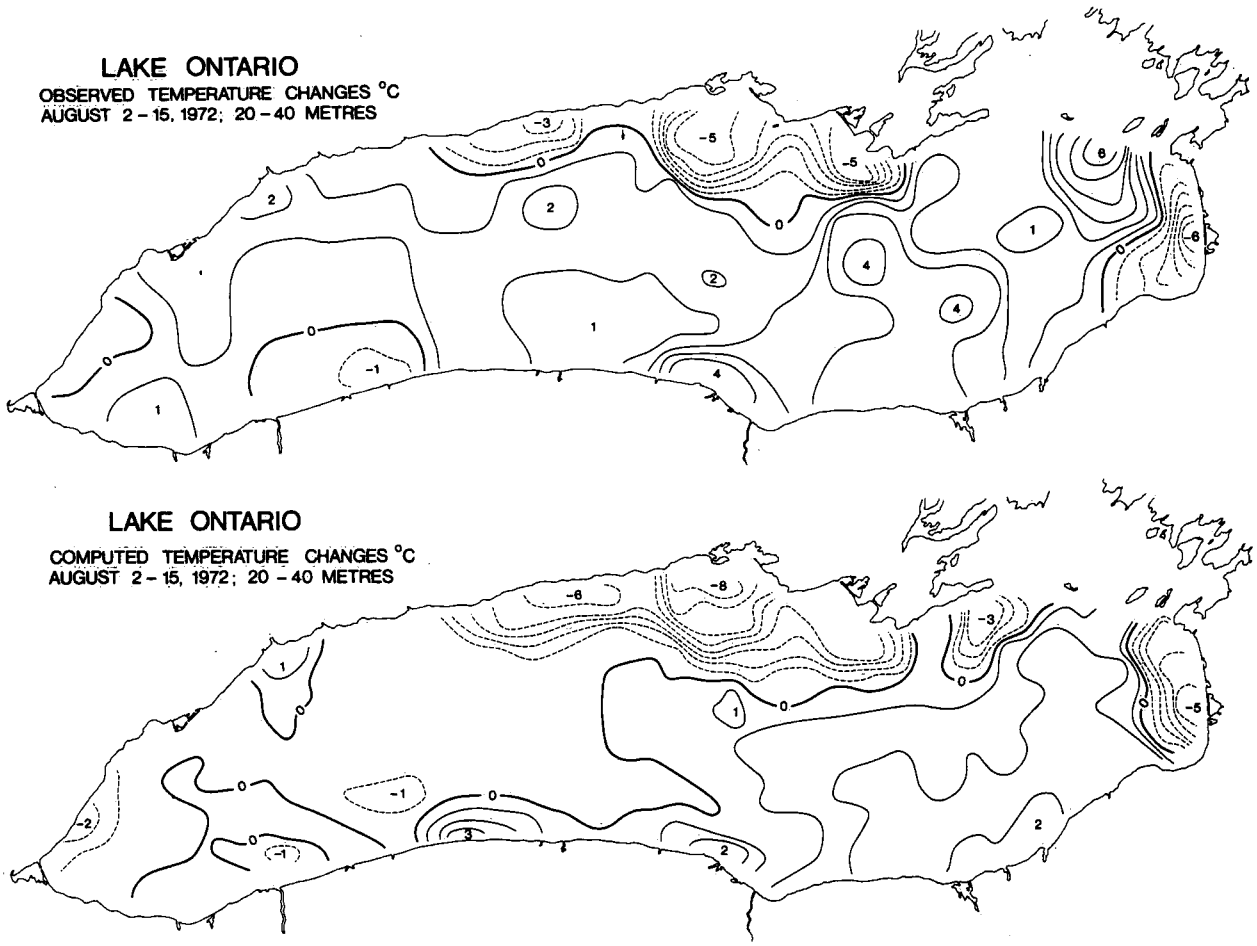

Figure 4.2.7 Observed and computed temperature changes over time interval 2-15 August 1972, for 20-40 m layer.

the state variables change with time according to a uniform set of biochemical reaction equations. Differences between the elements develop as a result of varying environmental conditions such as local temperature and loading regimes which are known from observations or derived from physical models. Except for the technical aspect of increased computational effort, the three-dimensionality of a model would add little of interest to the problem of ecosystem simulation if the volume elements remained completely independent. In practice, however, individual layers and zones of a large lake are coupled together by water movements and the complexity of a three-dimensional model is proportional to the manner in which this interaction is included.

The simplest method of simulating effects of water movements on biochemical variables is to invoke the concepts of turbulent diffusion, which lead to an exchange of these variables in proportion to the concentration gradients between adjacent volume elements. Indeed, this is the common way of dealing with vertical mixing between layers of a horizontally homogeneous lake model. For large enough time scales, all water transports, including horizontal circulations, can be visualized as some form of mixing and it will often be satisfactory to treat them in this fashion if the only aim is to design a management model of lake eutrophication. For shorter time scales, however, water movements can lead to large-scale transport ("advection") of dissolved or suspended substances in well-defined directions. Important effects of this type can occur during episodes of sustained upwelling or downwelling in nearshore zones of large lakes or seas. Inclusion of such transports in a three-dimensional model may contribute substantially to a proper interpretation of field observations and, consequently, can be essential for a realistic ecological simulation.

The present section is devoted to a discussion of the effects of water movements on the distribution of temperature, nutrients and biological matter. After a brief presentation of the computational framework, the vertical exchange across the thermocline is considered on a lake-wide scale, including upwelling as well as small-scale convection. This is followed by numerical computations of temperature and nutrient advection based on the hydrodynamic results presented in Section 4.2. The methodology used here is partially diagnostic to the extent that observed gradients of state variables are combined with computed water movements to evaluate mass exchanges.

Mathematical Formulation

Computations of mass exchanges between volume elements of a lake are based on the so-called advection-diffusion equation, which expresses the principle of mass conservation applied to each volume element. Consider a volume element within the lake bounded by imaginary surfaces which are permeable with regard to the flow of water and suspended or dissolved material. At any time the total mass of a given chemical substance in

this element can be expressed as the product of the mean concentration of this substance and the volume of the element. Now this mass can change by essentially three processes. The first one consists of transports by organized currents and vertical water motions through the various faces of the volume element, usually referred to as advection. The second process results from quasi-random fluid motions which tend to mix the properties of adjacent volume elements in a manner analogous to molecular diffusion. The third contribution comes from external sources or the internal exchange between individual chemical substances appearing as a source of one element and a sink of others. The advection-diffusion equation states that the time rate of change of mass of a given substance, contained in the element considered, can be computed by accumulating the above effects.

To express this conservation principle in mathematical form, assume that the lake is covered with a rectangular grid and that the interfaces between consecutive layers are fixed in space. Figure 4.3.1 presents two views of a volume element of the lake, the upper one taken from the top, the lower one from the side. T represents the concentration of the variable to be considered (units of mass/volume) and U, V, W are the components of the large-scale water transports through the western, southern, and bottom boundary of the volume element (units of volume/time). Index i runs from west to east, j runs from south to north, and k from the bottom to the surface. Deleted subscripts are understood to be equal to i, j, k. Note that the transports at the southern, western and lower boundary have the same subscript as the concentration at the centre of the volume element. The mass transport through the left side of the volume element may be written as

$$U_i(\alpha T_{i-1} + (1-\alpha)T_i)$$

and similar expressions hold for the other sides. For central differences $\alpha = 1/2$; for upstream differences $\alpha = 1$ or 0 depending on the sign of U. The transport components follow immediately from a hydrodynamic model such as the one discussed in section 4.2. The small-scale mixing across an interface is proportional to the concentration gradient between adjacent

elements. If A, B, C represent volume exchange components along the three coordinates in the same units as the water transports U, V, W, then the diffusive mass exchange through the left-hand side of the volume is

$$A_i(T_{i-1} - T_i)$$

with similar expressions holding for the other sides. The volume exchanges, A, B, C, can be estimated from heat or mass budgets or also from turbulent diffusion coefficients determined by dye experiments in lakes (see, for example, Murthy, 1975).

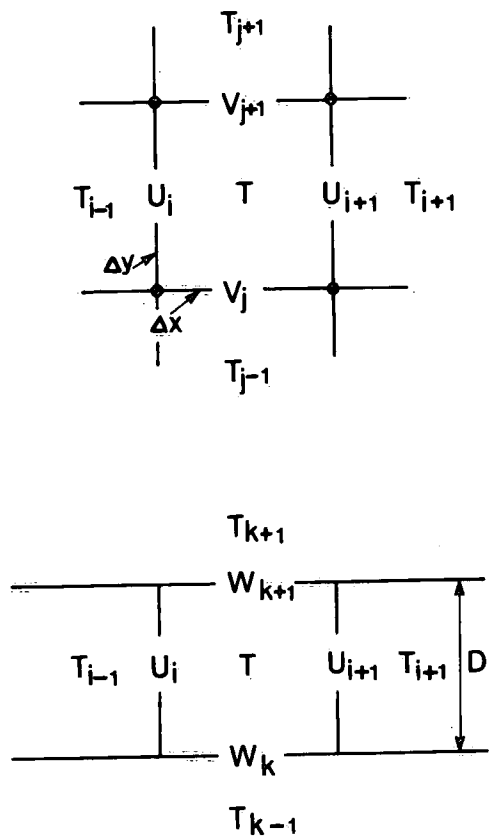

Figure 4.3.1 Horizontal and vertical structure of a typical volume element of a numerical model. T = temperature; U, V and W are transport components.

If the sum of all sources is represented by S (mass/time), then the complete conservation equation is

$$\frac{dM}{dt} = X_i - X_{i+1} + Y_i - Y_{i+1} + Z_k - Z_{k+1} + S$$

where

$$M = \Delta x \cdot \Delta y \cdot D \cdot T$$

$$X_i = U_i(\alpha T_{i-1} + (1-\alpha)T_i) + A_i(T_{i-1} - T_i)$$

$$Y_j = V_j(\alpha T_{j-1} + (1-\alpha)T_j) + B_j(T_{j-1} - T_j)$$

$$Z_k = W_k(\alpha T_{k-1} + (1-\alpha)T_k) + C_k(T_{k-1} - T_k)$$

The depth of the layer, D, will vary from point to point if the interfaces are not horizontal. This generalization can be readily incorporated (see Simons, 1973a) but for the moment there is no need to enter into this kind of detail.

Vertical Exchanges

In order to provide a basis for comparison between effects of large-scale water transports, vertical mixing, and biological processes included in plankton models, it is illustrative to consider first a horizontally uniform lake consisting of two or more layers. On a lake-wide scale, vertical mass exchanges include all scales of motion from small convective processes to large-scale upwelling of cold water in nearshore areas. Such vertical exchanges can be readily estimated from heat budgets. For Lake Ontario, three-dimensional descriptions of temperature are available from ship surveys at weekly intervals during 1972 (Boyce, 1978). This data base makes it possible to compute heat contents for any system of layers, whereupon vertical heat fluxes through the intermediate levels follow from heat content changes between consecutive ship surveys.

Let V be the volume of an arbitrary layer of water with average temperature T and let A_1 and A_2 be the areas of the upper and lower boundary and F_1 and F_2 the heat fluxes per unit area at these levels, then the heat balance equation is

$$F_1A_1 = F_2A_2 + \frac{\partial(TV)}{\partial t}$$

where ∂t is the time interval between cruises. Application of this equation to the lowest layer gives the flux through the first interface above the bottom if the heat flux at the bottom is neglected. This process is repeated for the layers and levels above. The exchange of water masses or effective exchange coefficient, E, can now be estimated by dividing the flux by the temperature difference between two adjacent layers, ΔT, thus

$$E = F/\Delta T$$

which has dimensions of a velocity, say m/day.

Naturally, the latter relationship cannot be used when the temperature gradient becomes very small or is directed against the heat flux. For predictive purposes, this causes no problems because such conditions can be taken to represent complete mixing, and hence can be readily incorporated in a model. For diagnostic computations, however, it is not possible to estimate water exchanges during the mixed period from the above equations. Consequently, the following computations are restricted to the stratified season. In that case, the mixing coefficients above may be multiplied with vertical gradients of observed limnological variables to estimate vertical mass exchanges of these variables.

Figure 4.3.2 shows upward mass exchanges at a depth of 20 m below the surface of Lake Ontario during the stratified season of 1972 (solid lines) as computed from exchange coefficients (Chapter 2.2) and observed vertical concentration gradients between the upper 20 m layer (Chapter 2.1). The volume of the upper layer is about 35.10^{10} m^3 and the variables selected here are soluble reactive phosphorus (SRP), nitrite and

nitrate (NO_3), total particulate carbon (TPC), and chlorophyll a (Chl a). This may be compared with the observed time rate of change of mass contained in the upper layer. If a simple linear data interpolation is used, the rate of change will be constant between consecutive ship cruises. These results are represented by the dashed curves in Figure 4.3.2. For a comparison between the solid and dashed curves, attention should be directed at the areas under the curves between consecutive cruises.

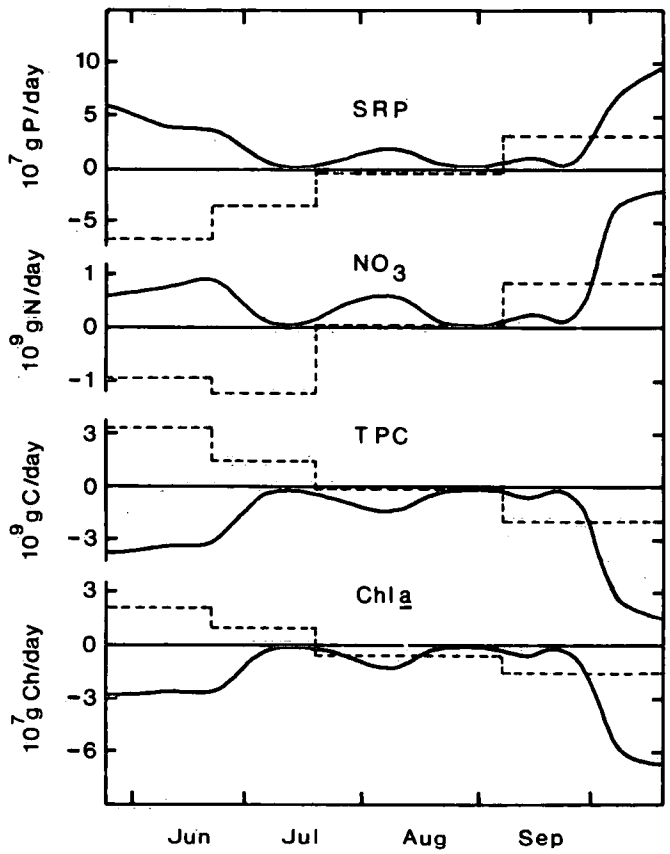

Figure 4.3.2 Upward mass exchanges computed at the 20-m level (solid lines) and observed rates of change between cruises (dashed lines).

It is seen from these results that the contributions from vertical mixing are typically of the same magnitude as the total rate of change of these variables. Since biological processes are essentially represented by the area between the solid and the dashed curves, it follows that during the spring season the observed rate of change is only

half the actual growth occurring with the help of mixing. Conversely, during the fall season, the observed rate of change is completely explained by mixing without invoking any biological activity. It is of particular interest to compare this internal loading of nutrients to the epilimnion of a lake with the external inputs. In the present case, the annual net loading to Lake Ontario during 1972 was about 1×10^7 g P/day for SRP and 1×10^8 g N/day of NO_3; that is much smaller than the mixing effects in spring and fall. From a modeling viewpoint, it is clear that a plankton model requires a very accurate description of the mass exchanges across the thermocline, and that it is not sufficient to simply divide the year in a mixed season and a stratified season without mixing.

Large-Scale Transports

The concept of mixing coefficients is only a first approximation to the problem of simulating mass exchanges between different volume elements of a large lake. A detailed analysis of local water quality variables shows significant time variations which are apparently due to advection of properties from other areas into the zone of interest. These variations therefore are directly related to organized large-scale water movements in specific directions. In particular, the nearshore zones are sensitive to the effects of wind-driven circulations because the latter lead to vertical motions in these areas. When combined with vertical concentration gradients and typical horizontal differences between shallow and deep water, these water motions cause sudden local concentration increases or decreases depending on the direction of the wind. Since it is not a practical proposition to measure three-dimensional circulations on a routine basis, one must resort to hydrodynamic models.

A numerical model for computing currents and temperatures in Lake Ontario has been described in Section 4.2. This model was used in some experiments to investigate the effects of large-scale circulation on the movement of dissolved or suspended material in Lake Ontario. Such simulations are based on the generalized advection-diffusion equation discussed at the beginning of this chapter. In one of the case studies presented by Simons (1972), the hydrodynamical model of Lake Ontario was run for actual wind conditions from 20 April 1971 to 14 May 1971. Inflow

and outflow from major rivers were included. If the results are averaged over the whole period, the circulation pattern appears as shown previously in Figure 4.2.2. Now assume that a continuous flow of some conservative substance originates from the Niagara River and is subjected to this circulation pattern. The computed concentrations after about three months then appear as shown at the top of Figure 4.3.3, where the concentration at the source is set equal to 10 units. If in addition we allow for diffusion of matter by employing a diffusion coefficient derived from dye release experiments (Murthy, 1976), the resulting distribution looks like the bottom of Figure 4.3.3. These results show in a qualitative way that wind-induced water circulations have a profound effect on the distribution of temperature and nutrients in Lake Ontario.

A quantitative evaluation of heat transports was carried out by Simons (1976a) as an extension of the hydrodynamic model verification described in Section 4.2. The model had a resolution of 5 km in the horizontal and consisted of four layers with fixed interfaces at 10, 20, and 40 metres below the surface. In this case the circulation model was run throughout the 1972 field year, but the temperatures were not predicted but continually updated by recourse to observations. The results were averaged over the inertial period (about 17 hours) and stored on magnetic tape for mass transport computations. For the latter purpose, the lake was divided into 21 zones with the mean depth contour separating shore zones from deep water. These zones were shown in Figure 4.1.1 together with the 5-km grid used for the hydrodynamic model. Computed water circulations were then combined with observed temperatures to estimate heat transports across the boundaries of these zones. Weekly estimates of heat budgets and surface fluxes for the same zones were used for model validation.

Figure 4.3.4 summarizes the salient results of this experiment. The left side of the figure presents results for combinations of zones, such as the north shore, deep lake, et cetera. The solid lines represent observed heat changes corrected for surface fluxes; the dashed lines indicate computed heat transports. The results for the whole lake are included as a measure of observational errors. The right-hand side of Figure 4.3.4 shows results for individual zones along the north shore. Inspection of

these figures makes it clear that considerable errors are present during the summer season, in particular toward the eastern half of the lake. This is probably due to lack of observations in this part of the lake and insufficient resolution of the hydrodynamic model (see also Bennett, 1977). In view of these results, further application of the hydrodynamic model output in this report will be restricted to the western half of the lake.

Figure 4.3.3 Computed dispersion of a conservative substance entering Lake Ontario via the Niagara River under the influence of currents displayed in Figure 4.2.2. Above - weak diffusion; below - strong diffusion.

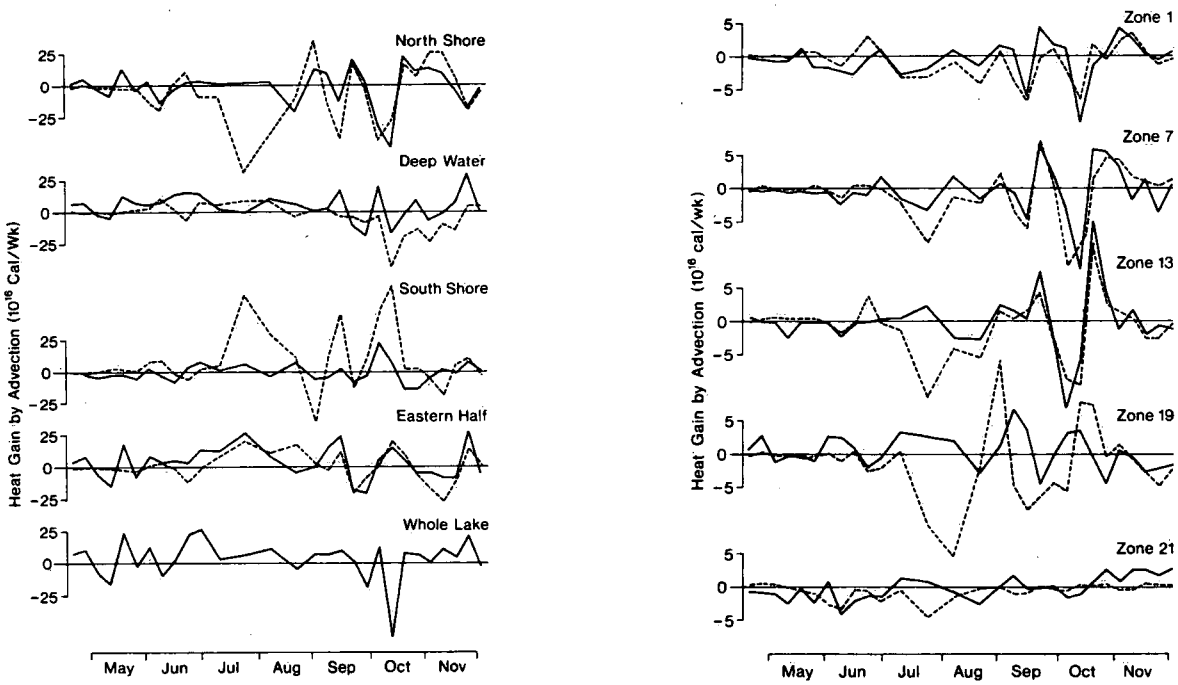

Figure 4.3.4 Comparison of measured (solid lines) and computed (dashed lines) heat gains due to currents for zones defined in Figure 4.1.1.

Nutrient Transports

Probably the most interesting aspects of large-scale water movements are the effects of wind-driven upwelling and downwelling on the ecological response of the nearshore zone. Without turning to complete three-dimensional water quality simulations, we may estimate the effects of such organized motions by combining the output from the hydrodynamic model with observed concentrations of nutrients and plankton. This approach is similar to the one used for the analysis of lake-wide vertical exchanges.

Let us consider a typical volume element in the upper layer of the nearshore zone (Figure 4.3.5). If C_1 is the mean concentration of the variable of interest for this volume, V, then the time rate of change of mass contained in the volume is $d(VC_1)/dt$. This change is partly due to biochemical processes within the volume, to loading from external sources, to sedimentation of particulate matter, and to mixing processes owing to small-scale motions not resolved by the hydrodynamic model. However, the change to be considered here is due to the large-scale vertical and horizontal water transports represented by W and U,

respectively, in Figure 4.3.5. If C_2 denotes the concentration in the underlying water and C_3 is the concentration of the adjacent surface water, then the mass change due to hydrodynamic transports may be approximated by

$$\frac{d}{dt}(VC_1) = W\left(\frac{C_1 + C_3}{2}\right)$$

where W and U have units of volume/time. If the volume element is limited in alongshore direction to a small part of the shore, there will also be effects of alongshore currents but these are in general negligible compared to those considered here. Furthermore, the interface concentrations can be approximated by a different weighting of upstream and downstream values but again such refinements may be dispensed with for the moment.

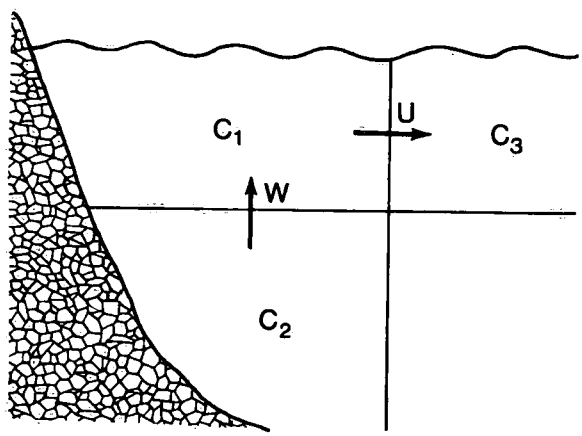

Figure 4.3.5 Typical volume element for upper layer of nearshore zone. C = concentration of chemical variables; U and W are transport components.

Figure 4.3.6 presents results of computations for zone 7 along the northern shore of Lake Ontario. This zone has been selected because it is a well-known upwelling area and because the hydrodynamic model was found to perform consistently well in this part of the lake (as discussed before). The solid lines represent net horizontal plus vertical mass transports into the upper 20-m layer of this zone, as computed from observed concentrations of variables (section 4.1) and water circulations

obtained from the hydrodynamic model. The data were interpolated in time by the method of cubic splines (see, e.g., Reinsch, 1967) to obtain a smoother variation between data points. As in Figure 4.3.2, the changes of mass in the volume element between consecutive cruises are again shown by the dashed lines. The volume is 1.4 10^{10} m^3 and the variables are the same as before.

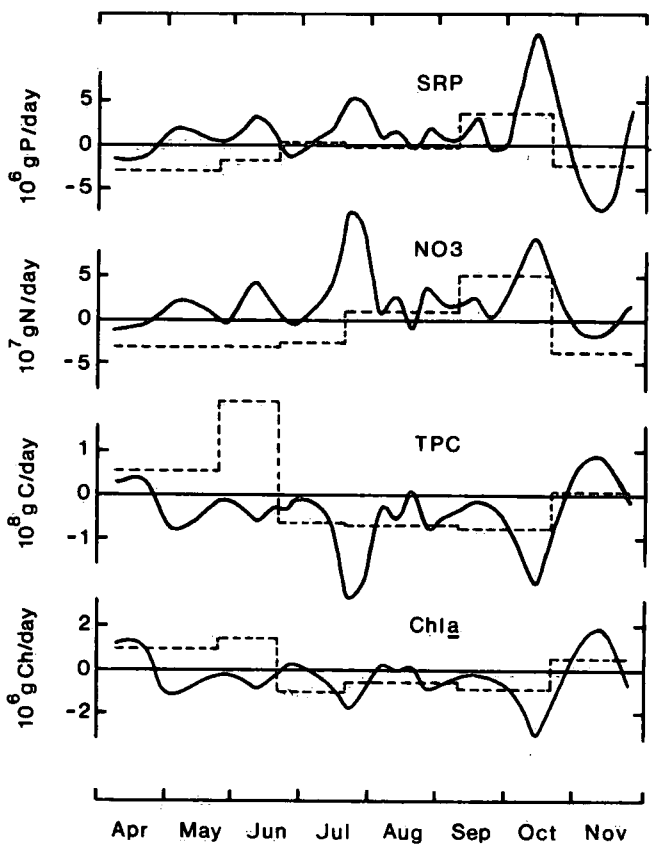

Figure 4.3.6 Computed transports of indicated variables into the upper 20-m layer of zone 7 of Figure 4.1.1 (solid lines) and observed rates of change between cruises (dashed lines).

It is seen that effects of water transports in the nearshore zone tend to be similar to effects of vertical mixing on a lake-wide scale. Since the spring bloom of phytoplankton occurs earlier along the shores, any vertical circulation in the early part of the year will represent a form of internal nutrient loading. In case of upwelling, nutrients will be transported up from the lower layer; in case of downwelling, the associated

horizontal surface motions toward the shore will transport nutrients from deep water to the shore zones. In summer, the horizontal gradients become less important but the vertical gradients and, consequently, the upwelling effects become more pronounced. It should be noted, however, that during this period small errors in computed water circulations will lead to large errors in transports of nutrients. This was noted previously in the context of model verification on the basis of heat advection. The large variations in nutrient advection during the fall season are caused by pronounced wind events during this period. It is seen that these mass transports are well reflected in the time variations of the mass contents, which was also found in the heat transport computations. Again, it may be pointed out that the internal loadings due to mass transports are far greater than the external inputs to this lake zone. The response of a nearshore zone can, therefore, not be simulated without regard to this interaction with the open lake.

4.4 Three-Dimensional Water Quality Models

This section is devoted to the coupling of physical and biochemical models for the purpose of obtaining a three-dimensional predictive water-quality model. As shown in Figure 4.4.1, the complete model is visualized as a combination of three major components, namely, the physical model, the biochemical model, and the interfacing model. The physical model consists of a package of modeling routines concerned with the hydrodynamic and thermodynamic properties of large water bodies, whereas the biochemical model simulates the various chemical, biological, and geological processes in the lake. The interfacing model is responsible for the coupling of physical and biological components and it coordinates the operation of the total model. In essence, the interfacing model is a transport model linking different compartments of the water body and various natural processes within each of these compartments. Mathematically, the interfacing model is formulated on the basis of the advection-diffusion equation presented in Section 4.3. This equation expresses the time rate of change of mass contained in a volume element as the sum of advection, diffusion, and sources. Once the time rate of change is known, it is a simple matter to compute the future concentrations from

the present one, at least for a reasonably short time step during which the environmental conditions may be considered quasi-invariant. After completing this computation for all the volume elements of the model, the advection, diffusion, and sources can be calculated for these new conditions and the cycle can be repeated until the desired prediction is completed. In practice, water quality models of this type may divide the water basin in more than one hundred compartments, and they will use time steps of one day or less to predict seasonal and yearly changes in a lake.

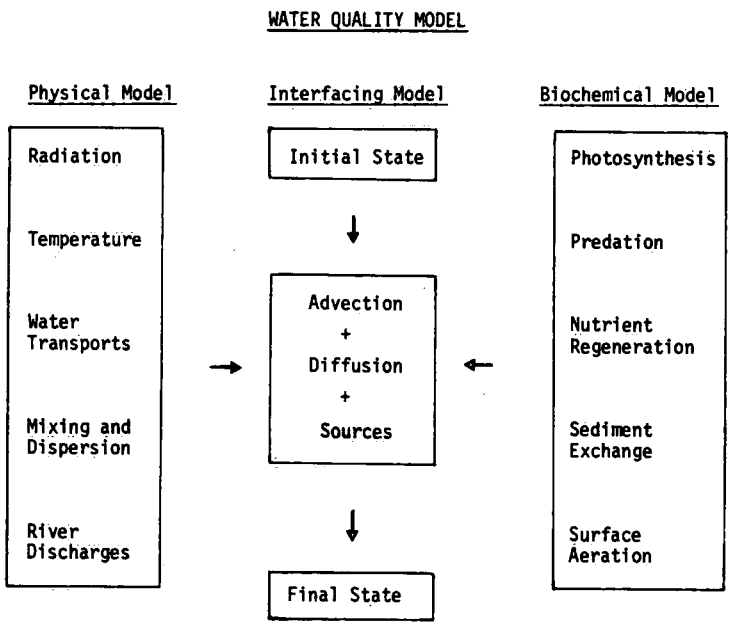

Figure 4.4.1 Structure of water quality model.

The synthesis model is coupled with the physical lake model through the advection-diffusion mechanism and with the biochemical models through the source terms in the governing equation. In turn, some of the biological models will draw directly upon the physical model for such parameters as temperature and radiation which strongly affect biological processes. Since the feedback from the biochemical model components on the physical model can be neglected to a first approximation, the most practical interfacing with the physical model will consist of computer disks or magnetic tapes. Thus the physical input for the water quality model is obtained first, partly from observations and partly from

hydrodynamic and thermodynamic models, and stored for subsequent use by the synthesis model. Since the required resolution in time and space is in general different for hydrodynamic versus water quality modeling, the first step is to make the necessary adjustments. The hydrodynamic models to be considered here have a typical horizontal resolution of 5 km and a time step of 15 minutes, much smaller than the corresponding values for the biological models mentioned above. Thus the output from the physical models is first averaged over time. This averaging period is not arbitrary, but it must be a multiple of the inertial period to eliminate the usually large inertial current oscillations induced by the earth's rotation. Since this period is about 17 hours for Lake Ontario, it should be noted that daily averages are particularly undesirable. Next, the hydrodynamic results are interpolated and integrated in space to obtain the flow of water perpendicular to any arbitrary boundary separating the volume elements of the biochemical model. Again, the operation is subject to certain conditions, in particular, the conservation of water mass for each compartment.

Lake Ontario Simulations

In a previous paper (Simons, 1976b) a description was presented of a three-dimensional modeling study of Lake Ontario during the 1972 International Field Year. The study combined radiation data, temperatures from ship cruises, vertical mixing coefficients derived from weekly heat budgets, water transports obtained from a four-layer circulation model, and a plankton model developed for Lake Ontario by Thomann *et al.*(1975). Similar three-dimensional experiments were carried out with other water quality models such as those discussed in Chapters 2.4 and 2.5 of the present report. In the meantime, a similar experiment has been reported by Chen and Smith (1977). In a way it may be considered a little premature to attempt such simulations, in view of the uncertainties surrounding limnological models which have been pointed out throughout this report. Indeed, this kind of study should be seen as simply another test to evaluate the sensitivity of ecological models to environmental parameters. Thus, the purpose is not so much to simulate or predict conditions in one particular location within a large lake, but rather to see what additional

information can be expected from a three-dimensional model, once we are able to simulate the basic ecological processes in the lake.

As expected, the major findings from our various three-dimensional experiments are very much alike, regardless of the ecological sub-models used in the different runs. In keeping with the approach followed throughout this report, we will illustrate them by recourse to one of the simpler models, namely, the two-component dynamic phosphorus model of Chapter 2.4. It has been noted before that this model incorporates essentially all the basic characteristics of typical plankton models. Thus, this sub-model was included in the three-dimensional model framework and the latter was run for the 1972/1973 field year, using the data base and hydrodynamic calculations discussed in Sections 4.1-2. Selected results are shown in Figure 4.4.2.

The upper part of Figure 4.4.2 compares epilimnion results from a horizontally mixed model with the values obtained if the results from the three-dimensional model are averaged over the whole epilimnion. It may be noted that the former solution differs from the two-layer results presented in Chapter 2.4, because the present calculation employed the four-layer structure of the hydrodynamic model. Although based on the same heat content data, the mixing coefficients depend on the vertical model structure as seen in Chapter 2.2, with the result that the model which was fitted so carefully to the data in Chapter 2.4, now exhibits considerable deviations from the same data. It is perhaps instructive to see that these variations exceed the differences between the horizontally mixed model and the averaged three-dimensional model results.

The lower part of Figure 4.4.2 compares epilimnion results for zones 7 and 12, i.e., the nearshore and the deep-water zone referred to in Section 4.1. The observations are indicated by circles and triangles, respectively. Two things may be noted here. The first one is that the time lag between nearshore and deep water observations during the spring season is also present in the model solutions. In the model, this time lag is due to the prescribed mixing regime. The second point is the sudden increase of SRP in the nearshore zone during the fall season. This is caused by large-scale wind-driven water movements as explained in Section 4.3. A final comment to be made is that the nearshore simulation of the organic phosphorus component shows little agreement with the data.

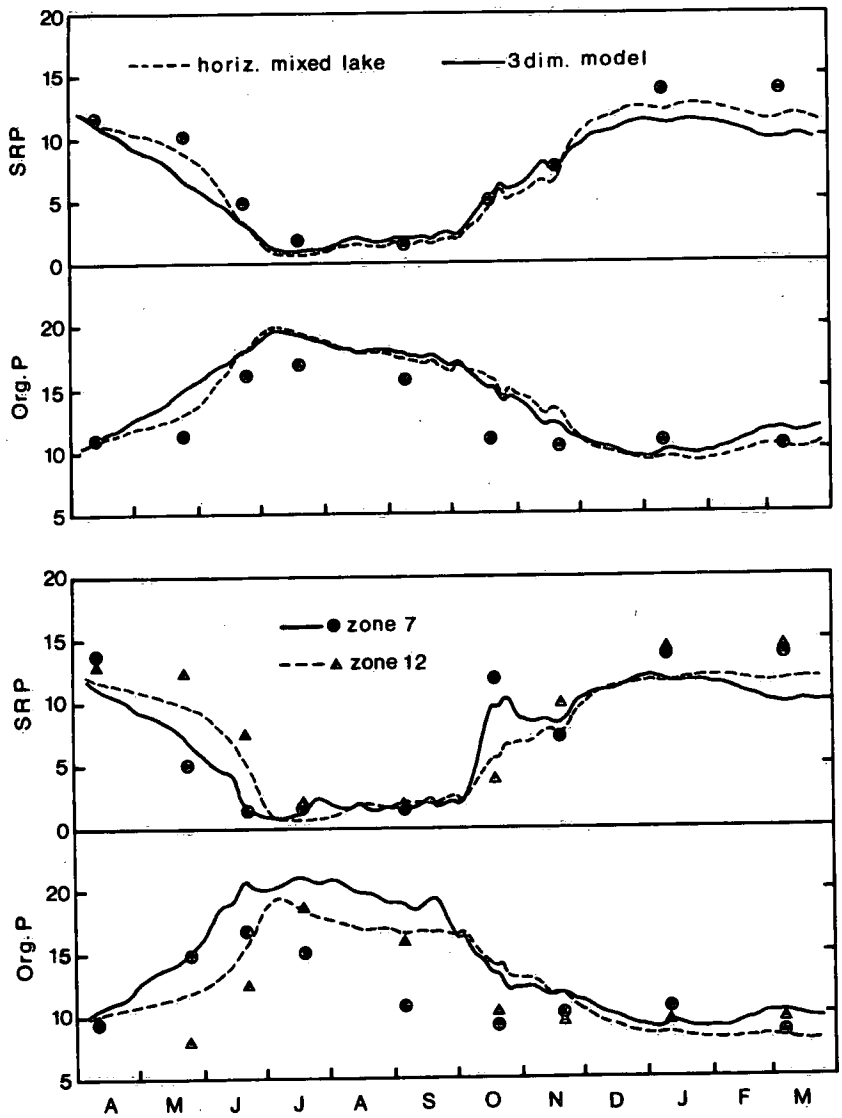

Figure 4.4.2 (Above) Results from three-dimensional, two-component phosphorus model, compared with results of horizontally mixed model and observations (circles) for epilimnion. (Below) results from the same model for zones 7 and 12 of Figure 4.1.1, again for the epilimnion.

The conclusions of our three-dimensional water quality modeling studies are probably best summarized as follows:

1. Lake-wide averages of solutions for the segmented lake model corresponded closely to results from a horizontally mixed model, implying that the lake-wide response of a large lake can be simulated reasonably well by the latter type of model.

2. Time lags between nearshore and deep water algal blooms in the early part of the year were properly simulated as a result of spatial variations in the onset of stratification and the associated variations of temperatures and vertical mixing.

3. Large-scale organized water movements during storm periods resulted in short-term fluctuations of solutions within the nearshore zone which may be as large as the kind of horizontal gradients observed between nearshore and offshore waters (see, for example, Simons, 1976b; figure 7).

Finally, in spite of all that has been said about the possible rewards of interdisciplinary research activities in limnology, the present investigation would suggest that but little can be gained from such efforts at the present time. The major gaps in our knowledge, be it primary production or hydrodynamic circulation, are still to be addressed by highly specialized disciplinary research. In recent years, computer modeling has developed into a powerful and exciting addition to the more conventional sciences, but the immediate practical benefits with regard to environmental management may have been somewhat oversold.

REFERENCES

AES., 1977. Maps of surface water temperature determined from the Airborne Thermometry Program. Hydro Meteorologic and Marine Applications Division, Atmospheric Environment Service, Downsview, Ontario.

Akima, H., 1970. A new method of interpolation and smooth curve fitting based on local procedures. J. Assoc. Comput. Mach., 17, 589-602.

Angström, A., 1956. On the computation of global radiation from records of sunshine. Ark. Geofys., 2, 471-479.

Bannerman, R.T., D.E. Armstrong, R.F. Harris, and G.C. Holdren. 1975. Phosphorus uptake and release by Lake Ontario sediments. Envir. Prot. Agency, Corvallis, Oregon, EPA-660/3-75-006, 51 pp.

Bennett, J.R., 1974. On the dynamics of wind-driven lake currents. J. Phys. Ocean., 4, 400-414.

Bennett, J.R., 1977. A three-dimensional model of Lake Ontario's summer circulation. I. Comparison with observations. J. Phys. Ocean., 7, 591-601.

Bertalanffy, L. Von, 1972. The history and status of general systems theory. In Trends in general systems theory. Edited by G.J. Klir. Wiley-Interscience, New York, 21-41.

Bierman, V.J., 1976. Mathematical model of the selective enhancement of blue-green algae by nutrient enrichment. In Modeling biochemical processes in aquatic ecosystems. Edited by R.P. Canale. Ann Arbor Science Publishers, Ann Arbor, 1-31.

Bolsenga, S.J., 1975. Estimating energy budget components to determine Lake Huron evaporation. Water Resour. Res., 11, 661-666.

Box, G.E.P. and G.M. Jenkins. 1970. Time Series Analysis, Forecasting and Control. Holden-Day Inc., San Francisco.

Boyce, F.M., 1978. Seasonal variations of vertical heat transports in Lake Ontario. Manuscript Rept., Canada Centre for Inland Waters, Burlington, Ontario.

Boyce, F.M., W.J. Moody and B.L. Killins, 1977. Heat content of Lake Ontario and estimates of average surface heat fluxes during IFYGL. Technical Bulletin No. 101, Inland Waters Directorate, Canada Centre for Inland Waters, Burlington, Ontario. 120 pp.

Boyd, J.D. and B.J. Eadie, 1977. Evaluation of U.S. IFYGL chemical data at the master stations, IFYGL Bulletin No. 21, 49-61.

Bryan, K., 1969. A numerical method for the study of ocean circulation. J. Comput. Phys., 4, 347-376.

Burns, N.M. and A.E. Pashley, 1974. In situ measurements of the settling velocity profile of particulate organic carbon in Lake Ontario. J. Fish. Res. Bd. Canada, 31, 291-297.

Cale, W.G. and P.L. Odell, 1978. Concerning aggregation in ecosystem modeling. In Theoretical Systems Ecology: Advances and Case Studies. Edited by E. Halfon. Academic Press, New York, (In Press).

Canada Centre for Inland Waters, 1977. Atmospheric Loading of the Lower Great Lakes. Report by Acres Consulting Limited. Under Contract DSS 01SS KL347-6-0146.

Casey, D.T. and S.E. Salbach, 1974. IFYGL stream materials balance study. Internat. Assoc. Great Lakes Res., Conf. Proc. 17, 668-681.

Chen, C.W., M. Lorensen, and D.T. Smith, 1975. A comprehensive water quality ecologic model for Lake Ontario. NOAA, GLERL, Ann Arbor, Mich., 202 pp.

Chen, C.W. and G.T. Orlob, 1975. Ecologic simulation for aquatic environments. In Systems analysis and simulation in ecology, edited by B.C. Patten, 3, 475-588. New York, Academic Press.

Chen, C.W. and D.J. Smith, 1977. Preliminary calibration of Lake Ontario water quality - ecological model. Great Lakes Envir. Res. Lab., Ann Arbor, Mich., NOAA Rept. No. 03-6-022-35162, 65 pp.

Dahlquist, G., 1974. Problems related to the numerical treatment of stiff differential equations. In: International Computing Symposium 1973, Gunther *et al* Eds. North Holland Publ. Co. Amsterdam, 307-314.

Davies, J.A. and W.M. Schertzer, 1974. Canadian radiation measurements and surface radiation balance estimates for Lake Ontario during IFYGL, Canada Centre for Inland Waters, Burlington, Ontario, 72 pp.

DiToro, D.M., D.J. O'Connor and R.V. Thomann, 1971. A dynamic model of the phytoplankton population in the Sacramento-San Joaquin Delta. Advances in Chemistry, Series 106, 131-180.

Dunbar, D.S., 1977. SMOOTH: A fortran programme for generating a 2D mass-consistent current field from scattered observations, CCIW Contract Report. June, 1977.

Elder, F.C., A.W. Anders, S.J. Eisenreich, T.J. Murphy, M. Sanderson and R.J. Vet, 1977. Atmospheric Loadings to Great Lakes. CCIW unpublished report.

El-Shaarawi and R.E. Kwiatkowski, 1978. Temporal and spatial variability of chlorophyll a and related parameters in Lake Ontario 1974. J. Great Lakes Res., 3, 177-183.

El-Shaarawi, A. and J. Whitney, 1977. On determining the number of samples required to estimate the phosphorus input contributed by Niagara River to Lake Ontario. Canada Centre for Inland Waters unpublished report.

Eppley, R.W., 1972. Temperature and phytoplankton growth in the sea. Fish. Bull., 70:1063-1085.

Fraser, A.S., 1976. Assessment of nitrogen and phosphorus trends in Lake Ontario 1968-1975. Canada Centre for Inland Waters manuscript.

Fraser, A.S., D.J. Casey and P.A. Clark, 1977. Materials balance for Lake Ontario during IFYGL (1972-1973). Canada Centre for Inland Waters unpublished report.

Great Lakes Water Quality Board, 1969. Report to the IJC on the Pollution of Lake Erie, Lake Ontario and the International Section of the St. Lawrence River. Vol. 2.

Gregor, D.J., 1977. Tributary loadings to the Great Lakes - comparison of methods. PLUARG CDN. Task D. unpublished report.

Halfon, E. and M.G. Reggiani, 1978. Adequacy of ecosystem models. Ecological Modelling, 4:41-50.

Hansen, W., 1956. Theorie zur Errechuung des Wasserstandes und der Strömungen in Randmeeren nebst Anwendungen. Tellus, 8. 287-300.

Humphrey, G.F., 1973. Photosynthetic and respiratory rates, and phosphorus content of algae grown at different phosphate levels, SPL. Publ., Mar. Biol. Ass. India, 74-79.

Hydroscience Inc., 1976. Assessment of the effects of nutrient loadings on Lake Ontario using a mathematical model of the phytoplankton. Report to the International Joint Commission.

International Joint Commission, Great Lakes Water Quality Board, Annual Reports 1974, 1975, 1976.

Imboden, D.M., 1974. Phosphorus models of lake eutrophication. Limnol. Oceanogr., 19, 297-304.

Imboden, D.M. and R. Gachter, 1978. A dynamic lake model for trophic state prediction. Ecol. Modelling, 4, 77-98.

Jerlov, N.G., 1968. Optical Oceanography. Elsevier Publishing Co., London, p. 199.

Jorgensen, S.E., 1976. A eutrophication model for a lake. Ecological Modeling, 2, 147-165.

Kendall, M.G. and A. Stuart, 1970. The advanced theory of statistics, 2. Inference and relationship, 3rd. ed. New York, Hafner Publ. Co., 391-407.

Kullenberg, G., C.R. Murthy and H. Westerberg, 1973. An experimental study of diffusion characteristics in the thermocline and hypolimnion regions of Lake Ontario. Internat. Assoc. Great Lakes Res., Conf. Proc. 16, 774-790.

Lam, D.C.L., 1978. Simulation of water circulations and chloride transports in Lake Superior for summer 1973, J. Great Lakes Res. (in press).

Lam, D.C.L. and T.J. Simons, 1976. Numerical computations of advective and diffusive transports of chloride in Lake Erie. J. Fish. Res. Bd. Can. 33, 537-549.

Marquardt, D.W., 1963. An algorithm for least squares estimation of nonlinear parameters, J. Soc. Indust. Appl. Math., 11, 431-441.

Mateer, C.L., 1955. A preliminary estimate of average insolation in Canada. Can. J. Agr. Sci., 35, 579-594.

Matheson, D.H., 1974. Measurements of atmospheric inputs to the Great Lakes. Canada Centre for Inland Waters unpublished report.

Mirham, G.A., 1972. Some practical aspects of the verification and validation of simulation models. Oper. Res. Q., 23, 17-29.

Murthy, C.R., 1976. Horizontal diffusion characteristics in Lake Ontario. J. Phys. Oceanogr., 6, 76-84.

Munawar, M., P. Stadelmann and I.F. Munawar, 1974. Phytoplankton biomass, species composition, and primary production at a nearshore and a midlake station of Lake Ontario during IFYGL. Internat. Assoc. Great Lakes Res., Conf. Proc. 17, 629-652.

Nunez, M., J.A. Davies and P.J. Robinson, 1971. Solar radiation and albedo at a Lake Ontario tower site. Canada Centre for Inland Waters. 82 pp.

O'Melia, R.R., 1972. An approach to the modeling of lakes. Swiss J. Hydrology, 34, 1-33.

Ongley, E.D., 1974. Hydrophysical characteristics of Great Lakes tributary drainage, Canada. Dept. of Geography, Queen's University, Kingston, Ontario.

Ontario Ministry of the Environment. Operating summary of water pollution control projects. Annual reports 1967-1976.

Park, R.A., 1974. A generalized model for simulating lake ecosystems. Simulation, 23, 33-50.

Parker, R.A., 1973. Some problems associated with computer simulation of an ecological system. In Mathematical theory of the dynamics of biological populations, ed. Bartlett and Hiorns, 269-288, London, Academic Press.

Parnas, H. and D. Cohen, 1976. The optimal strategy for the metabolism of reserve materials in micro-organisms. J. Theor. Biol., 56 (1), 19-56.

Philbert, F.J., 1973. The effect of sample preservation by freezing prior to chemical analysis of Great Lakes waters, International Association for Great Lakes Research, Conf. Proc. 16, 282-293.

Philbert, F.J. and W.J. Traversy, 1973. Methods of sample treatment and analysis of Great Lakes water and precipitation samples, International Association for Great Lakes Research, Conf. Proc. 16, 294-308.

Platt, T., K.L. Denman and A.D. Jassby, 1975. The mathematical representation and prediction of phytoplankton productivity. Environment Canada, Fish. Mar. Ser., Tech. Rept. 523, 121 pp.

Platzman, G.W., 1963. The dynamical prediction of wind tides on Lake Erie. Meteor. Monogr., 4, No. 26. 44 pp.

Reinsch, C.H., 1967. Smoothing by spline functions. Num. Math., 10, 177-183.

Robertson, A., F.C. Elder and T.T. Davies, 1974. IFYGL chemical intercomparisons, International Association for Great Lakes Research, Conf. Proc. 17, 682-696.

Sasaki, Y., 1970. Some basic formalisms in numerical variational analysis, Mon. Weather Rev., 98, 875-883.

Sauberer, F., 1962. Internationale Vereinigung fur theoretische und angewandte limnologie. Mitteilung No. 11.

Scavia, D., B.J. Eadie,and A. Robertson, 1976. An ecological model for Lake Ontario, model formulation, calibration and preliminary evaluation. Great Lakes Envir. Res. Lab., Ann Arbor, Mich., NOAA Tech. Rept. ERL 371-GRERL 12, 63 pp.

Schertzer, W.M., 1977. Energy budget and monthly evaporation estimates for Lake Superior. 1973. Canada Centre for Inland Waters.

Schertzer, W.M., F.C. Elder and J. Jerome, 1977. Measurements of vertical extinction and photic depth in Lake Superior 1973 and Lake Huron and Georgian Bay 1974 (presented at the 19th Conf. on Great Lakes Research) International Association for Great Lakes Research.

Sherman, C.A., 1976. A mass-consistent model for wind fields over complex terrain, UCRL-76171, U.C., Livermore, California, Dec. 1976.

Shiomi, M.T. and K.W. Kuntz, 1973. Great Lakes Precipitation Chemistry, Part I: Lake Ontario Basin. Proceedings 16th Conference, Internat. Assoc. Great Lakes Research, Conf. Proc. 16, 581-602.

Simons, T.J., 1971. Development of numerical models of Lake Ontario. Internat. Assoc. Great Lakes Res., Conf. Proc., 14, 654-669.

Simons, T.J., 1972. Development of numerical models of Lake Ontario, Part 2. Internat. Assoc. Great Lakes Res., Conf. Proc., 15, 655-672.

Simons, T.J., 1973a. Development of three-dimensional numerical models of the Great Lakes. Environment Canada, Scientific Series No. 12. 26 pp.

Simons, T.J., 1973b. Comparison of observed and computed currents in Lake Ontario during Hurricane Agnes, June, 1972. Internat. Assoc. Great Lakes Res., Conf. Proc. 16. 831-844.

Simons, T.J., 1974. Verification of numerical models of Lake Ontario I: Circulation in spring and early summer. J. Phys. Ocean., 4, 507-523.

Simons, T.J., 1975a. Verification of numerical models of Lake Ontario II: Stratified circulations and temperature changes. J. Phys. Ocean., 5, 98-110.

Simons, T.J., 1975b. Effective wind stress over the Great Lakes derived from long-term numerical model simulations. Atmosphere, 13, 169-179.

Simons, T.J., 1976a. Verification of numerical models of Lake Ontario III: Long-term heat transports. J. Phys. Ocean., 6, 372-378.

Simons, T.J., 1976b. Analysis and simulation of spatial variations of physical and biochemical processes in Lake Ontario. J. Great Lakes Res., 2, 215-233.

Snodgrass, W.J. and C.R. O'Melia, 1975. Predictive model for phosphorus in lakes. Envir. Sci. Technol., 9, 937-944.

Sonzogni, W.C., T.J. Monteith, W.N. Bach, and V.G. Hughes. 1978. United States Great Lakes Tributary Loadings. Report to PLUARG U.S. Task D.

Stadelmann, P. and A.S. Fraser, 1974. Phosphorus and nitrogen cycle on a transect in Lake Ontario during the International Field Year 1972-1973. Internat. Assoc. Great Lakes Res. Conf. Proc., 17, 92-108.

Stadelmann, P. and M. Munawar, 1974. Biomass parameters and primary production at a nearshore and a midlake station of Lake Ontario during IFYGL. Internat. Assoc. Great Lakes Res., Conf. Proc., 17, 109-119.

Stadelmann, P., J. Moore and E. Pickett, 1974. Primary production in relation to temperature structure, biomass concentration and light conditions at an inshore and offshore station in Lake Ontario. J. Fish. Res. Bd. Canada, 31, 1215-1232.

Steele, J.H., 1965. Notes on some theoretical problems in production ecology. Mem. Ist. Ital. Idrobiol., 18 (Suppl.) 383-398.

Steele, J.H., 1974. The structure of marine ecosystems. Cambridge, Mass., Harvard Univ. Press, 128 pp.

Strickland, J.D.H., 1958. Solar radiation penetrating the ocean. A review of requirements and methods of measurement with particular reference to photosynthetic productivity. J. Fish. Res. Bd. Canada, 15, 453-493. 1958.

Sweers, H.S., 1969. Structure dynamics and chemistry of Lake Ontario. Dept. of Energy, Mines and Resources, Ottawa, Manuscript Report Series 10.

Talling, J.F., 1965. Comparative problems of phytoplankton and photosynthetic productivity in a tropical and temperate lake. In Primary Productivity in Aquatic Environments. Edited by C.R. Goldman. Mem. 1st. Ital. Hydrobiol., 18, (Suppls), 399-424.

Thomann, R.V., R.P. Winfield and D.M. DiToro, 1974. Modeling of phytoplankton in Lake Ontario. Internat. Assoc. Great Lakes Res., Conf. Proc., 17, 135-149.

Thomann, R.V., D.M. DiToro, R.P. Winfield, and D.J. O'Connor, 1975. Mathematical modeling of phytoplankton in Lake Ontario, 1. Model development and verification. U.S.-EPA, Nat. Env. Res. Center, Corvallis, Oregon. EPA 660/3-75-005, 177 pp.

Thomann, R.V., R.P. Winfield, D.M. DiToro, and D.J. O'Connor, 1976. Mathematical modeling of phytoplankton in Lake Ontario, Part 2. Simulations using Lake 1 model. US-EPA, Env. Res. Lab., Duluth, Minnesota, EPA-600/3-76-065, 87 pp.

Thomson, K.P.B. and J. Jerome, 1973. Transmissometer measurements of the Great Lakes. Scientific Series #53, Inland Waters Directorate, Canada Centre for Inland Waters.

Thomson, K.P.B., J.H. Jerome and W.R. McNeil, 1974. Optical properties of the Great Lakes. Internat. Assoc. Great Lakes Res., Conf. Proc., 17, 811-822.

Traversy, W.J., 1971. Methods for chemical analysis of waters and wastewaters, Canada Dept. of Fisheries and Forestry, Inland Waters Branch, Water Quality Division Report.

Tyler, J.E., 1968. The Secchi disc. Limnol. and Oceanogr. 13, 1-6.

United States Geological Survey. Water resources data for New York.

Vollenweider, R.A., 1955. A nomogram for the determination of the transmission coefficient and some remarks on the method of its calculation, Swiss Journal of Hydrology, 17, 205-216.

Vollenweider, R.A., 1969. Possibilities and limits of elementary budget models for lakes. Arch. Hydrobiol. 66, 1-36 (in German).

Vollenweider, R.A., 1970. Models for calculating integral photosynthesis and some implications regarding structural properties of the community metabolism of aquatic systems. In Proc. IBP/PP Technical Meeting, Trebon, 14-21 September, 1969, 455-472.

Vollenweider, R.A., 1975. Input-output models with special references to the phosphorus loading concept in limnology. Swiss J. of Hydrology, 37, 53-84.

Vollenweider, R.A., and P.J. Dillon, 1974. The application of the phosphorus loading concept to eutrophication research. Nat. Res. Council Canada Rept. NRCC 13690, 42 pp.

Vollenweider, R.A., M. Munawar, and P. Stadelmann, 1974. A comparative review of phytoplankton and primary production in the Laurention Great Lakes. J. Fish. Res. Bd. Canada, 31, 739-762.

Watson, N.H.F., 1978. Seasonal distribution of crustacean zooplankton in relation to physical factors, Ch. 6 of "The status of the biota of Lake Ontario during IFYGL", edited by W.J. Christie and N.A. Thomas, IFYGL Final Report (to be published).

Watson, N.H.F., G.F. Carpenter, M. Munawar, 1975. Problems in the monitoring of biomass, Am. Soc. for Testing and Materials, Special Tech. Publ. 573, 311-319.

Webster, J.R., 1978. Hierarchical organization of ecosystems. In Theoretical Systems Ecology: Advances and Case Studies. Edited by E. Halfon. Academic Press, N.Y. (in press).

Willson, K.E., 1978. Nutrient loadings to Lake Ontario, 1966-1977. Canada Centre for Inland Waters, Burlington, Ontario.

Zeigler, B.P., 1976. Theory of Modelling and Simulation. Wiley-Interscience, New York, 425 pp.

ASSESSMENT OF WATER QUALITY SIMULATION CAPABILITY FOR LAKE ONTARIO